UNIVERSITÀ
DEGLI STUDI
DI PADOVA

Sede Amministrativa: Università degli Studi di Padova

Dipartimento di Fisica e Astronomia "G. Galilei"

CORSO DI DOTTORATO DI RICERCA IN: FISICA

CICLO: XXXIV

The role of variance in classical stochastic systems

Coordinatore: Ch.mo Prof. Franco Simonetto

Supervisore: Ch.mo Prof. Marco Baiesi

Dottorando: Ivan Di Terlizzi

ABSTRACT

We characterise stochastic systems by studying their variances. In particular, we tackle this topic from two points of view, by elaborating on the subject of *stochastic uncertainty relations* and by discussing a novel result that we term the *variance sum rule* for Langevin systems.
Stochastic uncertainty relations are inequalities that usually involve a *signal to noise ratio* $\boldsymbol{g}_O$, which can be regarded as a measure of the precision associated to the observable O, and a cost function $\mathcal{C}$ such that $\boldsymbol{g}_O \leq \mathcal{C}$. The thermodynamic uncertainty relation is one of the first examples of these stochastic inequalities and considers the average total entropy production $\langle \Sigma_{\text{tot}} \rangle$ in the cost function, thus refining the second law of thermodynamics. By means of an information-theoretic approach, we provide a new uncertainty relation for a system modelled by a linear generalised Langevin equation along with a novel *kinetic uncertainty relation*, where the upper bound to the precision is given by the *mean dynamical activity*, which quantifies the degree of agitation of a discrete system. We also show how the latter is often the main limiting factor for the precision in far-from-equilibrium conditions.
In the second part of the thesis we introduce some variance sum rules, which can be used to infer relevant dynamical parameters also for regimes far from equilibrium. We test our method on experimental data whose model parameters are known a priori, finding very good agreement between the results of the estimation procedure and the true values of the parameters. A specific sum rule for non-Markovian systems also shows good performances in estimating the memory kernel of complex fluids. Moreover, the same approach yields a solid formula for estimating the amount of entropy production. All of this shows that the indetermination of stochastic motion is a resource that we should continue to understand and exploit for measuring physical quantities.

Ringraziamenti

A distanza di otto anni dall'inizio del mio perocorso universitario, anni che sono volati e che già mi mancano, e arrivato alla conclusione della mia terza tesi, sento finalmente il dovere di dedicare un ringraziamento esteso a tutti coloro che, in un modo o nell'altro, mi hanno accompagnato durante questi intensi anni di transizione.
Il primo pensiero non può che andare al mio supervisor Marco che, nell'arco di questi anni, si è dimostrata essere innanzitutto una splendida persona nonchè un eccellente mentore. Grazie ai suoi insegnamenti ed alla sua immensa disponibiltà (anche in termini di tempo, specialmente nelle ultime settimane) sento finalmente di potermi definire un Fisico a tutti gli effetti. Grazie perché non avrei potuto scegliere un supervisor migliore.
Vorrei inoltre ringraziare Felix e Marta, con cui ho lavorato a stretto contatto negli ultimi tempi e a cui voglio un gran bene. Grazie perché, lavorando con loro, sono molto cresciuto professionalmente e anche perché (forse), grazie a loro, l'analisi dati non mi dispiace più così tanto. Forse...
Il primo ringraziamento non professionale non può che andare ai miei genitori e la mia amica di una vita Jole, che sono sempre stati i miei fan numero uno. Grazie semplicemente perché, se oggi sono così, è principalmente merito (o demerito, dipende dai punti di vista) vostro.
Un ringraziamento speciale non può che andare alla mia ragazza Giulia, che questi anni c'è sempre stata, per la sua immensa, enorme e sconfinata pazienza. Per merito suo sono sicuramente diventato una persona migliore (e anche più ordinata).
Ringrazio tutti i parenti, cugini e zii che, in misura variabile, hanno contribuito a farmi diventare quello che sono. Grazie in particolare a tutti i nonni che, anche se non tutti ci sono più, so che mi portano sempre nel loro cuore.
Un ringraziamento speciale e semi-professionale va anche al mio amico Miguel Angel Robert Muñoz El Borahẽo (per gli amici Mitch) con cui ho convissuto questo ultimo intenso mese di dottorato e cui va attribuito il merito della realizzazione delle figure più artistiche di questa tesi. Per questo vorrei semplicemente dire: "Muchas gracias Miguel!".
Come non menzionare poi tutti i conquilini con cui ho condiviso questi anni e che hanno visto il peggio di me senza scappare. Una ringraziamento speciale va a questo proposito a Marco Trenti (conosciuto ai più come *Mr El Tonahẽo* o semplicemenete *333*) e a Simone Frau, con cui ho sicuramente (e piacevolmente) sottratto più tempo agli studi durante questi anni padovani.
Grazie a tutti gli amici incontrati durante la mia carriera universitaria con cui ho studiato fino ad impazzire (vero Davide Chiappara?), senza di loro passare gli esami sarebbe stato sicuramente ancora più difficile.
Infine, grazie a tutti i Biscegliesi amici di una vita, che sono troppi da elencare, insieme a tutti gli amici conosciuti durante questi anni Padovani che hanno sicuramente reso questo lungo (ed allo stesso tempo breve) percorso indimenticabile.

Contents

CHAPTER 1

INTRODUCTION

Statistical mechanics is the field of physics whose aim is to characterise complex and chaotic systems, where many degrees are involved, by means of statistics and probability theory. Indeed, because a detailed description of these systems is often both theoretically and computationally impossible to tackle, one may resort to a coarse graining procedure where most of the *microscopic* degrees of freedom are eliminated and leading to a more simple yet at the same time effective model for the system in exam. This is often referred to as a *mesoscopic* level of description and, as consequence of the reduction of the degrees of freedom, the observable quantities exhibit a fluctuating behavior. For an observable O, the magnitude of these fluctuations can be quantified by the variance $\langle \Delta O^2 \rangle$ and its study can help to get a better insight into the microscopic structure of the system and the source of randomness.

Arguably the most important example of how the study of variances can be important dates back to the beginning of the XX century, when Einstein [1] managed to find a connection between the variance of the position of a Brownian particle and the microscopic proprieties of the fluid in which the colloidal particle is bathed. Because this variance is an easily measurable quantity, the aforementioned link between the microscopic world and the mesoscopic scale resulted in the first ever measure of the Boltzmann constant k_B and, as a consequence, led to final proof of the existence of atoms and molecules. Inspired by this remarkable result, the study of variances has evolved in parallel to technical developments until the present day where it is used, for example, to study the performances and efficiency of microscopic biological processes characterised by the presence of randomness [2, 3]. By following this path, in the present work we will deal with this issue of characterising stochastic systems by means of the study of variances. In particular, we will tackle this topic from the point of view of stochastic uncertainty relations, whose first example can be traced back to [4], and from the point of view of our novel result, i.e. the variance sum rule (VSR) for Langevin systems.

Stochastic uncertainty relations are inequalities that usually involve a *signal to noise ratio* (SNR) $\boldsymbol{g}_O$, which can be regarded as a measure of the precision associated to the observable O, and a cost function $\mathcal{C}$ such that $\boldsymbol{g}_O \leq \mathcal{C}$. These inequalities can be simultaneously regarded as an upper bound to the SNR, identifying $\mathcal{C}$ as a minimal cost to reach a certain precision, and as a lower bound to the cost function, which may be some quantity of interest to be minimised. In [4] the authors consider the average total entropy production $\langle \Sigma_{\text{tot}} \rangle$ (divided by two) as a cost function, hence making these *thermodynamic uncertainty relation* (TUR) a refinement of the second law of thermodynamics. Furthermore, for an appropriate (in a sense that must be specified) observable O, the SNR takes the form of

a squared average divided by its variance, i.e. $\boldsymbol{g}_O = \langle O \rangle^2 / \langle \Delta O^2 \rangle$. Indeed, it is rather intuitive to realise that, at fixed average, a higher variance, leading to a lower SNR, in turn corresponds to a lower precision. For example, if the observable O is the relative displacement of a molecular motor on a microtubule, one readily sees that this biological system may be interested in minimising the variance of such displacement, hence maximising g_O, in order to increase its performances and precision. As a consequence of the TUR, the SNR is bounded from above by the total entropy production which in turn implies that a certain precision may be reached at a minimal cost given by this upper bound. However, the TUR has a limited validity in the form presented above, i.e. discrete Markovian systems and continuous time and overdamped Langevin systems, both in a steady state and for observables O that are integrated currents. Indeed, since it was proposed, the original TUR has been further generalised leading to a plethora of different TURs [4, 5, 6, 7, 8, 9, 10, 11, 12, 13, 14, 15, 16, 17, 18, 19, 20, 21]. In this context, we contribute by deriving a novel example of a TUR for a linear non Markovian system, presented in Section 5.5 and based on the analytical calculations depicted in 3 and using an information theoretic approach, briefly discussed in Chapter 4. In this case, we manage to show that, in a steady state, the cost function becomes proportional to the entropy production rate hence providing an entropic bound for the SNR.

Furthermore, we also manage to derive a different stochastic bound which we call the kinetic uncertainty relation (KUR), generalising previously obtained results [22, 23, 24] and valid for Markovian jump systems with constant rates and arbitrary regimes and observables. In this case, the cost function is given by the mean dynamical activity $\langle \mathcal{K} \rangle_t$, which averages to the total number of jumps that the system performs in a certain time interval. Differently from entropy production, which can be linked to the amount of time symmetry breaking in a non equilibrium system [25, 26, 27, 28], the dynamical activity is a time symmetric quantity which, as a rich line of research [29, 30, 31, 32, 33, 34, 35] shows, plays an important role along with other time symmetric observables for the characterisation of non-equilibrium states. Indeed, we will show how, for some relevant examples such as the above-mentioned case of a molecular motor on a microtubule, it is the kinetic bound that gives the tightest constraint to the SNR of the observables in a far from equilibrium regime. This analysis in terms of uncertainty relation will hence add further insights into the role of such time symmetric, or *frenetic*, quantities for the description of non-equilibrium regimes.

The second part of this thesis, presented in Chapters 7 and 8, is again centred on the study of variances but this time in terms of a summation rule. Indeed, we will show how, at equilibrium, the behaviour of the sum of the variance of the relative displacement $\mathrm{Var}(x_t - x_0)$ and the variance of the integrated forces $\mathrm{Var}(\int_0^t \mathrm{d}t'\, F(x_{t'}, t'))$ for Markovian (Chapter 7) and non-Markovian (Chapters 8) Langevin systems is solely determined by the nature of the stochastic noise. Furthermore, we will show how, for Markovian systems in a non-equilibrium steady state (NESS), there is a finite correction to this sum rule which can be linked to the violation factor discussed in [36] and quantifying the amount of violation of the fluctuation-dissipation theorem (FDT) [37]. From this identification we will also be able to find a novel formula for the entropy production rate (Section 7.3.2.1) which may also be used in practical situation for entropy estimation.

The variance sum rule (VSR) may also be used for model parameter estimation.

For example, for a unidimensional Langevin system we will show how the VSR depends, in addition to the variances, on relevant system parameters as the friction coefficient or, in a non-Markovian setting, on the memory kernel of the system. Indeed, by computing the above-mentioned variances from experimental data coming from optical tweezers, we will show how the VSR can be used to estimate these dynamical parameters and to get further insight on the nature of the noise acting on the probe particle. In particular, for a simple Brownian particle trapped in an harmonic potential, the VSR offers an alternative procedure to estimate the friction coefficient γ and trap stiffness κ while for a DNA hairpin, briefly described in Section 8.3, we will propose a new method to extract the parameters of an effective non-Markovian memory kernel describing the zipping/unzipping equilibrium dynamics of these DNA hairpins. Finally, we will show how the non-Markovian VSR naturally leads to a reversed TUR for the thermodynamic work along with a lower bound to the Fano factor of the latter observable. We would also like to add that the results presented in this thesis regarding the VSR are not the whole story. Indeed, we are still working, at the time of writing this thesis, on further applications of our VSR which will be presented, along with the results shown here, in future papers written in collaboration with Marta Gironella, Marco Baiesi and Felix Ritort.

1.1 Outline of the thesis

This thesis is structured as follows. In 2 we briefly review basic concepts regarding the thermodynamics of mesoscopic systems along with the mathematical foundations of the most frequently employed models for the description of non-equilibrium phenomena and based on the theory of stochastic processes. We then focus in Chapter 3 on the specific non-Markovian stochastic process modelled by a linear generalised Langevin equation (GLE), which will be solved by means of our modified version of Laplace transforms. These results will be then used for the discussion of the non-Markovian TUR and VSR in Chapter 5 and 8, respectively. In Chapter 4 we will review some basic concepts of information geometry that prepares the discussion of stochastic uncertainty relations, which can be found in Chapter 5. In Chapter 6 we will solve some linear non-equilibrium models which will then be used in Chapter 7 to test the performances of the Markovian VSR. Finally, in Chapter 8, we will derive and discuss the non-Markovian VSR by highlighting its role in practical applications to experimental data.

CHAPTER 2

THERMODYNAMICS AND STOCHASTIC PROCESSES

2.1 Introduction: equilibrium statistical Physics

Since its early days, statistical physics has emerged as an extremely powerful and versatile theoretical framework for the description and characterisation of very complex and chaotic systems, where exact solutions of the underlying dynamical equations are unreachable. Arguably one of the most important and early accomplishments of statistical mechanics for equilibrium systems, was to find a connection between the macroscopic laws of thermodynamics, which fuelled the technological advancements that took place during the first industrial revolution, and the microscopic description of the individual atoms composing the system. Since then, what we now also call statistical thermodynamics has evolved into a comprehensive theoretical framework that describes classical thermodynamics as a set of emergent macroscopic phenomena arising from the microscopic properties of the individual components of the system.

The historical roots of this way of conceiving thermodynamics can be found in the second half of the nineteenth century when Ludwig Boltzmann, who can arguably be considered as the father of statistical mechanics, managed to find a statistical explanation to the second law of thermodynamics [38, 39]. His argument was based on an atomistic view of matter, which was not a well accepted idea at the time, and relied on the distinction between *macrostates*, i.e. states determined by macroscopic and experimentally accessible quantities, and *microstates*, i.e. those containing the whole information about the system and its single components. In formulae, Boltzmann described an isolated system, more precisely an ideal gas, at equilibrium and at a fixed energy E as being made of N particles, each characterised by its position $\boldsymbol{q}_i$ and momentum $\boldsymbol{p}_i$ leading to the microstate $\omega = \{\boldsymbol{x}_1, \boldsymbol{x}_2, \ldots, \boldsymbol{x}_N\}$, with $\boldsymbol{x}_i = \{\boldsymbol{q}_i, \boldsymbol{p}_i\}$. On the other hand, a macrostate M, or macroscopic configuration, describes the system in terms of a few macroscopic quantities such as number of particles N, total energy E and volume V, and depends at any moment on the microstate ω. The connection between microscopic and macroscopic properties can be found by considering some observable O, whose value in the microstate ω is $O(\omega)$, and the probability $p(\omega)$ that the system is in that microstate ω. Then, one can think of the measured value of O^{meas} in the macrostate as the average over the probability distribution $p(\omega)$ of the microstates, often referred to as *ensemble*, that is $O^{\text{meas}} = \langle O \rangle = \sum_\omega p(\omega) O(\omega)$. Of course, if N is very large, a single macrostate may correspond to many different microstates. This means that one can partition the set Ω of all possible microstates into subsets Ω_m of microstates that lead to the

same macrostate M. By postulating that, at equilibrium, every allowed microstate is equally probable, i.e. $p(\omega) = const$, one immediately sees that the probability p_m for a given microstate ω to be in Ω_m is equal to the ratio $|\Omega_m|/|\Omega|$, where $|\cdot|$ denotes the cardinality, or size, of the set. Under these hypothesis Boltzmann managed to show that, if the number N of particles composing the system is very large (such as for usual macroscopic systems where $N \propto 10^{23}$), then there is a $\Omega_{\widetilde{m}}$ whose size, or *volume*, is overwhelmingly larger then any other Ω_m, implying that $p_{\widetilde{m}} \approx 1$ and $p_{m \neq \widetilde{m}} \approx 0$. As a consequence, there is a certain macrostate $\widetilde{M}$ which is extremely more likely to be observed and hence the measured value of some observable O in the macroscopic state becomes

$$O^{\text{meas}} = \langle O \rangle = \sum_{\omega} p(\omega) O(\omega) = \sum_{m} p_m O_m \approx O_{\widetilde{m}} \,. \tag{2.1}$$

One can also show that the fluctuations around this average are of order N^{-1} justifying why, as a matter of fact, the outcome of a macroscopic experiment always gives the same result.

The link with thermodynamics can be made by means of Boltzmann's postulate of entropy, stating that the entropy S of an isolated system at equilibrium, with set of all possible macrostates given by $\mathcal{M} = \{M\}$, is proportional to the logarithm of the volume of microscopic configurations Ω compatible with $\mathcal{M}$, i.e.

$$S_{\text{eq}} = k_B \ln |\Omega| \approx k_B \ln |\Omega_{\widetilde{m}}| \equiv S_{\widetilde{M}} \tag{2.2}$$

where k_B is a constant bearing the name of Boltzmann itself and $S_{\widetilde{M}}$ is the entropy associated to the macrostate $\widetilde{M}$. This also explains why, classically, an isolated systems prepared in a certain macrostate M, corresponding to a set of microstates Ω_m and with entropy $S_M = \ln |\Omega_m|$, will evolve and explore all the available microstates with an equal a priori probability (Liouville's theorem) implying that, after some typical relaxation time, it will reach an equilibrium condition where, as a matter of fact, the system will spend most its time in the microstates corresponding to the most probable macrostate $\widetilde{M}$. As a consequence, the variation of entropy Σ, or *entropy production*, associated to this relaxation process, will be $\Sigma \equiv \Delta S = S_{\text{eq}} - S_M \approx S_{\widetilde{M}} - S_M \geq 0$ that is nothing else then the second law of thermodynamics, stating that an isolated system always evolves from a (macro)state with lower entropy to one of higher entropy. Indeed, from a statistical point of view, this just corresponds to the evolution of the system from a less probable state to a much more probable macrostates. The latter is exactly $\widetilde{M}$, the one that maximises the entropy and corresponding to thermodynamic equilibrium. One can also verify that equation (2.2) has all the proprieties expected from entropy like exstensivity, i.e. $S(N, E) \propto N$, and $\partial S(N, E)/\partial E = 1/T$, i.e. one recovers one of the Maxwell's relations in thermodynamics.

This is a groundbreaking result by Boltzmann. Even if its validity is limited to the framework of the kinetic theory of ideal gases, it embodies a very deep meaning. First of all, it implies the existence of atoms and molecules, something that was never really accepted until 1905 when Einstein proposed a method to measure the Boltzmann's constant using Brownian motion. Moreover, the laws of thermodynamics can be deduced by applying probability theory to the microscopic components of the system and their deterministic behaviour is just a consequence of

the law of large numbers. This in turn opens the door to the discussion of the laws of thermodynamics in a stochastic framework, concerning the regime of N not so large and where the usual thermodynamic laws are only valid on average.

For the sake of completeness, we also present the generalisation of Boltzmann's entropy formula (2.2), whose derivation is attributed to Willard Gibbs [40] and stating that the entropy of a system with a generic distribution of microstates , or ensemble, $p(\omega)$ is equal to

$$S = -k_B \sum_{\omega} p(\omega) \ln p(\omega) \,. \tag{2.3}$$

The relevant ensembles for the description of equilibrium systems, which can be regarded as a set of several copies ω of a system corresponding to all possible achievable microstates, each with a probability $p(\omega)$ of being realised, were first discussed by Gibbs and are as follows:

- for the scenario studied by Boltzmann, also known as *microcanonical ensemble*, one considers a system with a fixed number of particles N and a fixed energy E, corresponding to an isolated system, along with an equal a priori probability of being in a given microstate, i.e. $p(\omega) = 1/|\Omega| = const$. One immediately sees that, in this case, equation (2.3) trivially reduces to (2.2).

- If the system is closed, implying that no particle exchange is allowed while energy transfer with a heat bath at temperature T is, then one can show that the right choice for the distribution of the microstates is

$$p(\omega) = \frac{1}{\mathcal{Z}} \exp\left(-\frac{E(\omega)}{k_B T}\right) , \tag{2.4}$$

  where $E(\omega)$ is the energy associated to the microstate ω and $\mathcal{Z}$ is a normalisation factor also called *partition function*. This ensemble is also known as *canonical ensemble* and the corresponding distribution $p(\omega)$ is called the *canonical distribution*.

- Last but not least, the *grand canonical ensemble* deals with systems that can also exchange particles with a reservoir of heat and particles at a fixed temperature T and, moreover, at a fixed *chemical potential* μ. For the *grand canonical distribution* one finds that

$$p(\omega) = \frac{1}{\mathcal{Z}} \exp\left(-\frac{E(\omega) - \mu N(\omega)}{k_B T}\right) , \tag{2.5}$$

  where $E(\omega)$ and $N(\omega)$ are respectively the energy and the number of particles associated to ω.

The ensembles listed above form the building blocks of equilibrium statistical physics and, indeed, one can derive the laws of thermodynamics from the basic principles discussed in this introduction. For example, combining equation (2.4) and (2.3) one immediately sees that

$$S = \ln \mathcal{Z} + \frac{1}{T} \sum_{\omega} p(\omega) E(\omega) = \ln \mathcal{Z} + \frac{1}{T} \langle E \rangle \,. \tag{2.6}$$

By identifying the free energy $\mathcal{F}$ with $-k_B T \ln \mathcal{Z}$ and the average of the energy as the experimentally measured value in the sense shown in (2.1), one obtains the famous formula

$$\mathcal{F} = E^{\text{meas}} - TS \tag{2.7}$$

relating the energy available for thermodynamic work to the difference between the total amount of energy and the entropic forces, quantified by TS and whose effect is to lower the amount of "useful energy" of the system. With similar arguments, one can indeed derive a plethora of already known thermodynamic relation that are equivalent the the already known classical ones on average. Moreover, for macroscopic systems where the number of particles N involved is huge, these averages behave deterministically hence hiding the microscopic and probabilistic features on which the macroscopic averages rely on.

Even though the results presented above are in fact extraordinary, the idea of a world made of atoms found many difficulties in being accepted by the scientific community of the time also because, with what we have shown until now, no practical method to measure the Boltzmann's constant was provided. This can be instead achieved by studying another fundamental phenomenon in statistical physics, that is Brownian motion, first observed at the beginning of the eighteenth century by Robert Brown and modelled by Einstein in 1905. Einstein's model heavily relied on the atomistic hypothesis and by using it, he managed to connect a macroscopically observable quantity, i.e. the diffusion constant (estimated by measuring the variance of the displacement of a Brownian particle), to the microscopic Boltzmann's constant. A more detailed discussion of Brownian motion in the framework of Langevin dynamics and its implications is postponed to next sections, where a brief review on the thermodynamics of mesoscopic systems is also presented.

2.2 Non-equilibrium statistical physics

In the context of equilibrium systems, the main purpose of statistical physics is the deduction of thermodynamic proprieties of a system starting from its microscopic description. Nevertheless, during the last decades, statistical physics has become more and more an interdisciplinary area of research with applications ranging from pure physics to computer sciences, from chemistry to biology and from economics to logistics where, most of the times, interesting phenomena take place in a non-equilibrium regime. The latter is radically different from equilibrium situations mostly because of the breaking of time–reversal invariance, quantified by entropy production and determining the irreversible nature of non-equilibrium processes. For example, the relaxation process described in the previous section, where an isolated system evolves from a less probable macrostate to the most probable one such as the case depicted in Figure 2.1, exhibits a positive entropy production $\Sigma = S_{\widetilde{M}} - S_M \geq 0$ implying that it is an irreversible and spontaneous process. We further point out that, for macroscopic systems, irreversibility arises from the deterministic and reversible microscopic equations of motion as a statistical phenomenon explained by Boltzmann's argument. In addition to relaxation towards equilibrium, an important class of non-equilibrium systems are those that are driven out of equilibrium from an external or internal force, coming from example form a temperature gradient, a chemical potential or an external mechanical force. These could

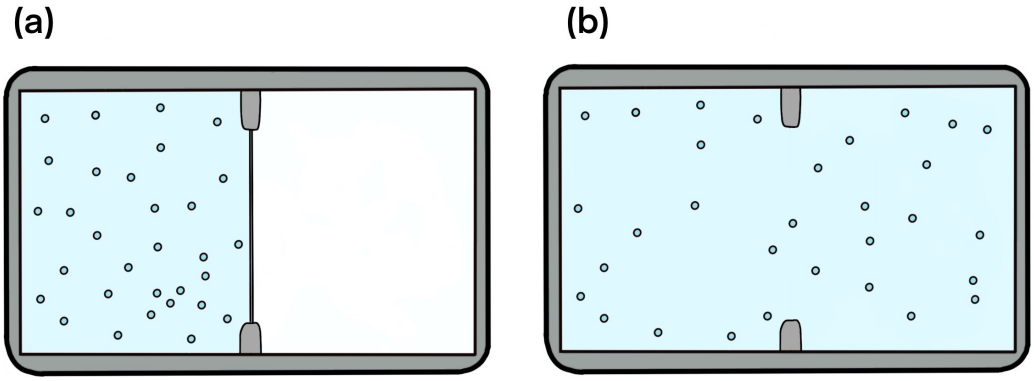

Figure 2.1: Free diffusing gas of N particles diffusing in an isolated environment. In (a), the gas is confined in the left region of the container with a gate separating it from the right one. As regards to (b) instead, the gate is opened and the gas can freely diffuse in both chambers. The evolution starts from a macrostate M_{in} coinciding with the microstate where all gas particles are in the left chamber. Using the binomial distribution with parameter $p = 1/2$ (chambers with equal volume), one sees that this microstate has a probability of occurring equal to $p(n_l = N, n_r = 0) = 2^{-N}\binom{N}{0} = 2^{-N}$, where n_l and n_r are the number of particles in the left and right chambers respectively. As regards to the final macrostate M_{fin} at equilibrium, a certain number $n < N$ of particles will be in the left part of the container while $N - n$ particle will be on the right. The probability of such a configuration is again obtained from the binomial distribution, i.e. $p^{\text{eq}}(n) \equiv p(n_l = n, n_r = N - n) = 2^{-N}\binom{N}{N-n}$ with moments equal to $\langle n\rangle^{eq} = N/2$ and $\langle \Delta n^2\rangle^{eq} = N/4$. If $N \gg 0$, this distribution becomes a Gaussian whose width is quantified by the ratio $\sigma = \langle \Delta n^2\rangle^{\text{eq}}/(\langle n\rangle^{\text{eq}})^2 \approx N^{-1}$. Hence, for $N \approx 10^{23}$ $p(n)$ is a very peaked distribution around its mean value implying that states corresponding to microstates having n extremely close to the mean value $\langle n\rangle^{\text{eq}} = N/2$ are the only ones to be observed. This example illustrates the statistical nature of irreversibility and explains why one will never see a spontaneous return to the initial state, i.e. the one having less entropy.

be the cases for example of two heat baths with different temperatures exchanging heat, an internal combustion engine or the mechanical compression of a gas exerted through a piston, respectively. It can be verified that for all these processes the total entropy production of system and environment is again strictly greater than zero.

As one could easily guess, non-equilibrium is much more complicated then equilibrium also because the statistical ensembles listed in the previous section can not be used anymore and, moreover, few universal results exist for non-equilibrium dynamics, at least until the present day. Indeed, it is often impossible to identify the density of microstates needed, for example, to calculate the entropy (2.3) which in turn makes it very difficult to derive a macroscopic description of the system from its microscopic structure. Moreover, even if an effective macroscopic description, given by a set of differential equations, is available, the solution of these equation is most of the time unreachable. Suffice it to say that finding a general solution to the Navier-Stokes equations, governing the dynamics of Newtonian fluids and which can be obtained from a coarse-graining procedure carried out on the microscopic

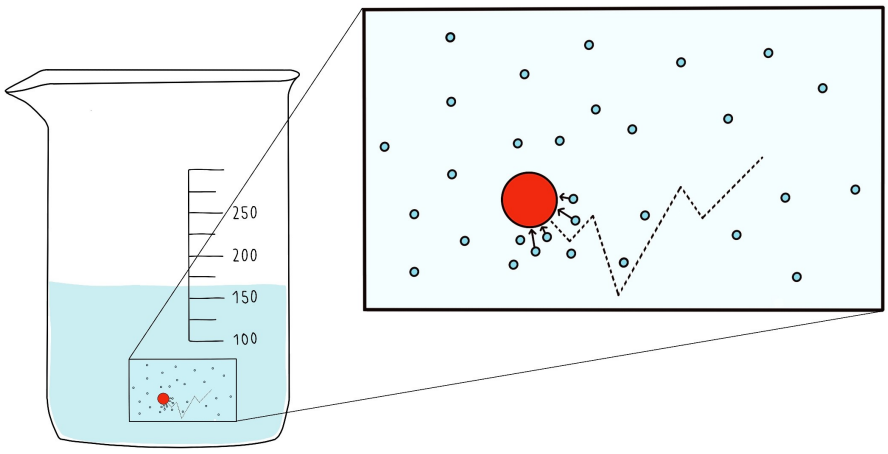

Figure 2.2: Graphical visualisation of a mesoscopic particle undergoing Brownian motion due to the temporary imbalances of forces caused by the components of the surrounding fluid.

components of the fluid, would win you one million dollars. More generally and as a matter of fact, what one usually does is to analyse case by case the system one is interested in by using ad hoc methods and few general principles.

The discussion on macroscopic non-equilibrium systems could of course continue for a plethora of more pages, but this is not the scope of this thesis. Instead, what we are more focused on is a mesoscopic level of description, where some coarse graining procedure has been carried out but until a certain level where statistical fluctuations are still relevant, in contrast to what happens on a macroscopic scale where fluctuations are negligible. Arguably one of the most important examples of this kind of systems is the one of a mesoscopic particle bathed in a fluid at thermal equilibrium at time T. This phenomenon is also called *Brownian motion* in honour of botanist Robert Brown who first described it in 1827 while studying pollen grains. Because the particle is mesoscopic, meaning that its mass is much larger then the mass of the particles composing the fluid but small enough that temporary imbalances of the forces due to the hits from the surrounding fluid's molecules are possible, one can integrate out the degrees of freedom relative to the particles of the fluid in order to obtain an effective equation of motion, based on Newton's second law and equal to

$$m\ddot{x}(t) = -\gamma\dot{x}(t) + F(x_t, t) + \gamma\sqrt{2D}\,\xi(t)\,. \tag{2.8}$$

Here, $x(t)$ and m are the position and mass of the mesoscopic particle, γ is its friction coefficient arising from the Stokes approximation which, in the small velocity regime, is the only source of dissipation in the system and $F(x_t, t)$ are some other non dissipative forces acting on the particle. Moreover, $\xi(t)$ is some Gaussian white noise such that $\langle\xi(t)\rangle = 0$ and $\langle\xi(t')\xi(t'')\rangle = \delta(t' - t'')$. The diffusion constant D instead, determines the strength of the random force and, as it will be shown in few lines, it is related to the Boltzmann's constant. This equation is named after Paul Langevin, which first proposed it to describe Brownian motion [41], originally not including the $F(x_t, t)$ term. Because of the stochasticity intrinsic to (2.8), if one

prepares say N different particles in the same initial position x_0, they will all diffuse and evolve in different ways performing a random erratic motion. Nevertheless, one can study the probability density function (PDF) $p(x_t, t)$ of the particle's position at time t which, for $F(x_t, t) = 0$, is a Gaussian. In this case, as we will discuss more in detail in the next chapter, the first moment of the distribution becomes $\langle x_t \rangle = \int \mathrm{d}x_t \, x_t \, p(x_t, t) = x_0$ while for its second moment, corresponding to the mean squared displacement of $N \to \infty$ different Brownian particles at time t starting at the same initial condition x_0 at time $t = 0$, one finds that

$$\lim_{t\to\infty} \langle \Delta x_t^2 \rangle = \lim_{t\to\infty} \int \mathrm{d}x_t \, (x_t - \langle x_t \rangle)^2 \, p(x_t, t) = 2Dt \,. \tag{2.9}$$

This result was first obtained by Einstein in 1905 without relying on the Langevin equation but rather by finding a connection between the density of Brownian particles $p(x_t, t)$ and the diffusion equation

$$\partial_t p(x_t, t) = D \partial_x^2 p(x_t, t) \,, \tag{2.10}$$

whose solution is a Gaussian distribution with second moment given by $\langle \Delta x_t^2 \rangle = 2Dt$ and where D is the same diffusion constant as before. Note that, in this context, the relation between the mean squared displacement and the diffusion constant holds at all times, this is due to the fact in its original work Einstein neglected inertial effects, corresponding to $m \ll \gamma$ in (2.8). The crucial feature of this result is that, by observing the diffusion of a sample of Brownian particles, one can experimentally measure the diffusion constant. Moreover, by considering a suspension of particles in a viscous fluid and in a gravitational field (see Figure 2.3), Einstein also managed to show that the diffusion constant is equal to

$$D = \frac{k_B T}{\gamma} \,. \tag{2.11}$$

This in turn has huge implications. Indeed, apart from the Boltzmann's constant, every quantity in (2.11) is experimentally accessible hence offering, for the first time in history, an experimental setup to estimate the Boltzmann's constant and, as a consequence, the Avogadro number N_A, i.e. the number of particles corresponding to a mole of a certain substance. This can be indeed considered the very first proof of the existence of atoms and molecules and it is needless to underline how much this is important.

Fuelled by these astonishing results, the study of mesoscopic systems has quickly developed into a rich and rapidly growing field of physics aimed to the description, for example, of the functioning of microscopic biological systems or the dynamics of chemical reactions when small quantities of reagents are involved [42]. Within this framework, one usually relies on the theory of stochastic processes of which the Langevin dynamics governed by (2.8) is just a particular example. A stochastic process is nothing else then a collection of random variables $X = \{X_i\}_{i=1,\dots,N}$ linked by some temporal causal relation, as it can be the sequence of the positions of a colloidal particle undergoing Brownian motion. Indeed, the latter is the prototype of a process taking values in a continuous set (R in this case) and with a continuous time parameter. After equation (2.8) was first proposed, researchers have been able to generalise it to what is now commonly referred to as the Langevin equation(s). Especially recently, where very precise experiments on colloidal particles

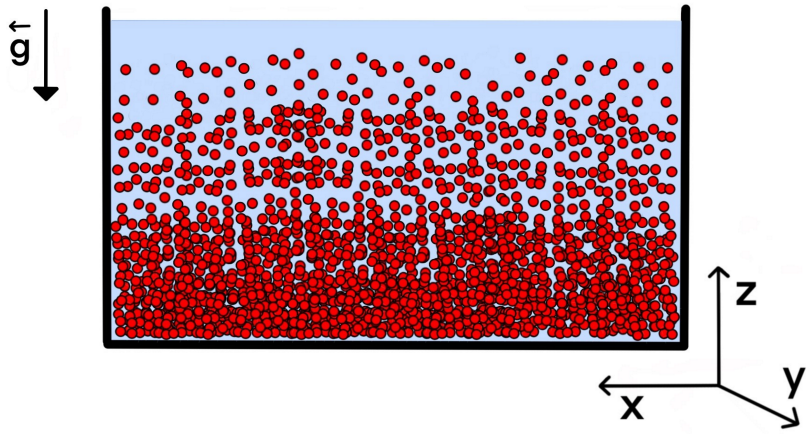

Figure 2.3: A collection of Brownian particles immersed in a fluid and in a gravitational field. The density density of particles $\rho(z)$ is the standard barometric distribution $\rho(z) = \rho_0 \exp\left[-\frac{mgz}{k_B T}\right]$, with m the mass of the colloidal particles, g the gravitational acceleration and z the height.
In a condition of dynamical equilibrium, the currents due to concentration gradients are quantified by Fick's law, i.e. $J^{\text{diff}} = -D\,\partial_z \rho(z) = \frac{mgD}{k_B T}\rho(z)$, and compete with the currents generated by the gravitational forces which are $J^{\text{grav}} = -\frac{mg}{\gamma}\rho(z)$, where γ is the friction coefficient of the particles, estimated through Stoke's approximation. If dynamical equilibrium holds, then $J^{\text{diff}} + J^{\text{grav}} = 0$, implying that $D = k_B T/\gamma$.

are possible thanks to *optical tweezers*, the Langevin equation has proven itself as an extremely powerful and versatile tool to model these experiments. Indeed, we will make large use of these equations in Chapter 7 with an eye to experimental applications. Another class of important stochastic processes are those still depending on a continuous time parameter but taking values in a discrete and numerable set. These states could stand, to give some examples, for the position of a reaction coordinate in a chemical network, for the chemo-mechanical state of a molecule or for the occupation number of some discrete energy levels, and so on. These kind of processes are often referred to as *continuous time Markov chains* or *jump processes* and they will be discussed in more detail in the next sections along with the above mentioned generalisation of equation (2.8).

The two classes of models cited above fall into the category of *Markovian*, or memoryless, processes meaning that every update of the process only depends on the previous step and not on the whole history of the system. Markovian processes are indeed a very powerful tool for the modelling of physical systems and, moreover, there are many mathematical theorems available which in turn help out in carrying out the calculations. Nevertheless, the Markovianity hypothesis is not always applicable on a certain mesoscopic scale of description, as for example in the case of a Brownian particle immersed in a solution of water and macro-molecules. Indeed, because the latter have a much larger mass then that of the water molecules, a net separation between the typical time scales of the Brownian particle and that of the components of the solution is no longer possible. This would imply that the noise appearing in the Langevin equation (2.8) can not be considered white, i.e. delta correlated, anymore and Markovianity is lost as a consequence. The study

of non-Markovian systems is hence of fundamental importance but much less is known about them from a mathematical point of view. In this thesis, we scratch the surface of the topic relative to non-Markovian dynamics by considering the generalised Langevin equation (GLE) (as the name suggests, it is the non-Markovian generalisation of the Langevin equation) with coloured noise, which will be widely used throughout the next sections and chapters.

2.3 Stochastic processes

Stochastic processes have been widely used in the last decades to model systems on a mesoscopic scale such as biological systems, molecular motors or chemical reaction networks. This has also been enormously fuelled by the technological advances carried out in this century, through which one is now able to manipulate and resolve the evolution and configurations of microscopic systems in unprecedented ways and precision. Because the systems listed above of course operate on a non equilibrium regime, they are characterised by some kind of dissipation or entropy production. For this reason, a lot of effort has been done in order to build a theory of stochastic thermodynamics in such a way that classical thermodynamics is obtained after the thermodynamic limit (in some sense that must be specified) is taken. Indeed, for some paradigmatic cases such as the motion of a colloidal particle modelled by (2.8) and for some sub-classes of jump processes, one is able to obtain the stochastic analogous of the usual laws of thermodynamics. In this context, thermodynamic quantities become stochastic, i.e. their value depends on the particular realisation of the dynamics of the system. This in turn implies that, for example, for one particular trajectory a Brownian particle in a non-conservative field, one could observe a negative variation of total entropy, which seems to be in contrast the second law of thermodynamics. Nevertheless, the latter can be recovered after performing an averaging procedure over all possible realisation of the dynamics, hence leading to $\langle \Sigma \rangle \geq 0$. Because of what has been shown in (2.1), in the thermodynamic limit the probability distribution of the macrostates become so sharp that, as a matter of fact, the averages start behaving deterministically.

As for macroscopic systems, the distance from equilibrium of a given stochastic process is quantified by the breaking of time-reversal invariance which can be linked, in some cases, to entropy production [25, 26, 27, 28]. As a consequence, it is clear how thermodynamic quantities play a prominent role in the characterisation of non-equilibrium processes. However, a recently emerged body of work puts a strong accent on the role played in non-equilibrium by time symmetric quantities [29, 30, 31, 32, 33, 34, 35], also referred to as *frenetic quantities*. The latter encode the information about the kinetic features of the dynamic and are complementary to thermodynamic aspects in which, by definition, thermodynamics is usually interested. For example, in Chapter 5 we will show how the maximum precision, in a sense that will be specified later, associated to a given process is both determined by thermodynamic and kinetic aspects. This behaviour will be quantified by the *thermodynamic uncertainty relation* and the *kinetic uncertainty relation* (one of the main original results of this thesis), the first one being more relevant close to equilibrium while the second one being often more important far from equilibrium. Moreover, the fact that kinetic aspects become relevant for the latter case

is not new, as it can be deduced the rich literature regarding far from equilibrium response theory [43, 44, 45, 46, 47, 48, 49, 50, 51, 33, 34]. Indeed, in this context the authors show how entropy production and time-invariance symmetry breaking are the only quantities determining the response of a system close to equilibrium but again, time-symmetric quantities start to arise while moving further and further into non-equilibrium. A more detailed and comprehensive treatment of frenetic aspects of stochastic processes can be found for example in [52, 53].

To conclude, in the next sections we will discuss some fundamental models used in non-equilibrium statistical physics by putting an accent on thermodynamic and kinetic aspects of the dynamics. These concepts will then be employed in Chapter 3, 5, 6, 7 and 8, where the original work of the author of this thesis is presented.

2.3.1 Jump processes

A jump process X_t, or continuous time Markov chain, is an ordered collection of random variables $X_t = \{X_{t_n}\}_{0\leq t_n\leq t}$ characterised by a continuous time parameter t and a numerable state space $\mathcal{S}$ such that $X_{t_n} \in \mathcal{S}$ for every index n. In other words, a jump process is a stochastic process that performs N_J random transitions among discrete states at exponentially distributed times and one of its possible realisation is depicted in Figure 2.4. The fact of the jump times being exponentially distributed is necessary and sufficient condition for the process to be Markovian and this can be put in formulae in the following way

$$P\left(X_{t+dt} = i | X_t = k\right) = W_{ik}(t)\, dt \quad \text{for} \quad i \neq k \tag{2.12}$$

$$P\left(X_{t_0+t} = k | X_{t_0} = k\right) = \exp\left[\int_{t_0}^{t_0+t} \mathrm{d}t'\, W_{kk}(t')\right], \tag{2.13}$$

where dt is an arbitrary infinitesimal time such that the probability of two jumps occurring in this time interval in negligible and $W_{ik}(t)$ is the *transition rate matrix* which determines the dynamics of the system. The latter is such that each one of its non diagonal elements is larger or equal then zero while its diagonal elements, denoted by $-\lambda_k(t)$, are negative. Moreover, for each column of the matrix, the sum of all its elements is equal to 0 so that

$$\sum_i W_{ik}(t) = 0 \qquad \lambda_k(t) = -W_{kk}(t) = \sum_{i\neq k} W_{ik}(t)\,, \tag{2.14}$$

meaning that $\lambda_k(t)$ is equal to the sum of the positive transition rates in its column. This propriety is crucial for the conservation of probability which in turn can be obtained from the master equation

$$\partial_t p_i(t) = \sum_k J_{ik}(t) \qquad J_{ik}(t) = W_{ik}(t)\, p_k(t) - W_{ki}(t)\, p_i(t)\,, \tag{2.15}$$

where $p_i(t)$ is the probability of the of state i of being occupied at time t. Clearly, it also holds that $\sum_i p_i(t) = 1$. Moreover, the probability currents $J_{ik}(t)$ can be regarded as expected directed current from state k to state i. These currents are such that they are anti-symmetric with respect to the flipping of the state indexes, i.e.

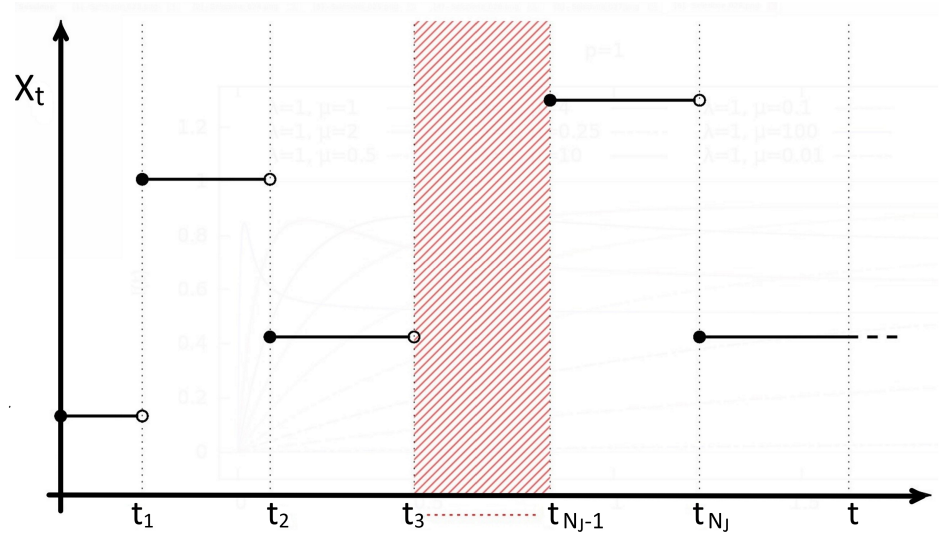

Figure 2.4: Example of a particular realisation of the jump process X_t up to time t and jumping times $\{t_1, t_2, \ldots, T_{N_J}\}$

$J_{ik}(t) = -J_{ki}(t)$, which is feature of time anti-symmetric quantities, as it will be clear at the end of this section. In addition, these flows are also deeply related to entropy production as it can indeed be seen by studying the equilibrium and stationary solution associated to (2.15), corresponding to time independent probabilities $p_i \implies \partial_t p_i = \sum_k J_{ik}(t) = 0$. This can happen in two ways:

- each of the probability currents $J_{ik} = 0$ at all times, which is only possible for time independent transition rates. This condition is referred to as equilibrium and corresponds to the absence of net flows among each bond between state i and k.

- The sum $\sum_k J_{ik}(t)$ being equal to zero along with at least two non zero currents, compensating each other. This would correspond to a non-equilibrium steady state where net currents are present along with, because it is not equilibrium, some form of entropy production. The latter statement is also true for arbitrary non-equilibrium states.

This implies that entropy production is equal to zero, i.e. the system is in an equilibrium state, if and only if all the currents J_{ik}^{eq} are zero at all times. This will be also made clear by equation (2.24).

Before going on, we recall the fundamental propriety of Markov processes which can be expressed in terms of conditional probabilities. To do so, we define a path probability density function associated to the probability of observing a particular realisation of the process $X_t = \{X_{t_n}\}_{0 \leq n \leq N = t/dt}$ as

$$P(\omega_t) = P(X_{t_N} = i_N, X_{t_{N-1}} = i_{N-1}, \ldots, X_0 = i_0)\,, \tag{2.16}$$

where i_n is the state at time t_n and dt can be interpreted, in a physical flavour, as some small characteristic time on which an underlying microscopic process, determining the behaviour of the system on a mesoscopic scale, is taking place. On the other hand and from a mathematical point of view, the right hand side of (2.16) is

the joint PDF of N dependent random variables. This in turn implies that (2.16) can be rewritten in terms of conditional probabilities, i.e.

$$P(\omega_t) = P(X_{t_N} = i_N, \dots, X_{t_{M+1}} = i_{M+1} | X_{t_M} = i_M, \dots, X_0 = i_0) \cdot \\ \cdot P(X_{t_M} = i_M, \dots, X_0 = i_0) \tag{2.17}$$

for any $0 \leq M < N$. For a Markov processes, for which the dynamics starting from from some initial state i_n only depends on the initial state itself (memoryless propriety), equation (2.17) becomes

$$P(\omega_t) = P(X_{t_N} = i_N, \dots, X_{t_{M+1}} = i_{M+1} | X_{t_M} = i_M) P(X_{t_M} = i_M, \dots, X_0 = i_0) \,, \tag{2.18}$$

that is the well known Markov propriety. By iterating this procedure for all values $0 \leq n < N$, and by defining

$$p_{ik}(t, t_0) \equiv P(X_t = i | X_{t_0} = k) \,, \tag{2.19}$$

also called transition probabilities, one can readily obtain from (2.16)

$$P(\omega_t) = p_{i_0}(t_0) \prod_{n=0}^{n=N-1} p_{i_{n+1} i_n}(t_n + dt, t_n) \,. \tag{2.20}$$

We mention that the transition probabilities are also governed by the master equation (2.15), i.e.

$$\partial_t p_{i\, i_0}(t, t_0) = \sum_k \left(W_{ik}(t)\, p_{k\, i_0}(t, t_0) - W_{ki}(t)\, p_{i\, i_0}(t, t_0) \right) , \tag{2.21}$$

and that they are time independent at equilibrium or in a steady state. For the special case of continuous time Markov chain, whose transition probabilities are (2.12) and (2.13), one can also easily see that equation (2.20) becomes

$$P(\omega_t) = p_{i_0}(t_0) \exp\Big(- \int_0^t \mathrm{d}t'\, \lambda_{i_{t'}}(t') \Big) \prod_{n=0}^{N_J - 1} W_{i_{n+1}\, i_n}(t_n)\, \mathrm{d}t \,, \tag{2.22}$$

where N_J is the number of jumps performed up to time t. This result will be useful later on in Chapter 5.

With everything that was shown above, one is able to evaluate the average entropy production associated to an arbitrary dynamics. To do so, one uses a generalisation of (2.3) given by the Shannon's entropy which, for a stochastic process, is equal to

$$\langle \Sigma_{\mathrm{tot}} \rangle_t = - \int \mathrm{d}\omega_t\, P(\omega_t) \ln P(\omega_t) \,, \tag{2.23}$$

where the role of the subscript "tot" will be clarified later on and $\mathrm{d}\omega_t$ stands for an infinitesimal "path volume". More in general, this is valid for every probability distribution. Indeed, except for Boltzmann's constant, one sees that (2.3) can be obtained from (2.23) in the case of statistical ensembles. Finally, by combining (2.22),

(2.21) for a steady state and (2.23), one is able to get a standard result for the average entropy production associated to the steady state dynamics of a jump process, i.e.

$$\begin{aligned}\langle \Sigma_{\rm tot}\rangle_t^{\rm st} &= \int_0^t {\rm d}t' \sum_{ik} W_{ik}(t')\; p_{k,\,\rm st} \ln\left(\frac{W_{ik}(t')\,p_{k,\,\rm st}}{W_{ki}(t')\,p_{i,\,\rm st}}\right) = \\ &= \frac{1}{2}\int_0^t {\rm d}t' \sum_{ik} J_{ik,\,\rm st}(t') \ln\left(\frac{W_{ik}(t')\,p_{k,\,\rm st}}{W_{ki}(t')\,p_{i,\,\rm st}}\right) \geq 0\,,\end{aligned} \tag{2.24}$$

which is only defined under the assumption of microscopic reversibility, namely, if $W_{ik}(t) \neq 0$ for some (i,k), then also $W_{ki}(t) \neq 0$. This is also a necessary condition to compare a trajectory with its time reversal in order to obtain the famous fluctuation theorem [54, 55]

$$\langle \Sigma_{\rm tot}\rangle^{st} = \int {\rm d}\omega\; P(\omega_t) \ln\left(\frac{P(\omega_t)}{P^\dagger(\omega_t)}\right), \tag{2.25}$$

where $P(\omega_t)$ is given by (2.22) and $P^\dagger(\omega_t) = P(\theta\omega_t)$, with $\theta\omega_t$ standing for the time reversed trajectory and with inverted velocities.

It is clear that, for the special case of equilibrium dynamics where all the net currents J_{ik} are equal to zero, the average entropy production becomes zero itself, as expected. To make the role of these net flows even clearer, we define the number of jumps $n_{ik}(\omega_t)$ that the system performs between state k and i during the evolution of the path ω_t in the time interval $[0,t]$. We also present its infinitesimal form ${\rm d}n_{ik}(\omega_t)$, corresponding to the number of jumps the the systems makes during the interval $[t, t+dt]$, and whose average equals

$$\langle {\rm d}n_{ik}\rangle_t = W_{ik}(t)\,p_k(t)\,{\rm d}t\,. \tag{2.26}$$

By using this, one can introduce the class of integrated currents defined as

$$R(\omega_t, t) = \int_0^t \sum_{ik} \left({\rm d}n_{ik}(\omega_{t'}) - {\rm d}n_{ki}(\omega_{t'})\right) g_{ik}(t')\,, \tag{2.27}$$

where $g_{ik}(t)$ is some state bond dependent function and whose average can be readily computed as

$$\langle R\rangle_t = \int_0^t {\rm d}t' \sum_{ik} \left(W_{ik}(t')\,p_k(t') - W_{ki}(t')\,p_i(t')\right) g_{ik}(t') = \int_0^t {\rm d}t' \sum_{ik} J_{ik}(t')\,g_{ik}(t')\,. \tag{2.28}$$

The latter vanishes of course at equilibrium, where all probability currents are equal to zero. These observables are often referred to as irreversible or dissipative integrated currents, because they do not average to zero only in presence of dissipation. Moreover, entropy production is itself an irreversible current, as it can be seen from (2.24), and also the directed flow from state m to state n can be obtained from (2.27) by choosing $g_{ik}(t) = \delta_{ni}\delta_{mk}$. In addition, many quantities of experimental interest fall in this class of observables while modelling a mesoscopic system using stochastic jump processes. Some examples could be the amount of some product of interest created by some chemical reaction network or the displacement of a molecular motor on a microtubule. For all these reasons, one is interested in the characterisation

of these observables in order to study, for example, the efficiency and precision of some biological process. The latter is a very active line of research and many ways of defining the efficiency and precision of a process exist. Without going to much into detail, in Chapter 5 we will consider the *signal to noise ratio* (SNR)

$$\mathcal{g}_t^R \equiv \frac{\langle R \rangle_t^2}{\langle \Delta R^2 \rangle_t} \tag{2.29}$$

as the quantity encoding the precision associated to the observable $R(\omega_t, t)$. Here, $\langle \Delta R^2 \rangle_t = \langle R^2 \rangle_t - \langle R \rangle_t^2$ is the variance of the observable. We will show how, in a steady state, this precision is bounded from above by the entropy production (*thermodynamic uncertainty relation*), which is trivially true at equilibrium where both quantities are equal to zero. As a consequence, it will be clear how, in the vicinity of equilibrium, entropy production plays a prominent role in determining the magnitude and precision of irreversible current. This also resembles what happens in the case of response theory where the response of a system near equilibrium is solely determined by entropy production. But this is not the whole story. Indeed, as briefly discussed in the previous section, time-symmetric quantities must be taken into account to properly characterise non-equilibrium regimes. We will add further empirical evidences to this argument by showing how, far from equilibrium and for some relevant examples, the SNR (2.29) is more tightly bounded by the average of the time symmetric quantity

$$\mathcal{K}(\omega_t) = \sum_{k,\, i \neq k} n_{ik}(t) = \frac{1}{2} \int_0^t \left(\sum_{k,\, i \neq k} \mathrm{d}n_{ik}(\omega_{t'}) + \sum_{k,\, i \neq k} \mathrm{d}n_{ki}(\omega_{t'}) \right), \tag{2.30}$$

counting the jumps of the system. Hence,

$$\langle \mathcal{K} \rangle_t = \sum_{k,\, i \neq k} \langle n_{ik} \rangle_t = \frac{1}{2} \sum_{k,\, i \neq k} \tau_{ik}(t)\,, \tag{2.31}$$

is the total average number of jumps that the system performs up to time t. In the literature, this quantity is often referred to as *mean dynamical activity*. We also point out that, as it will explained later in Chapter 5, this quantity provides an upper bound to the SNR only for jump processes defined by time independent transition rates W_{ik}. Furthermore, we introduced the *traffic* $\tau_{ik}(t)$ defined as

$$\tau_{ik}(t) = W_{ik}(t)\, p_k(t) + W_{ki}(t)\, p_i(t) \tag{2.32}$$

and quantifying the "activity" of the bond (i, k). By comparing equation (2.30) and (2.31)with (2.27) and (2.28), one notes that the symmetric traffic $\tau_{ik}(t)$ plays the same role in the averaging of $\mathcal{K}(\omega_t)$ as the probability current $J_{ik}(t)$ does for the irreversible integrated current $R(\omega_t, t)$. Indeed, the dynamical activity $\mathcal{K}$ is an example of reversible integrated quantity (with $g_{ij}(t) = 1/2$) which, perhaps surprisingly, often gives the tightest bound to the precision of irreversible currents in a regime far from equilibrium. To conclude this short preview of what we called the *kinetic uncertainty relation* (KUR), whose derivation ad discussion is postponed to Section 5.3, we also point out that, differently from the *thermodynamic uncertainty relation* (TUR) for jump processes, the KUR is also valid for arbitrary non equilibrium states and all kind of observables, not only dissipative currents.

Until now, the results presented in this section were given without any thermodynamic interpretation. This can be done by using a standard parametrisation [3, 52] for the transition rates, valid in the case of microscopic reversibility (i.e. $W_{ik}(t) \neq 0 \implies W_{ik}(t) \neq 0$ for each (i,k)) and given by

$$W_{ik}(t) = \sqrt{W_{ik}(t)W_{ki}(t)}\sqrt{\frac{W_{ik}(t)}{W_{ki}(t)}} \equiv a_{ik}(t)\, e^{s_{ik}(t)/2}\,, \tag{2.33}$$

$$a_{ik}(t) \equiv \sqrt{W_{ik}(t)W_{ki}(t)} = a_{ki}(t) \qquad s_{ik}(t) \equiv \ln\left(\frac{W_{ik}(t)}{W_{ki}(t)}\right) = -s_{ki}(t)\,. \tag{2.34}$$

In analogy to the arguments presented in the previous pages, we identify the symmetric part $a_{ik}(t)$ of the rates with those determining kinetic aspects of the dynamics and the anti-symmetric ones $s_{ik}(t)$ with those governing the behaviour of thermodynamic quantities. Indeed, as it has been known for a while in the literature [56, 57, 58, 59], by imagining the system to be in contact with an environment consisting of many equilibrium baths (of heat, particles, ecc..) one can interpret the $s_{ik}(t)$ with the local variation of entropy (per k_B) of the environment during the transition $k \to i$. If the bath is a heat reservoir, then this entropy change is due to the heat injected into the environment during the latter transition. Moreover, for time independent transition rates and by using the parametrisation (2.33) in equation (2.24) (and taking the average away) one easily sees that

$$\begin{aligned}\Sigma^{\text{st}}_{\text{tot}}(\omega_t) =& \frac{1}{2}\int_0^t \sum_{ik} \left(\mathrm{d}n_{ik}(\omega_{t'}) - \mathrm{d}n_{ki}(\omega_{t'})\right) \ln\left(\frac{W_{ik}\, p_{k,\text{st}}}{W_{ki}\, p_{i,\text{st}}}\right) = \\ =& \sum_{ik} n_{ik}(\omega_t)\left(s_{ik} - \Delta_{ik}\ln p\right)\,,\end{aligned} \tag{2.35}$$

where between the first and second line we used the anti-symmetry of the indexes of the logarithmic term appearing in the first line and, moreover, we also defined $\Delta_{ik}\ln p = \ln p_{i,\text{st}} - \ln p_{k,\text{st}}$. By noting that the sum over all states of the number of jumps can be seen as the sum over all jumping times N_J, one can further manipulate equation (2.35) to get

$$\begin{aligned}\Sigma^{\text{st}}_{\text{tot}}(\omega_t) =& \sum_{n=0}^{N_J-1}\left(s_{i_{n+1}\,i_n} + \Delta_{i_{n+1}\,i_n}\ln p\right) = \sum_{n=0}^{N_J-1} s_{i_{n+1}\,i_n} - \Delta_{i_{N_J},i_0}\ln p = \\ =& \Sigma^{\text{st}}_{\text{env}}(\omega_t) + \Sigma^{\text{st}}_{\text{sys}}(\omega_t)\,.\end{aligned} \tag{2.36}$$

One can hence identify two contributions to the entropy production, which justifies a posteriori its "tot" subscript. The first one, i.e. $\Sigma^{\text{st}}_{\text{env}}(\omega_t)$, comes from the sum over all jump times of all local entropy variations of the environment s_{ik}. If the environment consists in a unique thermal bath at temperature T, then one finds that $\Sigma^{\text{st}}_{\text{env}}(\omega_t) = \Delta Q/k_B T$, where ΔQ is the heat injected into the environment during the non-equilibrium process. The second contribution to the total entropy production, instead, stems from the system's internal entropy variation $\Sigma^{\text{st}}_{\text{sys}}(\omega_t) = -\Delta_{i_{N_J},i_0}\ln p$, i.e. the difference in Shannon entropy between the final and initial state. This term has of course zero average in a steady state, hence implying that

$$\langle \Sigma_{\text{tot}}\rangle^{\text{st}}_t = \langle \Sigma_{\text{env}}\rangle^{\text{st}}_t\,. \tag{2.37}$$

The anti-symmetric parameters s_{ik} are hence the only ones involved in determining the amount of entropy production and, moreover, one can prove that the equilibrium state distribution $p_{i,\mathrm{eq}}$ also depends uniquely on these parameters. This is of course not true outside equilibrium, where kinetic coefficients a_{ik} highly influence the dynamics of the system. Again, for a more detailed and comprehensive treatment of how this happens we refer to [52].

We conclude this section on Markov jump processes by briefly anticipating some of the topics of Chapter 5, where one of the main focuses will be the calculation of the *Fisher information*

$$\mathcal{I}(\alpha) = \int \mathrm{d}\omega \; p^{\alpha}(\omega) \left(\partial_{\alpha} \ln p^{\alpha}(\omega)\right)^2 , \tag{2.38}$$

where $p^{\alpha}(\omega)$ is some probability density function obtained from $p(\omega)$ by modifying the original dynamics via an α-dependent perturbation, where α is some parameter such that for $\alpha = 0$ one recovers the original dynamics. For each different perturbation, one gets a different result for the Fisher information. We will hence apply (2.38) to (2.22) by first perturbing the dynamics through a modification of the transition rates $W_{ik}(t) \to W^{\alpha}_{ik}(t)$. Indeed, in section 5.2.2 we will see how, for a particular modification influencing only the $s_{ik}(t)$ parameters in the rates, one gets that the Fisher information leads to the total entropy production and, as a consequence, to the thermodynamic uncertainty relation. Instead, for an alternative modification presented in section 5.3, this time influencing the symmetric parameters $a_{ik}(t)$, the Fisher information happens to be proportional to the average dynamical activity (2.31) hence leading to the kinetic uncertainty relation.

2.3.2 Langevin dynamics

In the previous section we discussed the case of Markov jump processes with continuous time and discrete states. This class of stochastic systems is particularly useful to model coarse-grained dynamics, taking place on some mesoscopic scale, where the set of states of interest can be efficiently approximated to be discrete. Of course, there are many cases where this is not the best path to follow, as it is the case of Brownian motion discussed in (2.2). In this context, we presented an effective stochastic differential equation (2.8) which, in the limit of large friction $m/\gamma \ll 1$, can be recast into

$$\dot{x}(t) = \mu F(x_t, t) + \sqrt{2D}\, \xi(t) , \tag{2.39}$$

where $\mu = \gamma^{-1}$ is the *mobility*, $D = \mu k_B T$ and $\xi(t)$, as usual, stands for a Gaussian white noise of average zero and normalised variance. This limit is also referred to as the *overdamped limit* and, for a constant force $F(x_t, t) = F$, it is known that the probability distribution for the position of the particle, starting at position x_0 at time $t = 0$, is equal to

$$p(x_t, t) = \frac{1}{\sqrt{4\pi D t}} \exp\left[-\frac{(x_t - x_0 - v_{\mathrm{d}} t)^2}{4Dt} \right] , \tag{2.40}$$

where we introduced the *drift velocity* $v_{\mathrm{d}} = \mu F$. This corresponds to the solution of the diffusion equation

$$\partial_t p(x_t, t) = -v_{\mathrm{d}}\, \partial_x p(x_t, t) + D \partial_x^2 p(x_t, t) \tag{2.41}$$

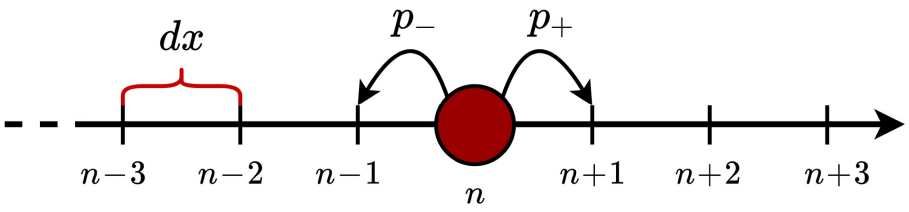

Figure 2.5: Biased random walk on a lattice with sites labelled by the index n. The spacing dx and microscopic time dt are taken such that the experimental resolution Δt is much larger then dt, i.e. $N = \Delta t/dt \gg 0$.

for the initial condition $p(x_t, t = 0) = \delta(x_t - x_0)$ and clearly coinciding with (2.10) for $v_d = 0$, hence recovering standard non-driven Brownian motion. These results, first proposed at the beginning of the XX century, were however more based on phenomenological arguments rather then on more rigorous justifications. Indeed, a more "microscopic" (not in the strict sense) approach can be used by means of discrete time Markov processes. The latter are similar to the processes presented in the previous section but of course, there are some differences. Without going too much into detail and by knowing that, from a microscopical and classical point of view, the system made of the Brownian particle and water molecules is discrete, one could imagine that the particle "lives" on a one dimensional lattice, depicted in Figure 2.5, with the probabilities of jumping to the right or the left being equal to p_+ and p_- (whit these probabilities finding a physical meaning only a posteriori). The next step consists in choosing the lattice spacing to be some microscopical characteristic length dx and in imagining the process as updating itself every time after a time interval dt has passed, the latter also being some microscopic characteristic time. Under these hypothesis and by defining the "continuous variables" $x = n\,dx$ and $t = N_J\,dt$, where n is the lattice index and N_J is the number of times the process has updated itself, one can use the discrete time master equation to show that the probability distribution $p(x_t, t)$ satisfies a partial differential equation equal to (2.41) in the limit of $dx, dt \to 0$. This also leads to the identification of $D = dx^2/2dt$ and $v = (p_+ - p_-)dx/dt$, meaning that the limits above must be taken carefully. This link between discrete and continuous dynamics can be further generalised by means of the so called Kramers–Moyal expansion of the Master equation [60, 61], which is applied to arbitrary transition probabilities on a d dimensional lattice. This procedure, which is treated in detail for example in [62, 63], leads to the famous Fokker-Plank equation which reads

$$\partial_t p(\boldsymbol{x}_t, t) = -\sum_{i=1}^{d} \partial_{x_t^i} \left(A_i(\boldsymbol{x}_t, t) p(\boldsymbol{x}_t, t)\right) + \sum_{ik=1}^{d} \partial_{x_t^i} \partial_{x_t^k} \left(D_{ik}(\boldsymbol{x}_t, t) p(\boldsymbol{x}_t, t)\right) , \tag{2.42}$$

where x_t^i and $A_i(\boldsymbol{x}_t, t)$, the *drift vector*, are d dimensional vectors while $D_{ik}(\boldsymbol{x}_t, t)$ is the state and time dependent $d \times d$ dimensional *diffusion matrix*. Moreover, it is clear that (2.41) is just a special case of the Fokker-Plank equation in one dimension with $A_i(\boldsymbol{x}_t, t) = v_d$ and $D_{ik}(\boldsymbol{x}_t, t) = D$. It can be shown that the solution $p(\boldsymbol{x}_t, t)$ of equation (2.42) is the same as the PDF associated to the stochastic differential equation

$$\dot{\boldsymbol{x}}(t) = \boldsymbol{A}(\boldsymbol{x}_t, t) + \sqrt{2\boldsymbol{D}(\boldsymbol{x}_t, t)} \cdot \boldsymbol{\xi}(t) , \tag{2.43}$$

which is the d dimensional generalisation of (2.39) and where we used vector notation instead of index notation. We mention that this equation can model a large number of systems, not only the motion of a Brownian particle in some force field, although we will always have in mind the latter case throughout this thesis. Moreover, from now on we will refer to (2.43) as the Langevin equation (LE) and all the variables denoted by x_t will be considered to be even, i.e. symmetric with respect to time reversal. This hypothesis will make many of the calculation presented later on in this section more simple and streamlined. Instead, a paradigmatic example of dynamics entailing odd variables will be discussed in detailed in the next chapter, where the complete Langevin equation, involving the mass of the Brownian particle, will be considered.

The last term in (2.43) is defined via the Ito product meaning that

$$\sqrt{2\boldsymbol{D}(\boldsymbol{x}_t,t)}\cdot\boldsymbol{\xi}(t)\,\mathrm{d}t=\sqrt{2\boldsymbol{D}(\boldsymbol{x}_t,t)}\cdot\mathrm{d}\boldsymbol{B}_t\,, \tag{2.44}$$

where $\mathrm{d}\boldsymbol{B}_t=\boldsymbol{B}_{t+dt}-\boldsymbol{B}_t\sim\mathcal{N}(0,\mathbb{1}_{d\times d}\,dt)$ is the multidimensional *Wiener process*. We point out that (2.44), also known as Ito prescription and leading to Ito stochastic calculus (where the chain rule does not hold anymore), corresponds to a particular interpretation of the underlying discrete dynamics, with characteristic time dt, from which the continuous stochastic PDE (2.43) are derived once the limit $dt\to 0$ is taken. Indeed, as it is known from the literature, the LE is not mathematically well defined in the strict sense and hence, one should always have in mind that the real dynamical equations are the discrete ones. We further add that the Ito prescription is particularly popular in applied mathematics and economics because of its averaging propriety, i.e. $\langle g(\boldsymbol{x}_t,t)\cdot\mathrm{d}\boldsymbol{B}_t\rangle=0$ for $g(\boldsymbol{x}_t,t)$ a *non anticipating function* (to know more about this topic we refer again to [63]). Instead, physicist usually prefer another prescription defined via the Stratonovich product which, for a generic matrix function $\boldsymbol{g}(\boldsymbol{x}_t,t)$, would lead to

$$\boldsymbol{g}(\boldsymbol{x}_t,t)\circ\boldsymbol{\xi}(t)\,\mathrm{d}t=\frac{\boldsymbol{g}(\boldsymbol{x}_{t+dt},t+dt)+\boldsymbol{g}(\boldsymbol{x}_t,t)}{2}\mathrm{d}\boldsymbol{B}_t\,. \tag{2.45}$$

For obvious reasons, this is also called mid-point prescription, leading to the Stratonovich stochastic calculus where the ordinary chain rule still holds. The reason why physicist often prefer the Stratonovich prescription, in addition to the propriety of preserving the chain rule, descends from the interpretation of the white noise as the limit of some coloured noise with characteristic time much smaller then the typical time on which the mesoscopic dynamics is taking place. Indeed, because the memory effects embodied by the coloured noise are symmetric in time, the Stratonovich interpretation (2.45) often becomes the most reasonable and physically funded choice.

The profound differences between the two prescriptions depicted above and their use are the subject of a wide and complex sub-field of stochastic calculus and their rigorous treatment is beyond the scope of this thesis (one can find more for example in [63]). Instead, we limit ourselves to showing the Langevin equation (2.43) using the Stratonovich prescription, that is

$$\dot{x}^i(t)=A^i(\boldsymbol{x}_t,t)-\sum_{kj=1}^{d}\sqrt{D_{kj}(\boldsymbol{x}_t,t)}\,\partial_{x_t^k}\sqrt{D_{ik}(\boldsymbol{x}_t,t)}+\sum_{k=1}^{d}\sqrt{2D_{ik}(\boldsymbol{x}_t,t)}\circ\xi^k(t) \tag{2.46}$$

and leading to the same Fokker-Plank equation depicted in (2.42). Note that for state independent diffusion matrix $\boldsymbol{D}(t)$ the two equations (2.43) and (2.46) coincide.

Lets reconsider for a moment the Fokker-Plank (FP) equation (2.42) using vector notation. One can see that it can be rewritten as

$$\partial_t p(\boldsymbol{x}_t, t) = -\nabla \cdot \boldsymbol{J}(\boldsymbol{x}_t, t) = -\nabla \cdot (\boldsymbol{\nu}(\boldsymbol{x}_t, t) p(\boldsymbol{x}_t, t)) \,, \tag{2.47}$$

with

$$\boldsymbol{\nu}(\boldsymbol{x}_t, t) = \boldsymbol{A}(\boldsymbol{x}_t, t) - \left(\nabla^{\mathrm{T}} \boldsymbol{D}(\boldsymbol{x}_t, t)\right)^{\mathrm{T}} - \boldsymbol{D}(\boldsymbol{x}_t, t) \, \nabla \, \ln\left(p(\boldsymbol{x}_t, t)\right) \,, \tag{2.48}$$

meaning that the FP equation can be recast into a continuity equation, implying the conservation of probability. Moreover, for future convenience we defined the *mean local velocity* $\boldsymbol{\nu}(\boldsymbol{x}_t, t)$ while the the probability current $\boldsymbol{J}(\boldsymbol{x}_t, t)$ appearing in the continuity equation (2.47) plays the same role as the currents $J_{ik}(t)$ did in the master equation (2.15). Indeed, the case of a time independent position PDF $p(\boldsymbol{x}_t) \implies \partial_t p(\boldsymbol{x}_t) = 0$ corresponds to two different cases:

- $\boldsymbol{J}(\boldsymbol{x}_t, t) = \boldsymbol{\nu}(\boldsymbol{x}_t, t) = 0$, meaning that the system is at equilibrium and implying that, as it will be clear from (2.52), there is no net entropy production during the evolution of the system.
- $\nabla \cdot \boldsymbol{J}(\boldsymbol{x}_t, t) = 0$, i.e. the probability current has zero divergence, meaning that the system is in a steady state. As always, because it is non-equilibrium, there is some form of entropy production involved in the dynamics of the system.

In analogy with what has been done in the previous section, one can define the *transition probability* $p(\boldsymbol{x}_t, t|\boldsymbol{x}_0, t_0)$, standing for the probability of observing the colloidal particle at the position $\boldsymbol{x}_t$ at time t given that it was at $\boldsymbol{x}_0$ at time $t = 0$ and governed by the same FP equation as (2.42), i.e.

$$\begin{aligned} \partial_t p(\boldsymbol{x}_t, t|\boldsymbol{x}_0, 0) = &- \sum_{i=1}^{d} \partial_{x_t^i} \left(A_i(\boldsymbol{x}_t, t) p(\boldsymbol{x}_t, t|\boldsymbol{x}_0, 0)\right) + \\ &+ \sum_{ik=1}^{d} \partial_{x_t^i} \partial_{x_t^k} \left(D_{ik}(\boldsymbol{x}_t, t) p(\boldsymbol{x}_t, t|\boldsymbol{x}_0, 0)\right) \,. \end{aligned} \tag{2.49}$$

The transition probabilities also obey the so called Einstein-Smoluchowski-Chapman –Kolmogorov (ESCK) relation

$$p(\boldsymbol{x}_t, t|\boldsymbol{x}_0, 0) = \int \mathrm{d}\boldsymbol{x}_{t'} \, p(\boldsymbol{x}_t, t|\boldsymbol{x}'_t, t') \, p(\boldsymbol{x}'_t, t'|\boldsymbol{x}_0, 0) \,, \tag{2.50}$$

a result that embodies the Markovian nature of the Langevin systems we are considering. By means of this, one can express the path probability $P(\omega_t)$ associated to the trajectory $\omega_t = \{x_{n\,dt}\}_{0 \leq n \leq t/dt}$, where dt is some characteristic microscopic time at which the process is taking place, that is

$$P(\omega_t) = p(\boldsymbol{x}_0, 0) \prod_{n=0}^{n=t/dt-1} p(\boldsymbol{x}_{(n+1)\,dt}, (n+1)\,dt|\boldsymbol{x}_{n\,dt}, n\,dt) \,. \tag{2.51}$$

Again, this can be used along with (2.23) to calculate the total average entropy associated to a given Langevin process [42, 64], that is

$$\langle \Sigma_{\text{tot}} \rangle_t = -\int \mathrm{d}\omega_t \, P(\omega_t) \ln P(\omega_t) = \int_0^t \mathrm{d}t' \left\langle \boldsymbol{\nu} \, \boldsymbol{D}^{-1} \boldsymbol{\nu} \right\rangle_{t'} . \tag{2.52}$$

From this one immediately sees that, for $\boldsymbol{J}(\boldsymbol{x}_t, t) = 0$ implying $\boldsymbol{\nu}(\boldsymbol{x}_t, t) = 0$, the total average entropy production vanishes, as expected for an equilibrium state. We also add that, in general, one can again decompose the total entropy production into a component accounting for the entropy injected into the environment and a second piece corresponding to the variation in entropy of the system, that is

$$\Sigma_{\text{tot}}(\omega_t) = \Sigma_{\text{env}}(\omega_t) + \Sigma_{\text{sys}}(\omega_t) \tag{2.53}$$

with

$$\Sigma_{\text{sys}}(\omega_t) = -\ln p(\boldsymbol{x}_t, t) + \ln p(\boldsymbol{x}_0, 0) \tag{2.54}$$

the difference of Shannon entropy between the initial and the final state and $p(\boldsymbol{x}_t, t)$ the solution of equation (2.47). Clearly, for a steady state or equilibrium, equation (2.54) averages to 0. Moreover, for the simple case of a Brownian particle in contact with a heat bath with temperature T, described by the multidimensional generalisation of (2.39), the entropy produced in the environment can be identified with the heat injected into the thermal bath, i.e.

$$\Sigma_{\text{env}}(\omega_t) = \frac{\Delta Q}{k_B T} = \beta \int_0^t \mathrm{d}t' \, \boldsymbol{F}^{\mathrm{T}}(\boldsymbol{x}_{t'}, t') \circ \dot{\boldsymbol{x}}(t') \, , \tag{2.55}$$

where $\beta = 1/k_B T$ and $\circ$ stands for the Stratonovich product (2.45). The latter is an example of the continuum analogous of (2.27), namely it is an irreversible integrated current which in general can be defined as

$$R(\omega_t, t) = \int_0^t \mathrm{d}t' \, \boldsymbol{g}(\boldsymbol{x}_{t'}, t') \circ \dot{\boldsymbol{x}}(t') \tag{2.56}$$

for some state and time dependent matrix $\boldsymbol{g}(\boldsymbol{x}_t, t)$ (of which the vector $\boldsymbol{F}(\boldsymbol{x}_t, t)$ is just an example). It can be also shown that (see [42] for example) these observables average to

$$\langle R \rangle_t = \int_0^t \mathrm{d}t' \left\langle \boldsymbol{g} \cdot \boldsymbol{\nu} \right\rangle_{t'} , \tag{2.57}$$

meaning that, indeed, these can be again identified with dissipative currents because at equilibrium, where no probability flow is present, their average becomes zero. Moreover, by choosing $\boldsymbol{g}(\boldsymbol{x}_t, t) = \boldsymbol{\nu}(\boldsymbol{x}_t, t)\boldsymbol{D}^{-1}(\boldsymbol{x}_t, t)$, one easily recovers (2.52) from (2.57), meaning that entropy production itself can be regarded as a dissipative integrated current. Because of this, and also because many other important and experimentally accessible quantities of interest fall into this class of observables, it is interesting to study the general behaviour of these currents. Indeed, in Chapter 5 we will study the precision associated to these observables, which again is upper bounded by entropy production. Sadly, a continuum generalisation of the kinetic uncertainty relation is still lacking and, as a consequence, the performances of the entropic bound can not be compared with any sort of kinetic bound.

2.3.2.1 Thermodynamics of a one dimensional Brownian particle in homogeneous media

As anticipated in equation (2.8), the unidimensional motion of a colloidal particle in an homogeneous fluid can be described by means of

$$m\ddot{x}(t) = -\gamma\dot{x}(t) + F(x_t, t) + \gamma\sqrt{2D}\,\xi(t)\,, \tag{2.58}$$

often referred to as the *underdamped* Langevin equation and where, as usual, $D = k_B T/\gamma$. With this paradigmatic example one can efficiently introduce and explore some of the main features and concepts of stochastic thermodynamics, but before doing so we express equation (2.58) in terms of a set of coupled stochastic equations

$$\begin{aligned} \dot{x}(t) &= v(t) \\ \dot{v}(t) &= -\frac{\gamma}{m}v(t) + \frac{1}{m}F(x_t, t) + \frac{\gamma}{m}\sqrt{2D}\,\xi(t)\,, \end{aligned} \tag{2.59}$$

where $v(t)$ is the velocity of the particle. Equation (2.59) can be regarded as a special case of (2.43) when the degrees of freedom $\boldsymbol{x}(t)$ are allowed to be odd variables too, such as the case of the velocity variables. Indeed, by setting

$$\boldsymbol{A}(x_t, v_t, t) = \begin{pmatrix} v(t) \\ -\frac{\gamma}{m}v(t) + \frac{1}{m}F(x_t, t) \end{pmatrix} \qquad \boldsymbol{D}(x_t, v_t, t) = \begin{pmatrix} 0 & 0 \\ 0 & \frac{\gamma^2 D}{m^2} \end{pmatrix} \tag{2.60}$$

one readily obtains (2.59) from (2.43). As a consequence, one can see that the transition probabilities $p(x_t, v_t, t|x_{t_0}, v_{t_0}, t_0)$ obey the FP equation, in this case also known as Kramer's equation, given by

$$\begin{aligned} \partial_t p(x_t, v_t, t|x_{t_0}, v_{t_0}, t_0) = &- \partial_{x_t}\left(v_t\, p(x_t, v_t, t|x_{t_0}, v_{t_0}, t_0)\right) + \\ &+ \frac{1}{m}\partial_{v_t}\left[\left(\gamma v_t - F(x_t, t)\right) p(x_t, v_t, t|x_{t_0}, v_{t_0}, t_0)\right] + \\ &+ \frac{\gamma^2 D}{m^2}\partial_{v_t}^2\, p(x_t, v_t, t|x_{t_0}, v_{t_0}, t_0) \end{aligned} \tag{2.61}$$

with initial condition given by $p(x_t, v_t, t_0|x_{t_0}, v_{t_0}, t_0) = \delta(x_t - x_{t_0})\delta(v_t - v_{t_0})$. The joint PDF for position and velocity (x_t, v_t) at time t can be readily obtained from the transition probability by integrating over the distribution of the initial conditions (x_{t_0}, v_{t_0}), i.e.

$$p(x_t, v_t, t) = \int \mathrm{d}x_{t_0}\mathrm{d}v_{t_0}\, p(x_t, v_t, t|x_{t_0}, v_{t_0}, t_0)p(x_{t_0}, v_{t_0}, t_0)\,. \tag{2.62}$$

To study the equilibrium and non-equilibrium dynamics of this system, we use the standard procedure of dividing the total force applied on the Brownian particle into a component arising from some externally controlled potential $U(x_t, \lambda_t)$, with λ_t being the time dependent control parameter, and a part corresponding to some non conservative force $f(x_t)$, i.e.

$$F(x_t, t) = -\partial_{x_t} U(x_t, \lambda_t) + f(x_t)\,. \tag{2.63}$$

By means of this, one can prove that for a confining potential $U(x_t, \lambda_t)$, for time independent control parameter $\lambda_t = \lambda$ and in the absence on non-conservative forces $f(x_t) = 0$, one recovers the standard Boltzmann distribution

$$p(x_t, v_t) = \exp\left[-\frac{m v_t^2}{2k_B T} - \frac{U(x_t, \lambda)}{k_B T}\right] / \mathcal{Z} \tag{2.64}$$

where one also uses that $D = k_B T/\gamma$ and where

$$\mathcal{Z} = \int \mathrm{d}x_t \mathrm{d}v_t \exp\left[-\frac{m v_t^2}{2k_B T} - \frac{U(x_t, \lambda)}{k_B T}\right] \tag{2.65}$$

is the *partition function* by means of which one can define the *free energy* $\mathcal{F} = -k_B T \ln \mathcal{Z}$.

Instead, if the external control parameter depends explicitly on time or a non-conservative force is acting on the colloidal particle (or both), then the system will be in a non-equilibrium state. As usual, this implies that there is some form of non zero entropy production which can be divided into an environmental contribution Σ_{env} and into a component accounting for the variation of the Shannon entropy of the system Σ_{sys}. As regards the first one, because the environment serves as a thermal bath of temperature T and by following Sekimoto's interpretation of stochastic energetics [65], one can see that the environmental contribution can be considered as the heat injected into the system, i.e. the amount of work done by the particle on the bath, that is

$$\Sigma_{\text{env}}(\omega_t) = \beta \Delta Q(\omega_t) = \beta \int_0^t \mathrm{d}t' \, F_{bath}(x_{t'}, t') \circ \dot{x}(t') \,, \tag{2.66}$$

where

$$F_{bath}(x_t, t) = \gamma\left(v_t - \sqrt{2D}\xi(t)\right) = F(x_t, t) - m\dot{v}(t) \tag{2.67}$$

can be obtained from the underdamped equation (2.59). Moreover, by combining equation (2.66) and (2.67) one obtains

$$\Delta Q(\omega_t) = \int_0^t \mathrm{d}t' \, F(x_{t'}, t') \circ \dot{x}(t') - \frac{m}{2}\left(v^2(t) - v^2(0)\right) \,, \tag{2.68}$$

where in order to obtain the last term on the right hand side one uses that, for the proprieties of Stratonovich stochastic calculus, it holds that $\circ\dot{x}(t')\mathrm{d}t' = \mathrm{d}x_{t'}$ hence leading to the usual rules of calculus. Note that (2.68) coincides with (2.55) in the overdamped limit. By further noting that the system's entropy production equals

$$\Sigma_{\text{sys}} = -\ln p(x_t, v_t, t) + \ln p(x_t, v_t, t_0) \,, \tag{2.69}$$

one finally gets an expression for the total entropy production

$$\begin{aligned}\Sigma_{\text{tot}} = \Sigma_{\text{env}} + \Sigma_{\text{sys}} = \int_0^t \mathrm{d}t' \, F(x_{t'}, t') \circ \dot{x}(t') - \frac{m}{2}\left(v^2(t) - v^2(0)\right) + \\ - \ln\left(\frac{p(x_t, v_t, t)}{p(x_{t_0}, v_{t_0}, t_0)}\right) \,,\end{aligned} \tag{2.70}$$

which can be shown averages to zero at equilibrium. By using this same procedure, in the next chapter we will show how this result is also valid for the non-Markovian

Langevin equation. In this context, we will also be interested in characterising the thermodynamic work $W(\omega_t)$ done on the particle, which can be found by means of the stochastic first law of thermodynamics. Indeed, by defining the change in internal energy of the system as the sum of the variations of potential and kinetic energy

$$\Delta E(\omega_t) = U(x_t, \lambda_t) - U(x_0, \lambda_0) + \frac{m}{2}\left(v^2(t) - v^2(0)\right) , \tag{2.71}$$

one can use the first law to get the thermodynamic work

$$W(\omega_t) = \Delta Q(\omega_t) + \Delta E(\omega_t) = \int_0^t \mathrm{d}\lambda_{t'}\, \partial_{\lambda_{t'}} U(x'_t, \lambda_{t'}) + \int_0^t \mathrm{d}t' f(x_{t'}, t') \circ \dot{x}(t') , \tag{2.72}$$

where we used (2.68) along with (2.71) and that

$$\begin{aligned} U(x_t, \lambda_t) - U(x_0, \lambda_0) &= \int_0^t \mathrm{d}U(x'_t, \lambda_{t'}) = \\ &= \int_0^t \mathrm{d}x_{t'}\, \partial_{x_{t'}} U(x'_t, \lambda_{t'}) + \int_0^t \mathrm{d}\lambda_{t'}\, \partial_{\lambda_{t'}} U(x'_t, \lambda_{t'}) \end{aligned} \tag{2.73}$$

along with $\circ\dot{x}(t')\mathrm{d}t' = \mathrm{d}x_{t'}$. We will show how all these these arguments are still applicable for the generalised Langevin equation (GLE), i.e. the non-Markovian version of (2.58) which reads

$$m\ddot{x}(t) = -\int_{t_m}^t \mathrm{d}t' \Gamma(t - t')\dot{x}(t') - \partial_{x_t} U(x_t, t) + f(x_t) + \eta(t) , \tag{2.74}$$

where $\Gamma(t)$ is some *memory kernel* that, as it can be deduced from its name, is accountable for the memory effects. As for the random force $\eta(t)$, it is a Gaussian distributed coloured noise such that $\langle \eta(t) \rangle = 0$ and $\langle \eta(t')\eta(t'') \rangle = k_B T \Gamma(|t' - t''|)$, the latter propriety being called the second fluctuation-dissipation theorem [37]. Note that, for $\Gamma(|t' - t''|) = 2\gamma\,\delta(t' - t'')$ one recovers (2.59) from (2.74). We will explicitly solve the GLE for the simple case of a parabolic potential of the form $U(x_t, \lambda_t) = \kappa(x_t - \lambda_t)^2/2$ by introducing a generalisation of the Laplace transform which becomes particularly useful to evaluate the large time limit of the dynamics of the system. By means of this we will also be able to explicitly evaluate many of the thermodynamic quantities presented in this section along with their averages and variances. These will be in turn used to discuss the performances of the non-Markovian uncertainty relation, presented in 5.5, and to test the validity of the non-Markovian variance sum rule (VSR) in Chapter 8.

Chapter 3

Generalised Langevin equation and Laplace transforms

3.1 Introduction

In this rather technical section, we discuss the method based on Laplace transforms to solve linear stochastic differential equations, which is particularly useful when memory effects, determined by the convolution of some memory kernel with the dynamical variables, are included. In particular, we will dedicate many pages to the solution of the generalised Langevin equation (2.74) for a moving parabolic potential. Because generating an initial condition for a Langevin equation with memory is a non-trivial issue, we introduce a generalisation of the Laplace transform as a useful tool for solving this problem, in which a limit procedure $t_m \to \infty$ may send the extension of memory effects to arbitrary times in the past. This method also allows us to compute average position, work, their variances and the entropy production rate of a particle dragged in a complex fluid by an harmonic potential, which could represent the effect of moving optical tweezers. For initial conditions in equilibrium we generalise the results by van Zon and Cohen [66], finding the variance of the work for generic protocols of the trap. In addition, we study a particle dragged for a long time captured in an optical trap with constant velocity in a steady state. Our formulas open the door to thermodynamic uncertainty relations in systems with memory, presented in Section (5.5).

3.2 Generalised Langevin equation

The driven diffusion process of a colloidal particle or bead immersed in a fluid has become a paradigm of non-equilibrium physics [28, 66, 67, 68, 65, 42, 69]. Fluctuations play a prominent role for this mesoscopic system due to the multitude of random hits on the particle by the molecules of the surrounding fluid. If these molecules are tinier and faster than the colloidal particle, a net separation of timescales between fast and slow degrees of freedom occurs and the colloidal particle undergoes Markovian dynamics. In this case, the motion of the particle can be equivalently described by using the Langevin equation (2.58), path integrals and the Fokker-Plank equation (2.61), see [62] for a (very) detailed treatment of this topic. Instead, if the particle is immersed in a solution containing for example long and complex polymers [70, 71], the above-mentioned separation of time scales is no longer possible and memory effects occur. In order to describe such kind of non-Markovian systems, one may then consider a generalised Langevin equation

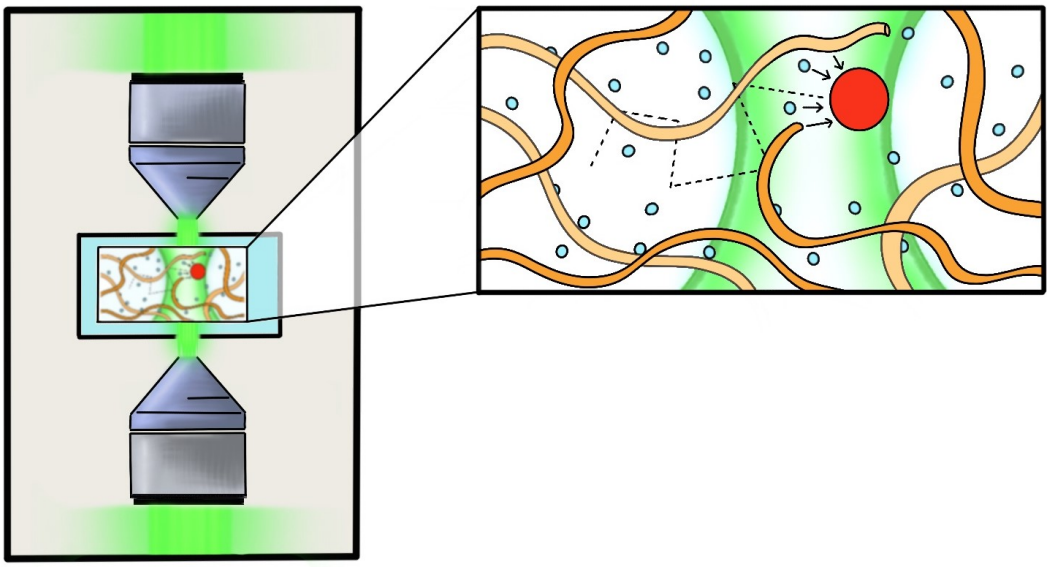

Figure 3.1: Brownian particle in a bath of polymers and trapped by optical tweezers.

(GLE) with constant diffusion coefficient, whose formal derivation can be found in [72, 73, 74]. For $t \geq 0$ this equation reads

$$m\ddot{x}(t) = -\int_{t_m}^{t} \mathrm{d}t' \, \Gamma(t-t')\dot{x}(t') - \partial_{x_t} U(x_t, t) + f(x_t) + \eta(t)\,, \tag{3.1}$$

where $\Gamma(t)$ is the memory kernel, $t_m \leq 0$ is the time to which the memory effects extend and $\eta(t)$ is a coloured Gaussian noise obeying $\langle \eta(t) \rangle = 0$. The GLE could also describe the motion of a particle under the effect of hydrodynamic backflow [75]. The fluctuation-dissipation relation [37] is still valid in the more general form $\langle \eta(t')\eta(t'') \rangle = k_B T \Gamma(|t' - t''|)$: thermodynamic equilibrium is present in the medium if its two effects (dissipation and noise) are proportional at all times. Note that a Markovian memory kernel $\Gamma^{\mathrm{Mark}}(t) = 2\gamma_0 \delta(t)$ would lead to the usual fluctuation-dissipation theorem while the consistency, instead, of equation (3.1) with the Markovian Langevin equation, is guaranteed by the Stratonovich convention for the integrals of delta functions, i.e. $\int_{t_m}^{t} \mathrm{d}t' \, f(t')\delta(t'-t) = f(t)/2$ (see [63] for a formal justification of this result). Indeed, because in this section we will deal with coloured noise and memory effects, the Markovian memory kernel must be regarded as the limit of some non-Markovian memory kernel whose characteristic time tends to zero, that is for example

$$\Gamma^{\mathrm{Mark}}(|t|) = \lim_{\tau \to 0} \frac{\gamma_0}{\tau} \mathrm{e}^{-|t|/\tau} = 2\gamma_0 \delta(t)\,. \tag{3.2}$$

As discussed in the previous section after equation (2.45), this interpretation of the white noise implies the Stratonovich prescription for the GLE. Moreover, the 2 factor on the right hand side of equation (3.2) is necessary as it can be readily seen from

$$\int_{-\infty}^{\infty} \mathrm{d}t' \, \Gamma^{\mathrm{Mark}}(|t'|) = \lim_{\tau \to 0} \int_{-\infty}^{\infty} \mathrm{d}t' \, \frac{\gamma_0}{\tau} \mathrm{e}^{-|t'|/\tau} = 2\gamma_0 \implies \int_{0}^{\infty} \mathrm{d}t' \, \Gamma^{\mathrm{Mark}}(t') = \gamma_0\,, \tag{3.3}$$

i.e. everything is consistent if a two factor is included in front of the Dirac delta in the Markovian memory kernel and if the integral of the delta centred on one of the integration boundaries gives an extra $1/2$ factor. We also add that, the generalisation of the FP equation to non-Markovian context is still an open problem and hence, determining the PDF associated to the GLE must be worked out case by case and by using ad hoc approaches.

The aim of this chapter is to solve the GLE with a parabolic confinement potential $U(x_t, t) = \frac{\kappa}{2}(x_t - \lambda_t)^2$ and without non-conservatives forces, obtained for instance by using optical tweezers centred on a moving coordinate λ_t,

$$m\ddot{x}(t) = -\int_{t_m}^{t} \mathrm{d}t'\, \Gamma(t-t')\dot{x}(t') - \kappa[x(t) - \lambda(t)] + \eta(t)\,. \tag{3.4}$$

The non-dynamical case was already discussed for example in [76]. Moreover, we will restrict ourselves to the case of a non-divergent time dependent effective friction coefficient $\widehat{\gamma}(t)$, i.e. such that $\widehat{\gamma} = \lim_{t\to\infty} \widehat{\gamma}(t) = \lim_{t\to\infty} \int_0^t \mathrm{d}t'\, \Gamma(t') < \infty$, which is a sensible physical requirement [77, 78].

One of the first analytical solutions for the GLE with $\kappa = 0$ and no external force can be found in [79]. It is obtained through the use of Laplace transforms and it is expressed in terms of the velocity susceptibility $\chi_v(t)$, a key quantity discussed in the next sections. In the paper [80], on which this chapter is based on, we obtain a more general solution in terms of the susceptibility and its integrals. This enables us to calculate averages and variances of relevant quantities such as position, thermodynamic work and entropy production, with a dynamics starting from different initial conditions. Some of these results are already known in the literature, especially for equilibrium initial conditions, see for example [81]. However, imposing a non-equilibrium steady state as initial condition is not trivial for the GLE, due to its memory. A scheme for achieving an initial condition with memory requires extending it far into the past. To this end, we introduce a modified version of Laplace transforms with arbitrary initial time t_m, which is then shifted back to minus infinity by taking an appropriate limit. The explicit dependence of the solution on t_m along with the well-defined limits of susceptibilities will make the procedure straightforward.

The following section introduces the technical details of the modified Laplace transform. In Sec. 3.4 we discuss the solution of the GLE and in Sec. 3.5 we show how to use the solution for computing relevant thermodynamic quantities. We show that the entropy production rate can be expressed in terms of a retarded velocity, which is equal to the usual velocity of the particle in the Markovian case, see (3.54). In section 3.6 we briefly discuss the overdamped case, corresponding to $m = 0$. Moreover, in Sec. 3.7, we apply the obtained results to the dynamics starting from equilibrium and to the case where initial conditions are taken in the infinite past, i.e. $t_m \to -\infty$, which can be seen as a generalised stationary state, in the sense that memory of initial conditions is lost. For the latter case we manage to show that the variance of the thermodynamic work is equal to that of a system prepared in equilibrium initial conditions for every driving protocol $\lambda(t)$ (see equation (3.89)), thus generalising the results by van Zon and Cohen [66]. Finally we consider the special case of a linear dragging protocol $\lambda(t) = vt$ with $t_m \to -\infty$, also discussed in [82], which can be considered as a steady state in the usual sense. For this scenario we show that quantities such as average position, velocity, work and entropy

production rate have the same structure as for Markov dynamics. The variances, however, are different.

3.3 Modified Laplace transform

A standard way of dealing with the linear GLE uses Laplace transforms. This technique is particularly useful when dealing with an initial condition at finite times, for instance when the system starts from equilibrium at time $t = 0$. If the initial time is rather taken infinitely back in the past, traditional Laplace transforms are no longer suitable to find a solution for the GLE. However, it is well known that, for Markovian dynamics, non-equilibrium steady states can be obtained from this limit. Hence, we would find it useful to have a framework in which Laplace transforms are available and steady states may be considered.

Our way to tackle this problem is to introduce a modified Laplace transform with an arbitrary initial time $t_m \leq 0$ that acts on a given function $g(t)$ as follows

$$\hat{g}^{\,t_m}(k) = \mathcal{L}_k^{t_m}[g(t)] = \int_{t_m}^{\infty} \mathrm{d}t\, \mathrm{e}^{-kt} g(t)\,. \tag{3.5}$$

The standard Laplace transform of course is recovered for $t_m \nearrow 0$.

The aim is to solve the GLE finding the explicit dependence of the solution on t_m and then, if interested in steady states, eventually take the limit $t_m \to -\infty$. For our purposes, we just need to know the effect of such modified transform on first and second derivatives of a function. They can be readily expressed as

$$\begin{aligned} \mathcal{L}_k^{t_m}[\dot{g}(t)] &= k\hat{g}^{\,t_m}(k) - g_{t_m}\mathrm{e}^{-kt_m}\,, \\ \mathcal{L}_k^{t_m}[\ddot{g}(t)] &= k^2\hat{g}^{\,t_m}(k) - kg_{t_m}\mathrm{e}^{-kt_m} - \dot{g}_{t_m}\mathrm{e}^{-kt_m}\,. \end{aligned} \tag{3.6}$$

Note that $\hat{g}^{\,t_m}(k)$ stands for the modified Laplace transform of the function $g(t)$ while $g_{t_m} \equiv g(t_m)$ and $\dot{g}_{t_m} \equiv \partial_t\, g(t)|_{t=t_m}$ are the function and its time derivative evaluated at time t_m .

Furthermore, it is not hard to show that the action of the modified Laplace transform on integrals is equal to the action of the standard transform, namely

$$\mathcal{L}_k^{t_m}\left[\int_{t_m}^{t} \mathrm{d}t'\, g(t')\right] = \frac{\hat{g}^{\,t_m}(k)}{k}\,. \tag{3.7}$$

We also need to know the effect of such transform on the convolution of a causal function $\mathcal{G}(t)$, i.e such that $\mathcal{G}(t<0) = 0$ (like the memory kernel $\Gamma(t)$ in our case), with an arbitrary $g(t)$

$$\mathcal{L}_k^{t_m}\left[\int_{t_m}^{t} \mathrm{d}t'\, \mathcal{G}(t-t')g(t')\right] = \int_{t_m}^{\infty} \mathrm{d}t \int_{t_m}^{t} \mathrm{d}t' \mathrm{e}^{-kt}\mathcal{G}(t-t')g(t')\,. \tag{3.8}$$

First, to compute an explicit version of this equation, we note that

$$\int_{t_m}^{\infty} \mathrm{d}t \int_{t_m}^{t} \mathrm{d}t' = \int_{t_m}^{\infty} \mathrm{d}t' \int_{t'}^{\infty} \mathrm{d}t \tag{3.9}$$

i.e. these integrals define the same region of integration so that (3.8) becomes

$$\begin{aligned}\mathcal{L}_k^{t_m}\left[\int_{t_m}^{t} \mathrm{d}t' \mathcal{G}(t-t')g(t')\right] &= \int_{t_m}^{\infty} \mathrm{d}t' \int_{t'}^{\infty} \mathrm{d}t\, \mathrm{e}^{-kt}\mathcal{G}(t-t')g(t') = \\ &\overset{u=t-t'}{=} \int_{t_m}^{\infty} \mathrm{d}t' \int_{0}^{\infty} \mathrm{d}u\, \mathrm{e}^{-ku}\mathrm{e}^{-kt'}\Gamma(u)g(t') = \\ &= \int_{t_m}^{\infty} \mathrm{d}t' \mathrm{e}^{-kt'}g(t') \int_{0}^{\infty} \mathrm{d}u\, \mathrm{e}^{-ku}\mathcal{G}(u) = \\ &= \mathcal{L}_k^{t_m}[g(t)]\,\mathcal{L}_k[\mathcal{G}(t)] = \hat{g}^{t_m}(k)\hat{\mathcal{G}}(k)\end{aligned} \tag{3.10}$$

which is a generalisation of the convolution theorem. It states that the modified Laplace transform of the convolution of a causal function $\mathcal{G}(t)$ with an arbitrary function $g(t)$ is equal to the product of the standard Laplace transform of the causal function, i.e. $\hat{\mathcal{G}}(k)$, and the modified Laplace transform of $g(t)$, that is $\hat{g}^{t_m}(k)$.

We conclude this section by remarking that, of course, the modified Laplace transform of a causal function is equal to the standard Laplace transform of that function.

3.4 GLE solution

By applying the modified Laplace transform (3.5) to the GLE (3.4) and by using the results obtained above

$$\mathcal{L}_k^{t_m}[m\ddot{x}(t)] = \mathcal{L}_k^{t_m}\left[-\int_{t_m}^{t} \mathrm{d}t'\,\Gamma(t-t')\dot{x}(t') - \kappa(x(t)-\lambda(t)) + \eta(t)\right] \tag{3.11}$$

we get

$$\begin{aligned}m\Big(k^2\hat{x}^{t_m}(k) - kx_{t_m}\mathrm{e}^{-kt_m} - v_{t_m}\mathrm{e}^{-kt_m}\Big) = \\ = -\hat{\Gamma}(k)\left[k\hat{x}^{t_m}(k) - x_{t_m}\mathrm{e}^{-kt_m}\right] - \kappa\hat{x}^{t_m}(k) + \kappa\hat{\lambda}^{t_m}(k) + \hat{\eta}^{t_m}(k)\,.\end{aligned} \tag{3.12}$$

Furthermore, with a bit of algebra one can isolate the position x from the other quantities obtaining

$$\hat{x}^{t_m}(k) = x_{t_m}\frac{\mathrm{e}^{-kt_m}}{k}(1-\kappa\hat{\chi}_x(k)) + mv_{t_m}\mathrm{e}^{-kt_m}\hat{\chi}_x(k) + (\kappa\hat{\lambda}^{t_m}(k) + \hat{\eta}^{t_m}(k))\hat{\chi}_x(k)\,, \tag{3.13}$$

where we introduced the "position susceptibility" $\chi_x(t)$ defined via its Laplace transform

$$\hat{\chi}_x(k) = [mk^2 + k\hat{\Gamma}(k) + \kappa]^{-1}\,. \tag{3.14}$$

In the following we will also use its integral $\chi(t)$ and its derivative $\chi_v(t)$ ("velocity susceptibility")

$$\chi(t) \equiv \int_0^t \mathrm{d}t'\chi_x(t')\,, \tag{3.15}$$

$$\chi_v(t) \equiv \partial_t\chi_x(t)\,. \tag{3.16}$$

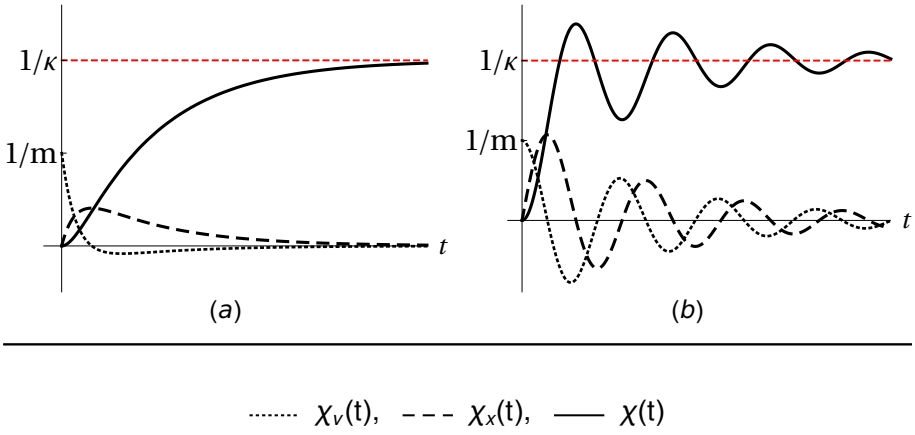

Figure 3.2: Underdamped ($m \neq 0$) susceptibilities for (a) Markovian memory kernel $\Gamma^{\text{Mark}}(t) = 2\gamma_0\delta(t)$ and (b) for non-Markovian memory kernel of the form $\Gamma^{\text{exp}}(t) = (\gamma/\tau)\exp[-t/\tau]\theta(t)$, where $\theta(t)$ is the Heaviside step function. In both cases we see that $\lim_{t\to 0}\chi_v(t) = 1/m$, $\lim_{t\to\infty}\chi_v(t) = 0$, $\lim_{t\to 0}\chi_x(t) = 0$, $\lim_{t\to\infty}\chi_x(t) = 0$, $\lim_{t\to 0}\chi(t) = 0$ and $\lim_{t\to\infty}\chi(t) = 1/\kappa$. In this underdamped case, all the mentioned limits remain valid for all memory kernels, see Appendix A.1.

In Appendix A.1 we discuss the limits of these susceptibilities for $t \to 0$ and $t \to \infty$. Two examples are shown in figure 3.2. We also stress that all the susceptibilities are of course causal functions, i.e. $\chi_*(t < 0) = 0$.

By defining the inverse of the modified Laplace transform through the usual Bromwich integral

$$g(t) = \frac{1}{2\pi i}\int_{\alpha-i\infty}^{\alpha+i\infty} \mathrm{d}k\, \mathrm{e}^{kt}\, \hat{g}^{t_m}(s)\,, \tag{3.17}$$

where α is such that the chosen vertical contour in the complex plane has all the singularities of $g(s)$ on its left, we see that $\mathcal{L}_k^{-1,t_m}\left[\mathrm{e}^{-kt_m}\right] = 2\delta(t-t_m)$ (the factor 2 is needed for consistency) and $\mathcal{L}_k^{-1,t_m}\left[\frac{\mathrm{e}^{-kt_m}}{k}\right] = \theta(t-t_m)$, where $\theta(t)$ is the Heaviside step function. Transforming back equation (3.12) to real time we obtain, for $t > 0 \geq t_m$,

$$\begin{aligned} x(t) =& x_{t_m}\left(\theta(t-t_m) - \kappa\int_{t_m}^{t}\mathrm{d}t'\chi_x(t-t')\theta(t'-t_m)\right) + \\ &+ 2mv_{t_m}\int_{t_m}^{t}\mathrm{d}t'\chi_x(t-t')\delta(t'-t_m) + \int_{t_m}^{t}\mathrm{d}t'\chi_x(t-t')\left[\kappa\lambda(t') + \eta(t')\right] = \\ =& x_{t_m}\left(1-\kappa\chi(t-t_m)\right) + mv_{t_m}\chi_x(t-t_m) + \int_{t_m}^{t}\mathrm{d}t'\chi_x(t-t')\left[\kappa\lambda(t') + \eta(t')\right]\,, \end{aligned} \tag{3.18}$$

that is the solution to the generalised Langevin equation. The velocity can be readily obtained by simply taking its time derivative:

$$v(t) = -\kappa x_{t_m}\chi_x(t-t_m) + mv_{t_m}\chi_v(t-t_m) + \int_{t_m}^{t}\mathrm{d}t'\chi_v(t-t')\left[\kappa\lambda(t') + \eta(t')\right] \tag{3.19}$$

where we used that for underdamped dynamics $\chi_x(0) = 0$, see Appendix A.1. Taking the averages of the above expressions and using that $\langle \eta(t) \rangle = 0$, we get

$$\langle x \rangle_{t_m,t} = \langle x_{t_m} \rangle (1 - \kappa\chi(t - t_m)) + m\langle v_{t_m} \rangle \chi_x(t - t_m) + \kappa \int_{t_m}^{t} \mathrm{d}t' \chi_x(t - t')\lambda(t') \tag{3.20}$$

$$\langle v \rangle_{t_m,t} = -\kappa\langle x_{t_m} \rangle \chi_x(t - t_m) + m\langle v_{t_m} \rangle \chi_v(t - t_m) + \kappa \int_{t_m}^{t} \mathrm{d}t' \chi_v(t - t')\lambda(t')\,, \tag{3.21}$$

with the notation $\langle \cdot \rangle_{t_m,t}$ meaning that initial conditions are taken at time t_m while the observation time is taken at time t.

3.4.1 Variance of the position and correlations

Another important quantity we are interested in is the variance of the position at time t. Given that the system started at time t_m with position x_{t_m} and velocity v_{t_m}, we have that

$$\langle \Delta x^2 \rangle_{t_m,t} = \langle (x_t - \langle x \rangle_{t_m,t})^2 \rangle_{t_m,t}\,. \tag{3.22}$$

Using the previously obtained expression for the position (3.18) and defining

$$\phi(t) = \int_{t_m}^{t} \mathrm{d}t' \chi_x(t - t')\eta(t')\,, \tag{3.23}$$

we find that (3.22) becomes

$$\begin{aligned} \langle \Delta x^2 \rangle_{t_m,t} =& \langle \phi^2(t) \rangle + \langle \Delta x_{t_m}^2 \rangle (1 - \kappa\chi(t - t_m))^2 + m^2 \langle \Delta v_{t_m}^2 \rangle \chi_x^2(t - t_m) \\ &+ 2m\mathrm{Cov}(x_{t_m}, v_{t_m})\chi_x(t - t_m)(1 - \kappa\chi(t - t_m))\,, \end{aligned} \tag{3.24}$$

where $\mathrm{Cov}(a, b) = \langle ab \rangle - \langle a \rangle \langle b \rangle$ is the covariance between the random variables a and b. Focusing on the the first term on the right hand side of (3.24), we further define the following quantity (also for future convenience):

$$\mathcal{C}(t', t'') = \langle \phi(t')\phi(t'') \rangle = \int_{t_m}^{t'} \mathrm{d}s' \int_{t_m}^{t''} \mathrm{d}s'' \chi_x(t' - s')\chi_x\left(t'' - s''\right) \langle \eta(s')\eta\left(s''\right) \rangle\,, \tag{3.25}$$

which in Appendix A.2 we show to be equal to

$$\begin{aligned} \mathcal{C}(t', t'') = k_B T \Big[&\chi(t' - t_m) + \chi(t'' - t_m) - \theta(t' - t'')\chi(t' - t'') + \\ &- \theta(t'' - t')\chi(t'' - t') - \kappa\chi(t' - t_m)\chi(t'' - t_m) - m\chi_x(t' - t_m)\chi_x(t'' - t_m) \Big]\,. \end{aligned} \tag{3.26}$$

The variance of the position can be obtained by evaluating this quantity at equal times (i.e. $t = t' = t''$) and then by plugging it into equation (3.24). From its definition (3.15), one immediately sees that $\chi(0) = 0$ so that

$$\langle \phi^2(t) \rangle = \mathcal{C}(t, t) = k_B T \Big[2\chi(t - t_m) - \kappa\chi^2(t - t_m) - m\chi_x^2(t - t_m) \Big]\,. \tag{3.27}$$

Finally, by using (3.24), we obtain an expression for the variance of the position from arbitrary initial conditions

$$\begin{aligned}\langle \Delta x^2\rangle_{t_m,t} =& k_B T\Big[2\chi(t-t_m) - m\chi_x^2(t-t_m) - \kappa\chi^2(t-t_m)\Big] + \\ &+ \langle \Delta x_{t_m}^2\rangle(1-\kappa\chi(t-t_m))^2 + m^2\langle \Delta v_{t_m}^2\rangle\chi_x^2(t-t_m) + \\ &+ 2m\mathrm{Cov}(x_{t_m}, v_{t_m})\chi_x(t-t_m)(1-\kappa\chi(t-t_m))\,.\end{aligned} \tag{3.28}$$

Note that, from (3.18) and (3.19) one sees that the stochastic behaviour of $x(t)$ and $v(t)$ is determined by the initial distribution of x_{t_m} and v_{t_m} and by a convolution involving the coloured noise $\eta(t)$. The latter is nothing else then a (continuous) sum of Gaussian random variables and hence it is Gaussianly distributed itself. This is a consequence of the GLE being linear, implying that if the initial probability distribution function (PDF) $p(x_{t_m}, v_{t_m}, t_m)$ is a (bivariate) Gaussian, so will be the $p_{t_m}(x_t, v_t, t)$ at time $t > t_m$. This also happens if arbitrary initial conditions are taken in the infinite past, i.e. if $t_m \to -\infty$. In fact, if a sufficiently large time has passed between the initial preparation of the system and the observation time t, which can be taken positive without loss of generality, the PDF regains its Gaussian character and can hence be written as

$$p_{t_m}(x_t, v_t, t) = \frac{1}{\sqrt{(2\pi)^2|\mathcal{S}_{t_m,t}|}}\exp\left[-\frac{1}{2}(\boldsymbol{x}_t - \langle \boldsymbol{x}\rangle_{t_m,t})\mathcal{S}_{t_m,t}^{-1}(\boldsymbol{x}_t - \langle \boldsymbol{x}\rangle_{t_m,t})\right], \tag{3.29}$$

with $\boldsymbol{x}_t = (x_t, v_t)$, $\langle \boldsymbol{x}\rangle_{t_m,t} = (\langle x\rangle_{t_m,t}, \langle v\rangle_{t_m,t})$ and $\mathcal{S}_{t_m,t}$ the covariance matrix

$$\mathcal{S}_{t_m,t} = \begin{pmatrix} \langle \Delta x^2\rangle_{t_m,t} & \mathrm{Cov}_{t_m}(x_t, v_t) \\ \mathrm{Cov}_{t_m}(x_t, v_t) & \langle \Delta v^2\rangle_{t_m,t}\,, \end{pmatrix} \tag{3.30}$$

whose components are the variances of position and velocity along with their covariances. We are hence interested in obtaining an expression for the missing components of the covariance matrix:

$$\begin{aligned}\langle \Delta v^2\rangle_{t_m,t} =& \langle (v_t - \langle v\rangle_{t_m,t})^2\rangle_{t_m,t} = \\ =& \partial_{t'}\partial_{t''}\langle (x_{t'} - \langle x\rangle_{t_m,t'})\,(x_{t''} - \langle x\rangle_{t_m,t''})\rangle_{t_m,t',t''}\big|_{t'=t''=t}\,,\end{aligned} \tag{3.31}$$

$$\begin{aligned}\mathrm{Cov}_{t_m}(x_t, v_t) =& \langle x_t v_t\rangle_{t_m,t} - \langle x\rangle_{t_m,t}\langle v\rangle_{t_m,t} = \\ =& \partial_{t'}\langle (x_t - \langle x\rangle_{t_m,t})\,(x_{t'} - \langle x\rangle_{t_m,t'})\rangle_{t_m,t,t'}\big|_{t'=t}\,,\end{aligned} \tag{3.32}$$

where we used that $\langle v\rangle_{t_m,t} = \partial_t\langle x\rangle_{t_m,t}$ because of the linearity of the GLE. Moreover, of course it holds that $\mathrm{Cov}_{t_m}(x_t, v_t) = \mathrm{Cov}_{t_m}(v_t, x_t)$. (3.31) and (3.32) can be computed similarly to the variance of the position (3.28):

$$\begin{aligned}\langle \Delta v^2\rangle_{t_m,t} =& k_B T\Big[1/m - m\chi_v^2(t-t_m) - \kappa\chi_x^2(t-t_m)\Big] + \kappa^2\langle \Delta x_{t_m}^2\rangle\chi_x^2(t-t_m) + \\ &+ m^2\langle \Delta v_{t_m}^2\rangle\chi_v^2(t-t_m) - 2\kappa m\mathrm{Cov}(x_{t_m}, v_{t_m})\chi_v(t-t_m)\chi_x(t-t_m)\,,\end{aligned} \tag{3.33}$$

$$\begin{aligned}\mathrm{Cov}_{t_m}(x_t, v_t) =& k_B T\Big[\chi_x(t-t_m) - m\chi_v(t-t_m)\chi_x(t-t_m) - \kappa\chi_x(t-t_m)\chi(t-t_m)\Big] + \\ &- \kappa\langle \Delta x_{t_m}^2\rangle\chi_x(t-t_m)(1-\kappa\chi(t-t_m)) + \\ &+ m^2\langle \Delta v_{t_m}^2\rangle\chi_x(t-t_m)\chi_v(t-t_m) + \\ &+ m\mathrm{Cov}(x_{t_m}, v_{t_m})\big(\chi_v(t-t_m)(1-\kappa\chi(t-t_m)) - \kappa\chi_x^2(t-t_m)\big)\,,\end{aligned} \tag{3.34}$$

where we used the convention for the Heaviside step function for which $\theta(0) = 1/2$ as well as $\chi_v(0) = 1/m$. Hence, equations (3.28), (3.33) and (3.34) are the explicit expressions of the components of the covariance matrix.

3.5 Thermodynamic quantities

This section is devoted to the analysis of relevant thermodynamic quantities such as entropy production, entropy production rate and thermodynamic work.

3.5.1 Entropy production and entropy production rate

Entropy production, plays a crucial role in non-equilibrium dynamics and its proprieties have been already briefly discussed in the previous chapter in the context of Markovian dynamics. It encodes the information about the irreversibility of a given process and the same thing happens for systems with memory. Indeed, for a colloidal particle in contact with a non-Markovian heat bath, the entropy production for a stochastic trajectory ω_t during a time interval $[0, t]$ can be again split into two parts

$$\Sigma_{\text{tot}}(\omega_t) = \Sigma_{\text{env}}(\omega_t) + \Sigma_{\text{sys}}(\omega_t) \tag{3.35}$$

with

$$\begin{aligned} \Sigma_{\text{env}}(\omega_t) &= \beta \Delta Q(\omega_t)\,, \\ \Sigma_{\text{sys}}(\omega_t) &= -\ln p_{t_m}(x_t, v_t, t) + \ln p_{t_m}(x_0, v_0, 0)\,, \end{aligned} \tag{3.36}$$

where $\Delta Q(\omega_t, t)$ is the heat injected into the heat reservoir, β is the inverse temperature (hence $\Sigma_{\text{env}}(x, t)$ is the entropy change in the reservoir) and $\Sigma_{\text{sys}}(x, t)$ is the difference between the Shannon entropy of the final and initial states of the system. In particular, for Gaussian PDFs, it holds that

$$\Sigma_{\text{sys}}(\omega_t, t) = \frac{1}{2} \ln \left[\frac{|\mathcal{S}_{t_m,t}|}{|\mathcal{S}_{t_m,0}|} \right] , \tag{3.37}$$

where $|\mathcal{S}_{t_m,t}|$ is the determinant of the covariance matrix (3.30) at time t.

In analogy to (2.66), we can define the heat absorbed from the bath by means of

$$\Delta Q(\omega_t) = \int_0^t \mathrm{d}t' F_{bath}(\omega_t, t') \circ \dot{x}(t')\,, \tag{3.38}$$

where $F_{bath}(\omega_t, t)$ is the force exerted from the particle on the bath, i.e., using the GLE (3.1),

$$\begin{aligned} F_{bath}(\omega_t, t) &= \int_{t_m}^t \mathrm{d}t' \Gamma(t - t') \dot{x}(t') - \eta(t) \\ &= \kappa\lambda(t) - m\ddot{x}(t) - \kappa x(t)\,. \end{aligned} \tag{3.39}$$

Equation (3.38) thus becomes

$$\begin{aligned} \Delta Q(\omega_t) &= \int_0^t \mathrm{d}t' \left[\kappa\lambda(t') - m\ddot{x}(t') - \kappa x(t') \right] \circ \dot{x}(t') = \\ &= \kappa \int_0^t \mathrm{d}t' \lambda(t') \dot{x}(t') - \frac{m}{2}[\dot{x}^2(t) - \dot{x}^2(0)] - \frac{\kappa}{2}[x^2(t) - x^2(0)] = \\ &= W(\omega_t) - \Delta E(\omega_t)\,, \end{aligned} \tag{3.40}$$

where

$$W(\omega_t) = -\int_0^t \mathrm{d}\lambda_{t'}\,\partial_{\lambda_{t'}} U(x_{t'},\lambda_{t'}) = -\kappa\int_0^t \mathrm{d}\lambda_{t'}\,(x(t')-\lambda(t'))\,, \tag{3.41}$$

$$\Delta E(\omega_t) = \frac{m}{2}[v^2(t)-v^2(0)] + \frac{\kappa}{2}[(x(t)-\lambda(t))^2 - x^2(0)]\,, \tag{3.42}$$

again in analogy to (2.71) and (2.72) and hence recovering the first law of thermodynamics at a stochastic level [65, 42].

Taking the average of (3.38), as $\langle r^2\rangle = \langle \Delta r^2\rangle + \langle r\rangle^2$ for any stochastic variable r and since for underdamped dynamics $\dot{x}(t) = v(t)$, we get

$$\begin{aligned}\langle \Sigma_{\mathrm{env}}\rangle_{t_m,t} = \beta\langle \Delta Q\rangle_{t_m,t} =& \beta\kappa\int_0^t \mathrm{d}t'\lambda(t')\langle v\rangle_{t_m,t'} + \\ &- \frac{\beta m}{2}(\langle v\rangle^2_{t_m,t} - \langle v\rangle^2_{t_m,0} + \langle \Delta v^2\rangle_{t_m,t} - \langle \Delta v^2\rangle_{t_m,0}) + \\ &- \frac{\beta\kappa}{2}(\langle x\rangle^2_{t_m,t} - \langle x\rangle^2_{t_m,0} + \langle \Delta x^2\rangle_{t_m,t} - \langle \Delta x^2\rangle_{t_m,0})\,.\end{aligned} \tag{3.43}$$

At this stage one can not further simplify this expression for the entropy production. On the other hand, we can obtain a much more compact form for the entropy production rate, defined as

$$\langle \sigma_{\mathrm{tot}}\rangle_{t_m,t} = \partial_t \langle \Sigma_{\mathrm{tot}}\rangle_{t_m,t}\,. \tag{3.44}$$

For the system entropy production rate we immediately see from (3.37) that

$$\langle \sigma_{\mathrm{sys}}\rangle_{t_m,t} = \frac{\partial_t |\mathcal{S}_{t_m,t}|}{2|\mathcal{S}_{t_m,t}|}\,. \tag{3.45}$$

From equation (3.43) instead we get that

$$\begin{aligned}\langle \sigma_{\mathrm{env}}\rangle_{t_m,t} =& \beta\partial_t\langle x\rangle_{t_m,t}\left[\kappa\lambda(t) - m\partial_t^2\langle x\rangle_{t_m,t} - \kappa\langle x\rangle_{t_m,t}\right] + \\ &- \frac{\beta\kappa}{2}\partial_t\langle \Delta x\rangle_{t_m,t} - \frac{\beta m}{2}\partial_t\langle \Delta v\rangle_{t_m,t}\,,\end{aligned} \tag{3.46}$$

where again we used that $\langle v\rangle_{t_m,t} = \langle \dot{x}\rangle_{t_m,t} = \partial_t\langle x\rangle_{t_m,t}$. Consider now the term between square brackets on the right hand side of equation (3.46) and name it

$$\mathcal{V}(t,t_m) = \kappa\lambda(t) - m\partial_t^2\langle x\rangle_{t_m,t} - \kappa\langle x\rangle_{t_m,t}\,. \tag{3.47}$$

Taking its modified Laplace transform we obtain

$$\begin{aligned}\mathcal{L}_k^{t_m}[\mathcal{V}(t,t_m)] =& \kappa\hat{\lambda}^{t_m}(k) - \kappa\mathcal{L}_k^{t_m}[\langle x\rangle_{t_m,t}] - mk^2\mathcal{L}_k^{t_m}[\langle x\rangle_{t_m,t}] \\ &+ mk\langle x_{t_m}\rangle \mathrm{e}^{-kt_m} + m\langle v_{t_m}\rangle \mathrm{e}^{-kt_m}\,,\end{aligned} \tag{3.48}$$

where we used the formula for the modified Laplace transform of a second derivative (3.6). Moreover, looking back to the expression for the average of the position (3.20) we note that it can be effectively written as

$$\langle x\rangle_{t_m,t} = \mathcal{I}(t,t_m) + \kappa\int_{t_m}^t \mathrm{d}t'\chi_x(t-t')\lambda(t')\,, \tag{3.49}$$

where $\mathcal{I}(t,t_m) = \langle x_{t_m}\rangle(1-\kappa\chi(t-t_m)) + m\langle v_{t_m}\rangle\chi_x(t-t_m)$ contains the information relative to initial conditions, in particular $\mathcal{I}(t_m,t_m) = \langle x_{t_m}\rangle$.

Going back to equation (3.48), recalling the definition of the position susceptibility via its Laplace transform ($\hat{\chi}_x(k) = [mk^2 + k\hat{\Gamma}(k) + \kappa]^{-1}$) and using that for the first term on the right hand side of equation (3.49) we have that

$$\hat{\mathcal{I}}^{t_m}(k) = \langle x_{t_m}\rangle \frac{\mathrm{e}^{-kt_m}}{k}(1-\kappa\hat{\chi}_x(k)) + m\langle v_{t_m}\rangle \mathrm{e}^{-kt_m}\hat{\chi}_x(k)\,, \tag{3.50}$$

along with the generalised convolution theorem for the second one, we get

$$\begin{aligned}
\mathcal{L}_k^{t_m}\left[\mathcal{V}(t,t_m)\right] =& \kappa\hat{\lambda}^{t_m}(k) - \kappa\mathcal{L}_k^{t_m}\left[\langle x\rangle_{t_m,t}\right] - mk^2\mathcal{L}_k^{t_m}\left[\langle x\rangle_{t_m,t}\right] + \\
&+ mk\langle x_{t_m}\rangle \mathrm{e}^{-kt_m} + m\langle v_{t_m}\rangle \mathrm{e}^{-kt_m} = \\
=& \kappa\left[1-\kappa\hat{\chi}_x(k) - mk^2\hat{\chi}_x(k)\right]\hat{\lambda}^{t_m}(k) - (mk^2+\kappa)\hat{\mathcal{I}}^{t_m}(k) + \\
&+ mk\langle x_{t_m}\rangle \mathrm{e}^{-kt_m} + m\langle v_{t_m}\rangle \mathrm{e}^{-kt_m} = \\
=& \hat{\Gamma}(k)\left[\kappa k\hat{\chi}_x(k)\hat{\lambda}^{t_m}(k) + k\hat{\mathcal{I}}^{t_m}(k) - \mathcal{I}(t_m,t_m)\mathrm{e}^{-kt_m}\right] = \\
=& \hat{\Gamma}(k)\mathcal{L}_k^{t_m}\left[\partial_t\langle x\rangle_{t_m,t}\right]\,.
\end{aligned} \tag{3.51}$$

Its inverse can be calculated using again the convolution theorem

$$\mathcal{V}(t,t_m) = \int_{t_m}^{t} \mathrm{d}t'\,\Gamma(t-t')\langle v\rangle_{t_m,t'} = \int_0^{t-t_m} \mathrm{d}t'\,\langle v\rangle_{t_m,t-t'}\Gamma(t') = \widehat{\gamma}(t-t_m)\langle v_{\mathrm{ret}}\rangle_{t_m,t}\,, \tag{3.52}$$

where

$$\widehat{\gamma}(t) = \int_0^t \mathrm{d}t'\,\Gamma(t') \tag{3.53}$$

is the time dependent effective friction coefficient and $\widehat{\gamma} = \lim_{t\to\infty}\widehat{\gamma}(t)$ is its asymptotic limit for long times. Moreover, we define the *retarded velocity* as

$$\langle v_{\mathrm{ret}}\rangle_{t_m,t} = \frac{1}{\widehat{\gamma}(t-t_m)}\int_0^{t-t_m}\mathrm{d}t'\,\langle v\rangle_{t_m,t-t'}\Gamma(t') \tag{3.54}$$

which can be interpreted as a quantity converging to the real velocity for $t\to\infty$, i.e.

$$\begin{aligned}
\lim_{t\to\infty}\langle v_{\mathrm{ret}}\rangle_{t_m,t} &= \lim_{t\to\infty}\frac{1}{\widehat{\gamma}(t-t_m)}\int_0^{t-t_m}\mathrm{d}t'\,\langle v\rangle_{t_m,t-t'}\Gamma(t') \approx \\
&\approx \lim_{t\to\infty}\frac{\langle v\rangle_{t_m,t}}{\widehat{\gamma}(t-t_m)}\int_0^{t-t_m}\mathrm{d}t'\Gamma(t') = \lim_{t\to\infty}\langle v\rangle_{t_m,t}\,.
\end{aligned} \tag{3.55}$$

The same decoupling between the kernel and the average velocity can be obtained for $t_m\to-\infty$ if one is able to show that $\langle v\rangle_{t_m,t} = \langle v\rangle_{t-t_m}$. It will be for example the case of a trapped particle dragged at a constant velocity, i.e. $\lambda(t) = vt$. In fact, under these hypothesis and with a calculation analogous to that of equation (3.55), we see that

$$\lim_{t_m\to-\infty}\langle v_{\mathrm{ret}}\rangle_{t-t_m} = \lim_{t_m\to-\infty}\frac{1}{\widehat{\gamma}(t-t_m)}\int_0^{t-t_m}\mathrm{d}t'\,\langle v\rangle_{t-t_m-t'}\Gamma(t') = \lim_{t_m\to-\infty}\langle v\rangle_{t-t_m}\,. \tag{3.56}$$

Moreover, note that for Markovian dynamics defined by a memory kernel $\Gamma^{\text{Mark}}(t) = 2\gamma_0\delta(t)$ it holds that $\widehat{\gamma} = \widehat{\gamma}(t) = \gamma_0$ and $\langle v_{\text{ret}}\rangle_{t_m,t} = \langle v\rangle_{t_m,t}$ for every t.

Finally, putting together equation (3.46) and (3.52), we get

$$\langle\sigma_{\text{env}}\rangle_{t_m,t} = \beta\widehat{\gamma}(t-t_m)\langle v\rangle_{t_m,t}\langle v_{\text{ret}}\rangle_{t_m,t} - \frac{\beta\kappa}{2}\partial_t\langle\Delta x^2\rangle_{t_m,t} - \frac{\beta m}{2}\partial_t\langle\Delta v^2\rangle_{t_m,t} \tag{3.57}$$

while for the total entropy production rate (assuming that $p_{t_m}(x_t, v_t, t)$ is Gaussian) we have that

$$\langle\sigma_{\text{tot}}\rangle_{t_m,t} = \beta\widehat{\gamma}(t-t_m)\langle v\rangle_{t_m,t}\langle v_{\text{ret}}\rangle_{t_m,t} - \frac{\beta\kappa}{2}\partial_t\langle\Delta x^2\rangle_{t_m,t} - \frac{\beta m}{2}\partial_t\langle\Delta v^2\rangle_{t_m,t} + \frac{\partial_t|\mathcal{S}_{t_m,t}|}{2|\mathcal{S}_{t_m,t}|}. \tag{3.58}$$

3.5.2 Work

In accordance to stochastic energetics [65, 42], we consider equation (3.41) as the work done on a particle by a time dependent external potential, harmonic in our case, meaning that for a particular stochastic trajectory ω_t taking place during the time interval $[0,t]$ one gets

$$\begin{aligned} W(\omega_t) &= -\int_0^t \mathrm{d}\lambda_{t'}\, U'(x_{t'} - \lambda(t')) = \\ &= -\kappa\int_0^t \mathrm{d}\lambda_{t'}\,(x(t') - \lambda(t')) = \frac{\kappa\lambda(t)^2}{2} - \kappa\int_0^t \mathrm{d}\lambda_{t'}\, x(t') \end{aligned} \tag{3.59}$$

where we restricted ourselves to the case where $\lambda(0) = 0$. We can calculate the work as a function of the external protocol and the susceptibilities (3.14) and (3.15) by just plugging the explicit solution for the position of the particle (3.18) into (3.59), which reads

$$\begin{aligned} W(\omega_t) =& \frac{\kappa\lambda(t)^2}{2} - \kappa\Bigg[x_{t_m}\left(\lambda(t) - \kappa\int_0^t \mathrm{d}\lambda_{t'}\,\chi(t'-t_m)\right) + \\ &+ m v_{t_m}\int_0^t \mathrm{d}\lambda_{t'}\,\chi_x(t'-t_m) + \int_0^t \mathrm{d}\lambda_{t'}\int_{t_m}^{t'} \mathrm{d}t''\chi_x(t'-t'')\left[\kappa\lambda(t'') + \eta(t'')\right]\Bigg]. \end{aligned} \tag{3.60}$$

Its average can be obtained, again by noting that $\langle\eta(t)\rangle = 0$, as

$$\begin{aligned} \langle W\rangle_{t_m,t} = \frac{\kappa\lambda(t)^2}{2} - \kappa\Bigg[&\langle x_{t_m}\rangle\left(\lambda(t) - \kappa\int_0^t \mathrm{d}\lambda_{t'}\,\chi(t'-t_m)\right) + \\ &+ m\langle v_{t_m}\rangle\int_0^t \mathrm{d}\lambda_{t'}\,\chi_x(t'-t_m) + \\ &+ \kappa\int_0^t \mathrm{d}\lambda_{t'}\int_{t_m}^{t'} \mathrm{d}t''\chi_x(t'-t'')\lambda(t'')\Bigg]. \end{aligned} \tag{3.61}$$

It is well known that, for such linear systems, the PDF $P(W_t)$ of the work is Gaussian. In fact, differently from other quantities such as the position, the probability distribution of the work at $t = 0$ is always a Dirac delta centred in 0, i.e.

$P(W_t, t=0) = \delta(W_t)$, as it can be easily seen from (3.60). Since such distribution is the limit of a Gaussian for a random variable with vanishing variance, and given the linearity of the GLE, the PDF of the work stays Gaussian at all times. Hence, in addition to the average $\langle W\rangle_{t_m,t}$, again we need its variance to completely characterise the PDF. It can be calculated similarly to the variance of the position (3.22), starting from the definition of work (3.59),

$$\begin{aligned}\langle \Delta W^2\rangle_{t_m,t} =&\langle (W(\omega_t) - \langle W\rangle_{t_m,t})^2\rangle_{t_m,t} = \kappa^2 \left\langle \left(\int_0^t \mathrm{d}\lambda_{t'}\,(x_{t'} - \langle x\rangle_{t_m,t'})\right)^2 \right\rangle_{t_m,t} = \\ =&\kappa^2 \int_0^t \mathrm{d}\lambda_{t'} \int_0^t \mathrm{d}\lambda_{t''}\, \mathcal{C}(t',t'') + \kappa^2 \langle \Delta x_{t_m}^2\rangle \left(\lambda(t) - \kappa \int_0^t \mathrm{d}\lambda_{t'}\,\chi(t'-t_m)\right)^2 + \\ &+ m^2\kappa^2 \langle \Delta v_{t_m}^2\rangle \left(\int_0^t \mathrm{d}\lambda_{t'}\,\chi_x(t'-t_m)\right)^2 + \\ &+ 2m\kappa^2 \mathrm{Cov}(x_{t_m}, v_{t_m}) \left(\lambda_t - \kappa \int_0^t \mathrm{d}\lambda_{t'}\,\chi(t'-t_m)\right) \int_0^t \mathrm{d}\lambda_{t'}\,\chi_x(t'-t_m)\,,\end{aligned} \tag{3.62}$$

where $\mathcal{C}(t',t'')$ was defined in (3.25). By computing the first term in the second line we get

$$\begin{aligned}\langle \Delta W^2\rangle_{t_m,t} =&k_B T\kappa^2 \left[2\lambda(t) \int_0^t \mathrm{d}\lambda_{t'}\,\chi(t'-t_m) - 2\int_0^t \mathrm{d}\lambda_{t'} \int_0^{t'} \mathrm{d}\lambda_{t''}\,\chi(t'-t'') + \right. \\ &\left. - \kappa \left(\int_0^t \mathrm{d}\lambda_{t'}\,\chi(t'-t_m)\right)^2 - m\left(\int_0^t \mathrm{d}\lambda_{t'}\,\chi_x(t'-t_m)\right)^2\right] + \\ &+ \kappa^2 \langle \Delta x_{t_m}^2\rangle \left(\lambda(t) - \kappa \int_0^t \mathrm{d}\lambda_{t'}\,\chi(t'-t_m)\right)^2 + \\ &+ m^2\kappa^2 \langle \Delta v_{t_m}^2\rangle \left(\int_0^t \mathrm{d}\lambda_{t'}\,\chi_x(t'-t_m)\right)^2 + \\ &+ 2m\kappa^2 \mathrm{Cov}(x_{t_m}, v_{t_m}) \left(\lambda(t) - \kappa \int_0^t \mathrm{d}\lambda_{t'}\,\chi(t'-t_m)\right) \int_0^t \mathrm{d}\lambda_{t'}\,\chi_x(t'-t_m)\,,\end{aligned} \tag{3.63}$$

that is the expression for the variance of the work for an arbitrary initial distribution of position and velocities. Although it might look rather complicated, in the next section we will see that the above equation simplifies significantly for some usual initial distributions.

3.6 Overdamped dynamics

Until now we restricted our discussion to underdamped dynamics, namely considering a finite mass for the particle and hence including inertial effects in the GLE (3.4). Instead, the overdamped case can be considered by taking $m = 0$, corresponding to the following GLE

$$\int_{t_m}^t \mathrm{d}t'\,\Gamma(t-t')\dot{x}(t') = -\kappa[x(t) - \lambda(t)] + \eta(t)\,. \tag{3.64}$$

Its solution can be obtained with the same procedure used for the underdamped case with the main difference consisting in a different definition of the position susceptibility

$$\hat{\chi}_x^{\text{over}}(k) = [k\hat{\Gamma}(k) + \kappa]^{-1} \tag{3.65}$$

and, as a consequence, of the other susceptibilities

$$\chi^{\text{over}}(t) \equiv \int_0^t \mathrm{d}t' \chi_x^{\text{over}}(t') \,, \tag{3.66}$$

$$\chi_v^{\text{over}}(t) \equiv \partial_t \chi_x^{\text{over}}(t) \,. \tag{3.67}$$

It is important to underline that one can not explicitly calculate the underdamped susceptibilities and take the massless limit $m \to 0$ afterwards because this would lead to inconsistencies, as it can be seen in [83]. However, the direct solution of the overdamped dynamics (3.64) can be found (dropping the "over" superscript):

$$x(t) = x_{t_m}\left(1 - \kappa\chi(t - t_m)\right) + \int_{t_m}^t \mathrm{d}t' \chi_x(t - t') \left[\kappa\lambda(t') + \eta(t')\right] \tag{3.68}$$

with its average equal to

$$\langle x \rangle_{t_m,t} = \langle x_{t_m} \rangle \left(1 - \kappa\chi(t - t_m)\right) + \kappa \int_{t_m}^t \mathrm{d}t' \chi_x(t - t')\lambda(t') \tag{3.69}$$

and with variance

$$\langle \Delta x^2 \rangle_{t_m,t} = k_B T \Big[2\chi(t - t_m) - \kappa\chi^2(t - t_m)\Big] + \langle \Delta x_{t_m}^2 \rangle (1 - \kappa\chi(t - t_m))^2 \,. \tag{3.70}$$

The velocity is computed by taking the derivative of (3.68),

$$v(t) = -\kappa x_{t_m} \chi_x(t - t_m) + \int_{t_m}^t \mathrm{d}t' \chi_v(t - t') \left[\kappa\lambda(t') + \eta(t')\right] + \chi_x(0) \left[\kappa\lambda(t) + \eta(t)\right] \,. \tag{3.71}$$

Since in the overdamped case $\chi_x(0) \neq 0$ (see Appendix A.1), the velocity is proportional to the noise $\eta(t)$, corresponding to the well known singularity of Brownian motion. This feature disappears once the average is taken,

$$\langle v \rangle_{t_m,t} = -\kappa \langle x_{t_m} \rangle \chi_x(t - t_m) + \kappa \int_{t_m}^t \mathrm{d}t' \chi_v(t - t')\lambda(t') + \kappa\chi_x(0)\lambda(t') \,. \tag{3.72}$$

On the other hand, the variance of the velocity is not well defined as the $\chi_x(0)\eta(t)$ term again yields some mathematical problems. Indeed, trying to calculate this variance, one finds a term of the form $\chi_x^2(0)\langle \eta(t)\eta(t) \rangle = k_B T \chi_x^2(0)\Gamma(0)$, which is a singular quantity (consider Markov dynamics for example), see again Appendix A.1 for more details.

For a Gaussian PDF, obtained for example starting from equilibrium initial conditions or by sending $t_m \to -\infty$ and $t \geq 0$, we get the following expressions for the total entropy production rate

$$\langle \sigma_{\text{tot}} \rangle_{t_m,t} = \beta \widehat{\gamma}(t - t_m) \langle v \rangle_{t_m,t} \langle v_{\text{ret}} \rangle_{t_m,t} - \frac{\beta\kappa}{2} \partial_t \langle \Delta x^2 \rangle_{t_m,t} + \frac{\partial_t \langle \Delta x^2 \rangle_{t_m,t}}{2 \langle \Delta x^2 \rangle_{t_m,t}} \,. \tag{3.73}$$

As for the work and its variance, again making the same reasoning as in the previous section, we get

$$\begin{aligned}\langle W\rangle_{t_m,t} = \frac{\kappa\lambda(t)^2}{2} - \kappa\Bigg[\langle x_{t_m}\rangle\left(\lambda(t) - \kappa\int_0^t \mathrm{d}\lambda_{t'}\chi(t'-t_m)\right) + \\ + \kappa\int_0^t \mathrm{d}\lambda_{t'}\int_{t_m}^{t'}\mathrm{d}t''\chi_x(t'-t'')\lambda(t'')\Bigg],\end{aligned} \tag{3.74}$$

$$\begin{aligned}\langle \Delta W^2\rangle_{t_m,t} =& k_BT\kappa^2\Bigg[2\lambda(t)\int_0^t \mathrm{d}\lambda_{t'}\chi(t'-t_m) - 2\int_0^t \mathrm{d}\lambda_{t'}\int_0^{t'}\mathrm{d}\lambda_{t''}\chi(t'-t'')+ \\ &- \kappa\left(\int_0^t \mathrm{d}\lambda_{t'}\chi(t'-t_m)\right)^2\Bigg] + \kappa^2\langle\Delta x_{t_m}^2\rangle\left(\lambda(t) - \kappa\int_0^t \mathrm{d}\lambda_{t'}\chi(t'-t_m)\right)^2.\end{aligned} \tag{3.75}$$

3.7 Applications

In this paragraph we apply the general formulas derived in the previous sections to specific initial conditions. In particular, we will discuss two cases:

- Dynamics starting from an equilibrium condition, generated by a trap left still for a long time with its minimum at $x = 0$, implying that $\langle x_0\rangle_t^{\mathrm{eq}} = 0$ and $\langle v_0\rangle_t^{\mathrm{eq}} = 0$. The protocol starts at $t = 0$ and no memory with the past is established, meaning that $t_m = 0$.
- Dynamics starting in the infinite past, corresponding to $t_m \to -\infty$, where memory of initial conditions is lost. Moreover, we will show that for the particular case of a linear dragging protocol $\lambda(t) = vt$, the system reaches a non-equilibrium steady state. This happens because the system can be mapped, through a Galileian transformation, to a reference frame where an equilibrium distribution is achieved in the limit $t_m \to -\infty$.

Of course, for a given protocol, in both cases the dynamics of the system becomes the same in the limit of large observation times $t \to \infty$.

Moreover, we stress that all the formulae presented in this section are both valid for underdamped and overdamped dynamics, with the only difference that the susceptibilities must be calculated at the beginning by choosing respectively a finite or a null mass for the particle.

3.7.1 Dynamics starting from equilibrium

For a colloidal particle trapped in a parabolic potential with stiffness κ, the equilibrium PDF at time $t_m = 0$ has a Gaussian shape,

$$P^{\mathrm{eq}}(x_0, v_0) = \frac{1}{\sqrt{(2\pi)^2|\mathcal{S}_0^{\mathrm{eq}}|}}\exp\left[-\frac{1}{2}(\boldsymbol{x}_0 - \langle\boldsymbol{x}_0\rangle^{\mathrm{eq}})\left(\mathcal{S}_0^{\mathrm{eq}}\right)^{-1}(\boldsymbol{x}_0 - \langle\boldsymbol{x}_0\rangle^{\mathrm{eq}})\right], \tag{3.76}$$

with parameters given by

$$\langle\boldsymbol{x}_0\rangle^{\mathrm{eq}} = \begin{pmatrix}\langle x_0\rangle^{\mathrm{eq}}\\ \langle v_0\rangle^{\mathrm{eq}}\end{pmatrix} = \begin{pmatrix}0\\0\end{pmatrix}, \tag{3.77}$$

$$\mathcal{S}_0^{eq} = \begin{pmatrix} \langle \Delta x_0^2 \rangle^{\text{eq}} & \text{Cov}^{\text{eq}}(x_0, v_0) \\ \text{Cov}^{\text{eq}}(x_0, v_0) & \langle \Delta v_0^2 \rangle^{\text{eq}} \end{pmatrix} = \begin{pmatrix} k_B T/\kappa & 0 \\ 0 & k_B T/m \end{pmatrix} . \tag{3.78}$$

Using equations (3.77) and (3.78), we can evaluate the evolution of all the quantities discussed in the previous section, starting from the probability distribution defined above and for an arbitrary $\lambda(t)$. Starting from the average of the position (3.20) and velocity (3.21) we find that

$$\langle \boldsymbol{x} \rangle_t^{\text{eq}} = \begin{pmatrix} \langle x \rangle_t^{\text{eq}} \\ \langle v \rangle_t^{\text{eq}} \end{pmatrix} = \kappa \begin{pmatrix} \int_0^t \mathrm{d}t' \chi_x(t-t')\lambda(t') \\ \int_0^t \mathrm{d}t' \chi_v(t-t')\lambda(t') \end{pmatrix} \tag{3.79}$$

while for the covariance matrix, using equations (3.28), (3.33) and (3.34) we get that

$$\mathcal{S}_t^{eq} = \begin{pmatrix} \langle \Delta x^2 \rangle_t^{\text{eq}} & \text{Cov}^{\text{eq}}(x_t, v_t) \\ \text{Cov}^{\text{eq}}(x_t, v_t) & \langle \Delta v^2 \rangle_t^{\text{eq}} \end{pmatrix} = \begin{pmatrix} k_B T/\kappa & 0 \\ 0 & k_B T/m \end{pmatrix} , \tag{3.80}$$

i.e. if we start from equilibrium and the trap stiffness κ does not change, then the covariance matrix remains constant in time for every choice of $\lambda(t)$.

Going forward to the estimate of thermodynamic work, from (3.61) and (3.63) and again using that $\lambda(0) = 0$ along with $\chi(t) = \int_0^t \mathrm{d}t' \chi_x(t)$, we get that

$$\langle W \rangle_t^{eq} = \kappa \left(\frac{\lambda(t)^2}{2} - \kappa \int_0^t \mathrm{d}\lambda_{t'} \int_0^{t'} \mathrm{d}\lambda_{t''} \chi(t'-t'') \right) , \tag{3.81}$$

$$\langle \Delta W^2 \rangle_t^{eq} = 2k_B T \kappa \left(\frac{\lambda(t)^2}{2} - \kappa \int_0^t \mathrm{d}\lambda_{t'} \int_0^{t'} \mathrm{d}\lambda_{t''} \chi(t'-t'') \right) , \tag{3.82}$$

i.e.

$$\langle \Delta W^2 \rangle_t^{eq} = 2k_B T \langle W \rangle_t^{eq} . \tag{3.83}$$

Since the PDF of the work $P(W_t)$ is Gaussian, an integral fluctuation theorem for the thermodynamic work $W(x_t, v_t, t)$ holds (see [81] for details) and a Jarzynski equality would follow [84].

Finally, since the covariance matrix and its determinant are both constants, a very simple expression can be found for the rate of entropy production

$$\langle \sigma_{\text{env}} \rangle_t^{\text{eq}} = \frac{\widehat{\gamma}(t) \langle v \rangle_t^{\text{eq}} \langle v_{\text{ret}} \rangle_t^{\text{eq}}}{k_B T} , \tag{3.84}$$

where again

$$\langle v_{\text{ret}} \rangle_t^{\text{eq}} = \frac{1}{\widehat{\gamma}(t)} \int_0^t \mathrm{d}t' \langle v \rangle_{t-t'}^{\text{eq}} \Gamma(t') . \tag{3.85}$$

3.7.2 Initial conditions in the infinite past

We discuss the evolution of all the quantities presented in the previous sections when the initial conditions are taken in the infinite past, i.e. $t_m \to -\infty$. This can be considered as a "stationary state" in a generalised sense, meaning that memory of initial conditions is lost and, as we will see in few lines, that the covariance matrix

has become constant. This can be easily seen again by considering the limits of the susceptibilities discussed in the appendix. For position and velocity, using again equations (3.20) and (3.21), what we get is

$$\langle \boldsymbol{x} \rangle_{-\infty,t} = \kappa \begin{pmatrix} \int_{-\infty}^{t} \mathrm{d}t' \chi_x(t-t')\lambda(t') \\ \int_{-\infty}^{t} \mathrm{d}t' \chi_v(t-t')\lambda(t') \end{pmatrix} . \tag{3.86}$$

As for the covariance matrix, we again use the expressions for the variance of position and velocity (3.28) and (3.33) alongside with their covariance (3.34), finding that

$$\lim_{t_m \to -\infty} \mathcal{S}_{-\infty,t} = \begin{pmatrix} \langle \Delta x^2 \rangle_{-\infty,t} & \mathrm{Cov}_{-\infty}(x_t, v_t) \\ \mathrm{Cov}_{-\infty}(x_t, v_t) & \langle \Delta v^2 \rangle_{-\infty,t} \end{pmatrix} = \begin{pmatrix} k_B T/\kappa & 0 \\ 0 & k_B T/m \end{pmatrix} . \tag{3.87}$$

As in the previous example starting form equilibrium, also for this sort of steady state we have that the covariance matrix does not depend on time for every driving protocol $\lambda(t)$.

The average work can be readily calculated using that $\chi(\infty) = 1/\kappa$ along with $\chi_x(\infty) = 0$, namely

$$\langle W \rangle_{-\infty,t} = \kappa \left(\frac{\lambda(t)^2}{2} - \kappa \int_0^t \mathrm{d}\lambda_{t'} \int_{-\infty}^{t'} \mathrm{d}t'' \chi_x(t'-t'')\lambda(t'') \right) . \tag{3.88}$$

As for its variance instead, we obtain that

$$\langle \Delta W^2 \rangle_{-\infty,t} = \langle \Delta W^2 \rangle_t^{eq} = 2k_B T \kappa \left(\frac{\lambda(t)^2}{2} - \kappa \int_0^t \mathrm{d}\lambda_{t'} \int_0^{t'} \mathrm{d}\lambda_{t''} \chi(t'-t'') \right) \tag{3.89}$$

i.e. the variance of the work in the generalised steady state is equal to the one starting from equilibrium conditions (3.82) for every driving protocol $\lambda(t)$.

Finally, for the entropy production rate we use equation (3.58) along with the fact that the covariance matrix is constant in order to obtain

$$\langle \sigma_{\mathrm{tot}} \rangle_{-\infty,t} = \frac{\widehat{\gamma} \langle v \rangle_{-\infty,t} \langle v_{\mathrm{ret}} \rangle_{-\infty,t}}{k_B T} , \tag{3.90}$$

with

$$\langle v_{\mathrm{ret}} \rangle_{-\infty,t} = \frac{1}{\widehat{\gamma}} \int_0^{\infty} \mathrm{d}t' \langle v \rangle_{-\infty,t-t'} \Gamma(t') . \tag{3.91}$$

3.7.2.1 Steady state

A particularly interesting case to consider is a linear dragging protocol of the form $\lambda(t) = vt$, where a non-equilibrium steady state is reached in the limit $t_m \to -\infty$. To understand why this happens, we recall that one usually defines the stationary distribution as the solution of the Fokker-Planck equation when the PDF does not depend explicitly on time. Nevertheless, this definition becomes problematic when the drift term or the diffusion coefficient of the associated Langevin equation depend explicitly on time, as in the cases we are considering in this chapter. To tackle this problem, first of all we note that if a sufficiently large time has passed from the

beginning of the dynamics, i.e. if $t_m \to -\infty$, the PDF $p_{t_m}(x_t, v_t, t)$ at time $t \geq 0$ will be a bivariate Gaussian with the usual form

$$\lim_{t-t_m\to+\infty} p_{t_m}(x_t, v_t, t) = \frac{1}{\sqrt{(2\pi)^2|\mathcal{S}_{t_m,t}|}} \exp\left[-\frac{1}{2}(\boldsymbol{x}_t - \langle \boldsymbol{x}\rangle_{t_m,t})\mathcal{S}^{-1}_{t_m,t}(\boldsymbol{x}_t - \langle \boldsymbol{x}\rangle_{t_m,t})\right], \tag{3.92}$$

depending on time via the averages of position and velocity and the covariance matrix. From (3.87) we see that for initial conditions taken in the infinite past the covariance matrix does not depend on time for every driving protocol $\lambda(t)$, but this does not happen in general for the averages of position of velocity, as it can be seen from equation (3.86).

We outflank this problem by moving the centre of the harmonic trap at constant speed, i.e. $\lambda(t) = vt$, so that we get the following GLE

$$m\ddot{x}(t) = -\int_{t_m}^{t} \mathrm{d}t' \Gamma(t-t')\dot{x}(t') - \kappa\left[x(t) - vt\right] + \eta(t)\,. \tag{3.93}$$

Performing the change of variable $y(t) = x(t) - vt$, we see that the system can be mapped through a Galilean transformation to the centre of the trap reference frame. This is always a consistent procedure for a GLE, as shown in [85]. Moreover, note that this transformation does not change the covariance matrix and that the new PDF $p_{t_m}(y_t, \dot{y}_t, t)$ will be defined by the same matrix along with $\langle y\rangle_{t_m,t}$ and $\langle \dot{y}\rangle_{t_m,t}$, which we will be now explicitly calculated. The transformed GLE hence becomes

$$m\ddot{y}(t) = -\int_{t_m}^{t} \mathrm{d}t' \Gamma(t-t')\dot{y}(t') - v\int_{t_m}^{t} \mathrm{d}t' \Gamma(t-t') - \kappa y(t) + \eta(t) \tag{3.94}$$

and its solution can be found similarly to that for the original GLE. In particular we find that

$$\langle y\rangle_{t_m,t} = \langle y_{t_m}\rangle(1 - \kappa\chi(t-t_m)) + m\langle \dot{y}_{t_m}\rangle\chi_x(t-t_m) - v\int_0^{t-t_m} \mathrm{d}t' \chi(t-t_m-t')\Gamma(t')\,. \tag{3.95}$$

Taking the limit $t_m \to -\infty$ and using the limits derived in Appendix A.1, we see that

$$\begin{aligned} \lim_{t_m\to-\infty} \langle y\rangle_{t_m,t} &= -v\chi(\infty)\int_0^\infty \mathrm{d}t' \Gamma(t') = -\frac{\widehat{\gamma}v}{\kappa}\,, \\ \lim_{t_m\to-\infty} \langle \dot{y}\rangle_{t_m,t} &= 0\,, \end{aligned} \tag{3.96}$$

which are both constant. We conclude that for a harmonic potential with constant strength and with centre travelling at constant speed ($\lambda(t) = vt$) it is possible, through a Galilean transformation, to map the system to another one for which an equilibrium distribution exists. In fact, the PDF $p_{t_m}(y_t, \dot{y}_t, t)$ inherits the Gaussian character from the PDF of the original variable $x(t)$. Thus, the PDF for $y(t)$ becomes time independent because the covariance matrix and the averages of the dynamical variables (3.96) are constant. In this sense we mean that $p_{t_m}(x_t, v_t, t)$ becomes stationary as $t_m \to -\infty$.

Introducing now the notation $\langle\cdot\rangle^{ss}$, meaning that we are considering stationary averages in the sense discussed above, we note that

$$\langle x\rangle_t^{\mathrm{ss}} = vt + \lim_{t_m\to-\infty}\langle y\rangle_{t_m,t} = vt - \frac{\widehat{\gamma}v}{\kappa}\,, \qquad \langle v\rangle_t^{\mathrm{ss}} = v\,, \tag{3.97}$$

i.e. they do not depend on the specific form of the memory kernel but only on the limit of its time integral. Moreover, note that the expressions above exhibit the same structure as in the usual Markov case where instead of $\widehat{\gamma}$ there appears the conventional Stokes friction coefficient γ_0.

Consider now the thermodynamic work, in particular equations (3.61) and (3.63) for the specific case of $\lambda(t) = vt$. For the average work we find

$$\langle W\rangle_t^{\mathrm{ss}} = \frac{\kappa v^2 t^2}{2} - \kappa v \int_0^t \mathrm{d}t' \langle x\rangle_{t'}^{\mathrm{ss}} = \widehat{\gamma} v^2 t\,, \tag{3.98}$$

that again has the same form as the well known Markov case. For the variance of the work, instead, we use the limits of susceptibilities discussed in Appendix A.1, hence obtaining

$$\langle \Delta W^2\rangle_t^{\mathrm{ss}} = k_B T \kappa v^2 \left(t^2 - 2\kappa \int_0^t \mathrm{d}t' \int_0^{t'} \mathrm{d}t'' \chi(t'') \right) . \tag{3.99}$$

As for the entropy production rate we immediately see that it has the same form as for Markov dynamics with the usual substitution $\gamma_0 \to \widehat{\gamma}$

$$\langle \sigma_{\mathrm{tot}}\rangle_t^{\mathrm{ss}} = \frac{\widehat{\gamma}\langle v\rangle_t^{\mathrm{ss}} \langle v_{\mathrm{ret}}\rangle_t^{\mathrm{ss}}}{k_B T} = \widehat{\gamma} v^2\,, \tag{3.100}$$

because

$$\langle v_{\mathrm{ret}}\rangle_t^{\mathrm{ss}} = \frac{1}{\widehat{\gamma}} \int_0^\infty \mathrm{d}t' \langle v\rangle_{t-t'}^{\mathrm{ss}} \Gamma(t') = \frac{v}{\widehat{\gamma}} \int_0^\infty \mathrm{d}t' \Gamma(t') = v\,. \tag{3.101}$$

Moreover, the constancy of the entropy production rate is another indicator that the scenario discussed above is indeed a stationary state.

3.7.3 Example: exponentially decaying memory kernel

As a standard example for non-Markovian dynamics, we examine a GLE with exponentially decaying memory kernel, as in Maxwell model for viscoelasticity [86]. In particular, we examine two cases: underdamped dynamics and overdamped dynamics. For causality, in both cases it holds that the memory kernel $\Gamma^{\exp}(t < 0) = 0$.

3.7.3.1 Underdamped dynamics

We first discuss the underdamped GLE with a purely exponential memory kernel

$$\Gamma^{\exp}(t) = \frac{\gamma}{\tau} \exp[-t/\tau] \quad \text{for } t \geq 0\,. \tag{3.102}$$

The characteristic time τ could emerge, for example, from the relaxation of the molecules or polymers in the reservoir. In the limit $\tau \to 0$, the symmetrized memory kernel tends to twice the Dirac delta

$$\lim_{\tau\to 0} \Gamma^{\exp}(|t|) = 2\gamma\delta(t) \tag{3.103}$$

and the Markovian limit is recovered.

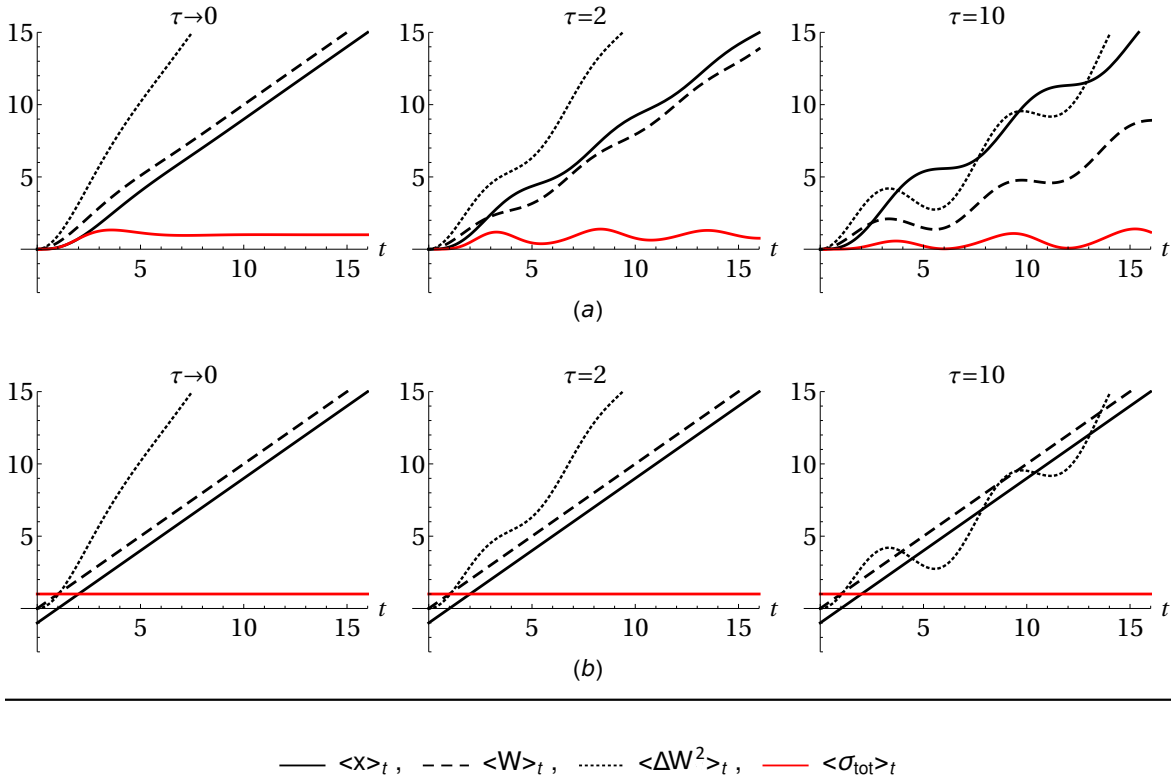

Figure 3.3: Time evolution of some of the quantities discussed in the previous sections starting from equilibrium (a) and from a stationary state (b) for linear dragging protocol $\lambda(t) = vt$. Parameters are set as $m = 1$, $\kappa = 1$, $\gamma = 1$ and $v = 1$. For (a) we see that as τ increases oscillations arise for all quantities while for (b) oscillations are visible only for $\langle \Delta W^2 \rangle_t^{ss}$ as it is equal to $\langle \Delta W^2 \rangle_t^{eq}$. Moreover, note that for the second column (i.e. $\tau = 2$), the effects of memory are still very present even at an observation time t equal to several multiples of τ.

For finite τ the underdamped susceptibilities display oscillations, as shown in figure 3.2. For memory kernels that are always positive, this feature is intimately related to the presence of a finite mass. In fact, as we will see in the next subsection, for overdamped dynamics oscillations appear only if the memory kernel has some negative components. This behaviour of the susceptibilities is of course reflected in all quantities considered in the previous sections, as one can see from figure 3.3(a), for a system starting from an equilibrium condition, even if the dragging protocol $\lambda(t) = vt$ is linear. In the stationary state, memory effects are not visible anymore in the averages of position, work and entropy production rate (they grow linearly, see figure 3.3(b)) but oscillations are still present in the variance of work, which we have shown to follow the same formula for transient dynamics and for the stationary state. The non-monotonicity with time of the work variance is clearly due to the memory stored by the complex fluid along with inertial effects. The variance of position and velocity are not shown in the figure as they are constant in both cases.

Finally, if we consider an intrinsically oscillating driving protocol of the form $\lambda(t) = A\sin(\omega t)$, the effects of memory may determine an increase of the amplitude of the already present oscillations, both from equilibrium (figure 3.4(a)), and in the steady state (figure 3.4(b)). Panels on the left in figure 3.4 represent the Marko-

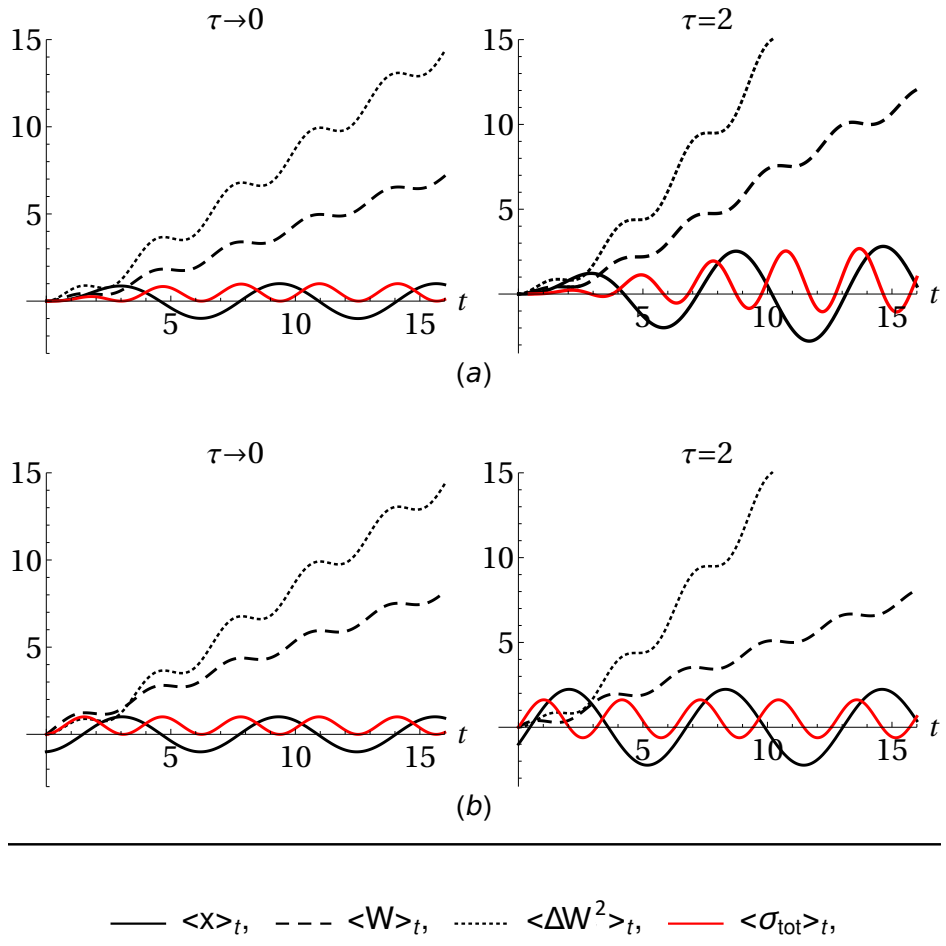

Figure 3.4: Evolution of the same thermodynamic quantities as in the previous figure starting from equilibrium (a) and for $t_m \to -\infty$ (b) for dragging protocol $\lambda(t) = Asin(\omega t)$. We set $m = 1$, $\kappa = 1$, $\gamma = 1$, $A = 1$ and $\omega = 1$. In both scenarios we observe an increasing amplitude of the oscillations that are already present because of the intrinsic oscillatory nature of the driving protocol. This is particularly evident for the average of the position. Another interesting feature that can be observed is that the entropy production rate can become negative as memory effects arise. Note that even in this case, differences between the two columns are still present at an observation time t much larger then τ.

vian limit while panels on the right show an example for an exponential memory kernel with $\tau = 2$. In the latter case, the average position fluctuates more, and the entropy production rate can become negative (while having a positive average over one cycle in the steady oscillatory regime).

We finish this section by noting that, even if the considered kernel is exponential, i.e. rapidly decaying, the effect of memory can extend to times much longer then the characteristic time τ of the kernel, as it can be seen from the figures.

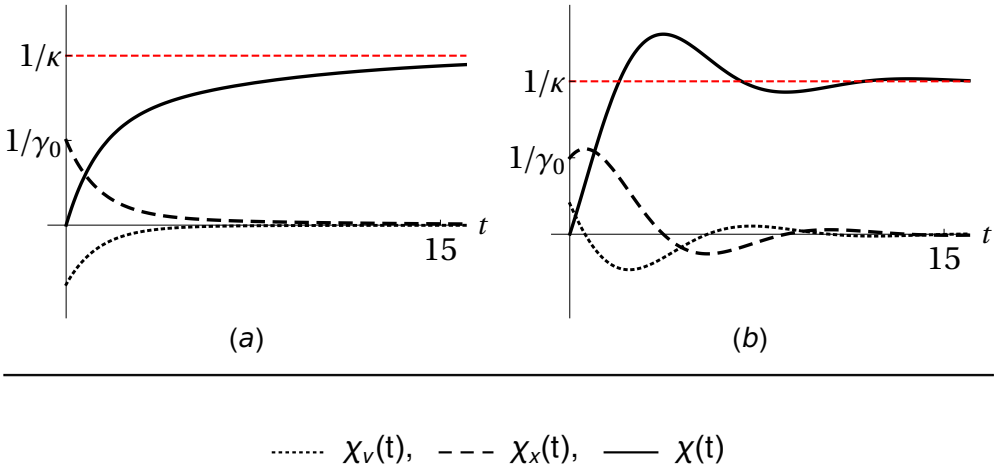

Figure 3.5: Overdamped ($m = 0$) susceptibilities for memory kernel of the form given in equation (3.104). For both figures we set $\kappa = 1$ and $\gamma_0 = 1$ while for the exponential part of the kernel we chose (a) $\gamma = 1$, $\tau = 5$ and (b) $\gamma = -0.9$, $\tau = 1$. The limits of the susceptibilities coincide with those calculated in Appendix A.1. Note that oscillations only appear in the case where the exponential part of the kernel is negative.

3.7.3.2 Overdamped dynamics

Here we consider the overdamped dynamics (3.64) with the memory kernel

$$\Gamma^{\exp}(t) = 2\gamma_0\delta(t) + \frac{\gamma}{\tau}\exp[-t/\tau] \quad \text{for } t \geq 0 \tag{3.104}$$

The Dirac delta part is necessary in the overdamped limit for reasons of mathematical consistency, as shown in Appendix A.1 and [87]. Examples of susceptibilities for this kind of dynamics are displayed in figure 3.5. In particular, one sees that for $\gamma \geq 0$ the susceptibilities exhibit no oscillations, differently from the case with $\gamma < 0$ that is more alike to the underdamped case. The similarities between the overdamped GLE with negative memory kernels and underdamped dynamics has already been discussed in [82]. For this reason, in the following discussion we will mainly focus on the case with positive memory kernel.

Figure 3.6 shows the behaviour of the same quantities considered in the previous subsection for a linear dragging protocol $\lambda(t) = vt$. The differences between the plots for different values of τ are smaller than in the underdamped case shown in figure 3.3. This is due to the absence of oscillations. Nevertheless, for integrated quantities such as average work and its variance, the effect of a finite τ is evident for every $t > 0$ (figure 3.7). In this case, the effects of memory determine a delay in the accumulation of thermodynamic work and in its variance. As a consequence, after some multiples of the characteristic time τ, we observe a constant difference between the averages (starting from equilibrium) and variances (both from equilibrium and stationary state) of work for different values of τ. This difference does not vanish in time and is also found for the entropy production (not shown). Thus, the exponential memory kernel influences the value of integrated quantities beyond its time scale τ even in the overdamped limit.

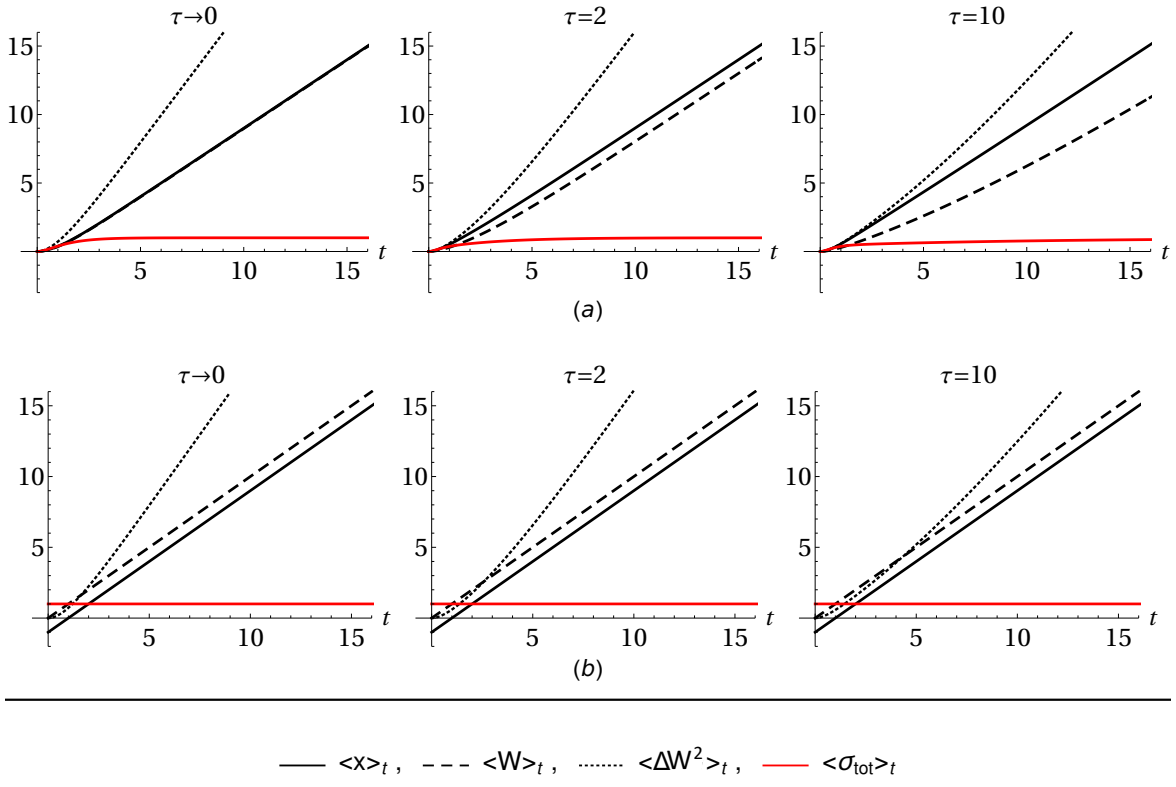

Figure 3.6: For the overdamped case, evolution of the same quantities considered for the underdamped case starting (a) from equilibrium and (b) from a stationary state, for linear dragging protocol $\lambda(t) = vt$. Parameters are set as $\kappa = 1$, $\gamma_0 = 0.5$, $\gamma = 0.5$ and $v = 1$. For (a) we see that the main differences between the plots are visible for average work and its variance while for (b) this only happens for $\langle \Delta W^2 \rangle_t^{ss}$ (that is, as we have shown in the previous sections, equal to the one starting from equilibrium $\langle \Delta W^2 \rangle_t^{eq}$).

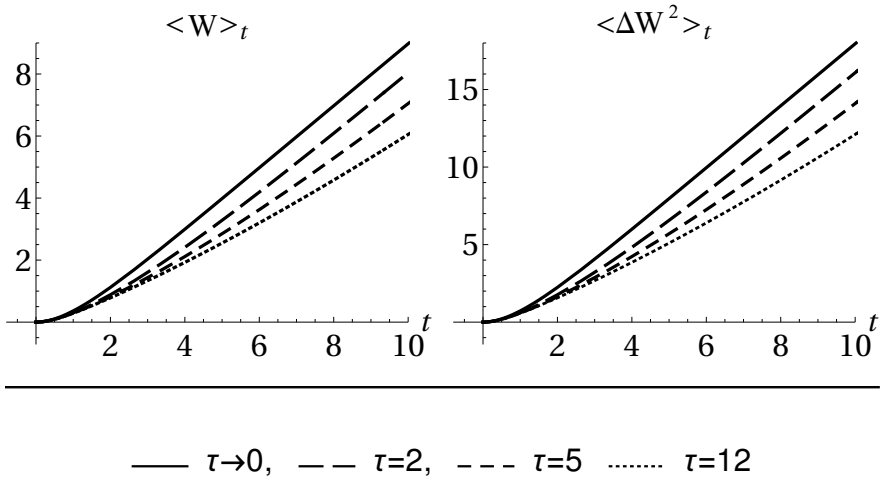

Figure 3.7: Evolution of average work starting from equilibrium on the left panel and variance of work (equal from equilibrium or from stationary state) on the right, for the overdamped case (parameters as in the previous figure).

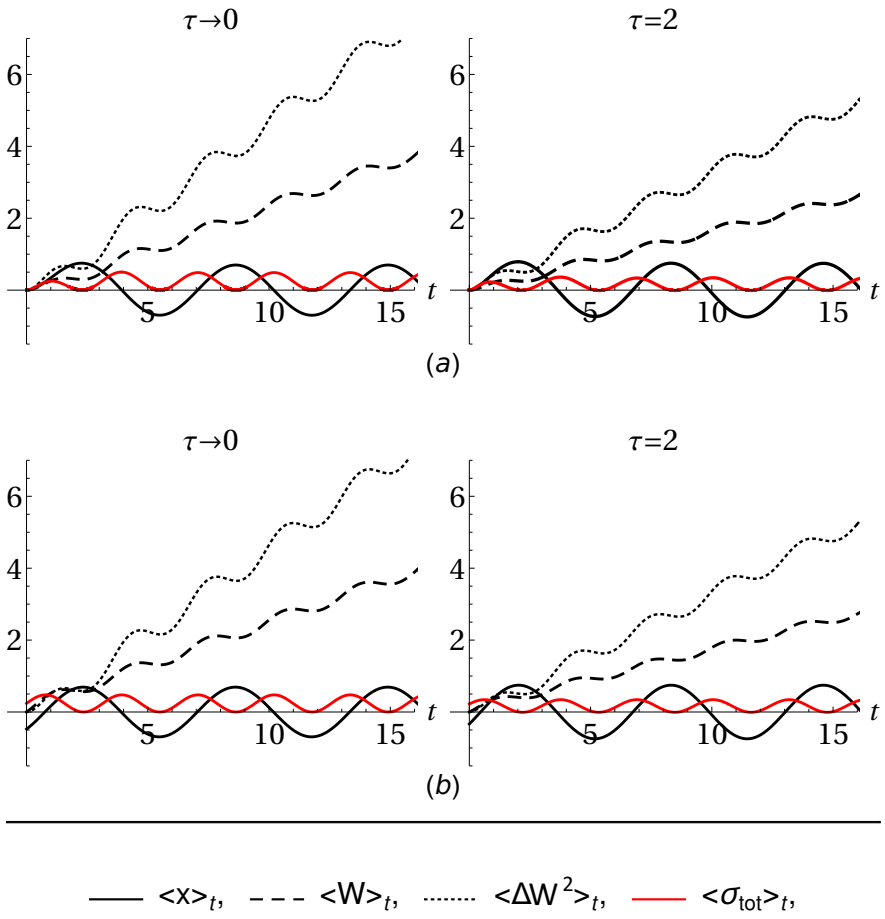

Figure 3.8: For the overdamped case, time evolution of the already discussed thermodynamic quantities from equilibrium (a) and for $t_m \to -\infty$ (b) for intrinsically oscillating dragging protocol $\lambda(t) = A\sin(\omega t)$. We chose $\kappa = 1$, $\gamma_0 = 0.5$, $\gamma = 0.5$, $A = 1$ and $\omega = 1$. As before, we note important differences between the two columns concerning integrated quantities such as average work and variance, while average position and total entropy production rate are basically unaffected by the presence of memory.

A similar behaviour is observed for the case of an intrinsically oscillating driving protocol $\lambda(t) = A\sin(\omega t)$. Indeed, figure 3.8 shows that the effects of memory are again very evident for average work and variance, while average position and entropy production rate are not strongly affected.

3.8 Chapter conclusions

The Gaussian process with memory is a classic in statistical mechanics. Yet, we have shown that further results can be derived for this process realised by a generalised Langevin equation for a particle driven by a harmonic trap with constant strength in a complex fluid. An explicit solution of the GLE is based on computing susceptibilities. In terms of these important dynamical quantities, several other expressions are derived.

For generic protocols and initial Gaussian conditions, the quantities we com-

puted for every time $t \geq 0$ are the average particle position (3.20), its autocorrelation function (3.26) and hence its variance (3.28), the average work done on the system (3.61), its variance (3.63), and the entropy production rate (3.58). These formulas can be simplified in some standard scenarios, e.g. starting from equilibrium or in steady states. Moreover, the variance of the work starting from equilibrium is equal to that for a steady state in a generalised sense and is proportional to the average of work starting from the same initial conditions. Since we can deal with various dragging protocols, this means that the two cumulants for the work (3.83) generalise formulas by van Zon and Cohen [66].

Especially aiming at dealing with steady states, everything starts by introducing a new Laplace transform with arbitrary initial time t_m. The explicit dependence of the solution on t_m along with the well-defined behaviour of the susceptibilities for the limits $t \to 0$ and $t \to \infty$ allow us to recognise a steady state for a linear dragging protocol $\lambda(t) = vt$ as $t_m \to -\infty$. More in general, for an arbitrary protocol, this limit leads to a loss of the information about the initial state. We can interpret it as a generalised steady state.

Going into some more details about the quantities calculated throughout the chapter, for a steady state generated by a linear dragging protocol we recognise the same structure of the average of position and of velocity, and of their covariance matrix, as for usual Markov dynamics. Finally, we are able to write the entropy production rate in terms of a quantity that we termed the retarded velocity, matching the usual velocity if no memory effects are included in the kernel.

In conclusion, we note that this framework yields average quantities but also their variances. Hence it is used to derive one of the first examples of thermodynamic uncertainty relations with memory [88, 89], whose derivation and discussion can be found in Section 5.5.

CHAPTER 4

INFORMATION GEOMETRY AND CRAMÉR-RAO BOUND

In this chapter we briefly review some fundamental concepts of information geometry which are propaedeutic to the derivation of stochastic uncertainty relations. This will be done by means of the Cramér-Rao bound, a fundamental result involving arguably the most important information-theoretic quantity, namely the *Fisher information*. Information geometry [90] is a branch of information theory that exploits differential geometry to describe information and to study probability theory and statistics. For this reason, we will start from the discussion of basic notions of differential geometry, found in Section 4.1 and mainly based on the second and third chapter of Carroll's book on general relativity [91]. This will in turn enable us to introduce the concept of *statistical manifold* in Section 4.2 and to derive the Cramér-Rao bound in Section4.3. The latter will then serve as a starting point for the discussion of stochastic inequalities

4.1 Basics of differential geometry

The foundation of differential geometry is mostly credited to Carl Friedrich Gauss and Bernhard Riemann, the latter being the first one to consider and describe the central concept of *manifold*. A manifold captures the idea of a space which may be curved and may have a non trivial topology but looks just like R^n locally. Two simple examples of manifolds are trivially R^n itself and the n-dimensional sphere S^n that looks flat, i.e. similar to R^n, in local regions but it is curved globally. The probably most eminent example of application of differential geometry is of course Albert Einstein's theory of general relativity, where space-time itself is considered as a 4-dimensional manifold and gravity becomes the manifestation of the curvature of space-time. The curvature is quantified by the *metric tensor*, a fundamental mathematical object that will be discussed later, and caused is by the presence of masses. As a consequence, a probe particle moving freely in such a curved space-time follows a minimum length path called *geodesics* that is, for flat spaces for example, nothing else then a straight line while for a sphere it would be a circle with the same centre of the sphere.

The obvious starting point for the discussion of the proprieties of manifolds is their definition [92]. An n-dimensional manifold is a set $\mathcal{M}$ that comes along with an indexed collection $\mathcal{A}$ of *charts* $(U_\alpha, \varphi_\alpha)$, such that:

- U_α is a subset of $\mathcal{M}$ and $\varphi_\alpha : U_\alpha \to \mathrm{R}^n$ is one-to one (or injective) $\mathcal{C}^\infty$ map, i.e. infinitely times differentiable, and whose image $\varphi_\alpha(U_\alpha)$ is an open set in R^n.

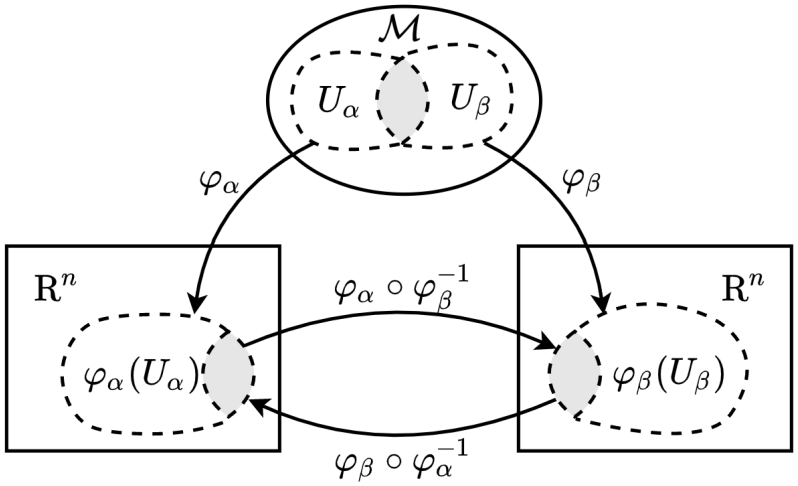

Figure 4.1: Commutative diagram showing the compatibility of the charts.

We point out that a map is a simple generalisation of a function between arbitrary sets and that as it holds for functions, any injective map is onto its image and hence $\varphi_\alpha : U_\alpha \to \varphi_\alpha(U_\alpha)$ is invertible. Moreover, we require its inverse to be a $\mathcal{C}^\infty$ map as well, in this case the map φ_α is also called a diffeomorphism.

- The set $\mathcal{U} = \{U_\alpha\}_{\alpha=1,\dots,N}$ is such that $\bigcup_{\alpha=1}^{N} U_\alpha = \mathcal{M}$, i.e. $\mathcal{U}$ covers $\mathcal{M}$.
- The charts $(U_\alpha, \varphi_\alpha)$ are smoothly sewn together, which means that if two charts overlap $U_\alpha \cap U_\alpha \neq \varnothing$, then the composition map $\varphi_\alpha \circ \varphi_\beta^{-1}$ is itself $\mathcal{C}^\infty$ from $\varphi_\beta(U_\alpha \cap U_\beta) \in \mathrm{R}^n$ to $\varphi_\alpha(U_\alpha \cap U_\beta) \in \mathrm{R}^n$, see Figure 4.1.

With these requirements the *maximum atlas* $\mathcal{A} = \{(U_\alpha, \varphi_\alpha)\}_{\alpha=1,\dots,N}$, i.e. the one containing every possible compatible chart, defines the differentiable manifold along with the set $\mathcal{M}$. In other words, a chart can be regarded as what we usually consider a coordinate system on the set U_α, and an atlas is a collection of charts which are smoothly related where they overlap. Moreover, the requirement of a maximal atlas is necessary as a means to avoid that two equivalent spaces endowed with different atlases are considered as different manifolds. Also, the fact that more charts are required, in addition of course to their compatibility, in order to define a manifold rather than just a single one can be easily understood as we consider the standard coordinate system for a 1-dimensional sphere, that is $\theta : \mathrm{S}^1 \to \mathrm{R}$. This map associates every point of the sphere with a value between 0 and 2π starting, for example, from the top of the circle where $\theta = 0$ and wrapping around counterclockwise up to 2π. The problem is that, if we want to include either the point $\theta = 0$ or $\theta = 2\pi$ in order to cover the whole circle, then the image $\theta(S)$ would not be open and hence one would violate the definition of manifold. Otherwise, if those points are not included, we fail to cover the whole sphere and hence we conclude that we need at least two charts to cover the whole manifold. The same issue appears with the 2-dimensional sphere where a canonical coordinate system called *stereographic projection* is often used. Indeed, in this case, one fails again to find a single chart covering the whole sphere for the same reasons as above. This is a common feature of many manifolds, especially compact ones, but there are also some that can be

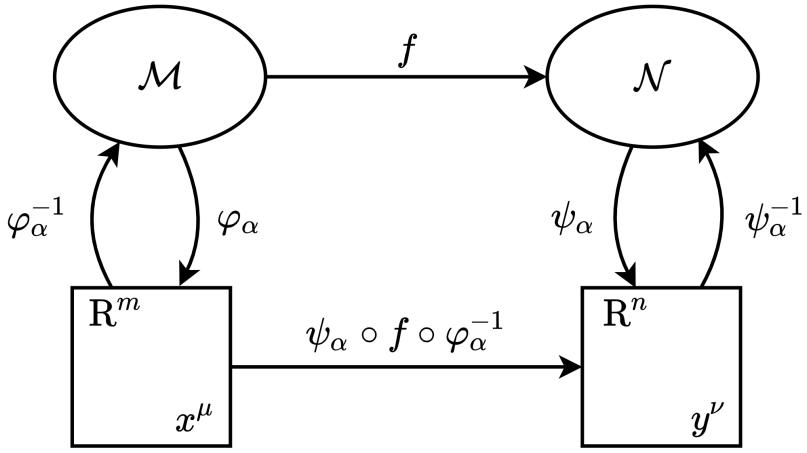

Figure 4.2: Commutative diagram for a function $f : \mathcal{M} \to \mathcal{N}$ and its composition with the charts defining the manifolds.

covered with a single chart, as is the case of the infinite cylinder $\mathrm{R} \times \mathrm{S}$. Nevertheless, when a global chart is not available, one still usually works with a one single chart and just keeps track of all the points which are not included. Finally, we point out that the requirement of the image $\varphi_\alpha(U_\alpha)$ associated to a given chart to be an open set in R^n is topologically founded (its deep reasons are beyond the scope of this work) and that the condition of the maps $\{\varphi_\alpha\}$ to be $\mathcal{C}^\infty$ is not necessary (we could replace it with $\mathcal{C}^p$, $p \geq 1$, and nothing would change in the discussion of the incoming lines).

The definition of manifold given above captures in formal terms the intuitive notion of a set that locally looks just like R^n but is not necessarily embedded in some higher-dimensional Euclidean space. The fundamental propriety of being similar to R^n, guaranteed by how the charts are constructed, introduces the possibility of doing standard calculus on manifolds, that is performing derivatives and integration. Indeed, consider a function between two manifolds $f : \mathcal{M} \to \mathcal{N}$ equipped with two set of charts $\{(U_\alpha, \varphi_\alpha)\}$ and $\{(V_\alpha, \psi_\alpha)\}$ and of dimension m and n respectively. In this case, one can not simply take the derivative of f because no notion of differentiability is defined in this case. Instead, the functions $\psi_\alpha \circ f \circ \phi_\alpha^{-1}$ are just functions between R^m and R^m (where they are defined) and of course one can consider the derivatives, for examples, with respect to the local coordinates $x^\mu \in \mathrm{R}^m$ (μ is an index going from 1 to m), so that the derivative of f can be defined as

$$\frac{\partial f}{\partial x^\mu} = \frac{\partial}{\partial x^\mu}(\psi_\alpha \circ f \circ \phi_\alpha^{-1})(x^\mu)\,, \tag{4.1}$$

see Figure 4.2 for the complete commutative diagram. Having said this, one can now discuss tangent spaces and vectors. Without going to much into detail, we can say that the tangent space to a point p of a manifold $\mathcal{M}$, that is $T_p\mathcal{M}$, is the *space of directional derivatives operators along all the curves passing by p*. To make an idea of what this means, lets consider a curve $\gamma(\lambda) : \mathrm{R} \to \mathcal{M}$ parametrised by a parameter λ and such that $\gamma(\lambda = 0) = p$. Using (4.1) and the diagram depicted in Figure 4.3, for some coordinate system x^μ on $\mathcal{M}$ one finds that the tangent vector to the curve becomes

$$V_\gamma(p) = \frac{\mathrm{d}}{\mathrm{d}\lambda}\varphi \circ \gamma\big|_{\lambda=0} = \frac{\mathrm{d}x^\mu}{\mathrm{d}\lambda}\Big|_{\lambda=0}, \tag{4.2}$$

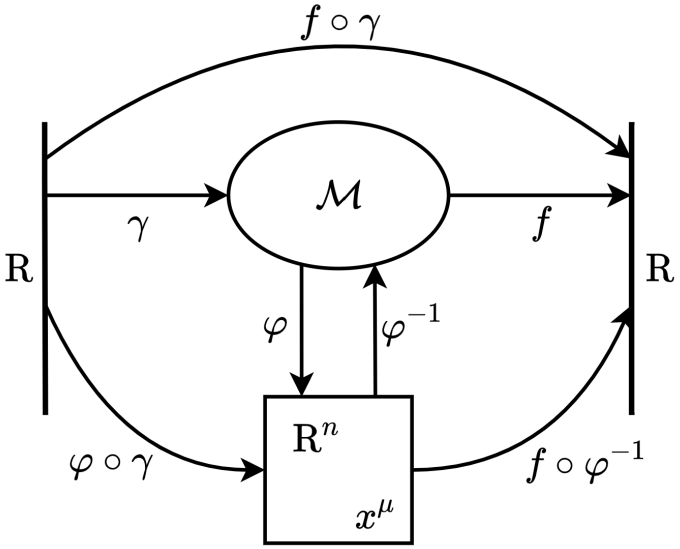

Figure 4.3: Commutative diagram for a curve $\gamma : \mathrm{R} \to \mathcal{M}$, a function $f : \mathcal{M} \to \mathrm{R}$ and their composition with the charts defining the manifold $\mathcal{M}$.

which also represent the velocity vector at which the coordinate x^μ is moving along γ (and where we have also dropped the indexes of the charts). One could say that the tangent space is the collection of all these tangent vectors associated to all the curves passing by p on $\mathcal{M}$, but this definition would be coordinate dependent, which should be clear from (4.2). Moreover, there exist infinitely many curves passing along p that have the same tangent vector as in equation (4.2). The solution to these issues is rather formal and passes through the definition of the equivalence class of curves such that, if two parametrised curves $\gamma_1(\lambda)$ and $\gamma_2(\lambda)$ are such that $\gamma_1(0) = \gamma_2(0) = p$ and $V_{\gamma_1}(p) = V_{\gamma_2}(p)$ for every coordinate chart φ, then they are considered equivalent, i.e $\gamma_1 \equiv \gamma_2$. Using this, one can now construct a vector space whose elements are all the tangent vectors to the point p on $\mathcal{M}$, one for each representative of the equivalence class defined above, that is the tangent space $T_p\mathcal{M}$. Note that this definition is coordinate independent and the identification between vectors and equivalence classes is unique. Actually, the elements of $T_p\mathcal{M}$ are not vectors in the common sense but, rather, a set of derivative operators that form a vector space and such that, if V is an element of this vector space and $f : \mathcal{M} \to \mathrm{R}$ a differentiable function defined around p, the action of V_γ on f gives a well-defined directional derivative along V, that is

$$V_\gamma(f) = \frac{\mathrm{d}}{\mathrm{d}\lambda} f(\gamma(\lambda)) \,, \tag{4.3}$$

for γ some representative of the equivalence class defined above (see again Figure 4.3 for the complete diagram). One can also indeed verify that the directional derivative operators form a vector space since, given two elements $\frac{\mathrm{d}}{\mathrm{d}\lambda}$ and $\frac{\mathrm{d}}{\mathrm{d}\eta}$, their sum $\frac{\mathrm{d}}{\mathrm{d}\lambda} + \frac{\mathrm{d}}{\mathrm{d}\eta}$ is still a directional derivative as it is clearly linear and, moreover, it can be shown that it respects the Leibniz rule of derivation. To sum up, the definition given above of tangent space $T_p\mathcal{M}$ formalises the intuitive idea of a space containing all possible directions in which one can tangentially pass through a point p on $\mathcal{M}$.

Having this formal definition in mind, one can now proceed to construct a useful basis for the tangent vector space. A convenient choice corresponds to take the set of partial derivatives with respect to some coordinate chart x^μ, i.e. $\partial_\mu \equiv \frac{\partial}{\partial x^\mu}$. Indeed, looking again at Figure 4.3 and using the definition of the directional derivative of an arbitrary function f (4.3) one can immediately see that

$$\begin{aligned} V_\gamma(f) &= \frac{\mathrm{d}}{\mathrm{d}\lambda} f \circ \gamma(\lambda) = \\ &= \frac{\mathrm{d}}{\mathrm{d}\lambda}[(f \circ \varphi^{-1}) \circ (\varphi \circ \gamma(\lambda))] = \\ &= \frac{\mathrm{d}}{\mathrm{d}\lambda}(\varphi \circ \gamma(\lambda)) \frac{\partial}{\partial x^\mu}(f \circ \varphi^{-1}) = \frac{\mathrm{d}x^\mu}{\mathrm{d}\lambda} \partial_\mu f \,, \end{aligned} \tag{4.4}$$

where between the second and the third line we used the chain rule and between the third and the last one we used the definition of the derivative of a function (4.1). Since the function f is arbitrary, one immediately sees that every vector, i.e. the differential operators V_γ, of the tangent space can be decomposed in a basis given by the partial derivatives $\{\partial_\mu\}$ with coefficients $\frac{\mathrm{d}x^\mu}{\mathrm{d}\lambda}$. The latter are often used to indicate the whole vector as the canonical base is implied. Moreover, from now on we use Einstein's notation of repeated indexes meant as summed over, as it is the case at the end of the last line of equation (4.4). We further add that as it is known, the position up and down of the indexes is important, as it will pointed out later, and that summed over indexes must be in a different position (one up and one down). Indeed, objects having components with upper indexes are called *contravariant* vectors, or just vectors, and belong to the tangent space $T_p\mathcal{M}$ while those having components with lower indexes are named as *covariant* vectors, covectors or one-forms, which live in the cotangent space $T_p^*\mathcal{M}$. The latter is nothing else then the dual space of $T_p\mathcal{M}$, i.e. the vector space of linear applications $\omega : T_p\mathcal{M} \to \mathrm{R}$. The classical example of a covector is the gradient of a function f, that is

$$\mathrm{d}f\left(\frac{\mathrm{d}}{\mathrm{d}\lambda}\right) = \frac{\mathrm{d}f}{\mathrm{d}\lambda} \,. \tag{4.5}$$

Just as the partial derivatives with respect to the coordinates x^μ provide a convenient basis for $T_p\mathcal{M}$, the gradients of the coordinate functions fulfil the role of being a good basis for the cotangent space. These gradients are also called the differentials $\mathrm{d}x^\mu$ and are such that

$$\mathrm{d}x^\mu(\partial_\nu) = \delta^\mu_\nu \,, \tag{4.6}$$

where δ^μ_ν is the Kronecker delta. As a consequence, any element ω of the cotangent space can be decomposed in this basis and be written as $\omega = \omega_\mu \mathrm{d}x^\mu$, where ω_μ are its components with lower indexes. Its action on a vector $V = V^\nu \partial_\nu$ hence becomes

$$\omega(V) = \omega_\mu V^\nu \mathrm{d}x^\mu(\partial_\nu) = \omega_\mu V^\nu \delta^\mu_\nu = \omega_\mu V^\mu \tag{4.7}$$

because for any vector or covector it holds that $V^\nu \delta^\mu_\nu = V^\mu$ and $\omega_\mu \delta^\mu_\nu = \omega_\nu$ respectively and because summed over indexes can be arbitrarily renamed.

Before moving on to the true reason why we introduced all these concept, it is worth mentioning one of the most important consequences of everything we have discussed so far. One of the most basic operations one can do in geometry and

physics is the a change of coordinates, lets say from x^μ to x^ν. Under this transformation, the basis vectors obtained from the new coordinate system can be expressed in terms of the old coordinates by using the chain rule, that is

$$\partial_\nu = \frac{\partial x^\mu}{\partial x^\nu}\partial_\mu \tag{4.8}$$

where $J^\mu_\nu = \frac{\partial x^\mu}{\partial x^\nu}$ is the Jacobian matrix of the transformation and has two indexes (one upper and one lower). It is straightforward now to find the law of transformation of the components of a vector in a new basis, i.e.

$$V = V^\mu \partial_\mu = V^\nu \partial_\nu = V^\nu \frac{\partial x^\mu}{\partial x^\nu}\partial_\mu \tag{4.9}$$

implying that

$$V^\nu = \frac{\partial x^\nu}{\partial x^\mu} V^\mu \,, \tag{4.10}$$

where $\frac{\partial x^\nu}{\partial x^\mu}$ is the inverse of the Jacobian matrix. This means that the vector components transform with the inverse of the matrix that transforms the basis vectors, this is why they are called *contravariant* vectors. In a similar way one could also show that, instead, the components of a one form transform with the Jacobian matrix as well, i.e.

$$\omega_\nu = \frac{\partial x^\mu}{\partial x^\nu}\omega_\mu \,. \tag{4.11}$$

This is why they are called *covariant* vectors. As it is known, the laws of transformation of coordinates play a central role in physics and, of course, it is impossible to summarise all the crucial consequences that derive from the proprieties depicted above in few lines. What we will do instead, will be to just say that writing equations in terms of vectors, covectors and their generalisation, i.e. tensors, all having a definite transformation law, is at the very least a fundamental feature of every equation relevant to physics. The last step towards the end of this short introduction to differential geometry consists in introducing the concept of tensor, based on the notion of tensor product. Given two vector spaces $\mathcal{V}, \mathcal{W}$ with elements (V, W) along with their duals $\mathcal{V}^*, \mathcal{W}^*$ with elements (V^*, W^*), then the vector space $\mathcal{V}^* \otimes \mathcal{W}^*$ with elements $V^* \otimes W^*$ is the space of bilinear functions such that

$$(V^* \otimes W^*)(V, W) = V^*(V)\, W^*(W) \,. \tag{4.12}$$

One can also build arbitrarily larger vector spaces by combining with the tensor product many different copies of vector and dual spaces. Indeed, for a given point p on a manifold $\mathcal{M}$, one can define a rank (r, s) tensor T^r_s as an element of

$$T^r_s \in \underbrace{T_p\mathcal{M} \otimes \cdots \otimes T_p\mathcal{M}}_{\text{r times}} \otimes \underbrace{T^*_p\mathcal{M} \otimes \cdots \otimes T^*_p\mathcal{M}}_{\text{s times}} \,, \tag{4.13}$$

which in components reads

$$T = T^{\mu_1,\ldots,\mu_r}_{\nu_1,\ldots,\nu_s}\, \partial_{\mu_1} \otimes \cdots \otimes \partial_{\mu_r} \otimes \mathrm{d}x^{\nu_1} \otimes \cdots \otimes \mathrm{d}x^{\nu_s} \,. \tag{4.14}$$

It is convenient, as usual, to forget about the elements of the basis and just use the components $T^{\mu_1,\ldots,\mu_r}_{\nu_1,\ldots,\nu_s}$. Nevertheless, for our purposes a tensor is nothing else then

a mathematical object that it has many indexes, namely a generalisation of vector and matrices, that transforms in a definite way, i.e.

$$T^{\mu'_1,\dots,\mu'_r}_{\nu'_1,\dots,\nu'_s} = \frac{\partial x^{\mu'_1}}{\partial x^{\mu_1}} \cdots \frac{\partial x^{\mu'_r}}{\partial x^{\mu_r}} \frac{\partial x^{\nu_1}}{\partial x^{\nu'_1}} \cdots \frac{\partial x^{\nu_s}}{\partial x^{\nu'_s}} T^{\mu_1,\dots,\mu_r}_{\nu_1,\dots,\nu_s} . \tag{4.15}$$

Again, we stress that the knowledge of transformation laws is a key feature of tensors and is the main reason why they are used in physics.

Among all possible tensors that one can built starting from tangent and cotangent spaces of a manifold, arguably the most important one is the metric tensor,

$$g = g_{\mu\nu}\, \mathrm{d}x^\mu \otimes \mathrm{d}x^\nu \tag{4.16}$$

that is also the main reason we introduced all the machinery of differential geometry. g is a $(0,2)$ symmetric tensor, i.e. such that $g_{\mu\nu} = g_{\nu\mu}$, with a non-null determinant $|g| \neq 0$. This last requirement guarantees the existence of an inverse $g^{\mu\nu}$ such that

$$g^{\mu\sigma}\, g_{\sigma\nu} = \delta^\mu_\nu . \tag{4.17}$$

Moreover, the action of the metric tensor on two vectors $V = V^\mu \partial_\mu$ and $W = W^\mu \partial_\mu$ follows from the definition of the metric (4.16) , of differential (4.6) and tensor product (4.12)

$$\begin{aligned} g(V,W) =& g_{\mu\nu}\, V^\rho\, W^\sigma\, \mathrm{d}x^\mu(\partial_\rho)\, \mathrm{d}x^\nu(\partial_\sigma) = \\ =& g_{\mu\nu}\, V^\rho\, W^\sigma\, \delta^\mu_\rho\, \delta^\nu_\sigma = \\ =& g_{\mu\nu}\, V^\mu\, W^\nu . \end{aligned} \tag{4.18}$$

The metric tensor, as well as any other quantity constructed from the tangent and cotangent space, has coordinates which in general depend on the point p of the manifold which actually makes it a tensor field $g_{\mu\nu}(x^\mu)$, i.e. a mathematical object that assigns a tensor to every point of the manifold. The fact that the components of the metric tensor are constant in at least one coordinate system assures that the space is flat. Moreover, it can be shown that the function

$$g_p : T_p\mathcal{M} \to T^*_p\mathcal{M} \tag{4.19}$$

is an isomorphism and hence, the metric tensor and its inverse can be used to raise and lower indexes, i.e. $v_\mu = g_{\mu\nu} v^\nu$ and $\omega^\mu = g^{\mu\nu}\omega_\nu$. In flat space and in the canonical basis, the metric tensor is just the identity and hence there is no difference between upper and lower indexes.

Arguably the most important propriety of the metric tensor is that it induces a scalar product on the manifold and, as a consequence, a notion of length and distance which is not intrinsic to the manifold. Indeed, by looking at equation (4.16) and dropping the tensor product sign, we can introduce the notion of infinitesimal line element

$$ds^2 = g_{\mu\nu}\, \mathrm{d}x^\mu \mathrm{d}x^\nu \tag{4.20}$$

which can informally be seen as the length of the infinitesimal displacement on the manifold associated to an infinitesimal change of coordinates x^μ. The length of a

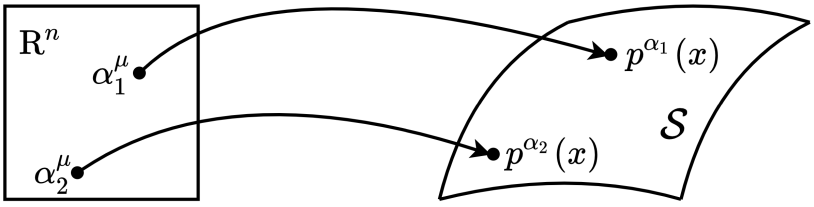

Figure 4.4: Definition of a statistical manifold.

path on $\mathcal{M}$, represented by the curve $\gamma : \mathrm{R} \to \mathcal{M}$ with $\gamma(0) = a$ and $\gamma(\Lambda) = b$ can be hence computed as

$$\mathcal{L}_\gamma(a,b) = \int_a^b ds = \int_0^\Lambda \mathrm{d}\lambda \sqrt{g\left(\frac{\mathrm{d}\gamma(\lambda)}{\mathrm{d}\lambda}, \frac{\mathrm{d}\gamma(\lambda)}{\mathrm{d}\lambda}\right)}\,. \tag{4.21}$$

The path that minimises this length functional is called a *geodesics*, that also is the trajectory of a free object moving in a curved space with a given metric. If the metric tensor is positive defined, it is also called a Riemannian metric and the manifold equipped with it is called a *Riemannian manifold*. This would imply that, for every vector $V = V^\mu \partial_\mu \neq 0$ and using (4.18), $g_{\mu\nu}$ is such that $g(V,V) = g_{\mu\nu}V^\mu V^\nu \geq 0$ and same thing for the length functional (4.21). For a given manifold, the existence of such a metric is guaranteed by a theorem by Riemann. Otherwise, for a n-dimensional manifold and a metric whose maximal subspace where it is positive defined is s-dimensional, with $s < n$, and same thing for the maximal r-dimensional subspace ($r = n - s$) where it is negative defined, one speaks then about a pseudo-Riemannian metric, whose existence is however not guaranteed for an arbitrary manifold. Nevertheless, if it exists, the pseudo-Riemannian metric is said to be of signature (r,s) and the positivity of the length of every vector is not true anymore. In general relativity, physicists are concerned with metric tensor fields, which are the solution of Einstein's equations for the gravitational field, that are of signature (3,1).

To sum up, in the last pages we scratched the surface of what the field of differential geometry is concerned about and, of course, many other concepts and mathematical techniques arise from the principles shown above. However, even with this basic knowledge, we will be able to tackle the issue of uncertainty relations in the context of information geometry. Indeed, the main ingredient for the reasoning that will follow will be the *Fisher information metric*, a metric that induces a notion of distance between parametrised statistical models which, as we will show in a few lines, can be regarded as a differentiable manifold.

4.2 Statistical manifolds and Fisher information

The starting point of this subsection is the definition of a parametrised statistical model, or just parametric model, that is a collection of parameter dependent PDFs $p(\omega|\alpha)$, defined on some sample space $\omega \in \Omega$, and such that $\alpha \in \mathcal{A} \subset \mathrm{R}^n$. In formulae

$$\mathcal{S} = \{p^\alpha = p(\omega|\alpha) \mid \alpha \in \mathcal{A}\}\,. \tag{4.22}$$

The key idea on which information geometry is based is that the set $\mathcal{A}$, called the parameter space, serves as a (possibly local) coordinate system for the statistical manifold $\mathcal{S}$, as it can be seen from Figure 4.4. This means that, for a given parameter vector α there is a probability distribution $p(\omega|\alpha)$, each labelled by a point $s(\alpha)$ in the manifold S. Moreover, if one assumes that $\mathcal{S}$ is such that the support of each PDF is invariant under arbitrarily change of parameters, then one can verify that all parametrisations related by a diffeomorphism, i.e. a differentiable isomorphism whose inverse is itself differentiable, can be considered to be equivalent. Because of that and because the parametrisations are taken as the charts for $\mathcal{S}$, we can indeed consider the latter to be a differentiable manifold whose charts are compatible and related by diffeomorphisms. A simple example of statistical manifold is the one represented by the family of Gaussian PDFs, that is

$$\mathcal{S}^{\text{Gauss}} = \{p^{\mu,\sigma} = p(x|\{\mu,\sigma\}) \mid \{\mu,\sigma\} \in \mathrm{R} \times \mathrm{R}^{+}\}\,, \tag{4.23}$$

$$p(x|\{\mu,\sigma\}) = \frac{1}{\sqrt{2\pi\sigma^2}} \exp\left[-\frac{(x-\mu)^2}{2\sigma^2}\right] \tag{4.24}$$

and, of course, it is 2-dimensional.

The next step consists in adding a metric to the manifold defined above. The natural choice falls on the so called *Fisher information matrix* $\mathcal{I}_{ij}(\alpha)$ defined as

$$\mathcal{I}_{ij}(\alpha) = g_{ij}(\alpha) = \int \mathrm{d}\omega\; p^{\alpha}(\omega)\, \partial_{\alpha_i} \ln p^{\alpha}(\omega)\, \partial_{\alpha_j} \ln p^{\alpha}(\omega)\;. \tag{4.25}$$

This metric, which is of course symmetric, induces a notion of distance on the manifold $\mathcal{S}$ and makes it possible to measures the "closeness" between two distribution functions. We can also verify that this metric is positive defined since, for every vector $V = V^i\, \partial_{\alpha_i}$ and using (4.18), it holds that

$$\begin{aligned} \mathcal{I}(V,V) &= \mathcal{I}_{ij}(\alpha)\, V^i V^j = \\ &= \int \mathrm{d}\omega\; p^{\alpha}(\omega)\, V^i \partial_{\alpha_i} \ln p^{\alpha}(\omega)\, V^j \partial_{\alpha_j} \ln p^{\alpha}(\omega) = \\ &= \int \mathrm{d}\omega\; p^{\alpha}(\omega) \left(V^i \partial_{\alpha_i} \ln p^{\alpha}(\omega)\right)^2 \geq 0\,. \end{aligned} \tag{4.26}$$

This makes it, of course, a Riemannian metric. To give an example, one can consider the case of a Gaussian statistical manifold defined in (4.23), for which

$$\ln p^{\mu,\sigma}(x) = -\ln\sigma - \ln\sqrt{2\pi} - \frac{(x-\mu)^2}{2\sigma^2}\,, \tag{4.27}$$

one finds that

$$\mathcal{I}_{ij}^{\text{Gauss}}(\{\mu,\alpha\}) = \begin{bmatrix} 1/\sigma^2 & 0 \\ 0 & 2/\sigma^2 \end{bmatrix}\,, \tag{4.28}$$

corresponding to the infinitesimal line element

$$ds^2 = \frac{\mathrm{d}\mu^2 + 2\,\mathrm{d}\sigma^2}{\sigma^2}\,. \tag{4.29}$$

The latter is very similar to another famous metric known as the Poincare metric,

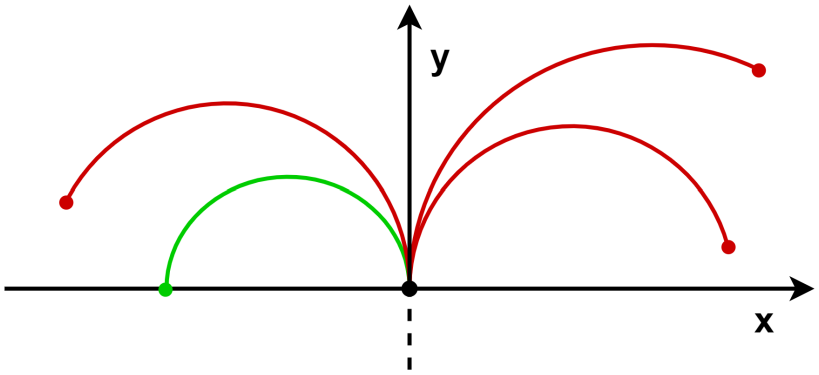

Figure 4.5: Visualisation of the Poincaré metric and its geodesics, consisting of arcs of circles (red lines). Straight lines are instead complete half circles (green line). The straight vertical line orthogonal to the x-axis is also considered a geodesic.

i.e. $ds^2 = (\mathrm{d}x^2 + \mathrm{d}y^2)/\sigma^2$, defined on the upper half plane and standard example of a 2-dimensional hyperbolic geometry, see Figure 4.5 for a graphical visualisation.

The notion of distance induced on the statistical manifold by the Fisher information metric can be also used to investigate classical speed limits [15, 93]. To do so, lets consider a curve $\gamma : \mathcal{A} \to \mathcal{S}$, where $\mathcal{A}$ is a one-dimensional parameter space parametrised by α, and such that $\gamma(\alpha_1) = p^{\alpha_1}(\omega)$, $\gamma(\alpha_2) = p^{\alpha_2}(\omega)$. The length of this path can be calculated by using equation (4.21)

$$\mathcal{L}_\gamma(\alpha_1, \alpha_2) \equiv \mathcal{L}_\gamma(p^{\alpha_1}(\omega), p^{\alpha_2}(\omega)) = \int_{\alpha_1}^{\alpha_2} \mathrm{d}\alpha \sqrt{\mathcal{I}\left(\frac{\mathrm{d}\gamma(\alpha)}{\mathrm{d}\alpha}, \frac{\mathrm{d}\gamma(\alpha)}{\mathrm{d}\alpha}\right)} = \int_{\alpha_1}^{\alpha_2} \mathrm{d}\alpha \sqrt{\mathcal{I}(\alpha)}\,, \tag{4.30}$$

where, of course, the result of the last integral in the previous line depends on γ, even if it is not explicitly shown. The path γ^* that minimises the length functional is of course a geodesics and we indicate the length associated to it as $\mathcal{L}^*(\alpha_1, \alpha_2)$. Moreover, it can be shown [94] that the latter is equal to

$$\mathcal{L}^*(\alpha_1, \alpha_2) \equiv \min_\gamma \mathcal{L}_\gamma(\alpha_1, \alpha_2) = 2 \arccos\left(\int \mathrm{d}\omega \sqrt{p^{\alpha_1}(\omega) p^{\alpha_2}(\omega)} \right). \tag{4.31}$$

The latter is also known as the *Bhattacharyya angle* or *statistical distance*, which is a distance in the strict mathematical sense, i.e it is symmetric and satisfies the triangle inequality. Note for example that, clearly, $\mathcal{L}^*(\alpha_1, \alpha_1) = 0$, i.e. the distance between a PDF and itself is 0. The Bhattacharyya angle, as the calculations done above clearly show, is a distance induced by the Fisher metric and, moreover, it also has a very nice geometric interpretation. Indeed, because the PDFs are of course normalised, their square root $\sqrt{p^\alpha(\omega)}$ can be seen as elements of an infinitely dimensional vector space whose (infinite) squared Euclidean norm is equal to one, i.e.

$$\int \mathrm{d}\omega \sqrt{p^\alpha(\omega)} \sqrt{p^\alpha(\omega)} = 1\,. \tag{4.32}$$

This norm derives from the infinite Euclidean inner product, appearing between parenthesis in the right hand side of (4.31). We can hence finally interpret the Bhattacharyya angle as the the length of an arc of a circle with maximal circumference

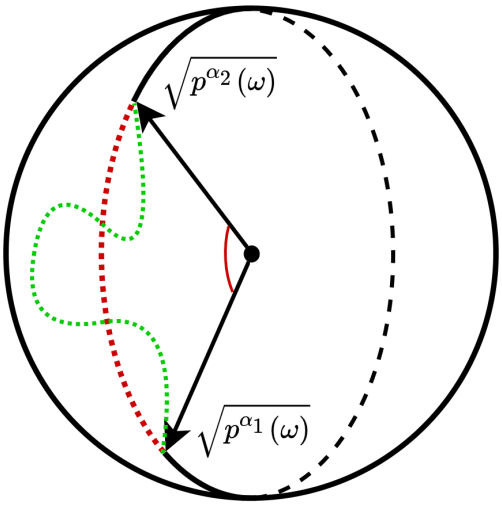

Figure 4.6: Geometrical interpretation of the Bhattacharyya angle. The green dotted line corresponds to a generic path with length $\mathcal{L}_\gamma(\alpha_1, \alpha_2)$ while the red one corresponds to a geodesics, i.e. an arc of circumference with maximal radius, with length $\mathcal{L}^*(\alpha_1, \alpha_2)$.

and lying on the surface of an infinite-dimensional sphere, on which the edges of $\sqrt{p^\alpha(\omega)}$ lie as well, see Figure 4.6 for a graphical intuition. We can also consider another functional that, for reasons that will be clear soon, will be denoted as *cost function*,

$$\mathcal{C}_\gamma(\alpha_1, \alpha_2) = \frac{1}{2}\int_{\alpha_1}^{\alpha_2} \mathrm{d}\alpha\, \mathcal{I}(\alpha)\,. \tag{4.33}$$

It is worth mentioning that this functional is minimised by the same path, which is unique because of the PDFs being normalizable, minimising the length functional (4.30). Moreover, by applying the Cauchy-Schwarz inequality to the latter, one immediately sees that

$$\Big(\mathcal{L}_\gamma(\alpha_1, \alpha_2)\Big)^2 = \Big(\int_{\alpha_1}^{\alpha_2} \mathrm{d}\alpha \sqrt{\mathcal{I}(\alpha)}\Big)^2 \leq \int_{\alpha_1}^{\alpha_2} \mathrm{d}\alpha\, \mathcal{I}(\alpha) \int_{\alpha_1}^{\alpha_2} \mathrm{d}\alpha = 2(\alpha_2 - \alpha_1)\mathcal{C}_\gamma(\alpha_1, \alpha_2)\,. \tag{4.34}$$

This implies that

$$\alpha_1 - \alpha_2 \geq \frac{\Big(\mathcal{L}_\gamma(\alpha_1, \alpha_2)\Big)^2}{2\mathcal{C}_\gamma(\alpha_1, \alpha_2)} \geq \frac{\Big(\mathcal{L}^*(\alpha_1, \alpha_2)\Big)^2}{2\mathcal{C}_\gamma(\alpha_1, \alpha_2)} \tag{4.35}$$

The last step to get an example of classical speed limit (SL), derived in [15], consists in taking time itself as the parameter on which the PDF depends on. Indeed, for a generic stochastic process one has that the PDF $p(\omega_t, t)$ evolves from a certain time t_0 up to a time t, i.e. $p(\omega_t, t = t_0)$ evolves in $p(\omega_t, t)$. Moreover, by following what has been done in [15], we introduce the *intrinsic velocity*

$$v_I(t) = \sqrt{\mathcal{I}(t)} \tag{4.36}$$

that can be interpreted as a velocity measuring how fast the PDF evolves from $p(\omega_t, t = t_0)$ to $p(\omega_t, t)$. We are also introducing the temporal Fisher information

$$\mathcal{I}(t) = \int \mathrm{d}\omega_t\; p\left(\omega_t, t\right) \Big(\partial_t \ln p\left(\omega_t, t\right)\Big)^2, \tag{4.37}$$

which, as it has been shown in [15], has many interesting proprieties. However, for the sake of simplicity, we just note that the length functional and the cost function can be written, in terms of the intrinsic velocity and by using equations (4.21) and (4.33), as

$$\mathcal{L}(t) \equiv \mathcal{L}_\gamma(t, t_0) = \int_{t_0}^{t} \mathrm{d}t'\, v_I(t') \qquad \mathcal{C}(t) \equiv \mathcal{C}_\gamma(t, t_0) = \int_{t_0}^{t} \mathrm{d}t'\, (v_I(t'))^2 \,. \tag{4.38}$$

From the equation on the left, one immediately understands the naming of intrinsic velocity for $v_I(t)$ and, as a consequence, one can interpret the cost function appearing in the equation on the right as a sort of integrated kinetic energy. With this in mind, one can finally specialise equation (4.35) to the case of time as a parameter hence obtaining

$$t \geq \frac{\left(\mathcal{L}(t)\right)^2}{2\mathcal{C}(t)} \geq \frac{\left(\mathcal{L}^*(t)\right)^2}{2\mathcal{C}(t)} \,, \tag{4.39}$$

that is the desired SL which provides a lower bound on time needed by the PDF to travel along a path of length $\mathcal{L}(t)$. One also understands the naming of the cost function for $\mathcal{C}(t)$, i.e. the more the system "pays" in terms of this (kinetic) cost the lowest the time evolution from an initial to a final state may be. Many more details on how this cost function can be linked to important thermodynamic quantities, such as entropy production, can be found in the references [15, 93]. We will instead limit ourselves to note that this bound is different with respect to the classical equivalents of the usual quantum SLs, known as the Mandelstam-Tamm and Margolus-Levitin type, found in [95]. Moreover, it is one of the first examples of SL entirely based on information geometric principles and gives a clear idea of how these limits can be studied using information-theoretic concepts. Indeed, in the last pages we have just scratched the surface of a very wide and active line of research which was worth mentioning. However, we will not follow this path in this thesis but, rather, we will use another fundamental result of information geometry that is the the Cramér–Rao bound, to which the next subsection is dedicated.

To recapitulate, we have obtained a Riemannian manifold $\mathcal{S}$, whose metric is the Fisher information metric and where each point is associated to a probability distribution on a sample space Ω. The proprieties of the geodesics on such manifold can be used to study classical SLs, i.e. lower bounds setting a minimum time needed for the evolution of the PDF from one state to another. These limits were first discussed in the context of quantum mechanics where information theory is used as well. Moreover, the Fisher metric is so important because it also encodes the amount of information that the random variable $\omega \in \Omega$ contains about the parameters α upon which the PDF depends. This statement can be quantified by the Cramér–Rao bound, which will be the main topic of the next subsection as well as the starting point of the discussion of uncertainty relations in the context of stochastic systems.

4.3 The Cramér–Rao bound and the fluctuation-response inequality

The Cramér–Rao (CR) bound [96, 97] is a central formula in statistics and estimation theory. In these fields, one is usually interested in estimating the value of a

given unknown parameter, such as the temperature in the case of the Ising model or the mean and variance of a Gaussian, on which the distribution of the data points depends on. This can be achieved through the use of *estimators*, which are random variables $O(\omega)$ defined on the sample space Ω and which may possibly be *unbiased*, i.e. such that their mean $\langle O \rangle^{\alpha} = \alpha$ is equal to the parameter one is trying to estimate. Of course, the quality of an estimator can be quantified by its variance since, the lower the variance, the lower will be the estimation error. In its most basic form and for the case of a PDF which depends solely on one parameter, the Cramér–Rao bound puts a lower bound to the variance of an arbitrary unbiased estimator given by the inverse of the Fisher information (4.25) (for a unidimensional parameter), that is

$$\langle \Delta O^2 \rangle^{\alpha} \geq \frac{1}{\mathcal{I}(\alpha)}, \tag{4.40}$$

$$\mathcal{I}(\alpha) = \int \mathrm{d}\omega \; p^{\alpha}(\omega) \left(\partial_{\alpha} \ln p^{\alpha}(\omega) \right)^2, \tag{4.41}$$

where $\langle \dots \rangle^{\alpha}$ is the average taken with respect to $p^{\alpha}(\omega)$. As one can see from (4.40), the higher the Fisher information $\mathcal{I}(\alpha)$, namely the information encoded in the PDF $p^{\alpha}(x)$ about the parameter α, the lower will be the bound on the variance of the unbiased estimator, thus allowing better estimates of the parameter α.

Nevertheless, the philosophy we are going to follow in this thesis, and in the next chapter in particular, is different. Indeed, we will consider the random variables $O(\omega)$ on Ω as *observables* of the system for a given stochastic process. The sample spaces we are going to consider are of two types:

- the space of stochastic trajectories associated to a given stochastic process $X(t) = \{X_i\}_{i,\dots,N \leq t/dt}$, i.e. the set of all possible realisations of the stochastic process X up to time t. As usual, we introduced an infinitesimal time dt at which the process updates itself. This definition includes the set of all paths generated by Langevin process or Markov jump processes, we will refer to this set as Ω_t and to its elements as ω_t. Important quantities that depend on the whole path are the entropy production $\Sigma(\omega_t)$ 2.24 and 2.52 and the dynamical activity $\mathcal{K}(\omega_t)$ 2.30, discussed in chapter 2.

- The space of all possible outcomes that a stochastic process $X(t)$ can give at a given time t. Consider again the example of Langevin equation. In this case, one could consider the PDF $p(x_t, t)$ obtained from the solution of a Fokker-Plank equation describing the probability of finding the Brownian particle in a certain position x_t at time t. It is clear that the sample space on which this PDF is defined is of the type as described above. We will use these kind of PDFs in the context of generalised Langevin systems, hence allowing us to consider any state dependent observable of the form $O(x_t)$.

Having this in mind, one can now consider the generalised Cramér-Rao bound, whose derivation descends from the Cauchy-Schwarz inequality applied to random variables and leading to the covariance inequality. The latter implies that, for two random variables $x_1(\omega)$ and $x_2(\omega)$, it holds that

$$\left(\mathrm{Cov}(x_1, x_2)\right)^2 \leq \langle \Delta x_1^2 \rangle \langle \Delta x_2^2 \rangle \tag{4.42}$$

and indeed, by choosing $x_1(\omega) = O(\omega)$ and $x_2(\omega) = \partial_\alpha \ln p^\alpha(\omega)$, where ∂_α indicates the derivative with respect to the parameter α, one readily gets

$$\frac{(\partial_\alpha \langle O \rangle_t^\alpha)^2}{\langle \Delta O^2 \rangle_t^\alpha} \leq \mathcal{I}_t(\alpha)\,, \tag{4.43}$$

that is the generalised CR bound. From this, one can also note that for an unbiased estimator such that $\langle O \rangle^\alpha = \alpha$, one recovers the basic CR bound (4.40) from (4.43). Moreover, note that we included the subscript t to the averages in (4.43) as all systems we are going to consider evolve in time.

The generalised CR bound is an extremely useful and powerful relation that exhibits a very similar structure to what one finds for the non-equilibrium inequalities. Indeed, as it was shown in [19, 15, 98, 99, 100], it is possible to exploit this result to derive uncertainty relations and to connect the Fisher information, a fundamental quantity in information theory, with thermodynamically relevant quantities. To do so, one has to parametrise the PDF $p(\omega_t)$ of a given stochastic process by performing an α-dependent perturbation of the dynamic of the process itself. Later, we will show "clever" α-perturbations that yield specific observables. Note that this perturbation must not be necessarily a physically realisable one but rather a virtual one. This can be done, for example, in the context of Langevin systems by adding a drift with a α prefactor to the Langevin equation

$$\begin{aligned} \dot{x}(t) = A(x_t, t) + \sqrt{2D(x_t, t)} \cdot \xi(t) \implies \\ \implies \dot{x}(t) = A(x_t, t) + \alpha Y(x_t, t) + \sqrt{2D(x_t, t)} \cdot \xi(t)\,, \end{aligned} \tag{4.44}$$

which will of course modify the PDF associated to this process

$$p(\omega_t) \implies p^\alpha(\omega_t)\,. \tag{4.45}$$

Once this parametrisation has been found, and we stress that this can be done for every stochastic process, one can hence calculate the modified averages and variances

$$\langle O \rangle_t^\alpha = \int \mathrm{d}\omega_t\, p^\alpha(\omega_t)\, O(\omega) \qquad \langle \Delta O^2 \rangle_t^\alpha = \langle O^2 \rangle_t^\alpha - (\langle O \rangle_t^\alpha)^2 \tag{4.46}$$

as well as the Fisher information (4.41) associated to this particular parametrisation. Moreover, one can also require that the α-perturbation is such that for $\alpha = 0$ one recovers the original dynamics and PDF, this is trivially true for example in (4.44). Under these hypothesis, one can expand all the terms in (4.43) around $\alpha \approx 0$ and may only consider the leading order, i.e.

$$\frac{(\partial_\alpha \langle O \rangle_t^\alpha|_{\alpha=0})^2}{\langle \Delta O^2 \rangle_t} \leq \mathcal{I}_t(\alpha)|_{\alpha=0}\,. \tag{4.47}$$

As one can easily see, the result does not depend explicitly on the perturbation parameter α even if the result itself depends on the choice of the modification induced into the PDF. This form of the CR bound will be used in the next chapter to obtain the *thermodynamic uncertainty relation* (TUR), as done in [19], along with our

kinetic uncertainty relation (KUR) in the context of Markovian jump processes. Furthermore, if the observable $\boldsymbol{O}$ is a d component vector, the CR bound (for small α) takes the following form

$$\left(\partial_\alpha \langle \boldsymbol{O} \rangle_t^\alpha|_{\alpha=0}\right)^{\mathrm{T}} \boldsymbol{\Xi}_{\boldsymbol{O},t}^{-1}\, \partial_\alpha \langle \boldsymbol{O} \rangle_t^\alpha|_{\alpha=0} \leq \mathcal{I}_t(\alpha)|_{\alpha=0} \tag{4.48}$$

where

$$\boldsymbol{\Xi}_{\boldsymbol{O},t} = \langle \boldsymbol{O}\boldsymbol{O}^{\mathrm{T}} \rangle_t - \langle \boldsymbol{O} \rangle_t \langle \boldsymbol{O} \rangle_t \tag{4.49}$$

is the covariance matrix associated to the observable $\boldsymbol{O}$. This result will allow us to show the proof, given for the first time in [19], of the TUR for multidimensional Langevin systems.

As a useful tool for the computation of stochastic uncertainty relation, we also present an equivalent formula to the CR bound in the limit of small α-perturbations, which was firstly derived by A. Dechant and S. Sasa in [19], i.e. the fluctuation-response inequality (FRI). For simplicity, we restrict this discussion to scalar observables for which the FRI takes the following form (for $\alpha \approx 0$)

$$\frac{(\langle O \rangle_t^\alpha - \langle O \rangle_t)^2}{\langle \Delta O^2 \rangle_t} \leq 2\mathcal{D}_{\mathrm{KL}}(p^\alpha \parallel p)\,, \tag{4.50}$$

where

$$\mathcal{D}_{\mathrm{KL}}(p^\alpha \parallel p) = \int \mathrm{d}\omega\, p^\alpha(\omega) \ln\left(\frac{p^\alpha(\omega)}{p(\omega)}\right). \tag{4.51}$$

is the Kullback–Leibler (KL) divergence, a quantity that measures the difference between probability distributions. For this reason, it is also called *relative entropy*. For finite α, the authors provide a correction to the r.h.s. of (4.50), but we will not use this result in this work.

The KL divergence is not a distance in the strict mathematical sense as it is not symmetric, i.e. $\mathcal{D}_{\mathrm{KL}}(q \parallel p) \neq \mathcal{D}_{\mathrm{KL}}(p \parallel q)$, and it does not satisfy the triangle inequality. However, for infinitesimally close distributions, one recovers the Fisher information, which is of course a genuine metric distance. To make things more clear, note that the KL divergence is strictly positive (this can be shown very easily) and its absolute minimum is zero, corresponding to the two distributions in the divergence to be equal, as it can be seen from (4.51). As a consequence, it can be shown that the expansion of the KL divergence around $\alpha \approx 0$ leads to

$$\mathcal{D}_{\mathrm{KL}}(p^\alpha \parallel p) \overset{\alpha\to 0}{\approx} \alpha\partial_\alpha \mathcal{D}_{\mathrm{KL}}(p^\alpha \parallel p)|_{\alpha=0} + \frac{\alpha^2}{2}\partial_\alpha^2 \mathcal{D}_{\mathrm{KL}}(p^\alpha \parallel p)|_{\alpha=0} = \frac{\alpha^2}{2}\mathcal{I}_t(\alpha)|_{\alpha=0}\,, \tag{4.52}$$

namely, the concavity of the KL divergence around its minimum is the Fisher information. Moreover, by taking the leading order in α of the numerator on the left hand side of equation (4.50) one sees that

$$\langle O \rangle_t^\alpha - \langle O \rangle_t \overset{\alpha\to 0}{\approx} \alpha\partial_\alpha \langle O \rangle_t^\alpha|_{\alpha=0} \tag{4.53}$$

and hence, by using this along with (4.52) and plugging everything into (4.50) one recovers (4.47).

We have hence presented two different information theoretic bounds involving two distinct fundamental quantities, i.e. the Fisher information and the KL divergence, which do coincide for small α-perturbations. Even though the result we are going to exploit coincides with latter case, the existence of these two bounds for arbitrary perturbations opens the door, along with the bounds shown in equations (4.35) and (4.39), to a deep study of stochastic uncertainty relations using information theoretic techniques. Moreover, it offers a clearer interpretation for the meaning of these inequalities, i.e. that the magnitude of the variation of the averages of the system's observable, due to a (virtual) perturbation and at fixed variance, is bounded from above by a quantity that measures, in a sense that must be mathematically specified, the distance between the perturbed and unperturbed PDF. Finally, we can outline the strategy which will be followed in this thesis in the context of this perturbative approach:

1. Consider a stochastic process, in our case a Langevin process or a Markovian jump process, along with a PDF associated to the process itself.

2. Perturb the original dynamics, such as in equation (4.44), in order to obtain a modified PDF $p^\alpha(\omega)$ depending on some parameter α.

3. Evaluate the perturbed average $\langle O\rangle_t^\alpha$, usually aiming to find something like $\langle O\rangle_t^\alpha = (1+\alpha)\langle O\rangle_t$ or $\langle O\rangle_t^\alpha = \langle O\rangle_{(1+\alpha)t}$. As it will be clear later, this will make the left hand side of both (4.43) and (4.50) physically accessible quantities.

4. Calculate the Fisher information or the KL divergence associated to the perturbation. Here, one usually tries to connect these quantities to entropy production, like we will see in Section 5.2, or, as we have proven in [101], to the mean dynamical activity $\langle \mathcal{K}\rangle_t$ (2.31).

5. Take the limit of $\alpha \to 0$.

Another interesting and powerful approach can be found in reference [15]. Here the authors take again time itself as the the parameter with respect to whom the Fisher information is calculated. Indeed, using (4.43) this would imply that

$$\frac{(\partial_t \langle O\rangle_t)^2}{\langle \Delta O^2\rangle_t} \leq \mathcal{I}(t)\,, \tag{4.54}$$

whit $\mathcal{I}(t)$ the temporal Fisher information (4.37). As in the previous section, the temporal Cramér-Rao bound (4.54) can also be used to study classical speed-limits but, once more, we refer to [15, 93] for further details. Instead, we will use equation (4.54) in Section 5.5 to derive a thermodynamic uncertainty relation for a system with memory and modelled by a linear GLE equation. In this case, we will consider state dependent PDFs associated to the process and, as a consequence, state dependent observables for the left hand side of (4.54).

For the sake of completeness, we also present another multidimensional version of the Cramér-Rao bound, which holds for an arbitrary number N of observables $\{O_i(\omega)\}_{i=1,\dots,N}$ and number of parameters on which the PDF depends on, say $\alpha = \{\alpha_i\}_{i=1,\dots,M}$. Indeed, by defining

$$\left(\mathbf{Z}^\alpha\right)_{ij} = \partial_{\alpha_i}\langle O_j\rangle_t^\alpha \qquad\qquad \left(\mathbf{\Xi}_t^\alpha\right)_{ij} = \langle O_i O_j\rangle_t^\alpha - \langle O_i\rangle_t^\alpha \langle O_j\rangle_t^\alpha \tag{4.55}$$

where the quantity on the left is an $M \times N$ matrix while the one on the right is the $N \times N$ dimensional covariance matrix between all observables. In terms of these quantities, the Cramér-Rao bound for an arbitrary number of observables can be formulated as follows

$$\boldsymbol{Z}^{\alpha}\left(\,\boldsymbol{\Xi}_{t}^{\alpha}\,\right)^{-1}\left(\boldsymbol{Z}^{\alpha}\right)^{\mathrm{T}} \leq \boldsymbol{\mathcal{I}}_{t}^{\alpha}\,, \tag{4.56}$$

where of course on the right we have the Fisher information matrix whose components have been defined in (4.25), i.e.

$$\left(\boldsymbol{\mathcal{I}}_{t}^{\alpha}\right)_{ij} = \int \mathrm{d}\omega\; p^{\alpha}\left(\omega, t\right) \partial_{\alpha_i} \ln p^{\alpha}\left(\omega, t\right) \partial_{\alpha_j} \ln p^{\alpha}\left(\omega, t\right)\,. \tag{4.57}$$

This multidimensional CR bound was used in reference [18] to derive a multidimensional TUR. In this paper, the author shows how the simultaneous measurement of many uncorrelated observable can indeed improve the lower bound to the entropy production until it is eventually saturated. This in turn offers the possibility of accurately estimating entropy production by measuring the highest possible number of operationally accessible observables.

Moreover, there is also a quantum version of the CR bound which has been used to derive quantum speed limits of the Mandelstam-Tamm type, see [102] for some examples, along with a quantum version of the thermodynamic uncertainty relation [100].

To conclude, we presented two different bounds, (4.43) and (4.50), which can be regarded as two possible starting points for the study of stochastic uncertainty relations. Indeed, many inequalities have been derived from them in the recent years. In the next chapter, we will show some possible applications of this information theoretic approach to stochastic uncertainty relations along with some novel original results.

CHAPTER 5

UNCERTAINTY RELATIONS

5.1 Introduction

During the last years, non-equilibrium statistical mechanics and the stochastic theory of thermodynamics at a mesoscopic scale have proven to be indispensable tools for the description of microscopic biological systems and the dynamics of bio-chemical reactions. As regards the latter, it is clear that the vast majority of the phenomena takes place in a non-equilibrium regime which is characterised by a positive entropy production Σ_{tot}. Indeed, as it is shown in Chapter 2, for an isolated stochastic system undergoing some thermodynamic transformation the second law of thermodynamics is valid on average $\langle \Sigma_{\text{tot}} \rangle_t > 0$. Despite being one of the most fundamental principle of physics, the second law of thermodynamics does not give any quantitative information about the production of entropy except that it is positive on average. A lot of effort has been made during the last decades to relate entropy production to important features of non-equilibrium processes and indeed it was found [25] that, in a steady state, it is linked to the ratio between the probability of a stochastic path $\mathrm{P}(\omega_t)$ and the probability of the (appropriately) time reversed trajectory $\mathrm{P}^\dagger(\omega_t)$

$$\langle \Sigma_{\text{tot}} \rangle^{\text{st}} = \int \mathrm{d}\omega_t \, \mathrm{P}(\omega_t) \ln \left(\frac{\mathrm{P}(\omega_t)}{\mathrm{P}^\dagger(\omega_t)} \right). \tag{5.1}$$

This result is known as the fluctuation theorem (FT), from which the second law can be derived, and is considered to be one of the most important theorems of stochastic thermodynamics. Nevertheless, if the system under investigation is extremely complex, it could be quite impossible to access and evaluate the path probability density function, as a consequence the estimation of entropy production can not be obtained using the FT.

Taking a step back, one can note that most of physical principles are expressed in terms of equalities and that the second law is arguably one of the most important exceptions. However, there are many other inequalities that can help in grasping important physical insights on the system under examination, the Heisenberg uncertainty principle and the so called quantum speed limits (SL) [102], which determine the minimum time needed to transform a quantum state to another, are just few of the possible examples. As it is well known, stochastic processes have many aspects in common with quantum mechanics because of their probabilistic nature, so it is reasonable to expect that such inequalities could also exist in the context of stochastic thermodynamics, and that is indeed the case. In 2015 Barato and Seifert conjectured the so called thermodynamic uncertainty relation (TUR) [4]

which stated that, for a certain class of stochastic processes and a current R of the system, it holds that

$$\frac{\langle R\rangle_t^2}{\langle \Delta R^2\rangle_t} \leq \frac{\langle \Sigma_{\rm tot}\rangle_t}{2k_B} \tag{5.2}$$

which can be seen as a refinement of the second law of thermodynamics. Moreover, the left hand side of (5.2) is a type of *signal to noise ratio* (SNR) and can be regarded as a measure of the precision associated to the observable R. Hence, the TUR gives an upper bound to this SNR which is given by the total entropy production up to time t. Precision can be a very relevant quantity for biological processes [2, 3] and biological systems may be interested in maximising this precision in order to enhance efficiency. The TUR hence sets a minimal cost for reaching a certain precision and implies that a higher SNR for a given observable can eventually be reached only at the cost of an increased dissipation. This is in line with the school of thought that living systems tend to maximise entropy production in order to increase their performances in the general sense. Nevertheless, this is strictly true only near equilibrium and indeed there are works such as [30, 33, 34, 52] that show that far from equilibrium there are kinetic effects, embodied by time symmetric quantities as opposite to entropy production, that must be taken into account for the complete characterisation of non-equilibrium states. To make an example, in [3] the authors show how the precision of a circadian clock, modelled by means of Markovian jump processes, does not monotonically increase with dissipation which is a clue of how kinetic effects may influence the region of parameter space where optimal performances are reached. In this context, we will add further insight on how time symmetric quantities determine the performances of non-equilibrium systems by means of our *kinetic uncertainty relation*, valid for Markovian jump processes and where the upper bound to the SNR is given by the time symmetric quantity $\langle \mathcal{K}\rangle_t$, often referred to as *mean dynamical activity*.

The TUR is the primary example a long list of recent non-equilibrium inequalities and includes the entropy production as a cost function [5, 6, 7, 8, 9, 10, 11, 12, 13, 14, 15, 16, 17, 18, 19, 20, 21] (dissipation may also limit the speed of a process [103]). Moreover, the TUR and its generalisations [22, 32, 23, 24, 101, 98, 104, 88, 98] are inequalities usually discussed and proven for discrete and continuous diffusive Markov systems. On the practical side, TURs may help in thermodynamic inference [105], for instance in evaluating the entropy production rate from data [10, 106, 107, 108, 109]. Theoretically, while the proof of the TUR in steady states is provided by the machinery of large deviation theory [7, 11], an approach by Dechant and Sasa (DS) [14, 19] adopts information theory as the main theoretical tool. Moreover, a unifying view [110] may explain the mechanism behind uncertainty relations.

This information-theoretic approach, which is based on the generalised Cramér-Rao (CR) bound (4.43)

$$\frac{(\partial_\alpha \langle O\rangle_t^\alpha)^2}{\langle \Delta O^2\rangle_t^\alpha} \leq \mathcal{I}_t(\alpha)\,, \tag{5.3}$$

and the fluctuation response inequality (FRI) (4.50), which (for small $\alpha \approx 0$) reads

$$\frac{(\langle O\rangle_t^\alpha - \langle O\rangle_t)^2}{\langle \Delta O^2\rangle_t} \leq 2\mathcal{D}_{\rm KL}(p^\alpha \parallel p)\,, \tag{5.4}$$

leads to quite general results for stochastic systems, finite times statistics, and regimes

outside steady states (the results above are presented, for simplicity, for scalar observables O). In the previous chapter we outlined some basic concepts of information geometry and discussed some formal details of the CR bound and the FRI. We also anticipated that, by means of a perturbative approach, we will show how the Fisher information and the Kullback-Leibler (KL) divergence may be linked to relevant thermodynamic and/or kinetic quantities. To this end, we present a very useful result obtained in [19] that gives the general expression for the KL divergence arising from the perturbation of a jump-diffusion process, i.e. involving both Langevin dynamics and discrete stochastic jumps. Such process is governed by a generalised Fokker Plank equation, which can be regarded as a combination of the diffusive FP (2.47) and the master (2.15) equation, i.e.

$$\partial_t p_i(\boldsymbol{x}_t, t) = -\nabla \cdot \boldsymbol{J}_i^{\text{diff}}(\boldsymbol{x}_t, t) + \sum_k \boldsymbol{J}_{ik}^{\text{jump}}(\boldsymbol{x}_t, t) \tag{5.5}$$

where

$$\begin{aligned} \boldsymbol{J}_i^{\text{diff}}(\boldsymbol{x}_t, t) &= \left(\boldsymbol{A}_i(\boldsymbol{x}_t, t) - \left(\nabla^{\mathrm{T}} \boldsymbol{D}_i(\boldsymbol{x}_t, t) \right)^{\mathrm{T}} - \boldsymbol{D}_i(\boldsymbol{x}_t, t) \, \nabla \, \ln p_i(\boldsymbol{x}_t, t) \right) p_i(\boldsymbol{x}_t, t) \\ \boldsymbol{J}_{ik}^{\text{jump}}(\boldsymbol{x}_t, t) &= W_{ik}(\boldsymbol{x}_t, t) \, p_k(\boldsymbol{x}_t, t) - W_{ki}(\boldsymbol{x}_t, t) \, p_i(\boldsymbol{x}_t, t) \, . \end{aligned} \tag{5.6}$$

This may be the case of a diffusing system whose chemo-mechanical configuration changes at exponentially distributed times and determined by the rates $W_{ik}(\boldsymbol{x}_t, t)$, hence changing the state dependent drift vector $\boldsymbol{A}_i(\boldsymbol{x}_t, t)$ and diffusion matrix $\boldsymbol{D}_i(\boldsymbol{x}_t, t)$. Without going too much into detail, in [19] the authors prove that a simultaneous perturbation of drift vector, transition rates and initial probability distribution as follows

$$\begin{aligned} \boldsymbol{A}_i(\boldsymbol{x}_t, t) &\to \boldsymbol{A}_i^\alpha(\boldsymbol{x}_t, t) = \boldsymbol{A}_i(\boldsymbol{x}_t, t) + \boldsymbol{Y}_i^\alpha(\boldsymbol{x}_t, t) \\ W_{ik}(\boldsymbol{x}_t, t) &\to W_{ik}^\alpha(\boldsymbol{x}_t, t) = W_{ik}(\boldsymbol{x}_t, t) \mathrm{e}^{\alpha \mathcal{Z}_{ik}^\alpha(\boldsymbol{x}_t, t)} \\ p_{i_0}(\boldsymbol{x}_0, 0) &\to p_{i_0}^\alpha(\boldsymbol{x}_0, 0) \, , \end{aligned} \tag{5.7}$$

which in turn determines a modification of the path probability distribution (PDF) $p(\omega_t) \to p^\alpha(\omega_t)$ (such as (2.22) and (2.51)), leads to a KL divergence which reads

$$\begin{aligned} \mathcal{D}_{\mathrm{KL}}(p^\alpha \parallel p) &= \int \mathrm{d}\omega_t \, p^\alpha(\omega_t) \ln \left(\frac{p^\alpha(\omega_t)}{p(\omega_t)} \right) \\ &= \int_0^t \mathrm{d}t' \left(\frac{1}{4} \langle \boldsymbol{Y}^\alpha \boldsymbol{D}^{-1} \boldsymbol{Y}^\alpha \rangle_{t'}^\alpha + \langle \mathcal{Z}^\alpha + \mathrm{e}^{-\mathcal{Z}^\alpha} - 1 \rangle_{t'}^\alpha \right) + \left\langle \ln \frac{p_0^\alpha}{p_0} \right\rangle_0^\alpha . \end{aligned} \tag{5.8}$$

As discussed in the previous chapter, we are interested in infinitesimal perturbations and indeed, for the particular case of

$$\begin{aligned} \boldsymbol{Y}^\alpha(\boldsymbol{x}_t, t) &= \alpha \boldsymbol{Y}(\boldsymbol{x}_t, t) \qquad\qquad \mathcal{Z}_{ik}^\alpha(\boldsymbol{x}_t, t) = \alpha \mathcal{Z}_{ik}(\boldsymbol{x}_t, t) \\ p_0^\alpha(x_0, 0) &= p_{i_0}(\boldsymbol{x}_0, 0) + \alpha \delta p_{i_0}(\boldsymbol{x}_0, 0) \end{aligned} \tag{5.9}$$

and for small α the authors also show that

$$\mathcal{D}_{\mathrm{KL}}(p^\alpha \parallel p) \overset{\alpha \to 0}{\approx} \frac{\alpha^2}{2} \mathcal{I}_t(\alpha)|_{\alpha=0} = \alpha^2 \int_0^t \mathrm{d}t' \left(\frac{1}{4} \langle \boldsymbol{Y} \boldsymbol{D}^{-1} \boldsymbol{Y} \rangle_{t'} + \frac{1}{2} \langle \mathcal{Z}^2 \rangle_{t'} \right) + \frac{\alpha^2}{2} \left\langle \frac{\delta p_0^2}{p_0^2} \right\rangle_0^\alpha . \tag{5.10}$$

By choosing "clever" perturbations on the dynamics of the system, DS showed that various forms of TUR hold for diffusion processes (we will present one example in the next section) and anticipated that a TUR holds also for Langevin dynamics with inertia. Following this approach, Van Vu and Hasegawa [98] also provided an explicit non-equilibrium inequality for inertial stochastic dynamics when reversible currents are present. Their formula shows that the mean entropy production cannot by itself constitute the cost function in inertial systems. In equilibrium, where on average dissipation is absent while currents are eventually present thanks to inertia, there is a form of dynamical activity that naturally enters in the upper bound. This is not a surprise because, as we will show in the next sections, the cost function can also include time-symmetric non-dissipative observables [22, 32, 23, 24, 98]. In particular, using the DS approach along with (5.10) for pure jump processes, we will show the existence of a KUR [101] that has the dynamical activity as a cost function.

The chapter is structured as follows. In the next section we will present one possible derivation of the TUR both for diffusive and jump systems and obtained in [19] by exploiting the above-mentioned information approach, followed by our KUR discussed with some examples in Section 5.3 and 5.4. Finally, in Section 5.5 we present an original example of TUR for non Markovian systems and obtained by means of the temporal Cramér-Rao bound (4.54)

$$\frac{(\partial_t \langle O \rangle_t)^2}{\langle \Delta O^2 \rangle_t} \leq \mathcal{I}(t)\,. \tag{5.11}$$

5.2 Thermodynamic uncertainty relation (TUR)

5.2.1 Diffusive systems

To get started, we consider a simple N dimensional Langevin system

$$\dot{\boldsymbol{x}}(t) = \boldsymbol{A}(\boldsymbol{x}_t) + \sqrt{2\,\boldsymbol{D}(\boldsymbol{x}_t)} \cdot \boldsymbol{\xi}(t)\,, \tag{5.12}$$

whose drift vector $\boldsymbol{A}(\boldsymbol{x}_t)$ and diffusion matrix $\boldsymbol{D}(\boldsymbol{x}_t)$ do not explicitly depend on time. As usual, $\boldsymbol{\xi}(t)$ is a white Gaussian noise with first moments given by $\langle \boldsymbol{\xi}(t) \rangle = 0$ and $\langle \xi_i(t') \xi_j(t)'' \rangle = \delta_{ij}\delta(|t' - t''|)$. The Fokker Plank equation, presented in (2.47) and associated to equation (5.12) leads to

$$\partial_t p(\boldsymbol{x}_t, t) = -\nabla \cdot \boldsymbol{J}(\boldsymbol{x}_t, t) = -\nabla \cdot (\boldsymbol{\nu}(\boldsymbol{x}_t, t) p(\boldsymbol{x}_t, t))\,, \tag{5.13}$$

$$\boldsymbol{\nu}(\boldsymbol{x}_t, t) = \boldsymbol{A}(\boldsymbol{x}_t) - \left(\nabla^{\mathrm{T}} \boldsymbol{D}(\boldsymbol{x}_t)\right)^{\mathrm{T}} - \boldsymbol{D}(\boldsymbol{x}_t)\, \nabla \ln\left(p(\boldsymbol{x}_t, t)\right), \tag{5.14}$$

where $\boldsymbol{J}(\boldsymbol{x}_t, t)$ is the probability current and $\boldsymbol{\nu}(\boldsymbol{x}_t, t)$ is the local mean velocity. In this section we are interested in the study of steady state dynamics, for which it holds that the PDF and the mean local velocity do not explicitly depend on time which in turn implies that

$$\partial_t p_{\mathrm{st}}(\boldsymbol{x}_t) = -\nabla \cdot (\boldsymbol{\nu}_{\mathrm{st}}(\boldsymbol{x}_t) p_{\mathrm{st}}(\boldsymbol{x}_t)) = 0\,, \tag{5.15}$$

$$\boldsymbol{\nu}_{\mathrm{st}}(\boldsymbol{x}_t) = \boldsymbol{A}(\boldsymbol{x}_t) - \left(\nabla^{\mathrm{T}} \boldsymbol{D}(\boldsymbol{x}_t)\right)^{\mathrm{T}} - \boldsymbol{D}(\boldsymbol{x}_t)\, \nabla \ln\left(p_{\mathrm{st}}(\boldsymbol{x}_t)\right). \tag{5.16}$$

The next step towards the TUR, consists in perturbing the steady state dynamics by adding an auxiliary drift vector proportional to the local mean velocity and leading to a new global drift vector

$$\boldsymbol{A}^{\alpha}(\boldsymbol{x}_t) = \boldsymbol{A}(\boldsymbol{x}_t) + \alpha\, \boldsymbol{v}_{\rm st}(\boldsymbol{x}_t)\,. \tag{5.17}$$

By plugging this modified drift vector into equation (5.16) and subsequently into equation (5.15), one obtains the modified PDF and local mean velocity associated to this perturbation

$$\boldsymbol{v}^{\alpha}_{\rm st}(\boldsymbol{x}_t) = \boldsymbol{A}^{\alpha}(\boldsymbol{x}_t) - \Big(\nabla^{\rm T}\boldsymbol{D}(\boldsymbol{x}_t)\Big)^{\rm T} - \boldsymbol{D}(\boldsymbol{x}_t)\,\nabla\,\ln\left(p_{\rm st}(\boldsymbol{x}_t)\right) = (1+\alpha)\boldsymbol{v}_{\rm st}(\boldsymbol{x}_t,t)\,, \tag{5.18}$$

$$(1+\alpha)\nabla^{\rm T}(\boldsymbol{v}_{\rm st}(\boldsymbol{x}_t,t)p^{\alpha}_{\rm st}(\boldsymbol{x}_t,t)) = 0\,. \tag{5.19}$$

This last equation implies that the modified PDF is the same as for the unperturbed process while the mean local velocity is rescaled by a factor $1+\alpha$.

Given this particular modification of the dynamics, one must choose a class of observables that "scale well" whit this perturbation. In this case, the natural choice falls on well known the class of *integrated currents* presented in (2.56), i.e.

$$\boldsymbol{R}(\omega_t,t) = \int_0^t {\rm d}t'\, \boldsymbol{g}(\boldsymbol{x}_{t'},t')\circ\dot{\boldsymbol{x}}(t') \tag{5.20}$$

where $\circ$ denotes the Stratonovich product. This is indeed a very important set of quantities of which the entropy production associated to the thermal bath is just an example. Indeed, one can recover the the heat dissipated into the environment (2.55) first by identifying the drift vector in (5.12) with a force $\boldsymbol{A}(\boldsymbol{x}_t) = \boldsymbol{\mu}\,\boldsymbol{F}(\boldsymbol{x}_t)$, where $\boldsymbol{\mu}$ is the mobility matrix, and then taking $\boldsymbol{g}(\boldsymbol{x}_t) = \beta\boldsymbol{F}^{\rm T}(\boldsymbol{x}_t)$ in (5.20).

One of the main feature of these observables, as discussed in Chapter 2, is that their average in a steady state can be explicitly written as a function of the mean local velocity. Indeed, by restricting ourselves to a time independent weight matrix $\boldsymbol{g}(\boldsymbol{x}_t)$, one finds that that is

$$\langle\boldsymbol{R}\rangle^{\rm st}_t = \int_0^t {\rm d}t'\,\langle\boldsymbol{g}\circ\dot{\boldsymbol{x}}\rangle^{\rm st}_{t'} = \int_0^t {\rm d}t'\,\langle\boldsymbol{g}\,\boldsymbol{v}_{\rm st}\rangle^{\rm st}_{t'} = \boldsymbol{J}_R\,t\,. \tag{5.21}$$

Here we also noted that $\boldsymbol{J}_R = \langle\boldsymbol{g}^{\rm T}\,\boldsymbol{v}_{\rm st}\rangle^{\rm st}_t$, which can be regarded as the rate associated to the current $\boldsymbol{R}(\omega_t)$, is constant because all equal time correlation functions, involving quantities that do not explicitly depend on time, are constant in the steady state. As a consequence, the perturbed average of an integrated current, associated to the modified dynamics due to (5.17), trivially becomes

$$\langle\boldsymbol{R}\rangle^{{\rm st},\alpha}_t = t\,\langle\boldsymbol{g}\,\boldsymbol{v}^{\alpha}_{\rm st}\rangle^{{\rm st},\alpha}_t = t\int {\rm d}\boldsymbol{x}_t\,\boldsymbol{g}(\boldsymbol{x}_t)\,\boldsymbol{v}^{\alpha}_{\rm st}(\boldsymbol{x}_t)\;p^{\alpha}_{\rm st}(\boldsymbol{x}_t) = (1+\alpha)\;\boldsymbol{J}_R\,t\,, \tag{5.22}$$

where for the last equality we used (5.18) and (5.19). This means that the averages evaluated in the perturbed dynamics are just rescaled by a factor $1+\alpha$, i.e.

$$\langle\boldsymbol{R}\rangle^{{\rm st},\alpha}_t = (1+\alpha)\langle\boldsymbol{R}\rangle^{\rm st}_t\,. \tag{5.23}$$

This in turn implies that, by specialising the multidimensional CR bound (4.48) to the case of one (infinitesimal) perturbation parameter, for these irreversible integrated currents one obtains

$$\partial_\alpha \langle \boldsymbol{R} \rangle_t^{\mathrm{st},\alpha}|_{\alpha=0} = \langle \boldsymbol{R} \rangle_t^{\mathrm{st}} \qquad \boldsymbol{\Xi}_{R,t} = \langle \boldsymbol{R}\boldsymbol{R}^{\mathrm{T}} \rangle_t^{\mathrm{st}} - \langle \boldsymbol{R} \rangle_t^{\mathrm{st}} \langle \boldsymbol{R}^{\mathrm{T}} \rangle_t^{\mathrm{st}} \tag{5.24}$$

$$\big(\langle \boldsymbol{R} \rangle_t^{\mathrm{st}}\big)^{\mathrm{T}} \big(\, \boldsymbol{\Xi}_{R,t}\big)^{-1} \langle \boldsymbol{R} \rangle_t^{\mathrm{st}} \leq \mathcal{I}_t(\alpha)|_{\alpha=0} \tag{5.25}$$

where $\boldsymbol{\Xi}_{R,t}$ is the covariance matrix (4.49) associated to the current R. Furthermore, if $\boldsymbol{g}(\boldsymbol{x}_t)$ appearing in (5.20) is a row vector, i.e. $\boldsymbol{g}(\boldsymbol{x}_t) = \boldsymbol{v}_t^{\mathrm{T}}$ for some vector $\boldsymbol{v}$, then the integrated current is a scalar function, as is the case, for example, of the total entropy production, and (5.25) becomes

$$\frac{\big(\langle \boldsymbol{R} \rangle_t^{\mathrm{st}}\big)^2}{\langle \Delta \boldsymbol{R}^2 \rangle_t^{\mathrm{st}}} \leq \mathcal{I}_t(\alpha)|_{\alpha=0}\,. \tag{5.26}$$

The right hand side of (5.25) and (5.26) can be readily evaluated for the perturbation (5.17) using the expression of the KL divergence for $\alpha \approx 0$ (5.10), that is

$$\mathcal{I}_t(\alpha)|_{\alpha=0} = \frac{2}{\alpha^2}\, \mathcal{D}_{\mathrm{KL}}(p^\alpha(x_t) \parallel p(x_t))|_{\alpha=0} = \frac{1}{2}\int_0^t \mathrm{d}t' \, \big\langle \boldsymbol{\nu}_{\mathrm{st}}\, \boldsymbol{D}^{-1}\, \boldsymbol{\nu}_{\mathrm{st}} \big\rangle_{t'}^{\mathrm{st}}\,, \tag{5.27}$$

where we identified $\boldsymbol{Y}^\alpha(\boldsymbol{x}_t) = \alpha \boldsymbol{Y}(\boldsymbol{x}_t) = \alpha\, \boldsymbol{\nu}_{\mathrm{st}}(\boldsymbol{x}_t)$. Moreover, note that the second last and last term of (5.10) do not appear in (5.27) because the initial distribution remains untouched by the perturbation we have chosen and because , of course, we are considering purely diffusive processes. As it is known in the literature, see again for example (2.52) or reference [42, 64], one can identify the total entropy production (in terms of k_B this time) with

$$\langle \Sigma_{\mathrm{tot}} \rangle_t = \int_0^t \mathrm{d}t' \, \big\langle \boldsymbol{\nu}\, \boldsymbol{D}^{-1}\, \boldsymbol{\nu} \big\rangle_{t'} \tag{5.28}$$

and hence, combining equation (5.26) with (5.25) or (5.27) one obtains

$$\big(\langle \boldsymbol{R} \rangle_t^{\mathrm{st}}\big)^{\mathrm{T}} \big(\, \boldsymbol{\Xi}_{R,t}\big)^{-1} \langle \boldsymbol{R} \rangle_t^{\mathrm{st}} \leq \frac{\langle \Sigma_{\mathrm{tot}} \rangle_t^{\mathrm{st}}}{2}\,, \qquad \frac{\big(\langle R \rangle_t^{\mathrm{st}}\big)^2}{\langle \Delta R^2 \rangle_t^{\mathrm{st}}} \leq \frac{\langle \Sigma_{\mathrm{tot}} \rangle_t^{\mathrm{st}}}{2} \tag{5.29}$$

that is the TUR for stationary states and vector/scalar integrated currents, respectively. Moreover, because the total entropy production is an integrated current itself with $\boldsymbol{g}(\boldsymbol{x}_t) = \big(\boldsymbol{D}^{-1}(\boldsymbol{x}_t)\boldsymbol{\nu}_{\mathrm{st}}\big)^{\mathrm{T}}$, the steady state average of the total entropy production can be written in terms of the *entropy production rate* σ_{tot}, i.e.

$$\langle \Sigma_{\mathrm{tot}} \rangle_t^{\mathrm{st}} = \sigma_{\mathrm{tot}}\, t \tag{5.30}$$

so that, by also rewriting the averages of the integrated currents in terms of their rates $\boldsymbol{J}_R$, one finally obtains from (5.29)

$$\boldsymbol{g}_t^R \equiv t\, \big(\boldsymbol{J}_R\big)^{\mathrm{T}} \, \big(\, \boldsymbol{\Xi}_{R,t}\big)^{-1} \, \boldsymbol{J}_R \leq \frac{\sigma_{\mathrm{tot}}}{2}\,, \qquad \boldsymbol{g}_t^R \equiv \frac{J_R^2}{\langle \Delta R^2 \rangle_t / t} \leq \frac{\sigma_{\mathrm{tot}}}{2} \tag{5.31}$$

where we introduced the *signal to noise ratio* $\boldsymbol{g}_t^R$ associated to the observable $R(\omega_t)$ and, moreover, we also dropped the superscript indicating the stationary average. Equation (5.31) is another form of the stationary TUR and is preferred to (5.29) because its right hand side, i.e. the upper bound, is finite and constant in the steady state. As discussed in the introduction to this chapter, the signal to noise ratio embodies the precision associated to the observable $R(\omega_t)$ and it is bounded from above by entropy production rate. For brevity, we do not present any applications of this diffusive TUR and refer to the rich literature (mentioned in the introduction of this chapter) for a comprehensive discussion of the implications of this TUR. Nevertheless, we will present some examples of the discrete TUR in Section 5.4 and compare its performances to those of our KUR (5.55).

5.2.2 Markov jump processes

The TUR can also be obtained for Markovian jump processes [19] defined on a numerable state space $S = \{s_i\}_{i=1,\dots,N}$ of N elements and continuous time. As explained in Chapter 2, the dynamics of such a process is entirely determined by the transition rate matrix $W_{ik}(t)$ and the evolution of the PDF is governed by the Master equation (2.15)

$$\partial_t p_i(t) = \sum_k J_{ik}(t) \qquad J_{ik}(t) = W_{ik}(t)\, p_k(t) - W_{ki}(t)\, p_i(t) \tag{5.32}$$

where $J_{ik}(t)$ is the probability current from the k^{th} site to the i^{th} site.

The steady state dynamics again corresponds to the probabilities p_i being not dependent on time which implies that

$$\partial_t p_{i,\,\text{st}} = \sum_k J_{ik,\,\text{st}}(t) = 0 \qquad J_{ik,\,\text{st}}(t) = W_{ik}(t)\, p_{k,\,\text{st}} - W_{ki}(t)\, p_{i,\,\text{st}}\,. \tag{5.33}$$

We perturb this steady state dynamics this time by modifying the transition rates as

$$W_{ik}^{\alpha}(t) = W_{ik}(t) \exp\big(\alpha \mathcal{Z}_{ik}\big) \overset{\alpha\to 0}{\approx} W_{ik}(t)(1 + \alpha \mathcal{Z}_{ik}) \tag{5.34}$$

$$\mathcal{Z}_{ik}(t) = \frac{W_{ik}(t)\, p_{k,\,\text{st}} - W_{ki}(t)\, p_{i,\,\text{st}}}{W_{ik}(t)\, p_{k,\,\text{st}} + W_{ki}(t)\, p_{i,\,\text{st}}}\,. \tag{5.35}$$

Note that, because $\mathcal{Z}_{ik}(t) = -\mathcal{Z}_{ki}(t)$, i.e. they have anti-symmetric indexes, this perturbation only acts on the s_{ij} parameters defined in (2.33) and this will lead, as it will be clear in the next pages, to an upper bound to the signal to noise ratio that is given by entropy production.

By putting the modified transition rates (5.35) into the steady state master equa-

tion (5.33) one sees that

$$\begin{aligned}\sum_k J^\alpha_{ik,\,\mathrm{st}}(t) &= \sum_k \left(W^\alpha_{ik}(t)\, p^\alpha_{k,\,\mathrm{st}} - W^\alpha_{ki}(t)\, p^\alpha_{i,\,\mathrm{st}}\right) = \\ &\overset{\alpha\to 0}{\approx} \sum_k \Bigg(W_{ik}(t)\, p^\alpha_{k,\,\mathrm{st}} - W_{ki}(t)\, p^\alpha_{i,\,\mathrm{st}} + \\ &\qquad + \alpha\left(W_{ik}(t)\, p_{k,\,\mathrm{st}} - W_{ki}(t)\, p_{i,\,\mathrm{st}}\right) \frac{W_{ik}(t)\, p^\alpha_{k,\,\mathrm{st}} + W_{ki}(t)\, p^\alpha_{i,\,\mathrm{st}}}{W_{ik}(t)\, p_{k,\,\mathrm{st}} + W_{ki}(t)\, p_{i,\,\mathrm{st}}} \Bigg) = \\ &\approx (1+\alpha) \sum_k \left(W_{ik}(t)\, p^\alpha_{k,\,\mathrm{st}} - W_{ki}(t)\, p^\alpha_{i,\,\mathrm{st}}\right) = 0\end{aligned} \tag{5.36}$$

meaning that the stationary modified probabilities obey to the same equations as the original ones and implying that $p^\alpha_{i,\,\mathrm{st}} = p_{i,\,\mathrm{st}}$. This in turn means that the modified probability currents are just the original ones but rescaled by a factor $1+\alpha$, i.e.

$$J^\alpha_{ik,\,\mathrm{st}}(t) = (1+\alpha)\, J_{ik,\,\mathrm{st}}(t)\,. \tag{5.37}$$

Again, one can consider the class of integrated currents in the case of Markov jump processes presented in (2.27) and defined as

$$R(\omega_t, t) = \int_0^t \sum_{ik} \left(\mathrm{d}n_{ik}(\omega_{t'}) - \mathrm{d}n_{ki}(\omega_{t'})\right) g_{ik}(t')\,. \tag{5.38}$$

The stationary average has also be found to be equal to

$$\langle R\rangle^{\mathrm{st}}_t = \int_0^t \mathrm{d}t' \sum_{ik} J_{ik,\,\mathrm{st}}(t')\, g_{ik}(t') \tag{5.39}$$

which, together with equation (5.37), implies that

$$\langle R\rangle^{\mathrm{st},\,\alpha}_t = \int_0^t \mathrm{d}t' \sum_{ik} J^\alpha_{ik,\,\mathrm{st}}(t')\; g_{ik}(t') = (1+\alpha)\langle R\rangle^{\mathrm{st}}_t\,. \tag{5.40}$$

So again, for integrated currents we managed to find a perturbation such that the perturbed average is proportional to the unperturbed one and rescaled by a factor $1+\alpha$. Hence, evaluating the left hand side of the Cramér-Rao bound for small perturbations (4.47) leads anew to

$$\frac{\left(\langle R\rangle^{\mathrm{st}}_t\right)^2}{\langle \Delta R^2\rangle^{\mathrm{st}}_t} \leq \mathcal{I}_t(\alpha)|_{\alpha=0}\,. \tag{5.41}$$

Regarding the Fisher information, as before one can exploit its relation with the KL divergence for small α which, together with (5.10), implies that

$$\mathcal{I}_t(\alpha)|_{\alpha=0} = \frac{2}{\alpha^2}\, \mathcal{D}_{\mathrm{KL}}(p^\alpha \parallel p)|_{\alpha=0} = \int_0^t \mathrm{d}t' \left\langle \mathcal{Z}^2\right\rangle_{t'} = \int_0^t \mathrm{d}t' \sum_{ik} W_{ik}(t')\; p_{k,\,\mathrm{st}}\; \mathcal{Z}^2_{ik}(t')\,, \tag{5.42}$$

where $\mathcal{Z}_{ik}(t)$ is given by (5.35). Moving forward with the calculations and using the so called log-mean inequality

$$\frac{2(b-a)^2}{b+a} \leq (b-a)\ln(b/a)\,, \tag{5.43}$$

valid for arbitrary positive a and b, along with (2.24), one sees that

$$\begin{aligned}
\mathcal{I}_t(\alpha)|_{\alpha=0} &= \int_0^t \mathrm{d}t'\, W_{ik}(t')\, p_{k,\mathrm{st}} \sum_{ik} \left(\frac{W_{ik}(t')\, p_{k,\mathrm{st}} - W_{ki}(t')\, p_{i,\mathrm{st}}}{W_{ik}(t')\, p_{k,\mathrm{st}} + W_{ki}(t')\, p_{i,\mathrm{st}}} \right)^2 \\
&= \frac{1}{2} \int_0^t \mathrm{d}t' \sum_{ik} \frac{\left(W_{ik}(t')\, p_{k,\mathrm{st}} - W_{ki}(t')\, p_{i,\mathrm{st}} \right)^2}{W_{ik}(t')\, p_{k,\mathrm{st}} + W_{ki}(t')\, p_{i,\mathrm{st}}} \leq \\
&= \frac{1}{4} \int_0^t \mathrm{d}t \sum_{ik} \left(W_{ik}(t')\, p_{k,\mathrm{st}} - W_{ki}(t')\, p_{i,\mathrm{st}} \right) \ln \left(\frac{W_{ik}(t')\, p_{k,\mathrm{st}}}{W_{ki}(t')\, p_{i,\mathrm{st}}} \right) = \\
&= \frac{1}{2} \int_0^t \mathrm{d}t' \sum_{ik} W_{ik}(t')\, p_{k,\mathrm{st}}\, \ln \left(\frac{W_{ik}(t')\, p_{k,\mathrm{st}}}{W_{ki}(t')\, p_{i,\mathrm{st}}} \right) = \frac{\langle \Sigma_{\mathrm{tot}} \rangle_t^{\mathrm{st}}}{2}\,,
\end{aligned} \tag{5.44}$$

i.e. the total entropy production is an upper bound to the Fisher information. Note that this definition of total entropy production relies on the hypothesis of microscopic reversibility, i.e. it must hold that if $W_{ik}(t) \neq 0 \implies W_{ki}(t) \neq 0$, so that the ratio appearing in the logarithm of equation's (5.44) last line is defined. This finally leads to

$$\frac{\left(\langle R \rangle_t^{\mathrm{st}} \right)^2}{\langle \Delta R^2 \rangle_t^{\mathrm{st}}} \leq \frac{\langle \Sigma_{\mathrm{tot}} \rangle_t^{\mathrm{st}}}{2} \tag{5.45}$$

where, differently from (5.29), entropy production is dimensionless. We further note that, for time independent jumping rates W_{ij} and by choosing a time independent weight matrix in (5.38), one can express (5.45) in terms of the entropy production rate and the rate of the currents $J_R = \langle R \rangle_t^{\mathrm{st}}/t$, hence obtaining

$$\boldsymbol{g}_t^R \equiv \frac{J_R^2}{\langle \Delta R^2 \rangle_t / t} \leq \frac{\sigma_{\mathrm{tot}}}{2} \tag{5.46}$$

that is the equivalent of (5.31) for Markov jump processes. We will consider some applications of this result in Section 5.4, where the performances of the TUR will be compared to those of the KUR. Indeed, for the examples that will be presented, we will show how near equilibrium the TUR is the most relevant bound because, as soon as the system starts to dissipate, currents start to appear and their signal to noise ratio $\boldsymbol{g}_t^R$ is tightly bounded by the entropy production rate. Instead, the kinetic constraint is the limiting factor for the precision of an observables in regimes far from equilibrium.

5.3 Kinetic uncertainty relation (KUR)

In this section we derive and discuss the kinetic uncertainty relation (KUR), a result we proposed [101] in 2019. The KUR is valid for Markov jump processes in continuous time, which describe a wide range of systems (molecules hopping between

states, chemical reactions, demographic dynamics, etc.). This inequality limits observable fluctuations from an angle totally distinct from the constraint of the TUR and is expressed as a function of time and of generic observables (with finite average). It embodies previous inequalities for non-equilibrium steady states [22, 23, 24] and is easily applicable to any dynamics without thermodynamic interpretation.

Consider again the master equation associated a jump process with constant jumping rates

$$\partial_t p_i(t) = \sum_k J_{ik}(t) \qquad\qquad J_{ik}(t) = W_{ik}\, p_k(t) - W_{ki}\, p_i(t)\,. \tag{5.47}$$

Moreover, consider a perturbation only involving the transition rates as defined in (5.7)

$$W^\alpha_{ik} = W_{ik} \mathrm{e}^{\alpha \mathcal{Z}^\alpha_{ik}} \tag{5.48}$$

and with $\mathcal{Z}^\alpha_{ik} = \mathcal{Z}^\alpha_{ki} = 1$, implying that

$$W^\alpha_{ik} \overset{\alpha\to 0}{\approx} (1+\alpha)\, W_{ik}\,. \tag{5.49}$$

In order to understand the effect of this perturbation on the dynamics of the system, lets consider equation (2.22), i.e. the probability of observing a given trajectory $\omega_t = \{i(t') | 0 \le t' \le t\}$ of a jump process where $i(t')$ is a piece-wise constant function of time which performs N_J jumps between states $\{i_0, ..., i_{N_J}\}$, given by

$$P(\omega_t) = p_{i_0}(t_0) \exp\Big(- \int_0^t \mathrm{d}t'\, \lambda_{i_{t'}} \Big) \prod_{n=0}^{N_J-1} W_{i_{n+1}\, i_n}\, \mathrm{d}t\,, \tag{5.50}$$

where $\lambda_i(t) = -W_{ii}(t) = \sum_{j\neq i} W_{ji}(t)$. For the perturbed rates defined in (5.49) the probability associated to a stochastic path becomes

$$\begin{aligned} P^\alpha(\omega_t) &= p_{i_0}(t_0) \exp\Big(- \int_0^t \mathrm{d}t'\, \lambda^\alpha_{i_{t'}} \Big) \prod_{n=0}^{N_J-1} W^\alpha_{i_{n+1}\, i_n}\, \mathrm{d}t = \\ &\overset{\alpha\to 0}{\approx} p_{i_0}(t_0) \exp\Big(- \int_0^t \mathrm{d}t'\, (1+\alpha)\, \lambda_{i_{t'}} \Big) \prod_{n=0}^{N_J-1} W_{i_{n+1}\, i_n}\, (1+\alpha)\, \mathrm{d}t = \\ &= P\big(\omega_{(1+\alpha)t}\big)\,, \end{aligned} \tag{5.51}$$

where in the second last line we noted that every $1+\alpha$ factor appearing in the formula can be reabsorbed into a time differential, i.e. $\mathrm{d}t'$ and $\mathrm{d}t$. Indeed, perhaps surprisingly, the rescaling of rates is equivalent to a global change in pace of the system and leads naturally to perturbed quantities that are just unperturbed ones evaluated at longer times. This implies that, for an arbitrary observable $O(\omega_t)$ which does not explicitly depend on time one has that

$$\langle O \rangle^\alpha_t = \langle O \rangle_{(1+\alpha)t}\,. \tag{5.52}$$

As usual, we can use the expression of the perturbed average as a function of α to evaluate the left hand side of (4.47) so that, for the perturbation we chose above, we get

$$\frac{\big(t \langle \dot{O} \rangle_t\big)^2}{\langle \Delta O^2 \rangle_t} \le \mathcal{I}_t(\alpha)|_{\alpha=0}\,. \tag{5.53}$$

As regards the right hand side of (5.53) one can readily evaluate it from (5.42) and by taking $\mathcal{Z}_{ik} = 1$

$$\mathcal{I}_t(\alpha)|_{\alpha=0} = \int_0^t \mathrm{d}t' \, \langle 1 \rangle_{t'} = \int_0^t \mathrm{d}t' \sum_{ik} W_{ik} \, p_k(t') = \sum_{ik} \int_0^t \langle \mathrm{d}n_{ik} \rangle_{t'} = \sum_{ik} \langle n_{ik} \rangle_t \,, \quad (5.54)$$

where we used the definition (2.26) $\langle \mathrm{d}n_{ik} \rangle_t = W_{ik} \, p_k(t) \, \mathrm{d}t$ for the average number of jumps in an infinitesimal time dt . Equation (5.54) implies that the Fisher information, for this particular perturbation, becomes equal to the average total number of jumps that the system performs in the time interval $[0, t]$, i.e. the dynamical activity presented in (2.30). The expectation $\langle \mathcal{K} \rangle_t$ is a measure of how on average the system has been active during the period $[0, t]$ and thus, the inequality (5.53) generates a KUR

$$\frac{\left(t \langle \dot{O} \rangle_t\right)^2}{\langle \Delta O^2 \rangle_t} \leq \langle \mathcal{K} \rangle_t \quad (5.55)$$

Note that, differently from the derivation of the TUR, no stationarity condition is required to obtain the KUR and also, there is no restriction on the observables for which the bound is valid, except that they must not depend explicitly on time. However, the KUR only holds for time independent transition rates.

In a steady state this equation matches previous formulas for currents [22] and counting observables [23]. Also, in the steady state one can rewrite the bound (5.55) in terms of the rates as

$$\boldsymbol{g}_t^O \equiv \frac{\left(\langle \dot{O} \rangle_t^{\mathrm{st}}\right)^2}{\langle \Delta O^2 \rangle_t^{\mathrm{st}} / t} \leq \kappa \,, \quad (5.56)$$

where $\kappa = \langle \mathcal{K} \rangle_t / t$ is constant because the average number of jumps, as it can be seen from (5.54), grows linearly with time in the steady state. Moreover, one also immediately sees that for integrated currents, for which it holds that $\langle R \rangle_t^{\mathrm{st}} = J_R \, t$, the stationary KUR becomes

$$\boldsymbol{g}_t^R = \frac{J_R^2}{\langle \Delta R^2 \rangle_t^{\mathrm{st}} / t} \leq \kappa \,. \quad (5.57)$$

To sum up, we have managed to derive a new inequality where the SNR is bounded from above by the time symmetric quantity that counts the average number of jumps in a time interval $[0, t]$. In the next section, we are going to consider some possible application of this bound and compare its performances with its thermodynamic counterpart (5.29).

5.4 TUR and KUR: examples

In this section we discuss some relevant applications of the bounds discussed above in the context of Markov jump processes. Indeed, one may wonder whether kinetic constraints are useful in thermodynamic systems because, close to equilibrium there is a finite activity (the system jumps also in equilibrium) while entropy production tends to zero. Hence, around equilibrium the TUR brings certainly a tighter constraint on a current precision than the KUR. Instead, as we will show, for all the

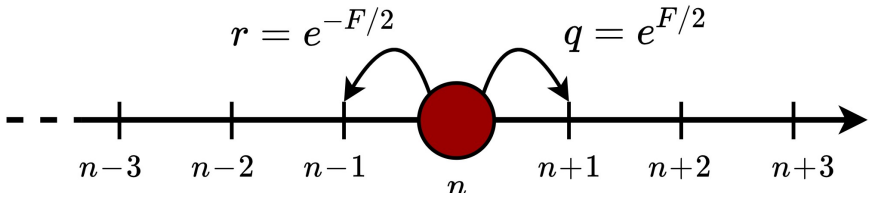

Figure 5.1: Biased Random walk with jumping rates parametrised by a non-equilibrium parameter F.

examples that we decided to consider the kinetic constraint becomes the most relevant one far from equilibrium, i.e. at regimes with a higher entropy production rate. More in detail, we will discuss the paradigmatic example of a biased random walk, the dynamics of a four state network with randomly generated transition rates and a model describing the motion of a molecular motor. In addition to these systems, which respect local detailed balance and have a well defined entropy production, we will also consider a non thermodynamic systems with an irreversible dynamics, i.e. a predator prey model where the occurrence of extinction is of course a permanent condition.

Biased Random walk is a fundamental, although very simple, example of jump process defined on an infinite and numerable sample space and depicted in Figure 5.1. In a physical flavour, one could imagine that a force F (normalised by unit displacement over $k_B T$) is applied toward positive values, and a walker jumps from n to $n+1$ with rate $q = \mathrm{e}^{F/2}$ or to $n-1$ with rate $r = \mathrm{e}^{-F/2}$ so that local detailed balance is fulfilled. In terms of the transition rate matrix, this corresponds to $W_{ik} = q\delta_{i-1,k} + r\delta_{i+1,k} - (q+r)\delta_{i,k}$ which implies that, the average total number of jumps or dynamical activity (5.58) becomes

$$\begin{aligned} \langle \mathcal{K} \rangle_t = \langle n_{\mathrm{tot}} \rangle_t = \sum_{i,k\neq i} \langle n_{ik} \rangle_t = \int_0^t \sum_{i,k\neq i} \langle \mathrm{d}n_{ik} \rangle_{t'} = \int_0^t \mathrm{d}t' \sum_{i,k\neq i} p_k(t') W_{ik} = \\ = (q+r) \int_0^t \mathrm{d}t' \sum_i p_i(t') = (q+r)t = \kappa t \,, \end{aligned} \tag{5.58}$$

where we used that $\langle \mathrm{d}n_{ik} \rangle_t = p_k(t) W_{ik}\, dt$ and noted that the rate of jumps is equal to $\kappa = q + r$. Moreover, it is clear that every time a jump occurs, the probabilities of jumping to the right or the left are equal to $p_+ = q/(q+r)$ and $p_- = r/(q+r)$ respectively. As a consequence, the average number of jumps towards the positive $\langle n_+ \rangle$ and negative $\langle n_+ \rangle$ direction become

$$\langle n_+ \rangle_t = p_+ \langle n_{\mathrm{tot}} \rangle_t = qt \qquad\qquad \langle n_- \rangle_t = p_- \langle n_{\mathrm{tot}} \rangle_t = rt \,. \tag{5.59}$$

By means of these averages, one can also compute the stationary average entropy production. Indeed, by noting that for the case we are considering the entropic parameters, defined in (2.33), are equal to $s_+ \equiv s_{i+1,i} = F$ and $s_- \equiv s_{i-1,i} = -F$, one readily sees that (2.35) becomes

$$\langle \Sigma_{\mathrm{tot}} \rangle_t^{\mathrm{st}} = \sum_{ik} s_{ik} \langle n_{ik} \rangle_t = s_+ \langle n_+ \rangle_t - s_- \langle n_- \rangle_t s_- = (q-r)Ft = \sigma_{\mathrm{tot}} t \,, \tag{5.60}$$

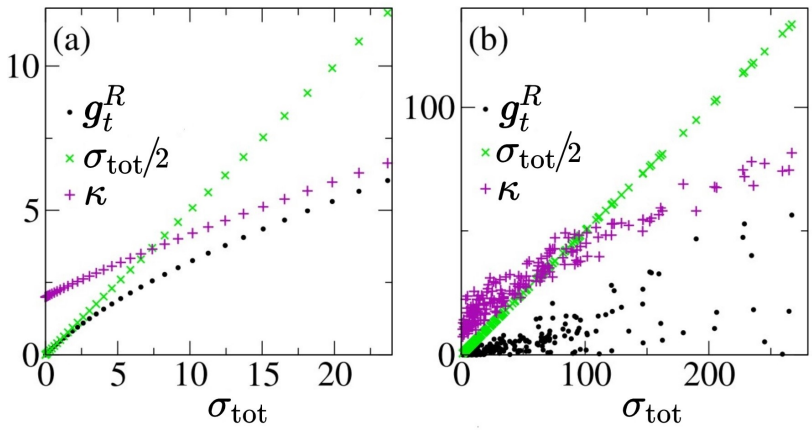

Figure 5.2: Biased Random walk with jumping rates parametrised by a non-equilibrium parameter F.

where clearly the entropy production rate equals $\sigma_{\rm tot} = (q-r)F$. This value exceeds the mean jumping rate $\kappa = (p+q)$ for sufficiently large forces, where the KUR becomes the limiting factor for the precision. For the latter, one could for example consider R equal to the displacement at time t from the initial position, that is an irreversible integrated current (2.27) with $g_{ik} = \delta_{i-1,k}$

$$R(\omega_t) = \int_0^t \sum_{ik} \left(\mathrm{d}n_{i,i-1}(\omega_{t'}) - \mathrm{d}n_{i-1,i}(\omega_{t'}) \right) = n_+(t) - n_-(t)\,, \tag{5.61}$$

i.e. it is the difference between the total number of jumps towards the right and the left. Its average is clearly $\langle R \rangle_t = \langle n_+ \rangle_t - \langle n_+ \rangle_t = (q-r)t$ while its variance, it can be shown, is equal to $\langle \Delta R^2 \rangle_t = 2(q+r)t$. These quantities can finally be used to evaluate the stationary SNR appearing on the left of (5.46) and (5.57)

$$\boldsymbol{g}_t^R = \frac{J_R^2}{\langle \Delta R^2 \rangle_t^{\rm st}/t} = \frac{(q-r)^2}{2(q+r)}\,, \tag{5.62}$$

where $J_R = \langle R \rangle_t^{\rm st}/t = q - r$. We plot this SNR in Figure 5.2(a) together with $\sigma_{\rm tot}/2$ and κ as a function of the mean dissipation rate $\sigma_{\rm tot}$ (points parametrised by increasing F). The figure visualises how $\boldsymbol{g}_t^R$ is first limited from above by the entropic constraint and then, getting farther from equilibrium by increasing $\sigma_{\rm tot}$, it becomes bounded by the frenetic limit $\sigma_{\rm tot} \leq \kappa$.

Random network. The generality of the nonequilibrium frenetic bounds on the precision of a stochastic current is illustrated with a second example, in which we focus on finite times. Let us consider networks of N states fully connected by transition rates $W_{ik} = \exp(s_{ik}/2)$ and reverse $W_{ki} = \exp(-s_{ik}/2)$, with s_{ik} drawn randomly from the interval $[-\Delta S_{\rm max}, \Delta S_{\rm max}]$. The entropy production in a trajectory of N_J jumps visiting states $\{i_0, i_1, \ldots, i_{N_J}\}$ is thus the sum $\Sigma_{\rm tot} = \sum_{n=0}^{N_J-1} s_{i_{n+1} i_n}$ plus boundary terms that do not matter after averaging in the steady state. Due to the randomisation, some networks dissipate on average more than others. Using for instance $N = 4$ and $\Delta S_{\rm max} = 5$, we generate a wide spectrum of $\sigma_{\rm tot}$ values. We first choose to observe the current $R(t) = n_{xy}(t) - n_{yx}(t)$ over the single bond (x, y)

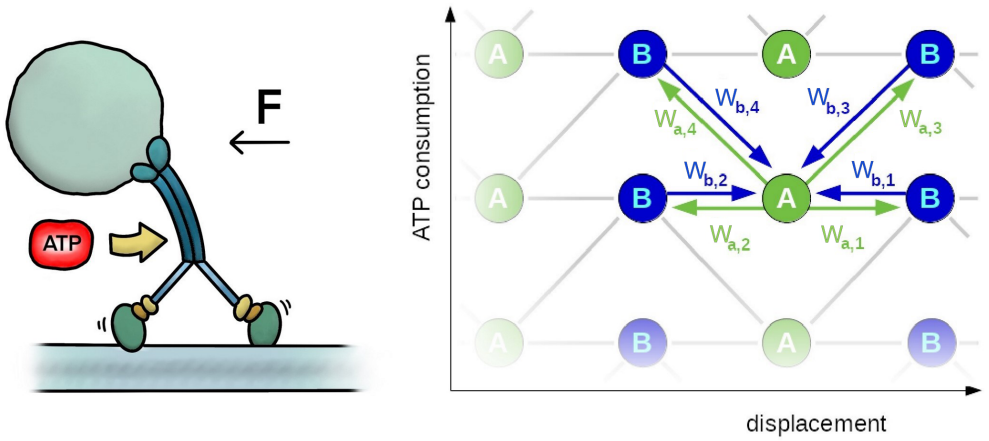

Figure 5.3: Sketch of possible transitions and relative transition rates in the kinesin model.

with largest $s_{xy} = \max_{ik} s_{ik}$ in each network. We thus count the jumps from x to y minus those from y to x up to time t, with $t = 1/\min_{i\neq j} W_{ik}$. In Figure 5.2(b) each point represents an average for a given random network. We see again that the time-dependent TUR ($\mathcal{g}_t^R \leq \sigma_{\text{tot}}/2$) limits the current precision near equilibrium while the KUR ($\mathcal{g}_t^R < \kappa$) is the limiting factor far from equilibrium.

Molecular motor. A molecular motor model confirms that the KUR is relevant in real non-equilibrium regimes. The model [111, 112] is based on parameters extracted from experimental data and describes the motion of a kinesin molecule on a microtubule while pulling against an external force $F < 0$. The microtubule can be regarded a one dimensional lattice with spacing $d = 4$nm while the Kinesin can be in one of two kinds of state, A (its legs are on the tubule) and B (one leg is raised). The full state space is infinite and characterised by the number n of half steps of the motor and by the number m of ATP consumed, after assuming for example $i = (0,0)$ to be of kind A. A jump from a state $i = (n,m)$ is to a neighbour of the opposite kind via one of four different transitions. For kind A these are: (1) right step with no ATP consumed, (2) left step with no ATP consumed, (3) right step with ATP consumed (which is the typical motor direction), (4) left step with ATP consumed. The opposite transitions from state B are also possible, see the scheme in Figure 5.3. In a notation consistent with the sketched transitions, we write their rates as $\boldsymbol{W}_a = (W_{a,1}, W_{a,2}, W_{a,3}, W_{a,4})$ and $\boldsymbol{W}_b = (W_{b,1}, W_{b,2}, W_{b,3}, W_{b,4})$. Thus, in total, there is a rate $\lambda_a = \boldsymbol{W}_a^{\mathrm{T}} \cdot \mathbf{1}$ to escape from A and $\lambda_b = \boldsymbol{W}_b^{\mathrm{T}} \cdot \mathbf{1}$ from B, where $\mathbf{1} = (1,1,1,1)$.

Kinesin is usually pulling cargoes with a force $F \approx pN$. For a scaled force $f = Fd/(k_B T)$ with sign $f < 0$ if F is opposite to the motion (it pulls on the left), the rates read

$$
\begin{aligned}
W_{a,1} &= \omega e^{-\epsilon+\theta_a^+ f}\,, & W_{b,1} &= \omega e^{-\theta_b^- f}\,,\\
W_{a,2} &= \omega' e^{-\epsilon-\theta_a^- f}\,, & W_{b,2} &= \omega' e^{\theta_b^+ f}\,,\\
W_{a,3} &= \alpha e^{-\epsilon+\theta_a^+ f} k_0[\mathrm{ATP}]\,, & W_{b,3} &= \alpha e^{-\theta_b^- f}\,,\\
W_{a,4} &= \alpha' e^{-\epsilon-\theta_a^- f} k_0[\mathrm{ATP}]\,, & W_{b,4} &= \alpha' e^{\theta_b^+ f}\,,
\end{aligned}
$$

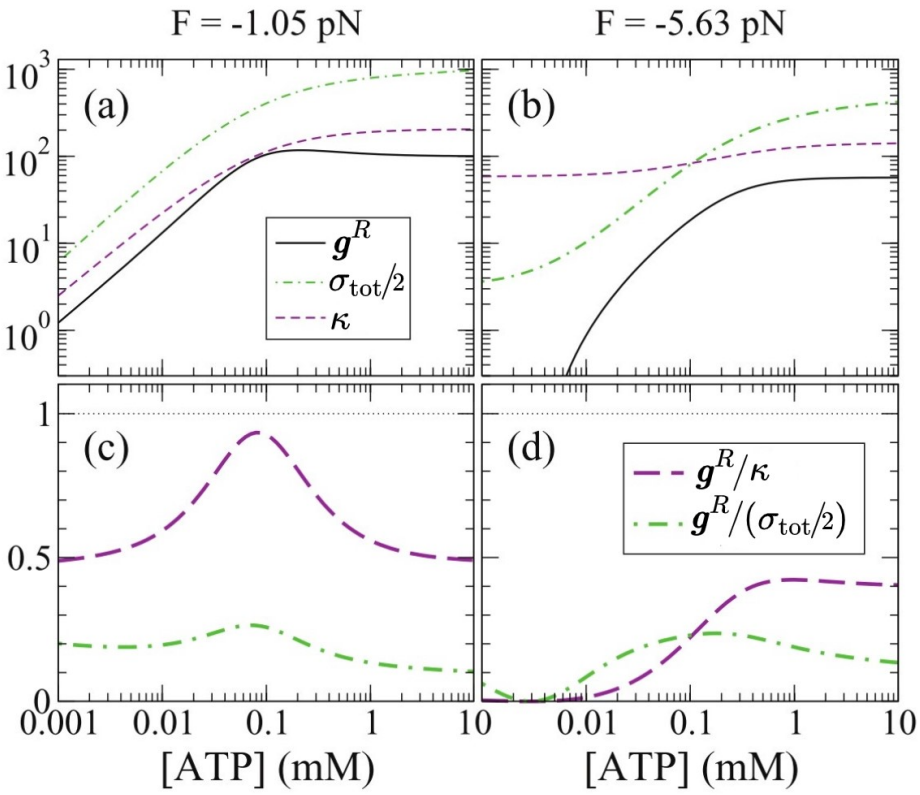

Figure 5.4: Model of kinesin pulling against a force F: left panels for $-F = 1.05$pN, right panels for $-F = 5.63$pN. (a), (b) Precision g^R of the molecular motor displacement in the steady state as a function of ATP concentration, together with half mean dissipation $\sigma_{\rm tot}/2$ and mean jumping rate κ. (c), (d) Ratio of the precision with these quantities. All plots highlight that in physiological conditions 1mM $\lesssim$ [ATP] $\lesssim$ 10mM it is the KUR that determines the upper limit of precision.

with values

$$\theta_a^+ = 0.25\,, \quad \theta_a^- = 1.83\,, \quad \theta_b^+ = 0.08\,, \quad \theta_b^- = -0.16\,,$$

and $k_0 = 1.4 \times 10^5 \mu\text{M}^{-1}$, $\epsilon = 10.81$, $\alpha = 0.57\text{s}^{-1}$, $\alpha' = 1.3 \times 10^{-6}\text{s}^{-1}$, $\omega = 3.4\text{s}^{-1}$, $\omega' = 108.15\text{s}^{-1}$. See Ref. [111] for all the details on these parameters.

To compute average quantities and variances we resort to large deviation theory [112, 113] and calculate the scaled cumulant generating function $\Lambda_O(s)$ associated to a given observable O. This can be done by first considering the generator $\mathbf{M}$ of the dynamics is the matrix entering in the master equation $\partial_t p = \mathbf{M}p$, where $p = (p_A, p_B)$ is the probability at time t to find the motor in A or B. The next step consists in "tilting" the generator with exponentials suitably coupled to the transitions. Let us define $\boldsymbol{v}_i = (e^{\gamma_{i,1}s}, e^{\gamma_{i,2}s}, e^{\gamma_{i,3}s}, e^{\gamma_{i,4}s})$ where γ's will define the observable O. With this definition, the tilted generator is written in a compact notation as

$$\mathbf{M}_O(s) = \begin{pmatrix} -\lambda_a & \boldsymbol{W}_b \cdot \boldsymbol{v}_b \\ \boldsymbol{W}_a \cdot \boldsymbol{v}_a & -\lambda_b \end{pmatrix}.$$

Its eigenvalue $\Lambda(s)$ (of the two) for which $\Lambda(0) = 0$ (i.e. the eigenvalue corresponding to the steady state of $\mathbf{M} = \mathbf{M}_O(0)$) is the scaled cumulant generating function of

O, namely the function determining its scaled cumulants in the limit of long time. For instance, the scaled average is

$$J_O = \lim_{t\to\infty} \langle O\rangle_t / t = \partial_s \Lambda_O(s)|_{s=0} \tag{5.63}$$

and the scaled variance is

$$C_2 = \lim_{t\to\infty} [\langle O^2\rangle_t - \langle O\rangle_t^2]/t = \partial_s^2 \Lambda_O(s)\Big|_{s=0} . \tag{5.64}$$

To obtain the mean dynamical activity κ one uses $\boldsymbol{\gamma}_a = \boldsymbol{\gamma}_b = \mathbf{1}$. For the entropy production $\sigma_{\rm tot}$ (with Boltzmann constant $k_B = 1$) the suitable

$$\boldsymbol{\gamma}_a = -\boldsymbol{\gamma}_b = (\ln W_{a,1}/W_{b,1}, \dots, \ln W_{a,4}/W_{b,4}) . \tag{5.65}$$

For an observable R equal to the displacement, in this model we have $\boldsymbol{\gamma}_a = -\boldsymbol{\gamma}_b = (d, -d, d, -d)$ and, by means of the procedure discussed above, one can compute the precision $\boldsymbol{\mathcal{g}}^R = J_R^2/C_2$ (all the results are obtained via Mathematica and here we do not report their long explicit formulae) and plot it as a function of growing ATP concentration, implying an increase of entropy production. Moreover, by also plotting $\sigma_{\rm tot}/2$ and κ one can evaluate the performances of the TUR and the KUR, the results are shown in Figure 5.4. We see that, in typical in vivo conditions ($-F \approx$ pN, ATP concentration 1mM $\lesssim$ [ATP] $\lesssim$ 10mM), $\kappa < \sigma_{\rm tot}/2$, i.e., it is the kinetic constraint that puts a ceiling on the precision of kinesin motion. At the smaller force [Fig. 5.4(a),(c)], there is a regime of almost optimised precision at around [ATP]$=$ 0.1mM. While a lower precision seems normal at small fuel concentrations, it is perhaps more surprising when the environment furnishes more resources. However, as already discussed in this thesis, this should not be considered unusual in life processes [3].

Predator prey model. The KUR is valid also for non-thermodynamic systems. We may for example consider processes without microscopic reversibility (some $W_{ik} \neq 0$ while $W_{ki} = 0$), where the TUR cannot be applied. The following example of population dynamics falls in this category.

Stochastic equations are routinely applied in studies of population dynamics, of which a simple model is the predator-prey dynamics that gives rise quasi-periodic oscillations (due to *stochastic amplification* [114]). The system is described by the number of predators (n individuals of kind A) and preys (m individuals of kind B) in a niche allowing at most N individuals, i.e., $n + m \leq N$. Working in the context of urn models [114], where also empty slots (E) are considered, the rates that describe the escape from a state $i = (n, m)$ are built upon microscopic processes (birth $BE \xrightarrow{b} BB$, death $A \xrightarrow{d_1} E$, $B \xrightarrow{d_2} E$ and predation $AB \xrightarrow{p_1} AA$, $AB \xrightarrow{p_2} AE$). They become $w^{(1)} = d_1 n$, $w^{(2)} = 2bm(N-n-m)/N$, $w^{(3)} = 2p_2 nm/N + d_2 m$, and $w^{(4)} = 2p_1 nm/N$, see the scheme in the inset of Figure 5.5.

As an observable, in this demographic model we consider the number $O(t)$ of predators' deaths (clearly originated by an irreversible process) up to time t, related to the transition 1 with rates $w^{(1)}(n, m)$. The system is simulated with a Gillespie algorithm [115] and is released at time zero from a given initial condition: (A) in steady state, (B) with an abundance of predators ($n/N = 3m/N = 0.6$), or (C) with

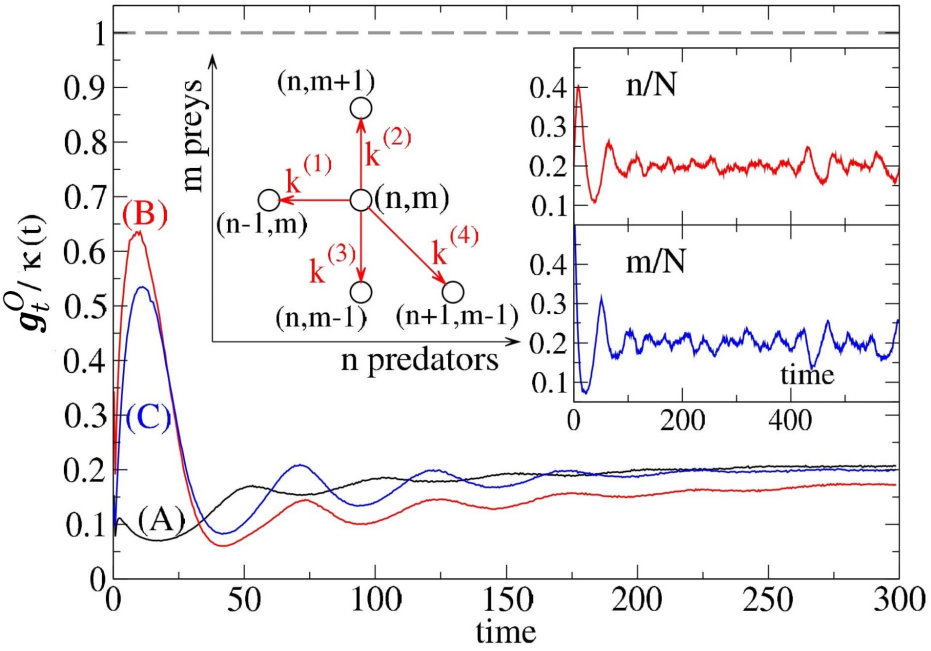

Figure 5.5: For the prey-predator model, we plot the KUR precision ratio $\boldsymbol{g}_O(t)/\kappa(t)$ for the counting O of predator deaths up to time t. Curves are for the three initial conditions discussed in the text ($N = 3200$, $b = 0.1$, $d_1 = 0.1$, $d_2 = 0$, $p_1 = 0.25$, $p_2 = 0.05$, curves from averages over 10^4 trajectories). The horizontal dashed line highlights that $\boldsymbol{g}_O(t)/\kappa(t) \leq 1$. The insets show a scheme of the transition rates of the model, and a relaxation trajectory from initial state of condition (C) toward a stochastic oscillatory regime.

an abundance of preys ($m/N = 3n/N = 0.6$). In the large inset of Fig. 5.5 we see an example of relaxation toward the regime with stochastic oscillations, for case (C). We collect the statistics of O in this transient phase. Fig. 5.5 shows that in all cases the ratio $g_O(t)/\kappa(t)$, associated to non equilibrium KUR (5.55) with $\kappa(t) = \langle \mathcal{K} \rangle_t / t$, is less then 1 as expected.

To compute the mean jumping rate $\kappa(t)$ in the simulation it is sufficient to record the total number of transitions in $[0, t]$ and average this value over many realisations of the process. We stress that in this system it is impossible to talk about irreversibility in the sense of ratios of reciprocal rates, W_{ik}/W_{ki}. Indeed such ratio is not defined for transitions 1 and 4, which do not have allowed reversals. Conversely, it seems a natural and easy procedure to count events to determine the mean dynamical activity.

Final considerations For thermodynamic systems, the KUR is complementary to the uncertainty relation based on thermodynamic considerations and focusing on dissipation. We have shown examples in which, by getting farther and farther from equilibrium dynamics, the kinetic constraints become more relevant than thermodynamic ones in limiting the precision of a given process. A model of kinesin suggests that the dispersion in the motion of this molecular motor, in physiological conditions, cannot be arbitrarily small due to the KUR. Moreover, the KUR is readily computed also in irreversible systems as those often modelled by discrete stochastic processes. With an example of predator-prey dynamics, we have illustrated how

the KUR puts a limit on the maximum precision of observables.

5.5 GLE based thermodynamic uncertainty relation

In this section we provide non-equilibrium inequalities for a simple system with memory, modelled by equation (3.4) and based on our paper [116]. This is achieved by applying the Cramér-Rao bound (4.54) to the joint PDF of position and velocity associated to the GLE. We will then proceed to consider a multidimensional generalisation of this scenario. A practical realisation of this dynamics is a colloidal bead dragged by optical tweezers in a complex medium [82, 117], say a viscoelastic fluid, or driven by a space-independent time-modulated force. Analytical solutions show that the average and variance of observables for this non-Markovian system also obey a form of generalised TUR, especially in the unidimensional case. In this inequality there appear instantaneous quantities: the instantaneous rate of entropy production is eventually present, while original TURs include the accumulated entropy production $\langle \Sigma_{\rm tot} \rangle_t$ and may reduce to forms including its rate only if a steady state is established. Similarly, the observable O entering in our formula is state dependent and its variance is meant as the instantaneous variance in a statistical ensemble at the same time. Thus, the formulas in this section are not for integrated currents, as in usual TURs, but for state-dependent quantities. The importance of such instantaneous quantities was recently highlighted in a novel version of TUR for Markovian systems [20] (see also previous examples [118]).

For the simplest one-dimensional Langevin dynamics without memory, implying equation (2.59) and with harmonic trap, both in steady states (where the trap has been moving with a steady velocity for a long time) and in transients from an initial equilibrium, but only for velocity-independent observables $O(x_t)$ in the latter case, we find that the entropy production rate is the only component of the cost function in the TUR. However, it comes with a prefactor depending on the trap strength and the fluid viscosity. The same holds by replacing Markovianity with the long time limit in systems with memory. The multidimensional generalisation, however, shows that such thermodynamic interpretation is not always possible. For the case of unbound diffusion we also find a rich phenomenology in which, under some specific conditions, there emerges entropy production as the upper bound of the non-equilibrium inequality.

We study a Langevin dynamics with coloured noise and friction with memory, by focusing first on the unidimensional case. We would like to characterise uncertainty relations for the motion of a colloidal particle in a complex viscoelastic fluid, subject to a harmonic potential due to the action of optical tweezers, and eventually to a time-modulated space-independent external force $f(t)$ that could represent a uniform electric field acting on a charged particle. With this addition, the GLE (3.4) becomes

$$m\ddot{x}(t) = -\int_{t_m}^{t} \mathrm{d}t' \, \Gamma(t-t')\dot{x}(t') - \kappa\left[x(t) - \lambda(t)\right] + f(t) + \eta(t)\,, \tag{5.66}$$

For future convenience, we collect the space-independent terms in

$$F(t) \equiv f(t) + \kappa\lambda(t)\,. \tag{5.67}$$

In this section we will only focus on processes for which the joint probability density function (PDF) of position and velocity at time t is Gaussian. For linear systems, as in our case, this can be obtained either by starting already from a Gaussian PDF $p(x_{t_m}, v_{t_m}, t_m)$, or by starting from an arbitrary distribution and wait long enough till it becomes a Gaussian. The latter scenario occurs if either $t_m \to -\infty$ or $t \to \infty$. Under these hypothesis, the PDF $p_{t_m}(x_t, v_t, t)$ is a bivariate Gaussian such that presented in (3.29)

$$p_{t_m}(x_t, v_t, t) = \frac{1}{\sqrt{(2\pi)^2 |\mathcal{S}_{t_m,t}|}} \exp\left[-\frac{1}{2}(\boldsymbol{x}_t - \langle \boldsymbol{x} \rangle_{t_m,t})^T \mathcal{S}^{-1}_{t_m,t} (\boldsymbol{x}_t - \langle \boldsymbol{x} \rangle_{t_m,t})\right], \quad (5.68)$$

with $\boldsymbol{x}_t = (x_t, v_t)$. Moreover, $\langle \boldsymbol{x} \rangle_{t_m,t} = (\langle x \rangle_{t_m,t}, \langle v \rangle_{t_m,t})$ and $\mathcal{S}_{t_m,t}$ are given by (3.20),(3.21) and (3.30), respectively. The distribution is of course completely characterised by the above mentioned quantities. We can hence apply the temporal Cramér-Rao bound (4.54) to (5.68) to obtain new stochastic inequalities involving average and variance of generic observables $O(x_t, v_t)$ depending on position and velocity. The bound hence becomes

$$\frac{\langle \dot{O} \rangle^2_{t_m,t}}{\langle \Delta O^2 \rangle_{t_m,t}} \leq \mathcal{I}_{t_m}(t)\,, \quad (5.69)$$

where $\mathcal{I}_{t_m}(t)$ is the temporal Fisher information depending on some initial condition at time t_m. Moreover, in reference [118], the authors Ito and Dechant find the expression for the temporal Fisher information associated to a Gaussian PDF, that is

$$\mathcal{I}_{t_m}(t) = (\langle \dot{x} \rangle_{t_m,t}, \langle \dot{v} \rangle_{t_m,t})^T \mathcal{S}^{-1}_{t_m,t} (\langle \dot{x} \rangle_{t_m,t}, \langle \dot{v} \rangle_{t_m,t}) + \frac{1}{2}\mathrm{tr}\left(\mathcal{S}^{-1}_{t_m,t} \dot{\mathcal{S}}_{t_m,t} \mathcal{S}^{-1}_{t_m,t} \dot{\mathcal{S}}_{t_m,t}\right), \quad (5.70)$$

where, as usual, the dot superscript stays for time derivative. In the next subsections we will calculate explicit expressions for the Fisher information starting from different initial conditions and eventually show their connection with the entropy production rate, derived in the previous chapter.

To sum up, the inequality defined by (5.69) and (5.70) is an instantaneous nonequilibrium uncertainty relation for processes with a Gaussian distribution and following a GLE with memory. Of course, this formula works also for Markov dynamics, see again [118]. By instantaneous we mean that both the observable O and the cost function on the right hand side are quantities that depend only on the (PDF of the) position and velocity at time t. Moreover, the Fisher information can be related to entropy production rates in some cases discussed in the following section.

5.5.0.1 Particle confined by a harmonic trap

For an active harmonic trap, we focus on two interesting regimes where the covariance matrix is constant and diagonal: the case $t_m \to -\infty$ and a dynamics starting from thermodynamic equilibrium. For this cases we find that (see equation (3.80) and (3.87))

$$\mathcal{S}^{\mathrm{eq}}_t = \mathcal{S}_{-\infty,t} = \begin{pmatrix} k_B T/\kappa & 0 \\ 0 & k_B T/m \end{pmatrix}. \quad (5.71)$$

This is obtained by using equations (3.28), (3.33) and (3.34) along with the limits of the susceptibilities calculated in A.1. Indeed, since κ is not modulated and since the force $f(t)$ is space-independent, we have that the covariance matrix remains constant.

In the first case, this *steady state* for the covariance matrix is achieved by starting from $t_m \to -\infty$. To justify terming steady state such regime, we anticipate that we will illustrate it for a particle that is being dragged since a long time by a trap moving at constant velocity. However, the results below hold also for a more complex scenario with general $\lambda(t)$ and $f(t)$.

Using again the limits of the susceptibilities, in particular using that that $\lim_{t\to\infty} \chi_v(t) = 0$, $\lim_{t\to\infty} \chi_x(t) = 0$ and $\lim_{t\to\infty} \chi(t) = 1/\kappa$, from (3.20) and (3.21) we obtain that

$$\langle x \rangle_t^{-\infty} = \int_{-\infty}^{t} \mathrm{d}t' \chi_x(t-t') F(t') \,, \tag{5.72}$$

$$\langle v \rangle_t^{-\infty} = \chi_x(0) F(t) + \int_{-\infty}^{t} \mathrm{d}t' \chi_v(t-t') F(t') \,. \tag{5.73}$$

where $\chi_x(0) \neq 0$ only for overdamped dynamics. Moreover, the notation $\langle \dots \rangle_t^{-\infty}$ denotes an average obtained for $t_m \to -\infty$. The asymptotic decay of the position susceptibility $\lim_{t\to\infty} \chi_x(t) = 0$ is expected in a constrained system (this will not be the case for $\kappa = 0$).

In the second case, equipartition as in (5.71) holds because we start at $t_m = 0$ at equilibrium under the potential $\kappa x_t^2/2$. This implies that $\langle v_0 \rangle = \langle x_0 \rangle = 0$, $\langle \Delta v_0^2 \rangle = k_B T/m$, $\langle \Delta x_0^2 \rangle = k_B T/\kappa$ and $\mathrm{Cov}(x_{t_0}, v_{t_0}) = 0$, so that the covariance matrix remains constant for all $t \geq 0$ (this can be checked by plugging the parameters just listed into equations (3.28), (3.33) and (3.34)). Moreover, it can be readily seen that

$$\langle x \rangle_t^{\mathrm{eq}} = \int_{0}^{t} \mathrm{d}t' \chi_x(t-t') F(t') \,, \tag{5.74}$$

$$\langle v \rangle_t^{\mathrm{eq}} = \chi_x(0) F(t) + \int_{0}^{t} \mathrm{d}t' \chi_v(t-t') F(t') \,. \tag{5.75}$$

For these two cases of confined particle, the estimates for the average of position and velocity and for the covariance matrix along with (5.69) and (5.70) lead to the uncertainty relation

$$\mathrm{g}^{\mathrm{trap}}_{O,t_m}(t) \leq \mathcal{C}^{\mathrm{trap}}_{t_m}(t) \tag{5.76}$$

with

$$\begin{aligned} \mathrm{g}^{\mathrm{trap}}_{O,t_m}(t) &\equiv \frac{\langle \dot{O} \rangle^2_{t_m,t}}{\langle \Delta O^2 \rangle_{t_m,t}} \\ \mathcal{C}^{\mathrm{trap}}_{x,v,t_m}(t) &\equiv \frac{\kappa \langle \dot{x} \rangle^2_{t_m,t} + m \langle \dot{v} \rangle^2_{t_m,t}}{k_B T} \,, \end{aligned} \tag{5.77}$$

where t_m is either 0 or $-\infty$, $\mathcal{C}^{\mathrm{trap}}_{t_m}(t)$ is the cost function and $\mathrm{g}^{\mathrm{trap}}_{O,t_m}(t)$ is essentially a (squared) signal-to-noise ratio (SNR), similar to those defined in (2.29), (5.31)

and (5.46), encoding the precision associated to the observable $O(x_t, v_t)$. Instead, if we consider the position PDF $p_{t_m}(x_t, t)$, obtained from the marginalisation of $p_{t_m}(x_t, v_t, t)$ with respect to v_t, we obtain another expression for the cost function $\mathcal{C}^{\text{trap}}_{t_m}(t)$ from the Fisher information, i.e.

$$\mathcal{C}^{\text{trap}}_{x,t_m}(t) \equiv \frac{\kappa \langle \dot{x} \rangle^2_{t_m,t}}{k_B T}\,, \tag{5.78}$$

which is also valid for overdamped dynamics, where $m = 0$. In this case, the bound is only valid for observables that depend solely on x_t, i.e. $O(x_t)$.

We have previously shown in (3.58) that, if the memory kernel is integrable, for large observation times the entropy production rate of the system becomes

$$\lim_{t\to\infty} \langle \sigma_{\text{tot}} \rangle_{t_m,t} = \lim_{t\to\infty} \langle \sigma_{\text{med}} \rangle_{t_m,t} = \frac{\widehat{\gamma}}{k_B T} \left(\lim_{t\to\infty} \langle \dot{x} \rangle_{t_m,t} \right)^2 . \tag{5.79}$$

In this limit equation (5.76) can be rewritten as

$$\lim_{t\to\infty} \mathrm{g}^{\text{trap}}_{O,t_m}(t) \leq \frac{\kappa}{\widehat{\gamma}} \langle \sigma_{\text{tot}} \rangle_{t_m,t} + \frac{m \langle \dot{v} \rangle^2_{t_m,t}}{k_B T}\,. \tag{5.80}$$

This means that for long times, instantaneous observables $O(x_t, v_t)$ have a SNR $\mathrm{g}^{\text{trap}}_{O,t_m}(t)$ bounded from above by the mean total entropy production rate times a ratio of the trap strength by the low-frequency damping coefficient, plus a positive term dependent on the average acceleration of the particle. Instead, for observables dependent solely on the position x_t or overdamped systems, the last term on the r.h.s. is not present and the bound has a purely entropic interpretation for large observation times. Again, as noted in [98], the dependence on odd variables, such as v_t, of the observables considered in the SNR ratio generates a new term in the cost function in addition to entropy production. However, for non-oscillating external forces such as $F(t) \propto t^n$ or more specifically $\lambda(t) = vt$, it holds that $\langle \dot{v} \rangle_t / \langle \dot{x} \rangle_t \to 0$ as $t \to \infty$ and hence, in this limit, the entropy production rate becomes the dominant component of the cost function in (5.80).

As an example, we consider a particularly interesting regime that can be achieved by choosing $\lambda(t) = vt$ and by sending $t_m \to -\infty$. Again in Chapter (3), we show that this can be considered as a steady state for which

$$\langle x \rangle^{ss}_t = vt - \frac{\widehat{\gamma} v}{\kappa}\,, \qquad \langle v \rangle^{ss}_t = \langle v_{\text{ret}} \rangle^{ss}_t = v\,, \qquad \langle \sigma_{\text{tot}} \rangle^{ss}_t = \widehat{\gamma} v^2 t\,. \tag{5.81}$$

Hence, in this case, we may express the cost function in terms of the instantaneous mean entropy production rate times $\kappa/\hat{\gamma}$ for all times and all observables $O(x_t, v_t)$, i.e.

$$\mathrm{g}^{ss,\text{trap}}_{O}(t) \leq \frac{\kappa}{\widehat{\gamma}} \langle \sigma_{\text{tot}} \rangle^{ss}_t\,. \tag{5.82}$$

Finally, in the Markovian (mk) case, inequality (5.80) is valid for every t_m and t. Indeed in this case

$$\Gamma^{\text{mk}}(t) = 2\gamma_0 \delta(t)\,, \quad \widehat{\gamma}^{\text{mk}}(t) = \int_0^t \mathrm{d}t' \, \Gamma^{\text{mk}}(t) = \gamma_0\,, \quad \langle v_{\text{ret}} \rangle^{\text{mk}}_{t_m,t} = \langle v \rangle^{\text{mk}}_{t_m,t} \tag{5.83}$$

and from equation (3.58) we get

$$\frac{\kappa}{\widehat{\gamma}}\langle\sigma\rangle^{\mathrm{mk}}_{t_m,t} = \frac{\kappa}{k_BT}(\langle\dot{x}\rangle^{\mathrm{mk}}_{t_m,t})^2\,, \tag{5.84}$$

$$\mathcal{C}^{\mathrm{mk,trap}}_{x,v,t_m}(t) = \frac{\kappa}{\gamma_0}\langle\sigma\rangle^{\mathrm{mk}}_{t_m,t} + \frac{m}{k_BT}(\langle\dot{v}\rangle^{\mathrm{mk}}_{t_m,t})^2\,, \tag{5.85}$$

$$\mathcal{C}^{\mathrm{mk,trap}}_{x,t_m}(t) = \frac{\kappa}{\gamma_0}\langle\sigma\rangle^{\mathrm{mk}}_{t_m,t}\,. \tag{5.86}$$

In the last line we noted that, for Markovian dynamics and observables that depend only on x_t as well as for overdamped dynamics, the cost function is always proportional to the entropy production rate.

5.5.0.2 Particle not confined

When no confinement is present ($\kappa = 0$), the only way to drive the system out of equilibrium is through the space-independent force $f(t)$. We again analyse two situations.

First, we consider an initial distribution that can be factorised as $p(x_0, v_0) = \delta(x_0 - \widetilde{x}_0)p^{\mathrm{eq}}(v_0)$ (a Dirac delta is a limit of a Gaussian), with

$$p^{\mathrm{eq}}(v_0) = \sqrt{\frac{m}{2\pi k_BT}}\exp\left[-\frac{mv_0^2}{2k_BT}\right] \tag{5.87}$$

and meaning that $\langle x_0\rangle = 0$, $\langle v_0\rangle = 0$, $\langle\Delta x_0^2\rangle = 0$, $\langle\Delta v_0^2\rangle = k_BT/m$ and $\mathrm{Cov}(x_{t_0}, v_{t_0}) = 0$. With this initial conditions we find that

$$\langle x\rangle^{dd}_t = \widetilde{x}_0 + \int_0^t \mathrm{d}t'\chi_x(t-t')f(t')\,, \quad \langle v\rangle^{dd}_t = \chi_x(0)f(t) + \int_0^t \mathrm{d}t'\chi_v(t-t')f(t')\,, \tag{5.88}$$

$$\mathcal{S}_t = \begin{pmatrix} 2k_BT\chi(t) & k_BT\chi_x(t) \\ k_BT\chi_x(t) & k_BT/m \end{pmatrix}. \tag{5.89}$$

Experimentally, this can obtained by selecting any occurrence where $x(t) = \widetilde{x}_0$ and use it as an initial point for the future dynamics. Note that this kind of initial distribution could have been also used for the trapped case but we simply chose not to consider it.

Otherwise, we can prepare the system in an initial equilibrium distribution with an optical trap, say with stiffness κ', and switch it off when the external force is turned on. This would correspond to $\langle v_0\rangle = \langle x_0\rangle = 0$, $\langle\Delta v_0^2\rangle = k_BT/m$, $\langle\Delta x_0^2\rangle = k_BT/\kappa'$ and $\mathrm{Cov}(x_{t_0}, v_{t_0}) = 0$, so that

$$\langle x\rangle^{\kappa'}_t = \int_0^t \mathrm{d}t'\chi_x(t-t')f(t')\,, \quad \langle v\rangle^{\kappa'}_t = \chi_x(0)f(t) + \int_0^t \mathrm{d}t'\chi_v(t-t')f(t')\,, \tag{5.90}$$

$$\mathcal{S}_t = \begin{pmatrix} k_BT(2\chi(t) + 1/\kappa') & k_BT\chi_x(t) \\ k_BT\chi_x(t) & k_BT/m \end{pmatrix}. \tag{5.91}$$

In both cases, using the limits of the susceptibilities for the diffusive scenario, one sees that the long time limit of the covariance matrix reads

$$\lim_{t\to\infty} \mathcal{S}_t = \begin{pmatrix} 2k_BTt/\gamma & k_BT/\gamma \\ k_BT/\gamma & k_BT/m \end{pmatrix} . \tag{5.92}$$

In all the cases shown above, the averages of position and velocity along with the covariance matrix fully characterise the joint PDF of position and velocity, as its Gaussian character is preserved by construction.

Moreover, for both scenarios we can effectively write the covariance matrix, its time derivative and its inverse as

$$\mathcal{S}_t = k_BT \begin{pmatrix} 2\chi(t) + \langle \Delta x_0^2 \rangle / k_BT & \chi_x(t) \\ \chi_x(t) & 1/m \end{pmatrix} , \tag{5.93}$$

$$\dot{\mathcal{S}}_t = k_BT \begin{pmatrix} 2\chi_x(t) & \chi_v(t) \\ \chi_v(t) & 0 \end{pmatrix} , \tag{5.94}$$

$$\mathcal{S}_t^{-1} = \frac{1}{k_BT|\widetilde{\mathcal{S}}_{t_m,t}|} \begin{pmatrix} 1 & -m\chi_x(t) \\ -m\chi_x(t) & 2m\chi(t) + m\langle \Delta x_0^2 \rangle / k_BT \end{pmatrix} , \tag{5.95}$$

where

$$|\widetilde{\mathcal{S}}_t| = \frac{m}{(k_BT)^2} |\mathcal{S}_t| = 2\chi(t) + \langle \Delta x_0^2 \rangle / k_BT - m\chi_x^2(t) \tag{5.96}$$

and $\langle \Delta x_0^2 \rangle = 0$ or $\langle \Delta x_0^2 \rangle = k_BT/\kappa'$ depending on the case considered.

By using equations (5.93), (5.94) and (5.95) along with the Cramér-Rao bound (5.69) and the expression of the temporal Fisher matrix for Gaussian PDFs (5.70) we get

$$\mathrm{g}_O^{\mathrm{diff}}(t) \leq \mathcal{C}^{\mathrm{diff}}(t) \tag{5.97}$$

with

$$\begin{aligned} \mathrm{g}_O^{\mathrm{diff}}(t) &\equiv \frac{\langle \dot{O} \rangle_t^2}{\langle \Delta O^2 \rangle_t / t} \\ \frac{\mathcal{C}_{x,v}^{\mathrm{diff}}(t)}{t} &\equiv \frac{1}{k_BT|\widetilde{\mathcal{S}}_t|} \left(\langle \dot{x} \rangle_t^2 + \frac{m\langle \Delta x^2 \rangle_t}{k_BT} \langle \dot{v} \rangle_t^2 - 2m\chi_x(t) \langle \dot{x} \rangle_t \langle \dot{v} \rangle_t \right) + \Phi(t) \end{aligned} \tag{5.98}$$

$$\begin{aligned} \Phi(t) &\equiv \frac{1}{2} \mathrm{tr} \left(\mathcal{S}_{t_m,t}^{-1} \dot{\mathcal{S}}_{t_m,t} \mathcal{S}_{t_m,t}^{-1} \dot{\mathcal{S}}_{t_m,t} \right) = \\ &= \frac{2\chi_x^2(t)}{|\widetilde{\mathcal{S}}_t|^2} \left(1 - m\chi_v(t) \left(1 - m\chi_v(t)/2 \right) \right) \xrightarrow{t\to\infty} \frac{\chi_x(t)}{2t\chi(t)} , \end{aligned} \tag{5.99}$$

where we used that $\langle \Delta x^2 \rangle_t = 2k_BT\chi(t) + \langle \Delta x_0^2 \rangle$ and that for free diffusion $\lim_{t\to\infty} \chi(t) = t/\widehat{\gamma}$, $\lim_{t\to\infty} \chi_x(t) = 1/\widehat{\gamma}$ and $\lim_{t\to\infty} \chi_v(t) = 0$. For the case of observables depending only on x_t, as well as for overdamped dynamics, it can be shown that the cost function reduces to

$$\frac{\mathcal{C}_x^{\mathrm{diff}}(t)}{t} \equiv \frac{\langle \dot{x} \rangle_t^2}{\langle \Delta x^2 \rangle_t} + \frac{1}{2} \left(\frac{\partial_t \langle \Delta x^2 \rangle_t}{\langle \Delta x^2 \rangle_t} \right)^2 = \frac{\langle \dot{x} \rangle_t^2}{\langle \Delta x^2 \rangle_t} + 2 \left(\frac{\chi_x(t)}{2\chi(t) + \langle \Delta x_0^2 \rangle} \right)^2 . \tag{5.100}$$

Note that the SNR $\mathrm{g}_O^{\mathrm{diff}}(t)$ and the cost function $\mathcal{C}^{\mathrm{diff}}(t)$ for this diffusive case are defined differently from (5.77). Now there is an additional factor t to let these quantities converge to a constant value at large observation times.

Finally, we consider the entropy production rate of the system

$$\langle \sigma_{\mathrm{sys}} \rangle_{t_m,t} = \frac{\partial_t |\mathcal{S}_{t_m,t}|}{2|\mathcal{S}_{t_m,t}|} = \frac{\chi_x(t)(1 - m\chi_v(t))}{2\chi(t) + \langle \Delta x_0^2 \rangle / k_B T - m\chi_x^2(t)} \xrightarrow{t\to\infty} \frac{\chi_x(t)}{2\chi(t)} \,. \tag{5.101}$$

Except for a factor $1/t$, we recover the same limit as for (5.99) as well as for the second term on the right hand side of (5.100). Moreover, if again we consider external forces that have a polynomial asymptotic behaviour $f(t) \propto t^n$, the term involving the squared derivative of the position in $\mathcal{C}_{x,v}^{\mathrm{diff}}(t)$ becomes dominant. As a consequence, using the expressions for the entropy production rate of the environment (3.57) as well as its long time limit (5.79), we get

$$\lim_{t\to\infty} \mathcal{C}^{\mathrm{diff}}(t) = \frac{\widehat{\gamma}\langle \dot{x} \rangle_t^2}{2k_B T} + \frac{\chi_x(t)}{2\chi(t)} = \frac{1}{2}(\langle \sigma_{\mathrm{tot}} \rangle_t + \langle \sigma_{\mathrm{sys}} \rangle_t) \,. \tag{5.102}$$

However, in general the term proportional to the squared acceleration may be not negligible. This is the case for example for an oscillating external force as $f(t) = A\sin(\omega t)$. Nevertheless, for overdamped dynamics ($m = 0$) and for observables only dependent on x_t, the limit (5.102) holds for all $f(t)$. Hence, again the presence of the odd variable v_t in the PDF modifies the interpretation of the cost function in the large time limit.

Finally, it worth considering the two paradigmatic cases where

(a) $f(t) = 0$, corresponding to $\langle \dot{x} \rangle_t = 0$ and $\langle \dot{v} \rangle_t = 0$ so that

$$\mathcal{C}^{\mathrm{diff}}(t) = t\Phi(t) \xrightarrow{t\to\infty} \langle \sigma_{\mathrm{sys}} \rangle_t = \langle \sigma_{\mathrm{tot}} \rangle_t \,, \tag{5.103}$$

(b) $f(t) = f$, corresponding to $\langle \dot{x} \rangle_t = f\chi_x(t)$ and $\langle \dot{v} \rangle_t = f\chi_v(t)$ and implying that

$$\mathcal{C}^{\mathrm{diff}}(t) \xrightarrow{t\to\infty} \frac{\widehat{\gamma}\langle \dot{x} \rangle_t^2}{2k_B T} = \frac{1}{2}\langle \sigma_{\mathrm{med}} \rangle_t = \frac{1}{2}\langle \sigma_{\mathrm{tot}} \rangle_t \,, \tag{5.104}$$

where we used that $\langle \sigma_{\mathrm{sys}} \rangle_t \propto t^{-1}$ as $t \to \infty$

We thus find different behaviours for the cost function in the large time limit depending on the external forces considered. While in all cases we recover the entropy production rate, there is a prefactor $1/2$ only for forced diffusion.

To sum up, for (i) underdamped dynamics, observables of the form $O(x_t, v_t)$ and external force with a polynomial large time limit $f(t) \propto t^n$, (ii) for underdamped dynamics and observables $R(x_t)$ and (iii) for overdamped dynamics, we recover an entropic interpretation of the cost function for the large time limit and the inequality reads

$$\lim_{t\to\infty} \mathrm{g}_O^{\mathrm{diff}}(t) \leq \frac{1}{2}(\langle \sigma_{\mathrm{tot}} \rangle_t + \langle \sigma_{\mathrm{sys}} \rangle_t) \,. \tag{5.105}$$

We close this section by noting that the bound above becomes valid for all times in the special case of Markovian dynamics in the overdamped limit and starting from an initial distribution that is a Dirac delta for the position and an equilibrium distribution for the initial velocitiy.

5.5.0.3 Multidimensional case

In this section we explore a multidimensional generalisation of our results in which uncoupled degrees of freedom may be subject to different temperatures. The starting point is of course the multidimensional GLE for the n-dimensional vector $\boldsymbol{x}_t$ with components x_t^i defined as

$$m\ddot{x}^i(t) = -\int_{t_m}^{t} \mathrm{d}t' \Gamma^i(t-t')\dot{x}^i(t') - \partial_{x_t^i} U(x_t) + f^i(t) + \eta^i(t)\,, \tag{5.106}$$

$$\langle \eta^i(t')\eta^j(t'')\rangle = k_B T^i \delta_{ij} \Gamma^i(|t'-t''|)\,. \tag{5.107}$$

We choose the external potential to have the following form

$$U(x_t,t) = \sum_i \frac{\kappa^i}{2}(x^i(t)-\lambda^i(t)) \quad \Longrightarrow \quad \partial_{x_t^i} U(x_t,t) = \kappa^i(x^i(t)-\lambda^i(t))\,. \tag{5.108}$$

With this choice of the confining potential the multidimensional GLE becomes

$$m\ddot{x}^i(t) = -\int_{t_m}^{t} \Gamma^i(t-t')\dot{x}^i(t')\mathrm{d}t' - \kappa^i x^i(t) + F^i(t) + \eta^i(t) \tag{5.109}$$

where we set $F^i(t) = \kappa^i\lambda^i(t) + f^i(t)$. By defining $\hat{\chi}_x(k) = \left[mk^2 + k\hat{\Gamma}^i(k) + \kappa^i\right]^{-1}$, one can solve (5.109) by noting that all n equations are uncoupled and can hence be solved independently, namely

$$\begin{aligned} x^i(t) =& x^i_{t_m}\Big(1-\kappa^i\chi^i(t-t_m)\Big) + m v^i_{t_m}\chi^i_x(t-t_m) + \\ &+ \int_{t_m}^{t} \mathrm{d}t' \chi^i_x(t-t')\Big[F^i(t') + \eta^i(t')\Big]\,. \end{aligned} \tag{5.110}$$

The averages of position and velocity can also be readily obtained

$$\langle x^i\rangle_{t_m,t} = \langle x^i_{t_m}\rangle\Big(1-\kappa^i\chi^i(t-t_m)\Big) + m\langle v^i_{t_m}\rangle\chi^i_x(t-t_m) + \int_{t_m}^{t}\mathrm{d}t'\chi^i_x(t-t')F^i(t')\,, \tag{5.111}$$

$$\begin{aligned} \langle v^i\rangle_{t_m,t} =& -\kappa^i\langle x^i_{t_m}\rangle\chi^i_x(t-t_m) + m\langle v^i_{t_m}\rangle\chi^i_v(t-t_m) + \\ &+ \chi^i_x(0)F^i(t) + \int_{t_m}^{t}\mathrm{d}t'\chi^i_v(t-t')F^i(t')\,, \end{aligned} \tag{5.112}$$

while the components of the $2n\times 2n$ multidimensional covariance matrix

$$\mathcal{S}_{t_m,t} = \begin{pmatrix} \mathrm{Cov}_{t_m}(x^i_t,x^j_t) & \mathrm{Cov}_{t_m}(x^i_t,v^j_t) \\ \mathrm{Cov}^T_{t_m}(x^i_t,v^j_t) & \mathrm{Cov}_{t_m}(v^i_t,v^j_t) \end{pmatrix} \tag{5.113}$$

are explicitly calculated in A.3.

In this section we will again focus on initial conditions such that the joint PDF $p_{t_m}(\boldsymbol{q}_t,t)$ is Gaussian, where we have set $\boldsymbol{q}_t = (\boldsymbol{x}_t,\boldsymbol{v}_t)$. In other words we are going to consider PDFs of the form

$$p_{t_m}(\boldsymbol{q}_t,t) = \frac{1}{\sqrt{(2\pi)^{2n}|\mathcal{S}_{t_m,t}|}}\exp\left[-\frac{1}{2}(\boldsymbol{q}_t-\langle\boldsymbol{q}\rangle_{t_m,t})^T\mathcal{S}^{-1}_{t_m,t}(\boldsymbol{q}_t-\langle\boldsymbol{q}\rangle_{t_m,t})\right]\,, \tag{5.114}$$

so that, for a given observable $\boldsymbol{O}(\boldsymbol{q}_t)$ with average

$$\langle \boldsymbol{O} \rangle_{t_m,t} = \int \mathrm{d}\boldsymbol{q}_t \, p_{t_m}(\boldsymbol{q}_t, t) \boldsymbol{O}(\boldsymbol{q}_t) \,, \tag{5.115}$$

the inequality deriving from the temporal and multidimensional Cramér-Rao bound reads

$$\langle \dot{\boldsymbol{O}} \rangle^T_{t_m,t} \mathcal{S}^{-1}_{\boldsymbol{O},t_m,t} \langle \dot{\boldsymbol{O}} \rangle_{t_m,t} \leq \langle \dot{\boldsymbol{q}} \rangle^T_{t_m,t} \mathcal{S}^{-1}_{t_m,t} \langle \dot{\boldsymbol{q}} \rangle_{t_m,t} + \frac{1}{2} \mathrm{tr} \left(\mathcal{S}^{-1}_{t_m,t} \dot{\mathcal{S}}_{t_m,t} \mathcal{S}^{-1}_{t_m,t} \dot{\mathcal{S}}_{t_m,t} \right) . \tag{5.116}$$

where $\mathcal{S}^{ij}_{\boldsymbol{O},t_m,t} = \langle O^i O^i \rangle_{t_m,t} - \langle O^i \rangle_{t_m,t} \langle O^i \rangle_{t_m,t}$, see again [118] for more details.

In the following we analyse this bound for the same cases of trapped dynamics and free diffusion discussed in the previous subsections.

Multidimensional confined particle. Here we consider the dynamics of a Brownian particle generated by a parabolic confining potential that is being dragged with a driving protocol $\boldsymbol{\lambda}(t)$, i.e.

$$U(\boldsymbol{x}_t, t) = \sum_i \frac{\kappa^i}{2} (x^i(t) - \lambda^i(t)) \tag{5.117}$$

with $\kappa_i \neq 0$ for every i. Moreover, remembering that for this scenario it holds that

$$\lim_{t\to\infty} \chi^i_v(t) = 0 \qquad \lim_{t\to\infty} \chi^i_x(t) = 0 \qquad \lim_{t\to\infty} \chi^i(t) = 1/\kappa^i \tag{5.118}$$

we immediately see from (A.28), (A.29) and (A.30) that, in the long time limit as well as for $t_m \to -\infty$, the covariance matrix becomes

$$\lim_{t-t_m\to\infty} \mathcal{S}_{t_m,t} = \lim_{t-t_m\to\infty} \begin{pmatrix} \mathrm{Cov}_{t_m}(x^i_t, x^j_t) & \mathrm{Cov}_{t_m}(x^i_t, v^j_t) \\ \mathrm{Cov}^T_{t_m}(x^i_t, v^j_t) & \mathrm{Cov}_{t_m}(v^i_t, v^j_t) \end{pmatrix} = \begin{pmatrix} k_B T^i \delta_{ij}/\kappa^i & 0 \\ 0 & k_B T^i \delta_{ij}/m \end{pmatrix} , \tag{5.119}$$

which is a constant matrix and also corresponds to the covariance matrix of a system that is in equilibrium. In fact, using this covariance matrix as initial condition at time t_m, we see that $\mathcal{S}_{t,t_m}$ remains constant at all times. We conclude that for the dynamics starting from an initial equilibrium condition and for a stationary state, i.e. $t_m \to -\infty$, the covariance matrix is always constant and diagonal. Moreover, from (5.111) and (5.112) we see that average positions and velocities can be in both cases effectively written as

$$\langle x^i \rangle_{t_m,t} = \int_{t_m}^t \mathrm{d}t' \chi^i_x(t-t') F^i(t') \tag{5.120}$$

$$\langle v^i \rangle_{t_m,t} = \chi^i_x(0) F^i(t) + \int_{t_m}^t \mathrm{d}t' \chi^i_v(t-t') F^i(t') \tag{5.121}$$

where $t_m = 0$ for equilibrium initial conditions or $t_m = -\infty$. Hence, for these initial setups, the inequality (5.116) becomes

$$\mathrm{g}^{\mathrm{trap}}_{\boldsymbol{O}}(t) \leq \mathcal{C}^{\mathrm{trap}}(t) \,, \tag{5.122}$$

with

$$\mathrm{g}_{O}^{\mathrm{trap}}(t) = \langle \dot{\boldsymbol{O}} \rangle_{t_m,t}^{T} \mathcal{S}_{\boldsymbol{O},t_m}^{-1} \langle \dot{\boldsymbol{O}} \rangle_{t_m,t} \,, \tag{5.123}$$

$$\begin{aligned} \mathcal{C}_{x,v,t_m}^{\mathrm{trap}}(t) &\equiv \sum_i \frac{\kappa_i \langle \dot{x}^i \rangle_{t_m,t}^2 + m \langle \dot{v}^i \rangle_{t_m,t}^2}{k_B T_i} \,, \\ \mathcal{C}_{x,t_m}^{\mathrm{trap}}(t) &\equiv \sum_i \frac{\kappa_i \langle \dot{x}^i \rangle_{t_m,t}^2}{k_B T_i} \,, \end{aligned} \tag{5.124}$$

where the range of validity of the two cost functions was discussed in the previous subsections.

Moving forward, we consider the total entropy production rate, which coincides with the entropy production rate of the environment because of the constancy of the covariance matrix, along with its large time limit

$$\lim_{t\to\infty} \langle \sigma_{\mathrm{tot}} \rangle_{t_m,t} = \lim_{t\to\infty} \langle \sigma_{\mathrm{med}} \rangle_{t_m,t} = \sum_i \frac{\widehat{\gamma}_i}{k_B T_i} \left(\lim_{t\to\infty} \langle v \rangle_{t_m,t} \right)^2 . \tag{5.125}$$

We see that, differently from the unidimensional case, it is not possible to find a simple proportionality relation between the first terms on the right hand side of (5.124) and the long time limit of the entropy production rate. We conclude that, for this multidimensional case, the cost functions in general have no entropic interpretation for large observation times. The recovery of a cost function proportional to the entropy production rate is only possible in specific cases: for example, for a dragging vector $\boldsymbol{\lambda}(t)$ with one nonzero component, or when all ratios $\kappa_i/\hat{\gamma}_i$ are the same.

Multidimensional particle not confined. We conclude this section by considering the case of diffusion without confinement. The GLE associated to this scenario is as follows:

$$m\ddot{x}^i(t) = -\int_{t_m}^{t} \mathrm{d}t' \Gamma^i(t-t') \dot{x}^i(t') + f^i(t) + \eta^i(t) \,. \tag{5.126}$$

In a similar way as for the unidimensional case, we chose

$$\mathcal{S}_0 = \begin{pmatrix} \mathrm{Cov}(x_0^i, x_0^j) & \mathrm{Cov}(x_t^0, v_t^0) \\ \mathrm{Cov}^T(x_0^i, v_0^j) & \mathrm{Cov}_{t_m}(v_0^i, v_0^j) \end{pmatrix} = \begin{pmatrix} \langle (\Delta x_0^i)^2 \rangle \delta_{ij} \,. & 0 \\ 0 & k_B T \delta_{ij}/m \end{pmatrix} \tag{5.127}$$

as the covariance matrix characterising the initial state at $t = 0$, with $\langle (\Delta x_0^i)^2 \rangle = k_B T/\kappa'^i$. This corresponds to an initial state where the particle has reached thermal equilibrium in a parabolic trap as in (5.117), with parameters $\{\kappa'^i\}$. The potential is then switched off at time $t = 0$ when $f(t)$ is turned on. As a consequence we have that $\langle x_0^i \rangle = 0$ and $\langle v_0^i \rangle = 0$. Moreover, in the limit of $\kappa'^i \to \infty$, the covariance matrix (5.127) is the same as the one of a joint PDF that is factorised as $P(\boldsymbol{x}_0, \boldsymbol{v}_0) = \prod_i \delta(x_0^i - \widetilde{x}_0^i) p^{\mathrm{eq}}(\boldsymbol{v}_0)$. This would rather correspond to $\langle x_0^i \rangle = \widetilde{x}_0^i$ and $\langle v_0^i \rangle = 0$. Both scenarios can hence be hence effectively described by the covariance matrix

$$\mathcal{S}_t = \begin{pmatrix} \left(\langle (\Delta x_0^i)^2 \rangle + 2 k_B T^i \chi^i(t) \right) \delta_{ij} & k_B T^i \chi_x^i(t) \delta_{ij} \\ k_B T^i \chi_x^i(t) \delta_{ij} & k_B T^i \delta_{ij}/m \end{pmatrix} \tag{5.128}$$

as well as by

$$\langle x^i\rangle_t = \widetilde{x}_0^i + \int_0^t \mathrm{d}t' \chi_x^i(t-t') f^i(t')\,, \tag{5.129}$$

$$\langle v^i\rangle_t = \chi_x^i(0) f^i(t) + \int_0^t \mathrm{d}t' \chi_v^i(t-t') f^i(t') \tag{5.130}$$

where $\widetilde{x}_0^i \neq 0$ only for $\{\kappa^i \to \infty\}$. With all these informations we are able to evaluate the bound (5.116)

$$\mathrm{g}_{\boldsymbol{O}}^{\mathrm{diff}}(t) \leq \mathcal{C}^{\mathrm{diff}}(t)\,, \tag{5.131}$$

with

$$\mathrm{g}_{\boldsymbol{O}}^{\mathrm{diff}}(t) = t\,\langle \dot{\boldsymbol{O}}\rangle_{t_m,t}^T \mathcal{S}_{\boldsymbol{O},t_m}^{-1}(t)\,\langle \dot{\boldsymbol{O}}\rangle_{t_m,t} \tag{5.132}$$

$$\frac{\mathcal{C}_{x,v,t_m}^{\mathrm{diff}}(t)}{t} \equiv \sum_i \frac{\langle \dot{x}^i\rangle_t^2 + m\big\langle \left(\Delta x^i\right)^2\big\rangle_t \langle \ddot{v}^i\rangle_t^2/k_BT - 2m\chi_x^i(t)\langle \dot{x}^i\rangle_t\langle \ddot{v}^i\rangle_t}{k_BT^i|\widetilde{\mathcal{S}}_t^i|} + \sum_i \Phi^i(t) \tag{5.133}$$

$$\Phi^i(t) \equiv \frac{2\left(\chi_x^i(t)\right)^2}{|\widetilde{\mathcal{S}}_t^i|^2}\Big(1 - m\chi_v^i(t)\Big(1 - m\chi_v^i(t)/2\Big)\Big) \xrightarrow{t\to\infty} \frac{1}{2t}\sum_i \frac{\chi_x^i(t)}{\chi^i(t)} \tag{5.134}$$

$$|\widetilde{\mathcal{S}}_t^i| = \big\langle \left(\Delta x^i\right)^2\big\rangle_t/k_BT^i - m(\chi_x^i(t))^2\,, \tag{5.135}$$

where again we used that $\big\langle \left(\Delta x^i\right)^2\big\rangle_t = 2k_BT^i\chi^i(t) + \big\langle \left(\Delta x_0^i\right)^2\big\rangle$ along with the limits of the susceptibilities.

Hence, similarly to the the confined case, there is no straightforward connection between the cost function (5.133) and the total entropy production (see (5.125)). However, if we consider free diffusion with $f^i(t) = 0$, that means $\langle x^i\rangle_t = 0$ and $\langle v^i\rangle_t = 0$, and note that

$$\langle \sigma_{\mathrm{sys}}\rangle_{t_m,t} = \frac{\partial_t|\mathcal{S}_{t_m,t}|}{2|\mathcal{S}_{t_m,t}|} = \sum_i \frac{\partial_t|\widetilde{\mathcal{S}}_{t_m,t}^i|}{2|\widetilde{\mathcal{S}}_{t_m,t}^i|} = \sum_i \frac{\chi_x^i(t)(1-m\chi_v^i(t))}{\big\langle \left(\Delta x^i\right)^2\big\rangle_t/k_BT - m(\chi_x^i(t))^2} \xrightarrow{t\to\infty} \sum_i \frac{\chi_x^i(t)}{2\chi^i(t)} \tag{5.136}$$

it is clear that, for this special case,

$$\lim_{t\to\infty} \mathcal{C}_{x,v,t_m}^{\mathrm{diff}}(t) = \langle \sigma_{\mathrm{sys}}\rangle_{t_m,t} = \langle \sigma_{\mathrm{tot}}\rangle_{t_m,t} \tag{5.137}$$

Finally, it is worth noting that, as usual, for observables that depend solely on $\boldsymbol{x}_t$, i.e. $\boldsymbol{O}(\boldsymbol{x}_t)$ as well as for overdamped dynamics, the cost function has a different form

$$\mathcal{C}_{x,t_m}^{\mathrm{diff}}(t) = \sum_i \left(\frac{\langle \dot{x}^i\rangle_t^2}{\big\langle \left(\Delta x^i\right)^2\big\rangle_t} + 2\left(\frac{\chi_x^i(t)}{2\chi^i(t) + \big\langle \left(\Delta x_0^i\right)^2\big\rangle}\right)^2 \right)\,. \tag{5.138}$$

Moreover, for overdamped free diffusion and for $\big\langle \left(\Delta x_0^i\right)^2\big\rangle \to 0$, i.e. $\kappa'^i \to \infty$ for every i, we get that for all times

$$\mathcal{C}_{x,t_m}^{\mathrm{diff}}(t) = \langle \sigma_{\mathrm{tot}}\rangle_{t_m,t} \tag{5.139}$$

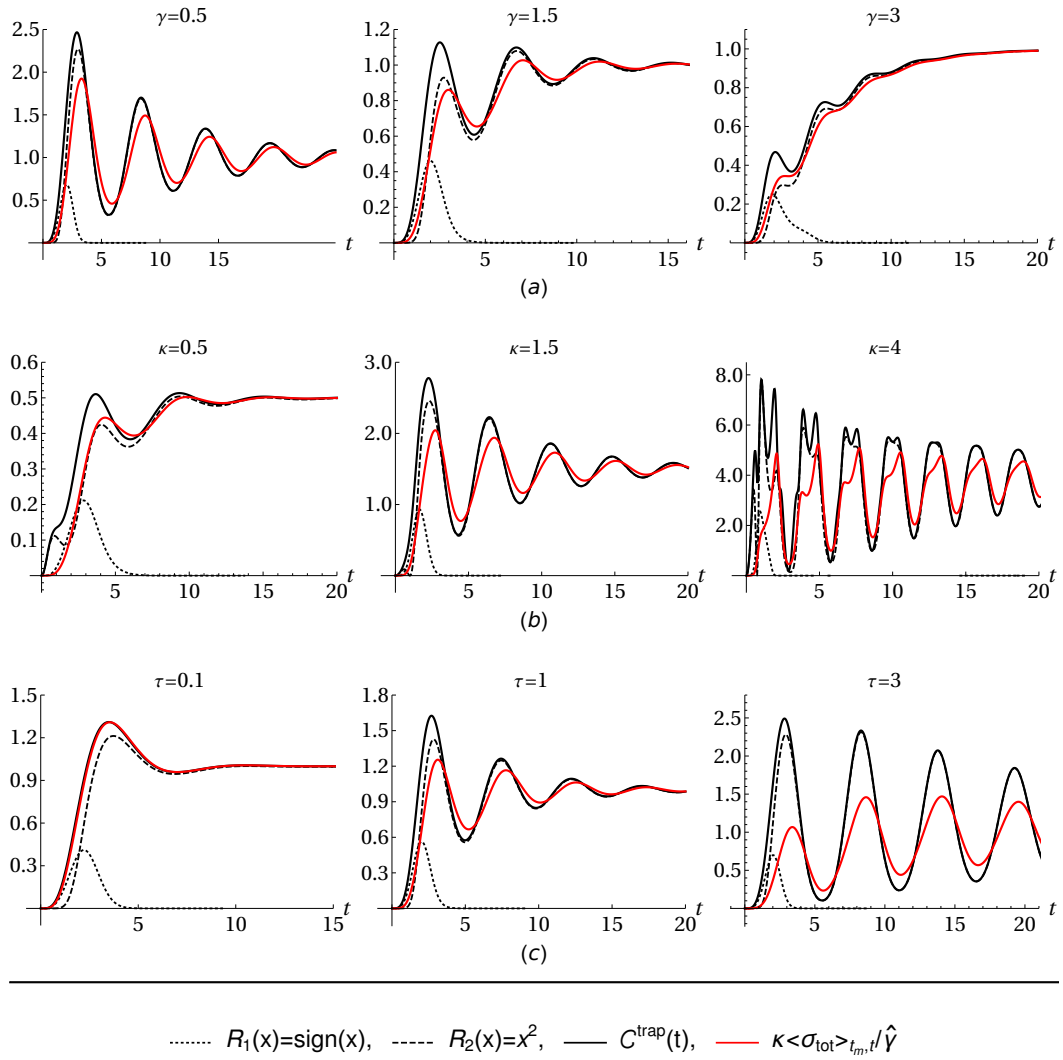

Figure 5.6: Upper bound (5.78) (dense black line) of the non-equilibrium inequality (5.76), and SNR ratios $g_O^{\text{trap}} = \langle \dot{O} \rangle_t^2 / \langle \Delta O^2 \rangle_t$ for two observables (dashed lines, see legend), for a pure exponential kernel ($\gamma_0 = 0$) and starting from equilibrium (parameters $m = 1$, $v = 1$, $\kappa = 1$, $\gamma = 1$ and $\tau = 1$). We also show the term $\kappa \langle \sigma_{\text{tot}} \rangle_t / \widehat{\gamma}$ (red line), which becomes the entropic bound for long times but in general is not a bound for the SNRs. In (a) we vary γ (quantities exhibit oscillations that become less pronounced as γ grows), in (b) we vary κ (oscillations become stronger and more persistent in time as κ becomes larger and the limit of the cost functions as well as the entropic bound grow linearly as the value of trap stiffness becomes larger), and in (c) we vary τ (note that for $\tau = 0.1$, i.e. at quasi-Markovianity, red and black continuous lines nearly coincide meaning that for Markovian dynamics the cost function becomes proportional to the entropy production rate).

5.5.1 Applications

We discuss some regimes for which it is possible to derive explicit analytical expressions for the SNRs and for the cost function or the entropy production rates. Moreover, we will focus on unidimensional underdamped dynamics and observables that depend only on spatial variables. This will allow us to observe the typical

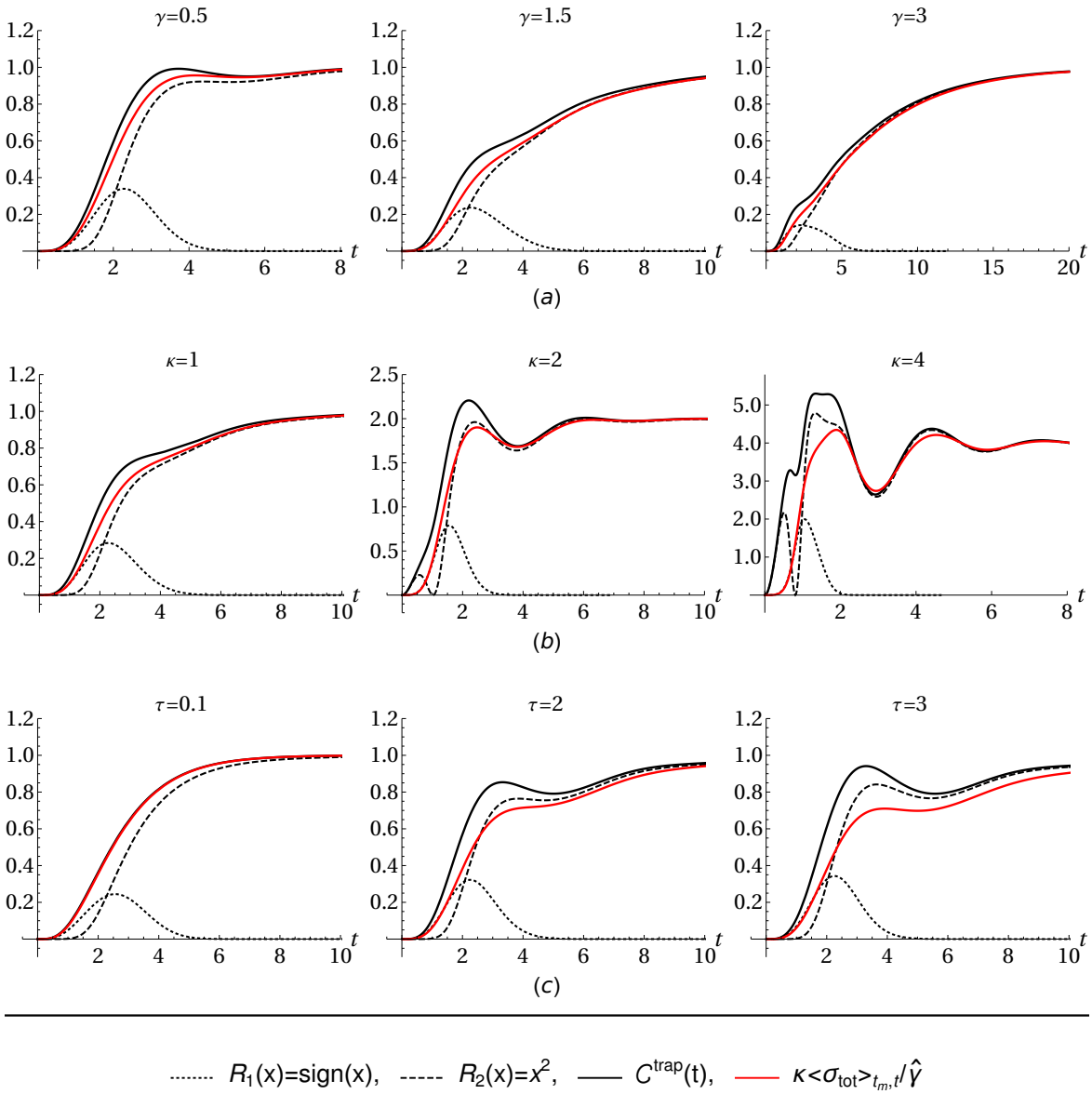

Figure 5.7: Similar to Figure 5.6 but for a complete exponential memory kernel with Markovian contribution $\gamma_0 = 0.5$ that smothers the oscillations.

oscillations associated to the underdamped scenario and will enable us to recover an entropic interpretation of the cost functions in the large time limit.

5.5.1.1 Exponential memory kernel with confinement

For our example, we focus on a simple memory kernel with one exponential component, with GLE

$$m\ddot{x}(t) = -\gamma_0 \dot{x}(t) - \frac{\gamma}{\tau}\int_{t_m}^{t} \mathrm{d}t' \, \mathrm{e}^{-(t-t')/\tau}\dot{x}(t') - \kappa\left[x(t) - vt\right] + \eta(t)\,, \tag{5.140}$$

where we set $\lambda(t) = vt$ and $f(t) = 0$. As already hinted in the previous section, with this linear dragging protocol a steady state is established for $t_m \to -\infty$.

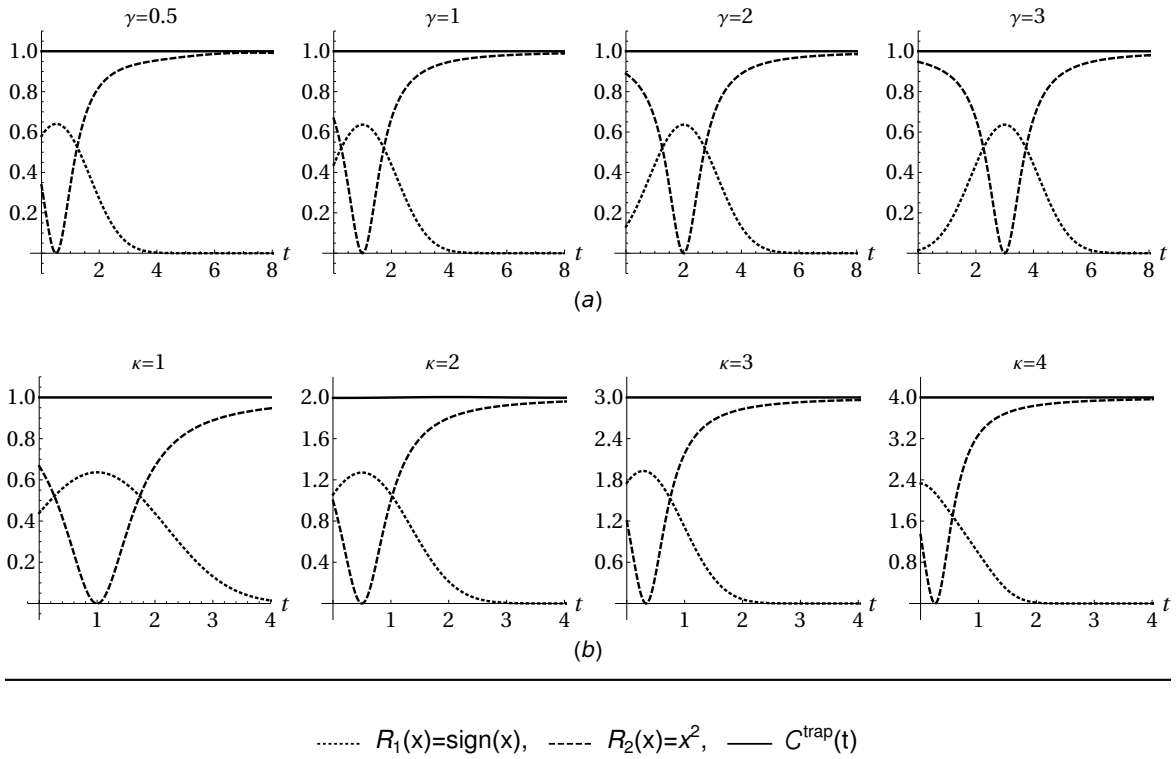

Figure 5.8: As in Figure 5.6 but for a trap dragging the particle with constant velocity (the "steady state") and passing with its minimum $\lambda(t) = vt$ at $\lambda(0) = 0$. In this case the cost function $\mathcal{C}^{\mathrm{trap,ss}}(t) = \kappa\langle\sigma_{\mathrm{tot}}\rangle_t^{\mathrm{ss}}/\widehat{\gamma} = \kappa v^2$ matches the entropic bound, proportional to the constant entropy production rate (see equation (5.81)). Variations of memory characteristic time are not considered as their effects are not present as $t_m \to -\infty$. (a) A larger value of γ corresponds to a shift of the minimum and maximum of the two SNRs towards larger observation times. The cost function remains unaffected by variations of γ. (b) As the trap stiffness grows, so does the cost function proportionally, while the minimum and maximum of the SNRs move towards smaller observation times.

Here we analyse the the bound (5.76) for two different observables, i.e. $O_1(x) = \mathrm{sign}(x)$ and $O_2(x) = x^2$, starting from equilibrium or from a stationary state. In the latter case, the bound becomes a full-fledged entropic bound (5.80).

As a first standard example for viscoelastic fluids, we analyse the case of an exponential memory kernel,

$$\Gamma^{\exp}(t) = 2\gamma_0\delta(t) + \sum_{i=1}\frac{\gamma_i}{\tau_i}\mathrm{e}^{-t/\tau_i}\,, \qquad \hat{\Gamma}^{\exp}(k) = \gamma_0 + \sum_{i=1}\frac{\gamma_i}{1+k\tau_i}\,, \tag{5.141}$$

with

$$\widehat{\gamma} = \int_0^\infty \mathrm{d}t'\,\Gamma(t') = \sum_{i=0}\gamma_i\,, \qquad 0 \le \widehat{\gamma} < \infty\,. \tag{5.142}$$

This is an important example, as a finite sum of suitably sized exponential terms can approximate, up to a finite time scale, every memory kernel even if $\widehat{\gamma}$ does not converge, see [77] for details.

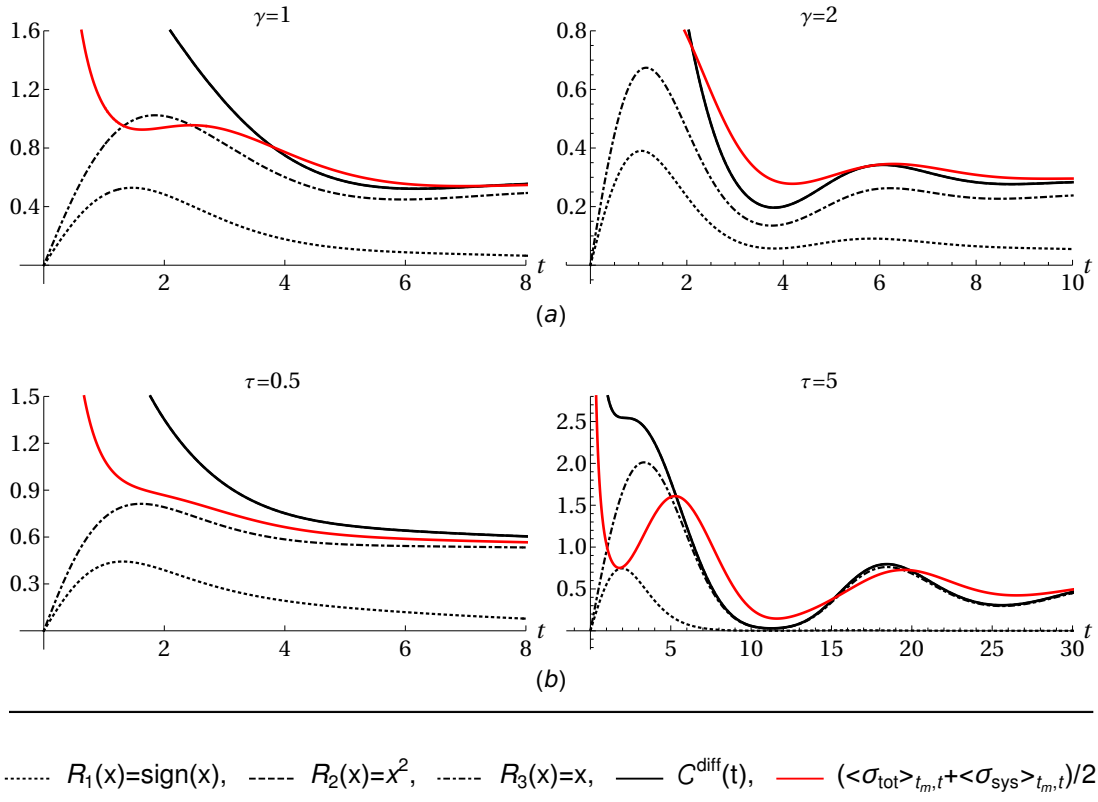

Figure 5.9: For free diffusion ($\kappa = 0$) under a constant force $f = 1$ from an initial distribution $p(x_{t_0}, v_{t_0}, t_0) = \delta(x - x_0)p^{\mathrm{eq}}(v_0)$: SNRs $g_O^{\mathrm{diff}} = t\langle \dot{O} \rangle_t^2 / \langle \Delta O^2 \rangle_t$ (dashed lines, see legend), cost function (dense black line) and entropic bound (red line) for pure exponential memory kernel ($\gamma_0 = 0$). As in previous figures, $m = 1$, $\gamma = 1$ and $\tau = 1$. In row (a) we vary γ. Differently from the bounded case (see Figure 5.6) oscillations become stronger in amplitude as γ increases while again the limit to which the cost functions and the entropy production rates does not change with γ. In (b) instead we vary τ. As before, the long time limit of the cost function is approached also by the corresponding entropic bound, while oscillations increase as the memory characteristic time gets larger. The bound is very quickly saturated for the observable $O_2(x) = x^2$, hence its SNR is not visible in the panels.

For a memory kernel that is purely exponential, i.e. when $\gamma_0 = 0$, we note that the SNRs as well as the bounds exhibit strong oscillations when starting from an equilibrium distribution, depending of course on the values of the parameters (Figure 5.6). When $\gamma_0 \neq 0$ instead, these oscillations are smothered (Figure 5.7). No significant difference is seen instead if we start from a stationary state (thus we show only the case $\gamma_0 = 0$ in Figure 5.8), in fact if $t_m \to -\infty$ the memory effects are lost and the dynamics only depends on the limit of the time dependent friction coefficient $\widehat{\gamma}$, see equation (5.81). In other words it is not possible anymore to distinguish the effects of the exponential part of the memory kernel from the Markovian one.

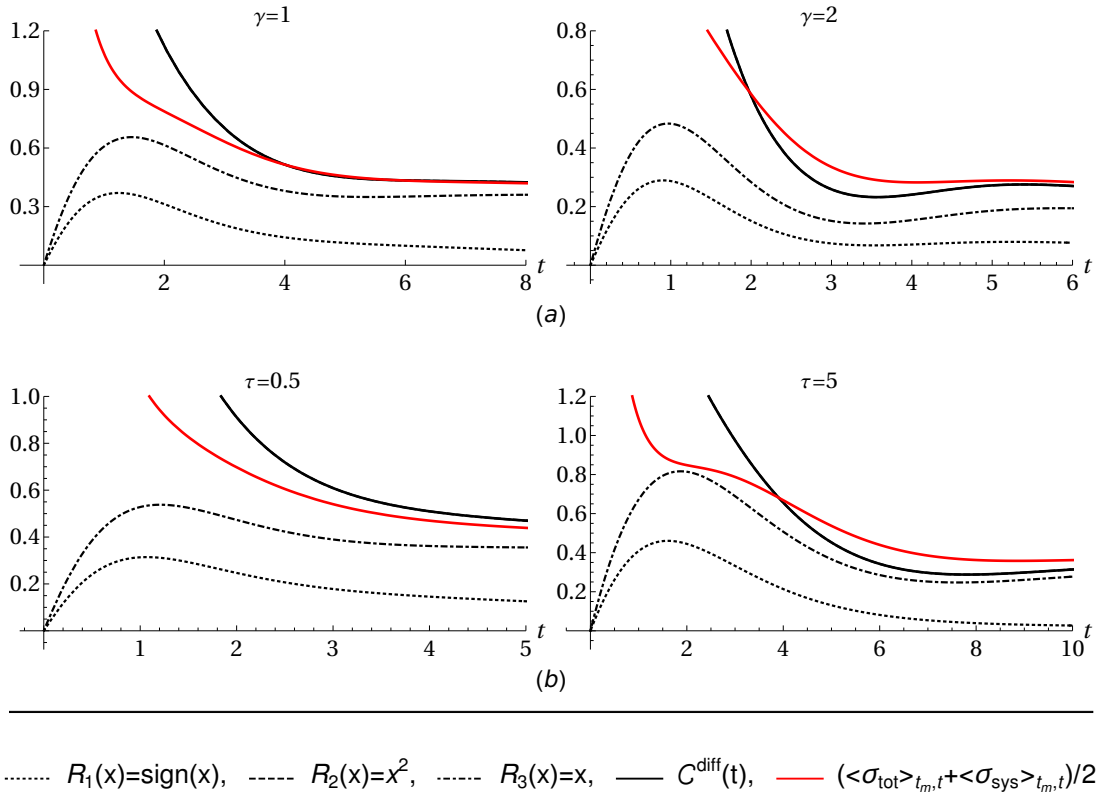

Figure 5.10: As in Figure 5.9 but for complete exponential memory kernel ($\gamma_0 = 0.5$, damping the oscillations) with initial distribution $P(x_{t_0}, v_{t_0}, t_0) = \delta(x - x_0)p^{\mathrm{eq}}(v_0)$.

5.5.1.2 Exponential memory kernel without confinement

We analyse diffusion dynamics ($\kappa = 0$) of the bead subject to an external force $f(t) = f$ that is constant both in space and time. The variance of the position grows in time, hence there exists no stationary distribution. Also the average position grows linearly in time due to f.

As in the previous subsection, for simplicity the associated GLE contains a single exponential with characteristic time τ,

$$m\ddot{x}(t) = -\gamma_0 \dot{x}(t) - \frac{\gamma}{\tau}\int_0^t \mathrm{d}t' \mathrm{e}^{-(t-t')/\tau}\dot{x}(t') + f + \eta(t)\,. \tag{5.143}$$

We thus discuss the bound (5.97) for the dynamics generated by the above equation, again noting the entropic nature of the bound in the large time limit. We will consider three observables: $O_1(x) = \mathrm{sign}(x)$, $O_2(x) = x^2$ and $O_3(x) = x$. The latter observable has a non-saturating SNR for this unbound diffusion dynamics.

Figure 5.9 and Figure 5.10 show the case of an initial distribution that is a Dirac delta for the starting position and an equilibrium distribution for the initial velocity, which implies $\langle \Delta x_0^2 \rangle = 0$. For small times this causes a divergence of the cost function $\mathcal{C}_x^{\mathrm{diff}}(t)$ due to its term $t(\partial_t \langle \Delta x^2 \rangle_t / \langle \Delta x^2 \rangle_t)^2$ in (5.100). While in this regime the bound becomes loose for $O_1(x)$ and $O_3(x)$ it is immediately saturated for $O_2(x)$.

However, if the dynamics starts from an equilibrium condition in an optical trap of stiffness κ' (implying $\langle \Delta x_0^2 \rangle = k_B T/\kappa'$) no divergences occur and the bound becomes tighter for all observables. This can be all seen in Figure 5.11, for $\gamma_0 = 0$. The case $\gamma_0 > 0$ yields similar plots with less oscillations.

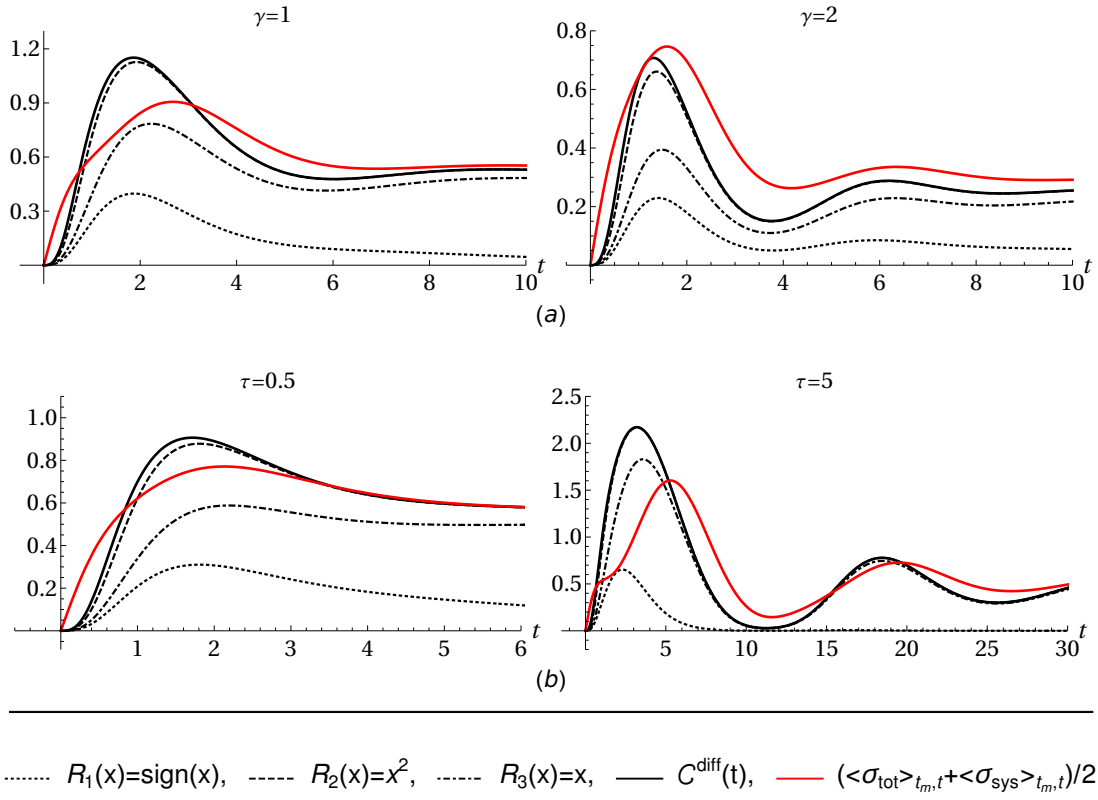

Figure 5.11: SNRs $g_O^{\mathrm{diff}} = t\,\langle \dot{O}\rangle_t^2 / \langle \Delta O^2\rangle_t$ (dashed lines, see legend), cost function (dense black line) and entropic bound (red line) for pure exponential memory kernel ($\gamma_0 = 0$) and for initial distribution $p(x_{t_0}, v_{t_0}, t_0) = p^{\kappa',\,\mathrm{eq}}(v_0)p^{\mathrm{eq}}(v_0)$ with $\langle \Delta x_0^2\rangle = k_B T/\kappa'$. In row (a) we chose $m = 1$, $f = 1$ and $\tau = 1$. A finite initial variance of the position avoids a divergence of the cost functions. Differently from the bounded case (see Figure 5.6) oscillations become stronger in amplitude as γ increases while again the long time limit of cost function and entropy production rate does not change with γ. For (b) instead we have $\gamma = 1$, $m = 1$ and $f = 1$. As before, the long time limit of the cost function and rates is the same for both values of τ while oscillations increase as the memory characteristic time grows larger. Again the bound is very quickly saturated for $O_2(x)$.

To summarise, the entropic bound is violated for finite times and is only valid asymptotically. It is perhaps surprising that the observable which goes closer to saturate the inequality is $O_2 = x^2$ instead of $O_3 = x$, which fully saturates the bound for trapped dynamics and, of course, for observables that are velocity-independent.

5.5.2 Conclusions

Considering a system as optical tweezers dragging a microbead in a complex fluid, we have considered a non-equilibrium inequality (5.69) for Langevin equations with memory kernel, for the cases in which the position evolves distributed as a Gaussian. This inequality covers also diffusion not bounded by a harmonic trap but driven by a homogeneous time-dependent field.

The inequality (5.69) quantifies how the signal-to-noise ratio of observables is bounded by a cost function. By focusing on instantaneous quantities as the bead position, it is in line with a recent TUR for Markovian dynamics [20] and embodies a previous Markovian version [15]. An approach based on instantaneous quantities is a viable option for dealing with non-Markovian systems, which have more complicated path weights than those of Markovian systems.

The cost function in the inequality (5.69) in general is not the entropy production, but it can become proportional to the entropy production rate in some limits. For a particle confined by a harmonic trap, (5.69) can be cast as (5.76), which becomes the TUR (5.80) in the limit of large observation times (again, this TUR contains the instantaneous entropy production rate, at variance with TURs in the literature). Moreover, for a particle dragged at constant velocity in a complex fluid by moving optical tweezers, the TUR (5.82) holds for all times if the dragging has been performed since a long time before the beginning of measurements.

For particles not constrained by optical tweezers, but eventually subject to a global force $f(t)$, the inequality reduces to (5.97). This may also become an instantaneous TUR with cost function proportional to some entropy production rates, see (5.105). For instance, for integrable memory kernels, at long times the effects of the memory are lost and essentially the system behaves as a Markovian one.

Markovian Langevin dynamics is a particular subclass of what we have described. In all cases we have analysed, a Markovian dynamics may lead more easily to a thermodynamic interpretation in which the entropy production rate is the function bounding the signal-to-noise ratio (besides constant prefactors). Indeed, we recover it for a particle dragged but starting from equilibrium, and also for a free overdamped particle starting from a given position (Dirac delta distribution initially). In the latter case the susceptibility is equal to $\chi(t) = 2Dt$, with diffusion constant D. Thus $\chi_x(t) = \partial_t \chi(t) = 2D$ and the ratio $(t\chi_x(t))/\chi(t) = 1$, so that from (5.105) we can infer the validity of the instantaneous TUR (5.105) for all times. A realisation of this scenario could be a charged particle driven by a homogeneous time-varying electric field in a fluid without memory.

The fact that a non-equilibrium inequality contains a cost function not directly related only to the entropy production is not surprising. As discussed in this thesis, many previous examples show that other non-dissipative aspects may be constraining the SNR of observables, in conjuction with or in alternative to the entropy production.

CHAPTER 6

SOLVED MODELS

In this chapter we present and solve three different linear models in a steady state, which will be used in the next chapter to discuss and apply our Markovian variance sum rule (VSR), valid for Langevin systems in a steady state and described by

$$\dot{\boldsymbol{x}}(t) = \boldsymbol{\mu}\boldsymbol{F}(\boldsymbol{x}_t, t) + \sqrt{2\boldsymbol{D}}\,\boldsymbol{\xi}(t)\,, \tag{6.1}$$

where $\boldsymbol{\mu}$ and $\boldsymbol{D}$ are the (constant) mobility and diffusion matrix, respectively, and $\boldsymbol{F}(\boldsymbol{x}_t, t)$ is the total force acting on the bead. In this setting, the VSR takes the following form

$$\mathrm{Cov}(\boldsymbol{x}_t - \boldsymbol{x}_0, \boldsymbol{x}_t - \boldsymbol{x}_0) + \int_0^t \mathrm{d}t' \int_0^t \mathrm{d}t''\, \mathrm{Cov}(\boldsymbol{\mu}\boldsymbol{F}(\boldsymbol{x}_{t'}, t'), \boldsymbol{\mu}\boldsymbol{F}(\boldsymbol{x}_{t''}, t'')) = 2\boldsymbol{D}t + 4\boldsymbol{\mathcal{V}}(t) \tag{6.2}$$

where

$$\boldsymbol{\mathcal{V}}(t) = \frac{1}{2}\int_0^t \mathrm{d}t' \int_0^{t'} \mathrm{d}t''\, \left(\mathrm{Cov}(\dot{\boldsymbol{x}}_{t''}, \boldsymbol{v}_0) + \mathrm{Cov}^{\mathrm{T}}(\dot{\boldsymbol{x}}_{t''}, \boldsymbol{v}_0)\right) \tag{6.3}$$

is a quantity involving the mean local velocity (2.48). In this chapter, which can be regarded as some anticipated appendices, we will restrict ourselves to calculating these quantities for the above-mentioned models and postpone a more detailed discussion of the application and relevance of the VSR and $\boldsymbol{\mathcal{V}}(t)$ to the next chapters.

Each system that we are going to consider is driven out of equilibrium by a different mechanism and are as follows:

- a 2D system trapped in a parabolic potential plus a non conservative force, the latter being accountable for the non equilibrium regime;
- another 2D system in a parabolic potential and in contact with two heat baths at different temperatures, also known as *Brownian gyrator*. In this case, it is the temperature gradient that drives the system out of equilibrium.
- A 1D system, again in a parabolic potential, plus a position independent random force proportional to $\sigma(t)$, the latter taking values $\{0, 1\}$ alternately with exponentially distributed waiting times. This is an example of a jump-diffusing process.

In addition, we will calculate the entropy production rate along with other interesting quantities related to these systems and whose usefulness will be clear in Chapter 7.

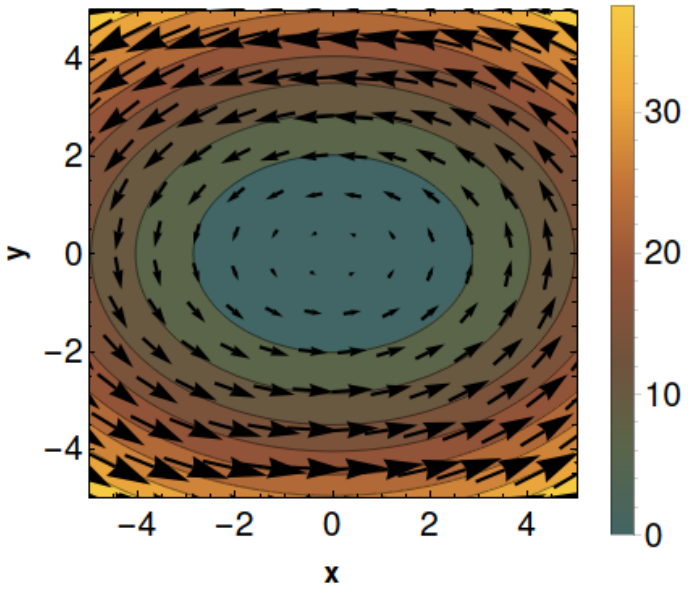

Figure 6.1: Non-conservative force field for $k_BT = \mu = \kappa = \rho = 1$ and $\alpha = 1/2$. The legend bar indicates the value of the potential $U(x_t, y_t)$ while the arrows correspond the vector field $\boldsymbol{f}(x_t, y_t)$. Note that they are tangent to the equipotential lines.

6.1 Linear non-conservative force

Lets consider the LE (2.43) in two dimensions, i.e. $\boldsymbol{x}_t = (x_t, y_t)$, with a parabolic potential given by $U(x_t, y_t) = \kappa_1 x_t^2/2 + \kappa_2 y_t^2/2$ and in the presence of a non conservative force $\boldsymbol{f}(x_t, y_t) = (-\rho_1 y_t, \rho_2 x_t)$. Moreover, we consider a diagonal diffusion matrix $D_{ij} = k_B T \mu \delta_{ij}$ where $\mu = 1/\gamma$ is the mobility of the particle. With this in mind, the LE can be written as the following set of coupled linear stochastic differential equations

$$\begin{cases} \dot{x}(t) = \mu \left(-\partial_{x_t} U(x_t, y_t) + f^x(x_t, y_t)\right) + \sqrt{2k_BT\mu}\, \xi^x(t) = \\ \qquad = -\mu\kappa_1 x(t) - \mu\rho_1 y(t) + \sqrt{2k_BT\mu}\, \xi^x(t) \\ \dot{y}(t) = \mu \left(-\partial_{y_t} U(x_t, y_t) + f^y(x_t, y_t)\right) + \sqrt{2k_BT\mu}\, \xi^y(t) = \\ \qquad = -\mu\kappa_2 y(t) + \mu\rho_2 x(t) + \sqrt{2k_BT\mu}\, \xi^y(t)\,. \end{cases} \tag{6.4}$$

One can easily verify that, by setting $\kappa_1 = \alpha\kappa$, $\kappa_2 = \kappa$, $\rho_1 = \rho$ and $\rho_2 = \alpha\rho$, the stationary solution of FP equation has a Gaussian shape of the following form

$$p_{\rm st}(\boldsymbol{x}_t) = p_{\rm st}(x_t, y_t) \propto \exp\left[-\frac{\alpha\kappa x_t^2 + \kappa y_t^2}{2k_BT}\right], \tag{6.5}$$

which implies that $\langle \boldsymbol{x}_t \rangle = 0$ and

$$\mathrm{Cov}(\boldsymbol{x}_t, \boldsymbol{x}_t) = \frac{k_BT}{\alpha\kappa}\begin{pmatrix} 1 & 0 \\ 0 & \alpha \end{pmatrix} \tag{6.6}$$

where $(\mathrm{Cov}(\boldsymbol{x}_t, \boldsymbol{x}_t))_{ij} = \langle x_t^i x_t^i \rangle - \langle x_t^i \rangle \langle x_t^i \rangle = \langle x_t^i x_t^i \rangle$ is the covariance matrix. Moreover, the mean local velocity defined in (2.48) becomes

$$\boldsymbol{v}_{st}(x_t, y_t) = \mu \left(-\nabla U(x_t, y_t) + \boldsymbol{f}(x_t, y_t)\right) - k_BT\mu\nabla \ln p_{\rm st}(x_t, y_t) = \mu \boldsymbol{f}(x_t, y_t)\,, \tag{6.7}$$

showing that the non-equilibrium state is due to the non conservative force $\boldsymbol{f}$.

In order to calculate relevant quantities associated to the dynamics defined in (6.4), we solve these equations by means of Laplace transforms. Indeed, similarly to what has been done for the unidimensional GLE in Chapter 3, by applying the Laplace transform to (6.4) one gets

$$\begin{cases} k\hat{x}(k) - x_0 = -\alpha\mu\kappa\hat{x}(k) - \mu\rho\hat{y}(k) + \sqrt{2k_BT\mu}\,\hat{\xi}^x(k) \\ k\hat{y}(k) - y_0 = -\mu\kappa\hat{y}(k) + \alpha\mu\rho\hat{x}(k) + \sqrt{2k_BT\mu}\,\hat{\xi}^y(k) \end{cases} \tag{6.8}$$

which can be rearranged to get

$$\begin{pmatrix} \hat{x}(k) \\ \hat{y}(k) \end{pmatrix} = \hat{\boldsymbol{\chi}}(k) \cdot \begin{pmatrix} x_0 + \sqrt{2k_BT\mu}\,\hat{\xi}^x(k) \\ y_0 + \sqrt{2k_BT\mu}\,\hat{\xi}^y(k) \end{pmatrix} \tag{6.9}$$

which is given in matrix notation and where we introduced the susceptibility matrix, defined via its Laplace transform, that is

$$\hat{\boldsymbol{\chi}}(k) = \frac{1}{(k+\alpha\mu\kappa)(k+\mu\kappa) + \alpha\mu^2\rho^2} \begin{pmatrix} k+\mu\kappa & -\mu\rho \\ \alpha\mu\rho & k+\alpha\mu\kappa \end{pmatrix}. \tag{6.10}$$

By further defining the function

$$\begin{aligned} \mathcal{T}(t) =& \mathcal{L}^{-1}\left[\frac{1}{(k+\alpha\mu\kappa)(k+\mu\kappa)+\alpha\mu^2\rho^2}\right] = \\ =& \frac{\sin\left(t\mu\sqrt{\alpha\rho^2 - \frac{(1-\alpha)^2\kappa^2}{4}}\right)}{\mu\sqrt{\alpha\rho^2 - \frac{(1-\alpha)^2\kappa^2}{4}}} \mathrm{e}^{-\kappa\mu(1+\alpha)t/2}, \end{aligned} \tag{6.11}$$

one can easily see that the susceptibility matrix becomes

$$\boldsymbol{\chi}(t) = \begin{pmatrix} \dot{\mathcal{T}}(t) + \mu\kappa\mathcal{T}(t) & -\mu\rho\mathcal{T}(t) \\ \alpha\mu\rho\mathcal{T}(t) & \dot{\mathcal{T}}(t) + \alpha\mu\kappa\mathcal{T}(t) \end{pmatrix}, \tag{6.12}$$

where we also used that $\dot{\mathcal{T}}(t) = \mathcal{L}^{-1}\left[k\hat{\mathcal{T}}(k)\right]$ because $\mathcal{T}(0) = 0$. By using this and by transforming back (6.9) into real time, the solution of (6.4) can be expressed as

$$x^i(t) = \chi_{ij}(t)\,x_0^j + \int_0^t \mathrm{d}t'\,\chi_{ij}(t-t')\,\xi^j(t'), \tag{6.13}$$

where summation over repeated indexes is intended. In a stationary state with PDF given by (6.5) it holds $\langle \boldsymbol{x}_t \rangle = (0,0)$ for every t and clearly (6.13) is consistent with this. Moreover, by using the equation above one can easily calculate the steady state correlation functions

$$\begin{aligned} \langle \boldsymbol{x}_t \boldsymbol{x}_0^{\mathrm{T}} \rangle =& \boldsymbol{\chi}(t)\langle \boldsymbol{x}_0 \boldsymbol{x}_0^{\mathrm{T}} \rangle = \boldsymbol{\chi}(t)\mathrm{Cov}(\boldsymbol{x}_0, \boldsymbol{x}_0) = \\ =& \frac{k_BT}{\alpha\kappa} \begin{pmatrix} \dot{\mathcal{T}}(t) + \mu\kappa\mathcal{T}(t) & -\alpha\mu\rho\mathcal{T}(t) \\ \alpha\mu\rho\mathcal{T}(t) & \alpha\dot{\mathcal{T}}(t) + \alpha^2\mu\kappa\mathcal{T}(t) \end{pmatrix}, \end{aligned} \tag{6.14}$$

where we used equation (6.6) and that, in the Ito convention, $\langle \boldsymbol{\xi}(t')\boldsymbol{x}_0\rangle = 0$ for every $t' \geq 0$. By means of (6.14), one can calculate the stationary entropy production rate, corresponding to the heat injected into the environment and which can be readily obtained from (2.52)

$$\sigma_{\text{tot}} = \partial_t \langle \Sigma_{\text{tot}}\rangle_t = \left\langle \boldsymbol{\nu}_{\text{st}}\, \boldsymbol{D}^{-1} \boldsymbol{\nu}_{\text{st}} \right\rangle_t = \frac{\mu\rho^2}{k_B T}\left(\langle y_t y_t\rangle + \alpha^2 \langle x_t x_t\rangle\right) = \frac{\mu\rho^2(1+\alpha)}{\kappa}, \quad (6.15)$$

where we used equation (6.7) along with $\langle \boldsymbol{x}_t \boldsymbol{x}_t\rangle = \langle \boldsymbol{x}_0 \boldsymbol{x}_0\rangle$ in this steady state (together with the fact that the average of $\boldsymbol{x}(t)$ is constant in time) and that $\mathcal{T}(0) = 0, \dot{\mathcal{T}}(0) = 1$.

Moreover, the correlation functions shown in (6.14) also serve as building blocks for the calculation covariances which will be needed in Chapter 7 to verify and discuss our variance our sum rule (6.2). With this in mind, we can proceed and calculate, for example, the covariance matrix of the relative displacement that is

$$\begin{aligned}\text{Cov}(\boldsymbol{x}_t - \boldsymbol{x}_0, \boldsymbol{x}_t - \boldsymbol{x}_0) =& \langle (\boldsymbol{x}_t - \boldsymbol{x}_0)(\boldsymbol{x}_t^{\mathrm{T}} - \boldsymbol{x}_0^{\mathrm{T}})\rangle - \langle (\boldsymbol{x}_t - \boldsymbol{x}_0)\langle \boldsymbol{x}_t^{\mathrm{T}} - \boldsymbol{x}_0^{\mathrm{T}})\rangle = \\ =& 2\langle \boldsymbol{x}_0 \boldsymbol{x}_0^{\mathrm{T}}\rangle - \langle \boldsymbol{x}_t \boldsymbol{x}_0^{\mathrm{T}}\rangle - \langle \boldsymbol{x}_t \boldsymbol{x}_0^{\mathrm{T}}\rangle^{\mathrm{T}} = \\ =& \frac{2k_B T}{\alpha\kappa}\begin{pmatrix} 1 - \dot{\mathcal{T}}(t) + \mu\kappa\mathcal{T}(t) & 0 \\ 0 & \alpha\left(1 - \dot{\mathcal{T}}(t) + \mu\kappa\mathcal{T}(t)\right)\end{pmatrix}.\end{aligned} \quad (6.16)$$

Another quantity we are interested in is the covariance matrix of the integral of the forces. It can be calculated by exploiting that

$$F(\boldsymbol{x}_t) = \begin{pmatrix} -\alpha\kappa x(t) - \rho y(t) \\ -\kappa y(t) + \alpha\rho x(t)\end{pmatrix}, \quad (6.17)$$

meaning that the correlation function $\left\langle \boldsymbol{F}(\boldsymbol{x}_{t'})\, \boldsymbol{F}^{\mathrm{T}}(\boldsymbol{x}_{t''})\right\rangle$ can be again expressed in terms of the components of (6.14), and that $\langle \boldsymbol{F}(\boldsymbol{x}_t)\rangle = 0$, which leads to

$$\begin{aligned}\text{Cov}\left(\int_0^t \mathrm{d}t' \boldsymbol{F}(\boldsymbol{x}_{t'}), \int_0^t \mathrm{d}t'' \boldsymbol{F}(\boldsymbol{x}_{t''})\right) =& \int_0^t \mathrm{d}t' \int_0^t \mathrm{d}t'' \langle \boldsymbol{F}(\boldsymbol{x}_{t'}) \boldsymbol{F}^{\mathrm{T}}(\boldsymbol{x}_{t''})\rangle = \\ =& \frac{2k_B T}{\kappa}\int_0^t \mathrm{d}t' \int_0^{t'} \mathrm{d}t'' \begin{pmatrix} (\alpha\kappa^2 + \rho^2)\dot{\mathcal{T}}(t'') + & 2\rho\kappa(1-\alpha)\dot{\mathcal{T}}(t'') \\ +\alpha\mu\kappa(\kappa^2+\rho^2)\mathcal{T}(t'') & \\ 2\rho\kappa(1-\alpha)\dot{\mathcal{T}}(t'') & (\kappa^2 + \alpha\rho^2)\dot{\mathcal{T}}(t'') + \\ & +\alpha\mu\kappa(\kappa^2+\rho^2)\mathcal{T}(t'')\end{pmatrix}.\end{aligned} \quad (6.18)$$

In a similar way, one can also calculate the violation factor, defined in (6.3) and equal to

$$\boldsymbol{\mathcal{V}}(t) = \frac{1}{2}\int_0^t \mathrm{d}t' \int_0^{t'} \mathrm{d}t'' \left(\text{Cov}(\dot{\boldsymbol{x}}_{t''}, \boldsymbol{\nu}_{\text{st},0}) + \left(\text{Cov}^{\mathrm{T}}(\dot{\boldsymbol{x}}_{t''}, \boldsymbol{\nu}_{\text{st},0})\right)\right). \quad (6.19)$$

Because $\boldsymbol{\nu}_{\rm st}(\boldsymbol{x}_t) = \mu \boldsymbol{f}(\boldsymbol{x}_t)$, implying that $\langle \boldsymbol{\nu}_{\rm st} \rangle = 0$, one gets that the terms involving the covariances in (6.19), i.e. $\mathrm{Cov}(\dot{\boldsymbol{x}}_t, \boldsymbol{\nu}_{{\rm st},0}) = \langle \dot{\boldsymbol{x}}_t \boldsymbol{\nu}_{{\rm st},0} \rangle$, can be again expressed in terms of the components of (6.14) hence leading to

$$\boldsymbol{\mathcal{V}}(t) = \frac{\mu^2 k_B T}{\kappa} \int_0^t \mathrm{d}t' \begin{pmatrix} \rho^2 \mathcal{T}(t') & \rho\kappa(1-\alpha)\mathcal{T}(t') \\ \rho\kappa(1-\alpha)\mathcal{T}(t') & \rho^2 \mathcal{T}(t') \end{pmatrix} . \tag{6.20}$$

The behaviour and relevance of all these quantities will be discussed in more detail in Section 7.3

6.2 Brownian gyrator

Brownian gyrators are nice minimal systems that can be used, for example, as models for microscopic heat engines operating on the nanoscale [119]. By following previous works on this topic such as [120, 121, 122, 123, 124], we consider a set of two LEs with a parabolic potential $U(x_t, y_t) = \kappa(x_t^2 + y_t^2)/2 + \alpha\,\kappa\, x_t\, y_t$, where $-1 < \alpha < 1$ is a factor determining the asymmetry of the potential landscape, and with diffusion matrix equal to

$$\boldsymbol{D} = \begin{pmatrix} k_B T_1 \mu_1 & 0 \\ 0 & k_B T_1 \mu_2 \end{pmatrix} \tag{6.21}$$

hence leading to

$$\begin{cases} \dot{x}(t) = -\mu_1 \partial_{x_t} U(x_t, y_t) + \sqrt{2 k_B T_1 \mu_1}\, \xi^x(t) = \\ \qquad = -\mu_1 \kappa x(t) - \mu_1 \alpha \kappa y(t) + \sqrt{2 k_B T_1 \mu_1}\, \xi^x(t) \\ \dot{y}(t) = -\mu_2 \partial_{y_t} U(x_t, y_t) + \sqrt{2 k_B T_2 \mu_2}\, \xi^y(t) = \\ \qquad = -\mu_2 \kappa y(t) - \mu_2 \alpha \kappa x(t) + \sqrt{2 k_B T_2 \mu_2}\, \xi^y(t) . \end{cases} \tag{6.22}$$

In a similar way as done for the system described in the previous subsection, one can apply the Laplace transform to (6.22) and, by turning to matrix notation and by doing some algebra, one gets

$$\begin{pmatrix} \hat{x}(k) \\ \hat{y}(k) \end{pmatrix} = \hat{\boldsymbol{\chi}}(k) \cdot \begin{pmatrix} x_0 + \sqrt{2 k_B T_1 \mu_1}\, \hat{\xi}^x(k) \\ y_0 + \sqrt{2 k_B T_2 \mu_2}\, \hat{\xi}^y(k) \end{pmatrix} , \tag{6.23}$$

where this time the susceptibility matrix is equal to

$$\hat{\boldsymbol{\chi}}(k) = \frac{1}{(k+\mu_1\kappa)(k+\mu_2\kappa) - \alpha^2 \mu_1 \mu_2 \kappa^2} \begin{pmatrix} k+\mu_2\kappa & -\alpha\mu_1\kappa \\ -\alpha\mu_2\kappa & k+\mu_1\kappa \end{pmatrix} . \tag{6.24}$$

Again, we define the function

$$\begin{aligned} \mathcal{T}(t) =& \mathcal{L}^{-1}\left[\frac{1}{(k+\mu_1\kappa)(k+\mu_2\kappa) - \alpha^2\mu_1\mu_2\kappa^2} \right] = \\ =& \frac{2 \sinh\left(\kappa t \sqrt{4\alpha^2 \mu_1 \mu_2 + (\mu_1 - \mu_2)^2}/2 \right)}{\kappa \sqrt{4\alpha^2 \mu_1 \mu_2 + (\mu_1 - \mu_2)^2}} \mathrm{e}^{-t\kappa(\mu_1+\mu_2)/2} , \end{aligned} \tag{6.25}$$

which is such that $\mathcal{T}(0) = 0$ (implying that $\dot{\mathcal{T}}(t) = \mathcal{L}^{-1}\left[k\hat{\mathcal{T}}(k)\right]$) and can be used to express the susceptibility matrix in real time as

$$\boldsymbol{\chi}(t) = \begin{pmatrix} \dot{\mathcal{T}}(t) + \mu_2\kappa\mathcal{T}(t) & -\alpha\mu_1\kappa\mathcal{T}(t) \\ -\alpha\mu_2\kappa\mathcal{T}(t) & \dot{\mathcal{T}}(t) + \mu_1\kappa\mathcal{T}(t) \end{pmatrix} . \tag{6.26}$$

Furthermore, by taking the inverse Laplace transform of (6.23), the solution of (6.22) can be written as

$$x^i(t) = \chi_{ij}(t)\, x_0^j + \int_0^t \mathrm{d}t'\, \chi_{ij}(t-t')\, \xi^j(t') \,. \tag{6.27}$$

From this, one can readily evaluate the stationary average of $\boldsymbol{x}_t$

$$\langle \boldsymbol{x} \rangle_t^{\mathrm{st}} = \langle \boldsymbol{x} \rangle_0^{\mathrm{st}} = \boldsymbol{\chi}(t)\, \langle \boldsymbol{x} \rangle_0^{\mathrm{st}} \,, \tag{6.28}$$

where $\langle \boldsymbol{x} \rangle_t^{\mathrm{st}} = \langle \boldsymbol{x} \rangle_0^{\mathrm{st}}$ is a consequence of the fact that neither the drift vector nor the diffusion matrix explicitly depend on time. Moreover, because the matrix $\boldsymbol{\chi}(t) \neq \mathbb{1}_2$ is not degenerate, the only possibility for (6.28) to hold corresponds to $\langle \boldsymbol{x} \rangle_0^{\mathrm{st}} = 0$. Another consequence of (6.27) is that, if $\boldsymbol{x}_0$ is distributed as a bivariate Gaussian, the same will be true for $\boldsymbol{x}_t$ at all times because a sum (or integral) of Gaussian random variables is itself Gaussian (remember that $\boldsymbol{\xi}(t)$ is also Gaussian). This feature is indeed a consequence of the linearity of equation (6.22) and, along with $\langle \boldsymbol{x} \rangle_0^{\mathrm{st}} = 0$, it implies that

$$p_{\mathrm{st}}(\boldsymbol{x}_t) \propto \exp\left(-\frac{1}{2} \boldsymbol{x}_t^{\mathrm{T}}\, \mathrm{Cov}^{-1}(\boldsymbol{x}_0, \boldsymbol{x}_0)\, \boldsymbol{x}_t \right) , \tag{6.29}$$

where

$$\mathrm{Cov}(\boldsymbol{x}_0, \boldsymbol{x}_0) = \begin{pmatrix} \langle \Delta x_0^2 \rangle & \mathrm{Cov}(x_0, y_0) \\ \mathrm{Cov}(x_0, y_0) & \langle \Delta y_0^2 \rangle \end{pmatrix} = \begin{pmatrix} \langle x_0^2 \rangle & \langle x_0 y_0 \rangle \\ \langle x_0 y_0 \rangle & \langle y_0^2 \rangle \end{pmatrix} \tag{6.30}$$

is, as usual, the covariance matrix. In order to evaluate its components, we resort to the discretised version of (6.22), i.e.

$$\begin{cases} x(t+dt) = x(t) - \mu_1\kappa x(t)\, dt - \mu_1\alpha\kappa y(t)\, dt + \sqrt{2k_B T_1 \mu_1}\, d\mathcal{B}^x(t) & (a) \\ y(t+dt) = y(t) - \mu_2\kappa y(t)\, dt - \mu_2\alpha\kappa x(t)\, dt + \sqrt{2k_B T_2 \mu_2}\, d\mathcal{B}^y(t) & (b) \end{cases} \tag{6.31}$$

where $\langle d\mathcal{B}^i(t) \rangle = 0$ and $\langle d\mathcal{B}^i(t)\, d\mathcal{B}^j(t) \rangle = \delta_{ij}\, dt$. By taking the square of (a) and (b) along with the product between (a) and (b) and by taking their average, one gets

$$\begin{cases} \langle x_{t+dt}^2 \rangle = \langle x_t^2 \rangle + \left(-2\mu_1\kappa \langle x_t^2 \rangle - 2\mu_1\alpha\kappa \langle y_t x_t \rangle + 2k_B T_1 \mu_1 \right) dt + o(dt) \\ \langle y_{t+dt}^2 \rangle = \langle y_t^2 \rangle + \left(-2\mu_2\kappa \langle y_t^2 \rangle - 2\mu_2\alpha\kappa \langle y_t x_t \rangle + 2k_B T_2 \mu_2 \right) dt + o(dt) \\ \langle x_{t+dt} y_{t+dt} \rangle = \langle x_t y_t \rangle - (\kappa(\mu_1+\mu_2)\langle x_t y_t \rangle + \alpha\mu_2\kappa\langle x_t^2 \rangle + \alpha\mu_1\kappa\langle y_t^2 \rangle) dt + o(dt) \,. \end{cases} \tag{6.32}$$

By further noting that, in a steady state, the correlation functions of random variables with constant average only depend on time differences (meaning for example that $\langle x_{t+dt}^2 \rangle = \langle x_t^2 \rangle$), one readily sees that (6.31) leads to a linear system of three

equations and three variables (i.e. $\langle x_t^2\rangle$, $\langle y_t^2\rangle$ and $\langle x_t\, y_t\rangle$, which are of course constant in time) whose solution reads

$$\begin{aligned}\langle x_0^2\rangle &= k_B\frac{T_1(\mu_1+\mu_2)+\alpha^2\mu_1(T_2-T_1)}{\kappa(1-\alpha^2)(\mu_1+\mu_2)}\\ \langle y_0^2\rangle &= k_B\frac{T_2(\mu_1+\mu_2)+\alpha^2\mu_2(T_1-T_2)}{\kappa(1-\alpha^2)(\mu_1+\mu_2)}\\ \langle x_0 y_0\rangle &= -\alpha k_B\frac{\mu_1 T_2+\mu_2 T_1}{\kappa(1-\alpha^2)(\mu_1+\mu_2)}\,.\end{aligned} \tag{6.33}$$

By means of these quantities we managed to fully determine the stationary PDF $p_{\rm st}(\boldsymbol{x}_t)$ (6.29) which in turn allows us to calculate the mean local velocity

$$\boldsymbol{v}_{st}(x_t,y_t) = -\boldsymbol{\mu}\nabla U(x_t,y_t) - \boldsymbol{D}\nabla \ln p_{\rm st}(x_t) = \begin{pmatrix} a_1 x_t - b_1 y_t \\ a_2 y_t - b_2 x_t\end{pmatrix}, \tag{6.34}$$

where $(\boldsymbol{\mu})_{ij} = \mu_i\delta_{ij}$ is the mobility matrix and

$$\begin{aligned} a_1 &= \frac{k_B T_1\mu_1\langle y_0^2\rangle}{\langle x_0^2\rangle\langle y_0^2\rangle - \langle x_0 y_0\rangle^2} - \mu_1\kappa \qquad & b_1 &= \frac{k_B T_1\mu_1\langle x_0 y_0\rangle}{\langle x_0^2\rangle\langle y_0^2\rangle - \langle x_0 y_0\rangle^2} + \alpha\mu_1\kappa\\ a_2 &= \frac{k_B T_2\mu_2\langle x_0^2\rangle}{\langle x_0^2\rangle\langle y_0^2\rangle - \langle x_0 y_0\rangle^2} - \mu_2\kappa \qquad & b_2 &= \frac{k_B T_2\mu_2\langle x_0 y_0\rangle}{\langle x_0^2\rangle\langle y_0^2\rangle - \langle x_0 y_0\rangle^2} + \alpha\mu_2\kappa\,. \end{aligned} \tag{6.35}$$

At this point, our aim would be to compute all the quantities that we derived in the last subsection, but this time the calculations are much longer and tedious. Hence, we will limit ourselves to present all the results by skipping most of the calculations and starting from the stationary entropy production which, similarly to (6.15), can be derived from (2.52) and it is equal to

$$\sigma_{\rm tot} = \left\langle \boldsymbol{v}_{\rm st}\,\boldsymbol{D}^{-1}\boldsymbol{v}_{\rm st}\right\rangle_t = \frac{\alpha^2\kappa\mu_1\mu_2(T_1-T_2)^2}{T_1T_2(\mu_1+\mu_2)}\,. \tag{6.36}$$

From this expression one can note that if the potential landscape is symmetric, corresponding to $\alpha = 0$, or if $T_1 = T_2$, the entropy production rate becomes equal to zero.

The next step consists in the calculation of the position correlation functions, i.e. the components of

$$\begin{aligned}\langle \boldsymbol{x}_t\boldsymbol{x}_0^{\rm T}\rangle =& \boldsymbol{\chi}(t)\langle \boldsymbol{x}_0\boldsymbol{x}_0^{\rm T}\rangle = \boldsymbol{\chi}(t){\rm Cov}(\boldsymbol{x}_0,\boldsymbol{x}_0) =\\ =& \begin{pmatrix} \left(\dot{\mathcal{T}}(t)+\kappa\mu_2\mathcal{T}(t)\right)\langle x_0^2\rangle + & \left(\dot{\mathcal{T}}(t)+\kappa\mu_2\mathcal{T}(t)\right)\langle x_0 y_0\rangle + \\ -\alpha\kappa\mu_1\mathcal{T}(t)\langle x_0 y_0\rangle & -\alpha\kappa\mu_1\mathcal{T}(t)\langle y_0^2\rangle \\ \left(\dot{\mathcal{T}}(t)+\kappa\mu_1\mathcal{T}(t)\right)\langle x_0 y_0\rangle + & \left(\dot{\mathcal{T}}(t)+\kappa\mu_1\mathcal{T}(t)\right)\langle y_0^2\rangle + \\ -\alpha\kappa\mu_2\mathcal{T}(t)\langle x_0^2\rangle & -\alpha\kappa\mu_2\mathcal{T}(t)\langle x_0 y_0\rangle \end{pmatrix},\end{aligned} \tag{6.37}$$

where in the first equality we used (6.27) along with the fact that $\langle \boldsymbol{\xi}(t')\,\boldsymbol{x}_0\rangle = 0$ almost everywhere. Note that, because $\mathcal{T}(0) = 0$ and $\dot{\mathcal{T}}(0) = 1$, for $t = 0$ (6.37)

trivially reduces to (6.30). Again, these correlations turn out to be very useful in the computation of the relative displacement covariance matrix, i.e.

$$\begin{aligned}\mathrm{Cov}(\boldsymbol{x}_t-\boldsymbol{x}_0,\boldsymbol{x}_t-\boldsymbol{x}_0) &= 2\langle \boldsymbol{x}_0\boldsymbol{x}_0^{\mathrm{T}}\rangle - \langle \boldsymbol{x}_t\boldsymbol{x}_0^{\mathrm{T}}\rangle - \langle \boldsymbol{x}_t\boldsymbol{x}_0^{\mathrm{T}}\rangle^{\mathrm{T}} = \\ &= 2\begin{pmatrix} \langle x_0^2\rangle - \langle x_t x_0\rangle & \langle x_0 y_0\rangle - (\langle x_t y_0\rangle + \langle y_t x_0\rangle)/2 \\ \langle x_0 y_0\rangle - (\langle x_t y_0\rangle + \langle y_t x_0\rangle)/2 & \langle y_0^2\rangle - \langle y_t y_0\rangle \end{pmatrix},\end{aligned} \tag{6.38}$$

of the covariance matrix of the integral of the forces

$$\begin{aligned}\mathrm{Cov}\left(\int_0^t \mathrm{d}t'\boldsymbol{F}(\boldsymbol{x}_{t'}),\int_0^t \mathrm{d}t''\boldsymbol{F}(\boldsymbol{x}_{t''})\right) &= \int_0^t \mathrm{d}t'\int_0^t \mathrm{d}t''\langle \boldsymbol{F}(\boldsymbol{x}_{t'})\boldsymbol{F}^{\mathrm{T}}(\boldsymbol{x}_{t''})\rangle = \\ = 2\kappa^2\int_0^t \mathrm{d}t'\int_0^{t'} \mathrm{d}t''&\begin{pmatrix} \mu_1^2(\langle x_{t''}x_0\rangle + \alpha^2\langle y_{t''}y_0\rangle + & \mu_1\mu_2(\alpha(\langle x_{t''}x_0\rangle + \langle y_{t''}y_0\rangle) + \\ +\alpha(\langle x_{t''}y_0\rangle + \langle y_{t''}x_0\rangle)) & +(1+\alpha^2)(\langle x_{t''}y_0\rangle + \langle y_{t''}x_0\rangle)/2) \\ \mu_1\mu_2(\alpha(\langle x_{t''}x_0\rangle + \langle y_{t''}y_0\rangle) + & \mu_2^2(\langle y_{t''}y_0\rangle + \alpha^2\langle x_{t''}x_0\rangle + \\ +(1+\alpha^2)(\langle x_{t''}y_0\rangle + \langle y_{t''}x_0\rangle)/2) & +\alpha(\langle x_{t''}y_0\rangle + \langle y_{t''}x_0\rangle)) \end{pmatrix},\end{aligned} \tag{6.39}$$

and of the Violation factor

$$\begin{aligned}\boldsymbol{\mathcal{V}}(t) =& \frac{1}{2}\int_0^t \mathrm{d}t'\int_0^{t'}\mathrm{d}t''\left(\mathrm{Cov}(\dot{\boldsymbol{x}}_{t''},\boldsymbol{\nu}_{\mathrm{st},0}) + \mathrm{Cov}^{\mathrm{T}}(\dot{\boldsymbol{x}}_{t''},\boldsymbol{\nu}_{\mathrm{st},0})\right) \\ =& \int_0^t \mathrm{d}t'\begin{pmatrix} a_1\langle x_{t'}x_0\rangle - b_1\langle x_{t'}y_0\rangle & \left(a_1\langle y_{t'}x_0\rangle + a_2\langle x_{t'}y_0\rangle + \right. \\ & \left. -b_1\langle y_{t'}y_0\rangle - b_2\langle x_{t'}x_0\rangle\right)/2 \\ \left(a_1\langle y_{t'}x_0\rangle + a_2\langle x_{t'}y_0\rangle + \right. & a_2\langle y_{t'}y_0\rangle - b_2\langle y_{t'}x_0\rangle \\ \left. -b_1\langle y_{t'}y_0\rangle - b_2\langle x_{t'}x_0\rangle\right)/2 & \end{pmatrix}\end{aligned} \tag{6.40}$$

where a_1, a_2, a_3, a_4 are given by (6.35). Again, we will study the behaviour of these covariances in 7.3, where they will be used to study the performances of our sum rule.

6.3 Stochastically switching trap

Finally, we consider the system composed by a Brownian particle at a temperature T and mobility μ, trapped in an harmonic potential whose center stochastically jumps between the positions $\{0,\Delta\lambda\}$, i.e. $U(x_t,t) = \kappa\left(x_t-\sigma_t\right)^2/2$. The stochastic variable σ_t, which is uncorrelated with the noise $\xi(t)$, takes values $\{0,1\}$ and undergoes a Markovian jumping dynamics, as those described in Section 2.3.1, with jumping rates $W_+ \equiv W_{10}$ and $W_- \equiv W_{01}$. By defining $W_{\mathrm{tot}} = W_+ + W_-$, one can also readily see that, in the stationary state, the average of σ_t becomes $m_{\mathrm{ss}} = \langle\sigma_t\rangle = W_+/W_{\mathrm{tot}}$. The dynamics of this system can be modelled by the Langevin equation

$$\begin{aligned}\dot{x}(t) &= \mu\left(-\kappa\left(x(t)-\Delta\lambda\sigma(t)\right)\right) + \sqrt{2k_BT\mu}\,\xi(t) = \\ &= \mu\left(-\kappa x(t) + \epsilon\sigma(t)\right) + \sqrt{2k_BT\mu}\,\xi(t),\end{aligned} \tag{6.41}$$

where we also defined $\epsilon = \kappa\Delta\lambda$. Furthermore, because in this steady state $\langle \dot{x}_t \rangle = 0$, one can readily compute the stationary average of the position of the particle which reads $\langle x_t \rangle = \epsilon m_{\rm ss}/\kappa$.

As we will show later, all the quantities we are interested in can be calculated in terms of the stationary correlation functions $C_{xx}(t) = \langle x_t\, x_0 \rangle$, $C_{x\sigma}(t) = \langle x_t\, \sigma_0 \rangle$, $C_{\sigma x}(t) = \langle \sigma_t\, x_0 \rangle$ and $C_{\sigma\sigma}(t) = \langle x_t\, \sigma_0 \rangle$ for $t \geq 0$. To compute these correlations we turn to a discrete description of the system, which can be modelled by the following set of stochastic equations

$$\begin{cases} x(t+dt) = x(t) - \mu\kappa x(t)\,dt + \mu\epsilon\sigma(t)\,dt + \sqrt{2k_B T\mu}\,d\mathcal{B}^x(t) & (a) \\ \sigma(t+dt) = \sigma(t) + (1-2\sigma(t))\theta(W_{1-\sigma_t,\sigma_t}dt - r) & (b) \end{cases} \tag{6.42}$$

where r is random variable with uniform probability distribution on $[0,1]$. By multiplying (a) in the latter equation by $x(0)$ and taking the stationary average, one obtains a first order differential equation that reads

$$\partial_t C_{xx}(t) = -\mu\kappa C_{xx}(t) + \mu\epsilon C_{\sigma x}(t)\,. \tag{6.43}$$

By multiplying the same line (a) in (6.42) by $\sigma(0)$, instead, one obtains

$$\partial_t C_{x\sigma}(t) = -\mu\kappa C_{x\sigma}(t) + \mu\epsilon C_{\sigma\sigma}(t)\,. \tag{6.44}$$

In a similar way, by multiplying line (b) in equation (6.42) by $x(0)$ and $\sigma(0)$, one can show that the following equations hold, i.e

$$\partial_t C_{\sigma x}(t) = W_+ \langle x_t \rangle - W_{\rm tot} C_{\sigma x}(t) \tag{6.45}$$

and

$$\partial_t C_{\sigma\sigma}(t) = W_+ m_{\rm ss} - W_{\rm tot} C_{\sigma\sigma}(t)\,. \tag{6.46}$$

These linear equations can be solved with standard techniques in terms of the initial conditions of the correlation functions at time $t = 0$. These (stationary) initial conditions can be calculated with the same method used in the previous sections and starting from the discretised equations (6.42). For brevity, we only present the results of this procedure, which are

$$\begin{aligned} C_{xx}(0) =& \frac{\epsilon^2 m_{\rm ss}^2}{\kappa^2} + \frac{k_B T}{\kappa} + \frac{\epsilon^2 \mu\, m_{\rm ss}(1-m_{\rm ss})}{\kappa(W_{\rm tot}+\mu\kappa)} \\ C_{\sigma x}(0) =& \frac{\epsilon^2 m_{\rm ss}^2}{\kappa} + \frac{\epsilon\,\mu\, m_{\rm ss}(1-m_{\rm ss})}{W_{\rm tot}+\mu\kappa} = C_{x\sigma}(0) \\ C_{\sigma\sigma}(0) =& m_{\rm ss}\,. \end{aligned} \tag{6.47}$$

By means of these quantities, one can readily solve equations (6.43), (6.44),(6.45)

and (6.46) finding that

$$\begin{aligned}
C_{xx}(t) =& \frac{\epsilon^2 m_{\rm ss}^2}{\kappa^2} + \left(\frac{k_B T}{\kappa} + \frac{\epsilon^2 \mu m_{\rm ss}(1-m_{\rm ss})}{\kappa(W_{\rm tot}+\mu\kappa)}\right) {\rm e}^{-\mu\kappa t} + \\
&+ \frac{\epsilon^2 \mu^2 m_{\rm ss}(1-m_{\rm ss})}{W_{\rm tot}^2 - \mu^2\kappa^2}\left({\rm e}^{-\mu\kappa t} - {\rm e}^{-W_+ t}\right) \\
C_{\sigma x}(t) =& \frac{\epsilon^2 m_{\rm ss}^2}{\kappa} + \frac{\epsilon\mu m_{\rm ss}(1-m_{\rm ss})}{W_{\rm tot}+\mu\kappa}{\rm e}^{-\mu\kappa t} \\
C_{x\sigma}(t) =& \frac{\epsilon^2 m_{\rm ss}^2}{\kappa} + \frac{\epsilon\mu m_{\rm ss}(1-m_{\rm ss})}{W_{\rm tot}+\mu\kappa}{\rm e}^{-\mu\kappa t} + \frac{\epsilon\mu m_{\rm ss}(1-m_{\rm ss})}{W_{\rm tot}-\mu\kappa}\left({\rm e}^{-\mu\kappa t} - {\rm e}^{-W_+ t}\right) \\
C_{\sigma\sigma}(t) =& m_{\rm ss}^2 + m_{\rm ss}(1-m_{\rm ss}){\rm e}^{-W_+ t}\,.
\end{aligned} \tag{6.48}$$

From these correlation functions, one can for example compute the variance of the relative displacement, that is

$$\begin{aligned}
{\rm Var}(x_t - x_0) =& \langle (x_t - x_0)(x_t - x_0)\rangle = 2(C_{xx}(0) - C_{xx}(t)) = \\
=& 2\left(\frac{k_B T}{\kappa} + \frac{\epsilon^2\mu m_{\rm ss}(1-m_{\rm ss})}{\kappa(W_{\rm tot}+\mu\kappa)}\right)(1-{\rm e}^{-\mu\kappa t}) + \\
&+ \frac{2\epsilon^2\mu^2 m_{\rm ss}(1-m_{\rm ss})}{\mu^2\kappa^2 - W_{\rm tot}^2}\left({\rm e}^{-W_+ t} - {\rm e}^{-\mu\kappa t}\right)\,.
\end{aligned} \tag{6.49}$$

Note that, for $\epsilon = 0$, one recovers the usual formula for the relative displacement of the Ornstein–Uhlenbeck process. As regards the variance of the time integrated forces, it can be readily computed by identifying the total forces acting on the bead as $F(x_t, t) = -\kappa x(t) + \epsilon\sigma(t)$, which leads to

$$\begin{aligned}
&{\rm Var}\Big(\int_0^t {\rm d}t' F(x_{t'}, t')\Big) = \int_0^t {\rm d}t' \int_0^t {\rm d}t'' {\rm Cov}(F(x_{t'}, t'), F(x_{t''}, t'')) = \\
&= 2\int_0^t {\rm d}t' \int_0^{t'} {\rm d}t'' \left(\kappa^2 C_{xx}(t'') + \epsilon^2 C_{\sigma\sigma}(t'') - \epsilon\kappa(C_{x\sigma}(t'') + C_{\sigma x}(t'')) - \langle F\rangle_{t''}^2\right) = \\
&= \frac{2k_B T t}{\mu} + \frac{2k_B T}{\mu^2\kappa}\left(1 - {\rm e}^{-\mu\kappa t}\right) + \frac{2\epsilon^2 m_{\rm ss}(1-m_{\rm ss})}{\mu\kappa(W_{\rm tot}+\mu\kappa)}\left(1 - \frac{W_{\rm tot}{\rm e}^{-\mu\kappa t}}{W_{\rm tot}-\mu\kappa} + \frac{\mu\kappa{\rm e}^{-W_{\rm tot} t}}{W_{\rm tot}-\mu\kappa}\right)
\end{aligned} \tag{6.50}$$

where we used that, because of the symmetry of the correlation functions $\langle F(x_{t'}, t')F(x_{t''}, t'')\rangle$, it holds that

$$\int_0^t {\rm d}t' \int_0^t {\rm d}t'' {\rm Cov}(F(x_{t'}, t'), F(x_{t''}, t'')) = 2\int_0^t {\rm d}t' \int_0^{t'} {\rm d}t'' {\rm Cov}(F(x_{t''}, t''), F(x_0, 0))\,. \tag{6.51}$$

Finally, we can also compute the average entropy production rate in a steady state, where the total entropy production can be identified with the amount of heat in-

jected into the environment and which can be obtained from equation (2.55), i.e.

$$\begin{aligned}
\sigma_{\text{tot}} =& \partial_t \langle \Sigma_{\text{env}} \rangle = \beta \partial_t \int_0^t \mathrm{d}t' \left\langle F(x_{t'}, t') \circ \dot{x}(t') \right\rangle = \\
=& \beta \partial_t \int_0^t \mathrm{d}t' \left\langle -\kappa x(t') \circ \dot{x}(t') + \epsilon \sigma(t') \circ \dot{x}(t') \right\rangle = \\
=& -\kappa \partial_t \left(\langle x_t^2 \rangle - \langle x_0^2 \rangle \right) + \epsilon \mu \partial_t \int_0^t \mathrm{d}t' \left\langle \sigma(t') \Big(-\kappa x(t') + \epsilon \sigma(t') + \sqrt{2 k_B T / \mu}\, \xi(t') \Big) \right\rangle = \\
=& \epsilon^2 \mu C_{\sigma\sigma} - \epsilon \mu \kappa C_{\sigma x}(0) = \\
=& \frac{\epsilon^2 \mu m_{\text{ss}} (1 - m_{\text{ss}}) W_{\text{tot}}}{W_{\text{tot}} + \mu \kappa},
\end{aligned} \tag{6.52}$$

where between the last two lines we used that $\langle x_t^2 \rangle = const$ and that $\langle \sigma(t) \xi(t) \rangle = 0$. Note that, as expected, the entropy production rate is zero for $\epsilon = 0$.

CHAPTER 7

MARKOVIAN VARIANCE SUM RULE

7.1 Introduction

Stochastic processes are extensively used, nowadays, to model and describe the dynamics of coarse grained mesoscopic systems or intrinsically random systems. As already discussed in the previous chapters, these processes are characterised by a path weight $P(\omega_t)$ (essentially, the path probability function (PDF)), such as (2.20) and (2.51), encoding the whole information about the dynamics. Indeed, in addition to their obvious role in calculating averages, variances and so on, the path PDFs can be used, for example, to calculate the entropy production associated to some non-equilibrium dynamics by means of Shannon's entropy (2.23) or, in the presence of a steady state and in the context of Markovian dynamics, by using the well known fluctuation theorems [25]. However, from a practical point of view, even if the functional form of the path PDF is known a priori, it is often very difficult if not impossible to gather a sufficient statistics to reconstruct the exact PDF in a proper way.

The problem of estimating probabilities and their evolution from raw data is a wide and extremely complex problem. Moreover, the abundance of data, the available computational power and the efficiency of the used algorithms play a prominent role in determining the final quality of the estimation procedure. For all these reasons, a comprehensive treatment of this topic is, of course, far beyond the scope of this thesis. Instead, in this chapter, we propose a new method, based on the estimation of variances of certain relevant observables, which can be used for the inference of model parameters and entropy production. This estimation technique is based on our main results, which we term the Markovian and non-Markovian variance sum rules (VSRs). For Markovian systems governed by the usual d-dimensional Langevin equation (LE) with constant diffusion matrix $\boldsymbol{D}$ and mobility matrix $\boldsymbol{\mu}$

$$\dot{\boldsymbol{x}}(t) = \boldsymbol{\mu}\boldsymbol{F}(\boldsymbol{x}_t, t) + \sqrt{2\boldsymbol{D}}\,\boldsymbol{\xi}(t)\,, \tag{7.1}$$

in the steady state with local mean velocity $\boldsymbol{\nu}$, the Markovian VSR takes the following form

$$\mathrm{Cov}(\boldsymbol{x}_t - \boldsymbol{x}_0, \boldsymbol{x}_t - \boldsymbol{x}_0) + \int_0^t \mathrm{d}t' \int_0^t \mathrm{d}t''\, \mathrm{Cov}(\boldsymbol{\mu}\boldsymbol{F}(\boldsymbol{x}_{t'}, t'), \boldsymbol{\mu}\boldsymbol{F}(\boldsymbol{x}_{t''}, t'')) = 2\boldsymbol{D}t + 4\boldsymbol{\mathcal{V}}(t) \tag{7.2}$$

where

$$\boldsymbol{\mathcal{V}}(t) = \frac{1}{2}\int_0^t \mathrm{d}t' \int_0^{t'} \mathrm{d}t'' \left(\mathrm{Cov}(\dot{\boldsymbol{x}}_{t''}, \boldsymbol{\nu}_0) + \mathrm{Cov}^{\mathrm{T}}(\dot{\boldsymbol{x}}_{t''}, \boldsymbol{\nu}_0)\right)\,. \tag{7.3}$$

is the integrated violation factor, involving the mean local velocity and hence equal to zero at equilibrium. The violation factor was first presented in [36] and derived for unidimensional systems, where it was shown that its magnitude can be regarded as a measure of the amount of violation of the fluctuation-dissipation theorem (FDT).

We anticipate that the VSR (7.2) has been verified by experiments performed with optical tweezers located at the *Small Biosystems Lab* (Barcelona) for the equilibrium dynamics of a colloidal bead in a parabolic potential and for the steady states dynamics of a stochastically switching harmonic trap described in Section 6.3. For more complicated non-equilibrium steady states, instead, we are still refining the experimental techniques aimed to the estimation of total forces.

To conclude this introductory section, we would like to acknowledge the merit for the experimental effort to Drss. Marta Gironella, who worked under the supervision of Prof. Felix Ritort at the the University of Barcelona. For this reason, we do not include any technical detail on the functioning of optical tweezers (a detailed description can be found for example in [125]). Indeed, for our purposes one just needs to know that the output of the experiments is a temporal series of forces applied on the colloidal bead by the trapping potential, i.e. the optical mini tweezers, with sampling frequency equal to $10^5 Hz$. Data analysis has been a joint work with Drss. Gironella. All the results presented in this chapter will be included in some papers [126] (in preparation at the time of writing this thesis) whose authors will be Ivan Di Terlizzi*, Marta Gironella*, Marco Baiesi and Felix Ritort.

7.2 Markovian variance sum rule: derivation

This technical section is devoted to the derivation of the VSR for the Markovian dynamics of a colloidal bead in d dimensions and in an homogeneous media, determined by the following Langevin equation

$$\dot{\boldsymbol{x}}(t) = \boldsymbol{\mu}\boldsymbol{F}(\boldsymbol{x}_t, t) + \sqrt{2\boldsymbol{D}}\,\boldsymbol{\xi}(t)\,. \tag{7.4}$$

The random noise, as usual, is Gaussian with moments equal to $\langle \xi^i(t')\rangle = 0$ and $\langle \xi^i(t')\xi^i(t'')\rangle = \delta_{ij}\,\delta(t'-t'')$. Instead, the diffusion matrix corresponds to $\boldsymbol{D} = k_B\boldsymbol{T}\boldsymbol{\mu}$ and it is defined via the mobility $\boldsymbol{\mu}$ and temperature $\boldsymbol{T}$ matrices. This hypothesis is valid in two distinct cases:

- the system is in contact with only one heat bath at temperature T, meaning that the temperature matrix is proportional to the identity matrix, i.e. $\boldsymbol{T} = T\mathbb{1}$, hence leading to $\boldsymbol{D} = k_B T\boldsymbol{\mu}$;
- the system is in contact with many heat baths. In this case, we consider a diagonal mobility matrix and same thing for $(\boldsymbol{T})_{ij} = T_i\,\delta_{ij}$, implying that $D_{ij} = k_B T_i\,\mu_{ii}\delta_{ij}$.

Hence, for the situations discussed above, the diffusion matrix can be written in terms of a commutative product of a temperature and a mobility matrix. In addition, the force term $\boldsymbol{F}(\boldsymbol{x}_t, t)$ can have an explicit time dependence due, for example, to a time dependent external protocol $\boldsymbol{\lambda}(t)$. In the case of conservative forces, for instance, it could take the form $\boldsymbol{F}(\boldsymbol{x}_t, t) = \nabla U(\boldsymbol{x}_t - \boldsymbol{\lambda}_t)$. The external protocol may

itself have a stochastic behaviour. If the statistics associated to the external protocol does not depend on trajectory ω_t, then we can take a specific realisation of $\lambda(t)$ in (7.4) and consider it deterministic. Once we will get the final formula, we will be able to average with respect all possible realisations of $\lambda(t)$ to get an experimentally accessible result. With this in mind, we proceed by considering an external force with an explicit, but deterministic time dependence.

Lets consider the time integral of equation (7.4) that is, rearranging the terms,

$$\Delta\boldsymbol{\mathcal{R}}_t \equiv \boldsymbol{x}(t) - \boldsymbol{x}(0) - \int_0^t \mathrm{d}t'\, \boldsymbol{\mu}\boldsymbol{F}(\boldsymbol{x}_{t'}, t') = \sqrt{2\boldsymbol{D}} \int_0^t \mathrm{d}t'\, \boldsymbol{\xi}(t')\,. \tag{7.5}$$

where we defined $\Delta\boldsymbol{\mathcal{R}}_t$ which is useful for calculations. Of course $\langle \Delta\boldsymbol{\mathcal{R}}_t \rangle = 0$. Consider now

$$\begin{aligned}
\mathrm{Cov}(\Delta\mathcal{R}^i_t, \Delta\mathcal{R}^j_t) =& \langle \Delta\mathcal{R}^i_t \Delta\mathcal{R}^j_t \rangle - \langle \Delta\mathcal{R}^i_t \rangle \langle \Delta\mathcal{R}^j_t \rangle = \\
=& \mathrm{Cov}(x^i_t - x^i_0, x^j_t - x^j_0) + \\
&+ \mu_{il}\,\mu_{jk} \int_0^t \mathrm{d}t' \int_0^t \mathrm{d}t''\, \mathrm{Cov}\left(F^l(\boldsymbol{x}_{t'}, t'), F^k(\boldsymbol{x}_{t''}, t'')\right) + \\
&- \mu_{jk} \int_0^t \mathrm{d}t'\, \mathrm{Cov}\left(x^i_t - x^i_0, F^k(\boldsymbol{x}_{t'}, t')\right) + \\
&- \mu_{ik} \int_0^t \mathrm{d}t'\, \mathrm{Cov}\left(x^j_t - x^j_0, F^k(\boldsymbol{x}_{t'}, t')\right) = 2D_{ij}\,t\,,
\end{aligned} \tag{7.6}$$

where, for the last term, we used the the second fluctuation dissipation theorem. We can rewrite equation (7.6) as

$$\begin{aligned}
&\mathrm{Cov}(x^i_t - x^i_0, x^j_t - x^j_0) + \mu_{il}\,\mu_{jk} \int_0^t \mathrm{d}t' \int_0^t \mathrm{d}t''\, \mathrm{Cov}\left(F^l(\boldsymbol{x}_{t'}, t'), F^k(\boldsymbol{x}_{t''}, t'')\right) = \\
=& 2D_{ij}\,t + \mu_{jk} \int_0^t \mathrm{d}t'\, \mathrm{Cov}\left(x^i_t - x^i_0, F^k(\boldsymbol{x}_{t'}, t')\right) + \mu_{ik} \int_0^t \mathrm{d}t'\, \mathrm{Cov}\left(x^j_t - x^j_0, F^k(\boldsymbol{x}_{t'}, t')\right)\,,
\end{aligned} \tag{7.7}$$

By focusing on the last two terms on the right hand side of (7.7) and noting that

$$\mu_{ij} \int_0^t \mathrm{d}t'\, F^j(\boldsymbol{x}_{t'}, t') = x^i(t) - x^i(0) - \sqrt{2D_{ij}} \int_0^t \mathrm{d}t'\, \xi^j(t')\,, \tag{7.8}$$

one immediately sees that

$$\begin{aligned}
&\mu_{jk} \int_0^t \mathrm{d}t'\, \mathrm{Cov}\left(x^i_t - x^i_0, F^k(\boldsymbol{x}_{t'}, t')\right) + \mu_{ik} \int_0^t \mathrm{d}t'\, \mathrm{Cov}\left(x^j_t - x^j_0, F^k(\boldsymbol{x}_{t'}, t')\right) = \\
=& 2\,\mathrm{Cov}(x^i_t - x^i_0\,,\, x^j_t - x^j_0) - \sqrt{2D_{jk}} \int_0^t \mathrm{d}t'\, \langle x^i_t\, \xi^k(t') \rangle - \sqrt{2D_{ik}} \int_0^t \mathrm{d}t'\, \langle x^j_t\, \xi^k(t') \rangle\,,
\end{aligned} \tag{7.9}$$

where we used that $\mathrm{Cov}(x^j_t\,,\, \xi^i(t')) = \langle x^j_t\, \xi^i(t') \rangle$ because $\langle \xi^i(t') \rangle = 0$ and that $\int_0^t \mathrm{d}t'\, \langle x^i_0\, \xi^j(t') \rangle = 0$ since $\langle x^i_0\, \xi^j(t') \rangle = 0$ almost everywhere on $[0, t]$ for every $\{ij\}$. In order to evaluate the correlations between position and noise we use the Furutsu-Novikov formula [127, 128] that relates the average of the functional derivative of

an observable, dependent on a Gaussian noise, with respect to the noise itself and the correlation between the noise and the observable. In our case, the result can be obtained by first considering the path probability density functional associated to all possible realisations of the stochastic noise $\{\boldsymbol{\xi}_t\}$

$$P(\{\boldsymbol{\xi}_t\}) \propto \exp\left[-\frac{1}{2}\int_0^t \mathrm{d}t'\, \boldsymbol{\xi}_{t'}^T\, \boldsymbol{\xi}_{t'}\right]. \tag{7.10}$$

From this one sees that, for a generic observable $O(\{\boldsymbol{\xi}_t\})$, it holds that

$$\begin{aligned}\left\langle \frac{\delta \mathcal{O}(\{\boldsymbol{\xi}_t\})}{\delta \xi^i_{t'}} \right\rangle &= \int \mathcal{D}[\{\boldsymbol{\xi}_t\}] P(\{\boldsymbol{\xi}_t\}) \frac{\delta \mathcal{O}(\{\boldsymbol{\xi}_t\})}{\delta \xi^i_{t'}} = -\int \mathcal{D}[\{\boldsymbol{\xi}_t\}] \frac{\delta P(\{\boldsymbol{\xi}_t\})}{\delta \xi^i_{t'}} \mathcal{O}(\{\boldsymbol{\xi}_t\}) = \\ &= \int \mathcal{D}[\{\boldsymbol{\xi}_t\}] P(\{\boldsymbol{\xi}_t\}) \mathcal{O}(\{\boldsymbol{\xi}_t\})\, \xi^i_{t'} = \langle \mathcal{O}(\{\boldsymbol{\xi}_t\})\, \xi^i_{t'} \rangle\end{aligned} \tag{7.11}$$

where at the end of the first line we performed an integration by parts and used that the path PDF goes to 0 at infinity. Using this, equation (7.9) becomes

$$\begin{aligned}&\mu_{jk}\int_0^t \mathrm{d}t'\, \mathrm{Cov}\left(x^i_t - x^i_0,\, F^k(\boldsymbol{x}_{t'}, t')\right) + \mu_{ik}\int_0^t \mathrm{d}t'\, \mathrm{Cov}\left(x^j_t - x^j_0,\, F^k(\boldsymbol{x}_{t'}, t')\right) = \\ &= 2\,\mathrm{Cov}(x^i_t - x^i_0\,,\; x^j_t - x^j_0) - \sqrt{2D_{jk}}\int_0^t \mathrm{d}t' \left\langle \frac{\delta x^i_t}{\delta \xi^k_{t'}} \right\rangle - \sqrt{2D_{ik}}\int_0^t \mathrm{d}t' \left\langle \frac{\delta x^j_t}{\delta \xi^k_{t'}} \right\rangle.\end{aligned} \tag{7.12}$$

Let us focus on the response function

$$\chi^{ij}(t,t') = \left\langle \frac{\delta x^i_t}{\delta \xi^j_{t'}} \right\rangle \tag{7.13}$$

with $t > t'$. As discussed in [46, 47, 50], if a perturbing potential is added to the unperturbed Hamiltonian so that

$$H_{tot}(\boldsymbol{x}_t, t) = H_0(\boldsymbol{x}_t, t) + H_p(\boldsymbol{x}_t, t) = H_0(\boldsymbol{x}_t, t) + h^j_t\, V^j(\boldsymbol{x}_t, t)\,, \tag{7.14}$$

then, the response with respect to h_t in the *steady state* is equal to

$$\begin{aligned}\left\langle \frac{\delta \mathcal{O}(x_t, t)}{\delta h^j_{t'}} \right\rangle = (k_B \boldsymbol{T})^{-1}_{jl} \Bigg(&\frac{\mathrm{d}}{\mathrm{d}t'} \langle \mathcal{O}(\boldsymbol{x}_t, t) V^l(\boldsymbol{x}_{t'}, t') \rangle - \frac{1}{2} \langle \mathcal{O}(x_t, t)\, (L_{t'} - L^*_{t'}) V^l(\boldsymbol{x}_{t'}, t') \rangle + \\ &- \frac{1}{2} \langle \mathcal{O}(\boldsymbol{x}_t, t)\, \partial_{t'} V^l(\boldsymbol{x}_{t'}, t') \rangle \Bigg).\end{aligned} \tag{7.15}$$

where T_{jl} is the diagonal temperature matrix and $L_{t'}$ and $L^*_{t'}$ are the generator of the dynamics and it conjugate, respectively. For the systems we are considering they are equal to

$$L_t = \mu_{ik} F^i(\boldsymbol{x}_t, t)\, \partial_{x^k_t} + D_{ik}\, \partial_{x^i_t} \partial_{x^k_t} \tag{7.16}$$

$$L^*_t = -\mu_{ik} F^i(\boldsymbol{x}_t, t) \partial_{x^k_t} - D_{ik}\, \partial_{x^i_t} \partial_{x^k_t} + 2 D_{ik} \left(\partial_{x^i_t} \log(p_{\mathrm{st}}(\boldsymbol{x}_t))\right) \partial_{x^k_t} \tag{7.17}$$

where Einstein's notation is understood and $p_{\mathrm{st}}(\boldsymbol{x}_t, t)$ is the stationary distribution obtained from the FP equation associated to (7.4). The same formal reasoning that lead to (7.15) can be applied to the thermal noise, which near equilibrium leads to the famous Onsager regression hypothesis. Indeed we see that the Langevin equation can be rewritten as

$$\dot{x}^i(t) = \mu_{ij} F^j(\boldsymbol{x}_t, t) + \sqrt{2D_{ij}}\, \xi^j(t) = \mu_{ij} \left(F^j(\boldsymbol{x}_t, t) + \mu^{-1}_{jl} \sqrt{2D_{lr}}\, \xi^r(t) \right), \tag{7.18}$$

meaning that the thermal noise can be seen as a small perturbation to the deterministic dynamics driven by $\boldsymbol{F}(\boldsymbol{x}_t, t)$ and arising from the perturbing Hamiltonian

$$H_p(\boldsymbol{x}_t, t) = x^j(t)\, \mu^{-1}_{jl} \sqrt{2D_{lr}}\, \xi^r(t)\,. \tag{7.19}$$

Moreover, comparing this last equation with (7.14), we identify

$$V^j(\boldsymbol{x}_t, t) = x^r(t)\, \mu^{-1}_{rl} \sqrt{2D_{lj}} \qquad\qquad h^j_t = \xi^j(t) \tag{7.20}$$

so that (7.15) specialises to

$$\left\langle \frac{\delta \mathcal{O}(\boldsymbol{x}_t, t)}{\delta \xi^j_{t'}} \right\rangle = (k_B \boldsymbol{T})^{-1}_{js} \sqrt{2D_{sl}}\, \mu^{-1}_{lr} \left(\frac{\mathrm{d}}{\mathrm{d}t'} \langle \mathcal{O}(\boldsymbol{x}_t, t)\, x^r_{t'} \rangle - \langle \mathcal{O}(\boldsymbol{x}_t, t) \left(L_{t'} - L^*_{t'} \right) x^r_{t'} \rangle / 2 \right) \tag{7.21}$$

as a consequence of μ_{ij} and D_{ij} being symmetric and $\partial_t V^j(\boldsymbol{x}_t, t) = 0$, because ∂_t is a partial derivative and $V^j(\boldsymbol{x}_t, t)$ in (7.20) does not depend explicitly on time. Going back to the position response function appearing in (7.12) and using this last result one gets

$$\chi^{ij}(t, t') = \left\langle \frac{\delta x^i_t}{\delta \xi^j_{t'}} \right\rangle = (k_B \boldsymbol{T})^{-1}_{js} \sqrt{2D_{sl}}\, \mu^{-1}_{lr} \left(\frac{\mathrm{d}}{\mathrm{d}t'} \langle x^i_t\, x^r_{t'} \rangle - \langle x^i_t \left(L_{t'} - L^*_{t'} \right) x^r_{t'} \rangle / 2 \right), \tag{7.22}$$

where we also defined the position's susceptibility $\chi^{ij}(t, t')$. Lets calculate the term involving the generators of the dynamics, i.e.

$$\begin{aligned} \left(L_{t'} - L^*_{t'} \right) x^r_{t'} =& 2 \left(\mu_{kl} F^k(\boldsymbol{x}_{t'}, t') \partial_{x^l_{t'}} + D_{kl} \partial_{x^k_{t'}} \partial_{x^l_{t'}} - D_{kl} \left(\partial_{x^k_{t'}} \log(p_{\mathrm{st}}(\boldsymbol{x}_t)) \partial_{x^l_{t'}} \right) x^r_{t'} = \right. \\ =& 2 \left(\mu_{kr} F^k(\boldsymbol{x}_{t'}, t') - D_{kr} \partial_{x^k_{t'}} \log(p_{\mathrm{st}}(\boldsymbol{x}_{t'})) \right) = 2 \nu^r_{\mathrm{st}}(\boldsymbol{x}_{t'}, t)\,, \end{aligned} \tag{7.23}$$

where $\nu^r_{\mathrm{st}}(\boldsymbol{x}_t, t)$, defined in (2.48), is the steady state mean local velocity. Hence, putting equation (7.23) into (7.22) (and renaming some indexes), one obtains that

$$\chi^{ij}(t, t') = (k_B \boldsymbol{T})^{-1}_{js} \sqrt{2D_{sl}}\, \mu^{-1}_{lr} \left(\frac{\mathrm{d}}{\mathrm{d}t'} \langle x^i_t\, x^r_{t'} \rangle - \langle x^i_t\, \nu^r_{t'} \rangle \right). \tag{7.24}$$

Furthermore, one can also note that

$$\begin{aligned}\sqrt{2D_{jk}}\chi^{ik}(t,t') =& \sqrt{2D_{jk}}(k_B\boldsymbol{T})^{-1}_{ks}\sqrt{2D_{sl}}\,\mu^{-1}_{lr}\left(\frac{\mathrm{d}}{\mathrm{d}t'}\langle x^i_t\, x^r_{t'}\rangle - \langle x^i_t\, v^r_{t'}\rangle\right)\\ =& \sqrt{2D_{jk}}\sqrt{2D_{ks}}(k_B\boldsymbol{T})^{-1}_{sl}\,\mu^{-1}_{lr}\left(\frac{\mathrm{d}}{\mathrm{d}t'}\langle x^i_t\, x^r_{t'}\rangle - \langle x^i_t\, v^r_{t'}\rangle\right)\\ =& 2D_{js}D^{-1}_{sr}\left(\frac{\mathrm{d}}{\mathrm{d}t'}\langle x^i_t\, x^r_{t'}\rangle - \langle x^i_t\, v^r_{t'}\rangle\right) =\\ =& 2\left(\frac{\mathrm{d}}{\mathrm{d}t'}\langle x^i_t\, x^j_{t'}\rangle - \langle x^i_t\, v^j_{t'}\rangle\right),\end{aligned} \tag{7.25}$$

where between the first and the second line we used that, if $\boldsymbol{T}$ and its inverse are diagonal (but not proportional to the identity), also $\boldsymbol{D}$ and $\boldsymbol{\mu}$ are diagonal and hence all matrices involved in the previous formula commute. Instead, if $\boldsymbol{T}$ is proportional to the identity, then it trivially commutes with all matrices. Moreover, for the same reason, we have that $\boldsymbol{D}^{-1} = (k_B\boldsymbol{T}\boldsymbol{\mu})^{-1} = k_B\boldsymbol{T}^{-1}\boldsymbol{\mu}^{-1}$, motivating the step between the second and the third line of (7.25). Finally, going back to equation (7.12) and using (7.25) we get

$$\begin{aligned}&\mu_{jk}\int_0^t \mathrm{d}t'\,\mathrm{Cov}\left(x^i_t - x^i_0, F^k(\boldsymbol{x}_{t'},t')\right) + \mu_{ik}\int_0^t \mathrm{d}t'\,\mathrm{Cov}\left(x^j_t - x^j_0, F^k(\boldsymbol{x}_{t'},t')\right) =\\ &= 2\,\mathrm{Cov}(x^i_t - x^i_0\,,\, x^j_t - x^j_0) - \sqrt{2D_{jk}}\int_0^t \mathrm{d}t'\,\chi^{ik}(t,t') - \sqrt{2D_{ik}}\int_0^t \mathrm{d}t'\,\chi^{jk}(t,t') =\\ &= 2\,\mathrm{Cov}(x^i_t - x^i_0\,,\, x^j_t - x^j_0) - 2\Bigg(2\langle x^i_t\, x^j_t\rangle - \langle x^i_t\, x^j_0\rangle - \langle x^j_t\, x^i_0\rangle +\\ &\qquad\qquad - \int_0^t \mathrm{d}t'\,\langle x^i_t\, v^j_{t'}\rangle - \int_0^t \mathrm{d}t'\,\langle x^j_t\, v^i_{t'}\rangle\Bigg) =\\ &= 2\Bigg(\langle x^i_0\, x^j_0\rangle - \langle x^i_t\, x^j_t\rangle + \int_0^t \mathrm{d}t'\,\langle x^i_t\, v^j_{t'}\rangle + \int_0^t \mathrm{d}t'\,\langle x^j_t\, v^i_{t'}\rangle - \langle x^i_t - x^i_0\rangle\langle x^j_t - x^j_0\rangle\Bigg),\end{aligned} \tag{7.26}$$

where we used that

$$\mathrm{Cov}(x^i_t - x^i_0\,,\, x^j_t - x^j_0) = \langle x^i_t\, x^j_t\rangle + \langle x^i_0\, x^j_0\rangle - \langle x^j_t\, x^i_0\rangle - \langle x^i_t\, x^j_0\rangle - \langle x^i_t - x^i_0\rangle\langle x^j_t - x^j_0\rangle\,. \tag{7.27}$$

In addition, we exploit that, in a steady state and with a constant diffusion matrix, $\boldsymbol{x}(t)$ can be decomposed into a deterministic and a random component $\boldsymbol{y}(t)$, the latter having constant average and implying that $\boldsymbol{x}(t) = \boldsymbol{v}t + \boldsymbol{y}(t)$ and $\langle\boldsymbol{x}\rangle_t = \boldsymbol{v}t + \langle\boldsymbol{y}\rangle$. This is indeed a consequence of Galilean invariance applied to the LE [85]. Furthermore, one also has that $\boldsymbol{v} = \langle\boldsymbol{v}_{\mathrm{st}}\rangle$, which is the reason for the latter of being called local mean velocity. By using this decomposition in the last line of (7.26) (except for a factor 2) and by then recollecting all the terms one gets

$$\begin{aligned}&\langle x^i_0\, x^j_0\rangle - \langle x^i_t\, x^j_t\rangle + \int_0^t \mathrm{d}t'\,\langle x^i_t\, v^j_{t'}\rangle + \int_0^t \mathrm{d}t'\,\langle x^j_t\, v^i_{t'}\rangle - \langle x^i_t - x^i_0\rangle\langle x^j_t - x^j_0\rangle =\\ &\qquad = \int_0^t \mathrm{d}t'\,\left(\langle(x^i_t - \langle x^i\rangle_t)\,v^j_{t'}\rangle + \langle(x^j_t - \langle x^j\rangle_t)\,v^i_{t'}\rangle\right)\end{aligned} \tag{7.28}$$

Moreover, for reasons that will be clear soon, the next step consists in evaluating

$$\begin{aligned}\langle x_0^i\, v_0^j\rangle + \langle x_0^j\, v_0^i\rangle =& \mu_{jk}\langle x_0^i\, F_0^k\rangle + \mu_{ik}\langle x_0^j\, F_0^k\rangle + \\ &- \int \mathrm{d}\boldsymbol{x}_0 \left(D_{jk}\partial_{x_0^k} p_{\mathrm{st}}(\boldsymbol{x}_0) x_0^i + D_{ik}\partial_{x_0^k} p_{\mathrm{st}}(\boldsymbol{x}_0) x_0^j\right) = \\ =& \mu_{jk}\langle x_0^i\, F_0^k\rangle + \mu_{ik}\langle x_0^j\, F_0^k\rangle + \int \mathrm{d}\boldsymbol{x}_0 \left(D_{ji}\, p_{\mathrm{st}}(\boldsymbol{x}_0) + D_{ij}\, p_{\mathrm{st}}(\boldsymbol{x}_0)\right) = \\ =& \mu_{jk}\langle x_0^i\, F_0^k\rangle + \mu_{ik}\langle x_0^j\, F_0^i\rangle + 2D_{ij}\,,\end{aligned} \tag{7.29}$$

where we used the definition (2.48) of the local mean velocity while between the second line and the third line we performed an integration by parts and used that the PDF is zero at infinity. In order to evaluate the terms involving the correlations with the forces, one considers the LE (7.4) in incremental form and using the Ito convention, that is

$$x^i(t+dt) = x^i(t) + \mu_{ij} F^j(\boldsymbol{x}_t, t)dt + \sqrt{2D_{ij}}\, d\mathcal{B}^j(t)\,, \tag{7.30}$$

with $\langle d\mathcal{B}^i(t)\rangle = 0$ and $\langle d\mathcal{B}^i(t)\, d\mathcal{B}^j(t)\rangle = \delta_{ij}\, dt$. By multiplying equation (7.30) by itself for two different indexes $\{ij\}$ and taking the average one gets

$$\langle x_{t+dt}^i x_{t+dt}^j\rangle = \langle x_t^i x_t^j\rangle + \mu_{jk}\langle x_t^i F_t^k\rangle dt + \mu_{ik}\langle x_t^j F_t^k\rangle dt + 2D_{ij}dt + o(dt)\,. \tag{7.31}$$

By using the decomposition used above and by noting that

$$\langle x_{t+dt}^i x_{t+dt}^j\rangle = \langle y_{t+dt}^i y_{t+dt}^j\rangle + v^i\langle y^j\rangle(t+dt) + v^j\langle y^i\rangle(t+dt) + v^i v^j t^2 + o(dt), \tag{7.32}$$

where $\langle y_{t+dt}^i\, y_{t+dt}^j\rangle = \langle y_t^i\, y_t^j\rangle$ because $\boldsymbol{y}(t)$ has a constant average and we are in a steady state, one gets from (7.31)

$$v^i\langle y^j\rangle dt + v^j\langle y^i\rangle dt = \mu_{jk}\langle x_t^i F_t^k\rangle dt + \mu_{ik}\langle x_t^j F_t^k\rangle dt + 2D_{ij}dt\,. \tag{7.33}$$

This finally implies that

$$\mu_{jk}\langle x_t^i F_t^k\rangle + \mu_{ik}\langle x_t^j F_t^k\rangle = v^i\langle y^j\rangle + v^j\langle y^i\rangle - 2D_{ij} \tag{7.34}$$

and hence (7.29) leads to

$$\langle x_0^i\, v_0^j\rangle + \langle x_0^j\, v_0^i\rangle = v^i\langle y^j\rangle + v^i\langle y^j\rangle\,. \tag{7.35}$$

The final step consist in noting that the correlations in the last line of equation (7.28) involve only quantities whose average is constant, which implies that these correlations are homogeneous in time. As a consequence, and by performing a change of variables, the right hand side of equation (7.28) becomes

$$\begin{aligned}&\int_0^t \mathrm{d}t' \left(\langle (x_{t'}^i - \langle x^i\rangle_{t'})\, v_0^j\rangle + \langle (x_{t'}^j - \langle x^j\rangle_{t'})\, v_0^i\rangle\right) = \\ &\qquad = \int_0^t \mathrm{d}t' \int_0^{t'} \mathrm{d}t'' \left(\langle (\dot{x}_{t''}^i - \langle \dot{x}^i\rangle_{t''})\, v_0^j\rangle + \langle (\dot{x}_{t''}^j - \langle \dot{x}^j\rangle_{t''})\, v_0^i\rangle\right) + \\ &\qquad\quad + \int_0^t \mathrm{d}t' \left(\langle (x_0^i - \langle x^i\rangle_0)\, v_0^j\rangle + \langle (x_{t'}^j - \langle x^j\rangle_{t'})\, v_0^i\rangle\right) = \\ &\qquad = \int_0^t \mathrm{d}t' \int_0^{t'} \mathrm{d}t'' \left(\mathrm{Cov}(\dot{x}_{t'}^i, v_0^j) + \mathrm{Cov}(\dot{x}_{t'}^j, v_0^i)\right)\end{aligned} \tag{7.36}$$

where between the first and the second line we added and subtracted $\int_0^t \mathrm{d}t' \langle (x_0^i - \langle x^i \rangle_0) v_0^j \rangle$ (same thing for switched indexes $\{ij\}$) and then noted that $x^i(t) - x^i(t) = \int_0^t \mathrm{d}t'\, \dot{x}^i(t')$. Instead, to get the final line from the previous one we use (7.35) along with the fact that, at time $t = 0$, it holds that $\langle \boldsymbol{x} \rangle_0 = \langle \boldsymbol{y} \rangle$. Finally, by plugging (7.36) into (7.26) and (7.7) afterwards, one gets

$$\mathrm{Cov}(x_t^i - x_0^i,\, x_t^j - x_0^j) + \mu_{il}\,\mu_{jk} \int_0^t \mathrm{d}t' \int_0^t \mathrm{d}t''\, \mathrm{Cov}\Big(F^l(\boldsymbol{x}_{t'}, t'),\, F^k(\boldsymbol{x}_{t''}, t'')\Big) = \\ = 2D_{ij}\,t + 4\mathcal{V}_{ij}(t) \tag{7.37}$$

where

$$\mathcal{V}_{ij}(t) = \frac{1}{2} \int_0^t \mathrm{d}t' \int_0^{t'} \mathrm{d}t''\, \Big(\mathrm{Cov}(\dot{x}_{t''}^i, v_0^j) + \mathrm{Cov}(\dot{x}_{t''}^j, v_0^i) \Big)\,. \tag{7.38}$$

is the multidimensional (integrated) version of the *violation factor* presented in [36], quantifying the amount of violation of the equilibrium fluctuation dissipation theorem. Indeed, the latter is of course equal to zero at equilibrium, where the probability current and the mean local velocity as a consequence are equal to zero.

7.3 Markovian variance sum rule: discussion and applications

The Markovian VSR

$$\mathrm{Cov}(\boldsymbol{x}_t - \boldsymbol{x}_0,\, \boldsymbol{x}_t - \boldsymbol{x}_0) + \int_0^t \mathrm{d}t' \int_0^t \mathrm{d}t''\, \mathrm{Cov}(\boldsymbol{\mu F}(\boldsymbol{x}_{t'}, t'),\, \boldsymbol{\mu F}(\boldsymbol{x}_{t''}, t'')) = 2\boldsymbol{D}\,t + 4\boldsymbol{\mathcal{V}}(t) \tag{7.39}$$

is a novel result relating the covariance of the relative displacement and the covariance of the integrated force (multiplied by the mobility Matrix). Its functional form depends on the presence (or absence) of the integrated violation factor $\boldsymbol{\mathcal{V}}(t)$, which is zero at equilibrium. For this reason, we divide this section in two distinct parts, hence discussing equilibrium or non-equilibrium regimes separately.

7.3.1 Equilibrium

As it is known from the literature, an equilibrium condition for a colloidal bead is reached when a static confining potential is applied to the bead and enough time has passed for the system to relax to equilibrium. If the trapping is due to optical tweezers, one can actually measure the forces acting on the particle as well as its position (the latter can be reconstructed from the forces by knowing the functional form of the trapping potential). As a consequence, one is also able to compute the terms involving the covariances in (7.39) and hence, the equilibrium VSR

$$\mathrm{Cov}(x_t^i - x_0^i,\, x_t^j - x_0^j) + \mu_{ik}\,\mu_{jl} \int_0^t \mathrm{d}t' \int_0^t \mathrm{d}t''\, \mathrm{Cov}(F^k(\boldsymbol{x}_{t'}),\, F^l(\boldsymbol{x}_{t''})) = 2k_B\,T_{ik}\,\mu_{kj}\,t\,, \tag{7.40}$$

where we used that $D_{ij} = T_{ik}\,\mu_{kj}$, leads to a set of time dependent equations with unknown variables given by the components of the mobility matrix and the temperatures. An example of such kind of dynamics can be found in Figure 7.1, row

(a), where the temporal evolution of the VSR and of the quantities involved in it are depicted for a Brownian gyrator, discussed in Section 6.2, with equal temperatures ($T_1 = T_2$, hence corresponding to equilibrium). Moreover, because the VSR (7.40) produces a different relation for each data point (given by the covariances) at every sampling time, one can robustly fit the unknown parameters by evaluating the behaviour of the covariances on a time window including many different time scales during which the variances evolve (from $t \approx 10^{-4}$ to $t \approx 10^{-1}$ for the experiments we are going to consider). Note that this cannot be done by naively taking the average of the integrated Langevin equation because, at equilibrium, the averages are constant in time and the computed quantities are hence static. Furthermore, additional information about the mobility tensor and the temperatures is contained in the noise amplitude and it is clear that the study of variances can also make use of this information. At this stage of the project, we still have not applied this method to multidimensional systems, but we are positive to say that it can be regarded as a valuable technique to estimate physical parameters in a robust way. Indeed, we already obtained very good results by applying this method to unidimensional systems such as the simple case of a Brownian particle trapped in a parabolic potential $U(x_t) = \kappa x_t^2/2$, where κ is the stiffness of the trap. In this setup, one has that the (measured) force $f(x_t)$ acting on the particle is equal to $f(x_t) = -\partial_{x_t} U(x_t) = -\kappa x_t$, which enables to rewrite the equilibrium VSR as

$$\frac{\gamma}{\kappa^2}\mathrm{Var}(f(x_t) - f(x_0)) + \frac{1}{\gamma}\int_0^t \mathrm{d}t' \int_0^t \mathrm{d}t'' \,\mathrm{Cov}(f(x_{t'}), f(x_{t''})) = 2k_B T t\,, \qquad (7.41)$$

where we used that, for such a system, $\gamma = \mu^{-1}$. We point out that, the trap stiffness, as well as the friction coefficient γ, are parameters not known a priori and must be estimated in some way. Indeed, because the forces $f(x_t)$ are experimentally accessible, one can compute the variances (and covariances) involving these forces and fit the best parameters γ and κ such that the VSR (7.41) is optimally satisfied. The results of this procedure (for two beads and four traces for each bead) are displayed in Figure 7.2 where, after the fitting procedure has been performed, we have plotted the left hand side (coloured lines) and right hand side (black dashed line) of (7.41) for the estimated optimal parameters. The latter are in very good agreement with the values obtained by means of another established method for the estimation of γ and κ, based on the analysis of the particle's power spectrum [125, 129]. Of course, one could also estimate the trap stiffness with the latter method and use (7.40) to estimate γ (or, in a multidimensional setting, the mobility tensor).

The method we just showed can hence be useful to estimate physically relevant model parameters but, as a matter of fact, there already exist other techniques that can be used to achieve the same scope. However, our method should be considered as a viable and complementary technique that may be used for the characterisation of diffusive systems modelled by a overdamped Langevin equation.

7.3.2 Non-equilibrium

Non-equilibrium regimes are known to be more difficult to deal with if compared to equilibrium conditions and the VSR makes no exception. Indeed, the integrated violation factor $\mathcal{V}(t)$ appearing on the right hand side of (7.39) involves correlations

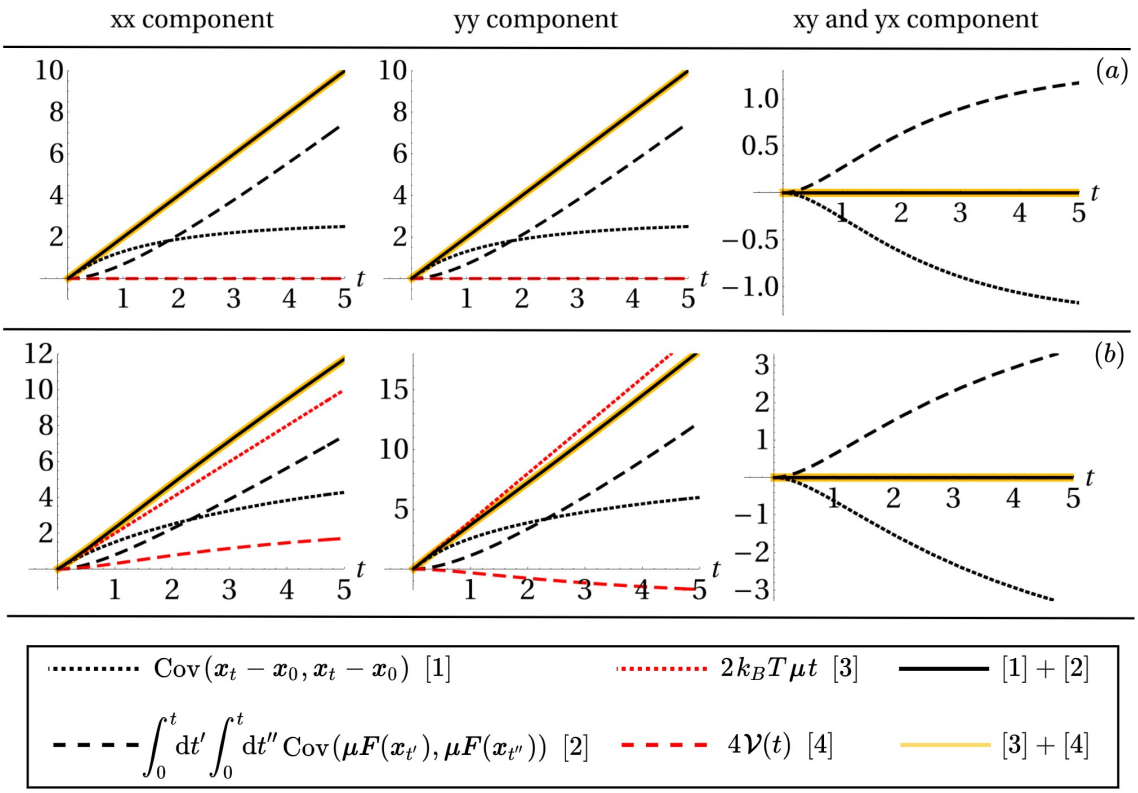

Figure 7.1: VSR for the Brownian gyrator presented in Section 6.2. The first row (a) has parameters equal to $k_B = \mu_1 = \mu_2 = T_1 = T_2 = \kappa = 1$ and $\alpha = 0.5$ and, because the two temperatures are equal, it corresponds to equilibrium. Indeed, the sum of the right terms on the right hand side of (8.35) (yellow line) scales linearly in time for all components of the sum rule with slope determined by the components of the mobility tensor. Instead, for row (b), we set $k_B = \mu_1 = \mu_2 = T_1 = \kappa = 1$, $T_2 = 2$ and $\alpha = 0.75$, hence corresponding to non equilibrium. Note that, also in this case, both sides of the sum rule are equal to zero for the xy component.

with the local mean velocity, which are often difficult to compute from an experimental point of view. Nevertheless, for the linear systems presented in Section 6.1 and 6.2, we manage to calculate $\mathcal{V}(t)$ and observe that it is finite at all times. Indeed, as one can see from Figure 7.1(b) and Figure 7.3, the finite contribution given by the violation factor modifies the linear relation of the variances observed for the equilibrium setting. This in turn implies that, if a finite deviation from the linear behaviour would be observed, this would imply that the system is in a non-equilibrium state. Indeed, we are planning to apply this method to more complicated system such that of a red blood cell trapped by optical tweezers and whose deviation from the equilibrium sum rule should indicate the presence of activity. Furthermore, because $\mathcal{V}(t)$ is itself a quantity of interest and linked to the amount of violation of the FDT, one can also exploit the VSR to compute this term which, as stated at the beginning of this section, may be difficult to evaluate in other ways. However, because a non-equilibrium (steady) state is generated by an additional force to that coming from the trapping potential, the total force acting on the particle is itself difficult to estimate. We are still working on how this estimation could be done precisely in non-trivial situations and hence we do not mention any further details on this issue.

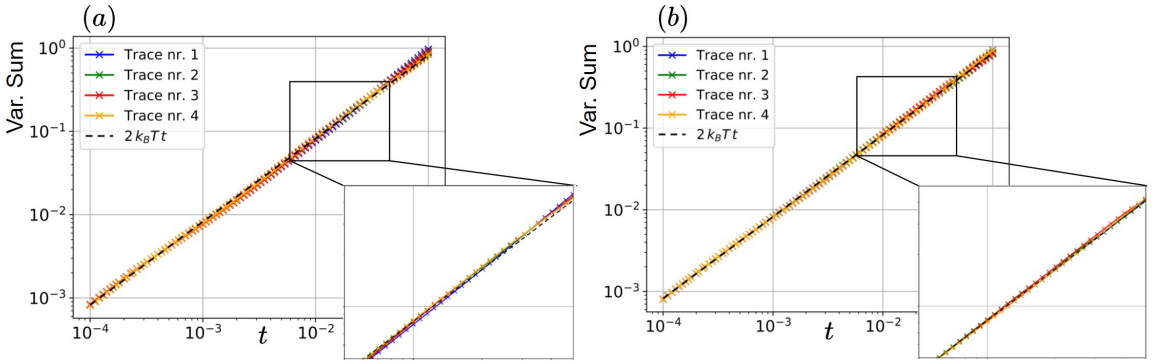

Figure 7.2: VSR for two different beads and four traces for each bead. Coloured lines correspond to the left hand side of equation (7.41) (for the optimal parameters $\widetilde{\gamma}, \widetilde{\kappa}$) while the black dashed lines correspond to its right hand side. By computing the variance of the relative displacement and of the integrated force, one is able to fit the optimal parameters $\widetilde{\gamma}, \widetilde{\kappa}$ such that the VSR is optimally satisfied. For Figure (a) we find:
Trace 1) $\widetilde{\gamma} = (2.85 \pm 5 \cdot 10^{-2}) \cdot 10^{-5}$ pNs and $\widetilde{\kappa} = (6.99 \pm 2 \cdot 10^{-2}) \cdot 10^{-2}$ pN/nm;
Trace 2) $\widetilde{\gamma} = (2.77 \pm 4 \cdot 10^{-2}) \cdot 10^{-5}$ pNs and $\widetilde{\kappa} = (6.94 \pm 3 \cdot 10^{-2}) \cdot 10^{-2}$ pN/nm;
Trace 3) $\widetilde{\gamma} = (2.88 \pm 3 \cdot 10^{-2}) \cdot 10^{-5}$ pNs and $\widetilde{\kappa} = (7.01 \pm 2 \cdot 10^{-2}) \cdot 10^{-2}$ pN/nm;
Trace 4) $\widetilde{\gamma} = (2.77 \pm 4 \cdot 10^{-2}) \cdot 10^{-5}$ pNs and $\widetilde{\kappa} = (6.99 \pm 3 \cdot 10^{-2}) \cdot 10^{-2}$ pN/nm.
For Figure (b), instead, we find that :
Trace 1) $\widetilde{\gamma} = (2.61 \pm 2 \cdot 10^{-2}) \cdot 10^{-5}$ pNs and $\widetilde{\kappa} = (6.91 \pm 3 \cdot 10^{-2}) \cdot 10^{-2}$ pN/nm;
Trace 2) $\widetilde{\gamma} = (2.63 \pm 1 \cdot 10^{-2}) \cdot 10^{-5}$ pNs and $\widetilde{\kappa} = (6.91 \pm 3 \cdot 10^{-2}) \cdot 10^{-2}$ pN/nm;
Trace 3) $\widetilde{\gamma} = (2.63 \pm 4 \cdot 10^{-2}) \cdot 10^{-5}$ pNs and $\widetilde{\kappa} = (6.86 \pm 4 \cdot 10^{-2}) \cdot 10^{-2}$ pN/nm;
Trace 4) $\widetilde{\gamma} = (2.68 \pm 3 \cdot 10^{-2}) \cdot 10^{-5}$ pNs and $\widetilde{\kappa} = (6.95 \pm 3 \cdot 10^{-2}) \cdot 10^{-2}$ pN/nm.
For both cases, the power spectrum method gives values $\gamma = (2.53 \pm 5 \cdot 10^{-2}) \cdot 10^{-5}$ pNs and $\kappa = (7.0 \pm 5 \cdot 10^{-1}) \cdot 10^{-2}$ pN/nm.

As discussed in the introduction to this chapter and as shown in the previous section, the main use of the VSR is to estimate model parameters by exploiting the information contained in the correlation functions defining the variances. To show a possible application of the VSR based method for non-equilibrium steady states, we consider the simple model described in Section 6.3 (see all details there) and whose stochastic evolution for its diffusive variable $x(t)$ corresponds to

$$\dot{x}(t) = \mu\left(-\kappa x(t) + \epsilon\sigma(t)\right) + \sqrt{2k_BT\mu}\,\xi(t)\,, \tag{7.42}$$

while $\sigma(t)$ jumps stochastically between the two states $\{0,1\}$. For this dynamics, an experimental estimation of the total forces is possible. To this end, and because the direct computation of the violation factor is more difficult with respect to the other cases considered as a consequence of the non-Gaussian shape of the PDF, we directly compute $\mathcal{V}(t)$ by means of the VSR and equations (6.49) and (6.50), i.e.

$$\begin{aligned}\mathcal{V}(t) = \mathrm{Var}(x_t - x_0) + \mu^2\mathrm{Var}\Big(\int_0^t \mathrm{d}t'\,F(x_{t'},t')\Big) - 2k_BT\mu t = \\ = \frac{4\epsilon^2 m_{\mathrm{ss}}(1-m_{\mathrm{ss}})}{\kappa(W_{\mathrm{tot}}+\mu\kappa)}\left(1 - \frac{W_{\mathrm{tot}}\mathrm{e}^{-\mu\kappa t}}{W_{\mathrm{tot}}-\mu\kappa} + \frac{\mu\kappa\mathrm{e}^{-W_{\mathrm{tot}}t}}{W_{\mathrm{tot}}-\mu\kappa}\right).\end{aligned} \tag{7.43}$$

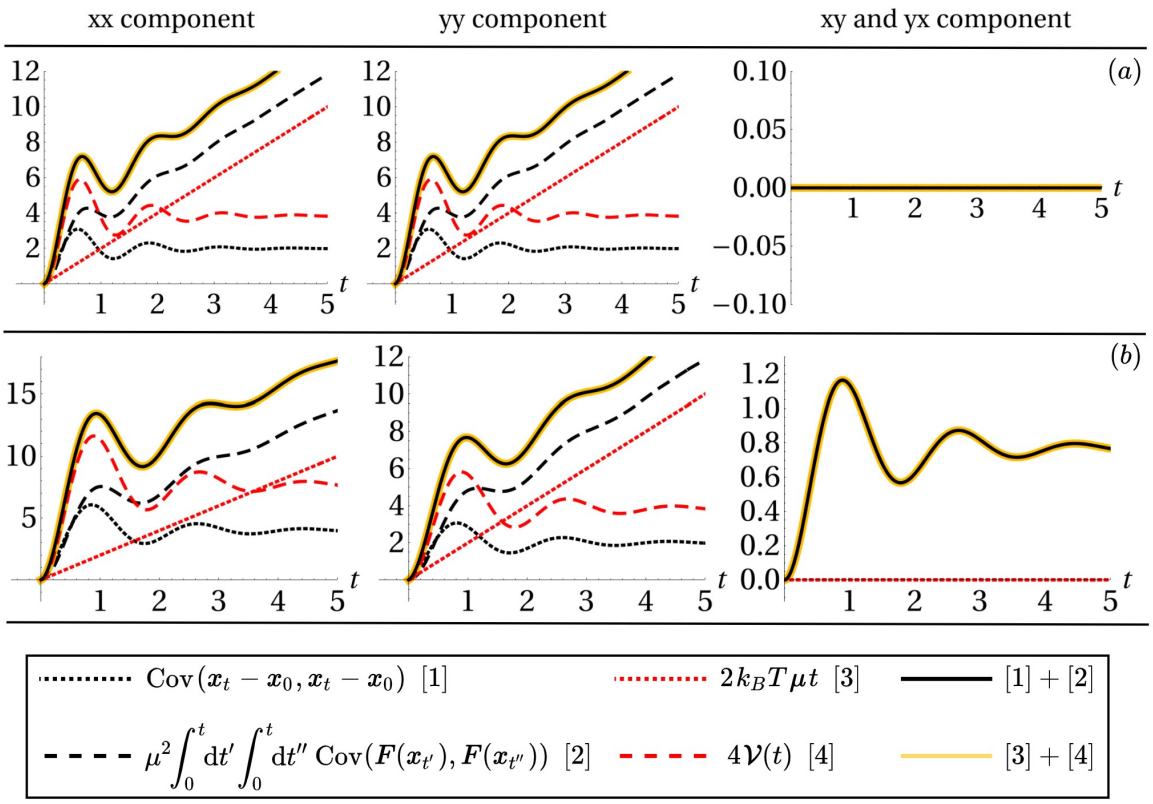

Figure 7.3: VSR for the case of a parabolic potential in a non-conservative force field depicted in Section 6.1. Row (a) corresponds to $k_BT = \mu = \kappa = \alpha = 1$ and $\rho = 4$. Because $\alpha = 1$, the xy component of the VSR is equal to zero at all times. Instead, in row (b), we consider $k_BT = \mu = T = \kappa = 1$, $\alpha = 0.5$ and $\rho = 4$. In this case, the xy component of the VSR has a non trivial behaviour and a finite limit, differently from all the cases considered until now.

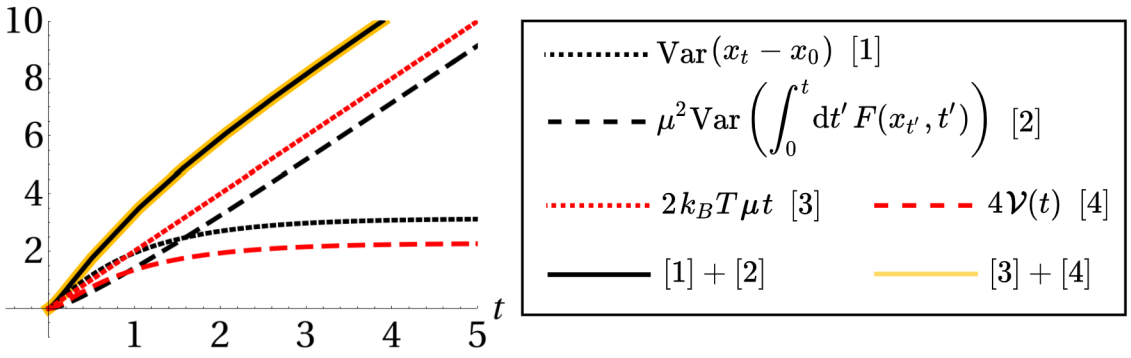

Figure 7.4: VSR for a stochastically switching trap described in section 6.3. Parameters are set to $k_BT = \mu = \kappa = 1$, $\epsilon = 5$, $m_{ss} = 1/2$ and $W_{tot} = 10$. Note that the integrated violation factor $\mathcal{V}(t)$ increases monotonically and reaches a finite value for large times.

The temporal evolution of all quantities shown above has been computed analytically and is depicted in Figure 7.4. In order to test the VSR based estimation method, we consider two time traces of a bead trapped in an harmonic poten-

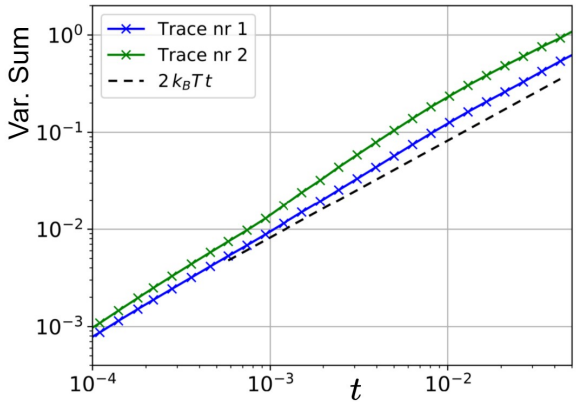

Figure 7.5: VSR based method for time traces of colloidal beads trapped in a stochastically jumping harmonic potential and modelled by equation (7.42). Coloured lines correspond to $\mathrm{Var}(x_t - x_0)/\mu + \mu\mathrm{Var}\left(\int_0^t \mathrm{d}t'\, F(x_{t'}, t')\right)$, i.e. the sum of the variances except for a factor μ^{-1}.
Trace nr. 1 is generated by using $\Delta\lambda = 200$nm and $W_{\mathrm{tot}} = 6$Hz and the VSR predicts $\widetilde{\Delta\lambda} = (193 \pm 9)$nm and $W_{\mathrm{tot}} = (5.7 \pm 0.4)$Hz.
Instead, Trace nr. 2 is generated by using $\Delta\lambda = 270$nm and $W_{\mathrm{tot}} = 10$Hz and the VSR predicts $\widetilde{\Delta\lambda} = (268 \pm 14)$nm and $W_{\mathrm{tot}} = (10.2 \pm 0.5)$Hz.

tial, generated by optical tweezers, whose center randomly jumps between two positions $\{0, \Delta\lambda\}$ ($\Delta\lambda = \epsilon/\kappa$) with exponentially distributed waiting times. Also, the two jumping rates are taken equal, i.e. $W_+ = W_- = W_{tot}/2$, implying that $m_{ss} = W_+/W_{tot} = 1/2$. Because the stochastic protocol $\sigma(t)$ is known a priori, one is able to recunstruct the total forces acting on the bead and, as a consequence, one is also able to calculate all the variances appearing in the VSR. Indeed, from an equilibrium estimate of $\gamma = \mu^{-1}$ and κ, which can be performed for example by means of our method, one is also able to compute the variance of the position (remember that $x_t = -f^{\mathrm{opt}}(x_t, t)/\kappa + \Delta\lambda\,\sigma_t$, where the force exerted by the optical tweezers $f^{\mathrm{opt}}(x_t, t)$ and σ_t are experimentally accessible) which in turn implies that an experimental estimate of the $\mathcal{V}(t)$ from the left hand side of (7.43) is possible. By fitting the latter with the right hand side of the (7.43) and with free parameters $\widetilde{\epsilon}$ and $\widetilde{W}_{\mathrm{tot}}$, one is able to find an estimate for these parameters. By comparing the results of this estimation with the real values ϵ and W_{tot} used in the experimental setup, one is able to test the performances of our method applied to real experimental data. The extracted parameters are in very good agreement with the experimentally used values ϵ and W_{tot} and the results of this estimation procedure can be found in Figure 7.5.

Further applications of this VSR based method in a non-equilibrium steady state, such as the case of a living red blood cell trapped by optical tweezers, will be presented in future papers.

7.3.2.1 Link to entropy production

Because the direct estimation of the probabilities is difficult in general, statistical physicists usually try to overcome this problem by finding alternative ways to esti-

mate relevant quantities characterising the dynamics (or equilibrium) of the system under examination. This would be the case, for example, for entropy production whose magnitude is directly related to the distance from equilibrium and to the amount of time-symmetry breaking. As we showed in Chapter 5, the TUR can be used to estimate a lower bound to the entropy production rate by measuring averages and variances of experimentally accessible observables. Furthermore, recent works [130, 131] have shown how the finite time generalisation of the TUR can be used to efficiently infer the entropy production rate by performing short time experiments and without needing the knowledge of the whole path PDF. In this sections, we present a novel formula for the entropy production, based on the VSR, which can be used to estimate the entropy production rate by means of short times experiments as well.

As discussed in the previous section, the non-equilibrium VSR is characterised by the presence of the integrated violation factor $\boldsymbol{\mathcal{V}}(t)$. In [36], the authors show that its one dimensional version is tightly linked to entropy production and, in a similar fashion, we are going to exploit this link in order to express the stationary entropy production rate as a function of the covariances appearing in the VSR. To do so, we consider the latter in component notation, that is

$$\begin{aligned} &\mathrm{Cov}(x_t^i - x_0^i,\, x_t^j - x_0^j) + \\ &+2\mu_{il}\,\mu_{jk}\int_0^t \mathrm{d}t' \int_0^{t'} \mathrm{d}t''\, \mathrm{Cov}\Big(F^l(\boldsymbol{x}_{t''}, t''),\, F^k(\boldsymbol{x}_0, 0)\Big) = 2D_{ij}\,t + 4\mathcal{V}_{ij}(t)\,, \end{aligned} \tag{7.44}$$

where, for reasons of symmetry, it holds that

$$\begin{aligned} \mu_{il}\,\mu_{jk}\int_0^t \mathrm{d}t' \int_0^t \mathrm{d}t''\, \mathrm{Cov}\Big(F^l(\boldsymbol{x}_{t'}, t'),\, F^k(\boldsymbol{x}_{t''}, t'')\Big) = \\ = 2\mu_{il}\,\mu_{jk}\int_0^t \mathrm{d}t' \int_0^{t'} \mathrm{d}t''\, \mathrm{Cov}\Big(F^l(\boldsymbol{x}_{t''}, t''),\, F^k(\boldsymbol{x}_0, 0)\Big)\,. \end{aligned} \tag{7.45}$$

By taking the second time derivative of (7.44) and by evaluating the result for $t = 0$, one readily gets that

$$\partial_t^2 \mathrm{Cov}(x_t^i - x_0^i,\, x_t^j - x_0^j)|_{t=0} + 2\mu_{il}\,\mu_{jk}\mathrm{Cov}\Big(F^l(\boldsymbol{x}_0, 0),\, F^k(\boldsymbol{x}_0, 0)\Big) = 4\partial_t^2 \mathcal{V}_{ij}(t)|_{t=0}\,, \tag{7.46}$$

where the last term can be evaluated from (7.38), that is

$$\begin{aligned} \partial_t^2 \mathcal{V}_{ij}(t) &= \Big(\mathrm{Cov}(\dot{x}_0^i, v_0^j) + \mathrm{Cov}(\dot{x}_0^j, v_0^i)\Big)/2 = \\ &= \Big(\mathrm{Cov}(v_0^i, v_0^j) + \mathrm{Cov}(v_0^j, v_0^i)\Big)/2 = \langle v_0^i v_0^j\rangle - v_{\mathrm{d}}^i v_{\mathrm{d}}^j\,, \end{aligned} \tag{7.47}$$

where we used that $\langle \dot{x}_0^i\rangle = \langle v_0^i\rangle = v_{\mathrm{d}}^i$ (with v_{d} the mean drift velocity) and that, as shown in [42] and for a generic $g(\boldsymbol{x}_t)$, it holds that $\langle g(\boldsymbol{x}_t)\dot{\boldsymbol{x}}_t\rangle = \langle g(\boldsymbol{x}_t)\boldsymbol{v}(\boldsymbol{x}_t)\rangle$. Hence, equation (7.47) enables us to rewrite (7.46) as

$$\langle v_0^i v_0^j\rangle = v_{\mathrm{d}}^i v_{\mathrm{d}}^j + \frac{1}{4}\partial_t^2 \mathrm{Cov}(x_t^i - x_0^i,\, x_t^j - x_0^j)|_{t=0} + \frac{1}{2}\mu_{il}\,\mu_{jk}\mathrm{Cov}\Big(F^l(\boldsymbol{x}_0, 0),\, F^k(\boldsymbol{x}_0, 0)\Big)\,. \tag{7.48}$$

By multiplying both sides of this equation by D^{-1}_{ij} and by summing over these indexes (summation signs are omitted and Einstein's notation is understood) one gets

$$\langle \nu^i_0 D^{-1}_{ij} \nu^j_0 \rangle = v^i_{\rm d} D^{-1}_{ij} v^j_{\rm d} + \frac{1}{4} D^{-1}_{ij} \partial^2_t \mathrm{Cov}(x^i_t - x^i_0, x^j_t - x^j_0)|_{t=0} + \\ + \frac{1}{2} D^{-1}_{ij} \mu_{il} \mu_{jk} \mathrm{Cov}\Big(F^l(\boldsymbol{x}_0, 0), F^k(\boldsymbol{x}_0, 0)\Big) . \tag{7.49}$$

The matrix multiplication in front of the covariance matrix can be readily evaluated by exploiting that, as discussed in the derivation of the Markovian VSR in Section 7.2, $D^{-1}_{ij} = (\boldsymbol{T}\boldsymbol{\mu})^{-1}_{ij} = T^{-1}_{ik} \mu^{-1}_{kj} = \mu^{-1}_{ik} T^{-1}_{kj}$ (because if $\boldsymbol{T}$ is diagonal and not proportional to the identity, then also $\boldsymbol{\mu}$ and as a consequence $\boldsymbol{D}$ are diagonal) and hence

$$\mathcal{M}_{lk} = D^{-1}_{ij} \mu_{il} \mu_{jk} = T^{-1}_{ir} \mu^{-1}_{rj} \mu_{jk} \mu_{il} = T^{-1}_{ki} \mu_{il} , \tag{7.50}$$

where we introduced the matrix $\mathcal{M}$ and used that, of course, $\boldsymbol{T}$ is symmetric. Furthermore, by noting that the left hand side of (7.49) can be identified with the total entropy production rate by means of equation (2.52), one finally gets from (7.49)

$$\sigma_{\rm tot} = \frac{1}{2} \boldsymbol{v}^T_{\rm d} \boldsymbol{D}^{-1} \boldsymbol{v}_{\rm d} + \frac{1}{4} \partial^2_t \langle (\boldsymbol{x}_t - \boldsymbol{x}_0)^T \boldsymbol{D}^{-1} (\boldsymbol{x}_t - \boldsymbol{x}_0) \rangle|_{t=0} + \\ + \frac{1}{2} \left\langle (\boldsymbol{F}(\boldsymbol{x}_0, 0) - \langle \boldsymbol{F}(\boldsymbol{x}_0, 0) \rangle)^T \boldsymbol{\mathcal{M}} (\boldsymbol{F}(\boldsymbol{x}_0, 0) - \langle \boldsymbol{F}(\boldsymbol{x}_0, 0) \rangle) \right\rangle , \tag{7.51}$$

where we used that

$$\partial^2_t \mathrm{Cov}(x^i_t - x^i_0, x^j_t - x^j_0)|_{t=0} = \partial^2_t \langle (x^i_t - x^i_0)(x^j_t - x^j_0) \rangle - 2 v^i_{\rm d} v^j_{\rm d} \tag{7.52}$$

because $\langle x^i_t - x^i_0 \rangle = v^i_{\rm d} t$.

Equation (7.51) is a new formula for the average entropy production rate, involving the (variances of the) position of the particle and the total force acting on it. Position and force are also needed for the usual direct estimation of the average entropy production rate in a steady state by means of the generalisation of equation (2.55) to more heat baths at different temperatures, i.e.

$$\sigma_{\rm tot} = \langle \Sigma_{\rm env} \rangle_t / t = \sum_i \frac{\langle \Delta Q_i \rangle_t}{t \, k_B T_i} = k_B^{-1} \int_0^t \mathrm{d}t' \, \langle (\boldsymbol{T}^{-1} \boldsymbol{F})^{\rm T} \circ \dot{\boldsymbol{x}} \rangle_{t'} / t , \tag{7.53}$$

where ΔQ_i is the amount of heat exchanged with the thermal bath at temperature $T_i = (\boldsymbol{T})_{ii}$. The need to apply the Stratonovich prescription (2.45) for the estimation of the stochastic integral above requires a sufficiently fast sampling rate with respect to the rate of variation of force. This requirement seems less strict for (7.51), it is expected to work as long as the second derivative in time is evaluated correctly thanks to a diffusive behaviour of the position. Anther appealing feature of (7.51) is that other quantities are instantaneous correlations and thus can be evaluated correctly at any experimental sampling rate.

For a quick comparison of the performances of (7.51) vs the classic formula (7.53) in correctly estimating the entropy production rate, we consider time traces of position and forces from the gyrator model described in Section 6.1 and described by

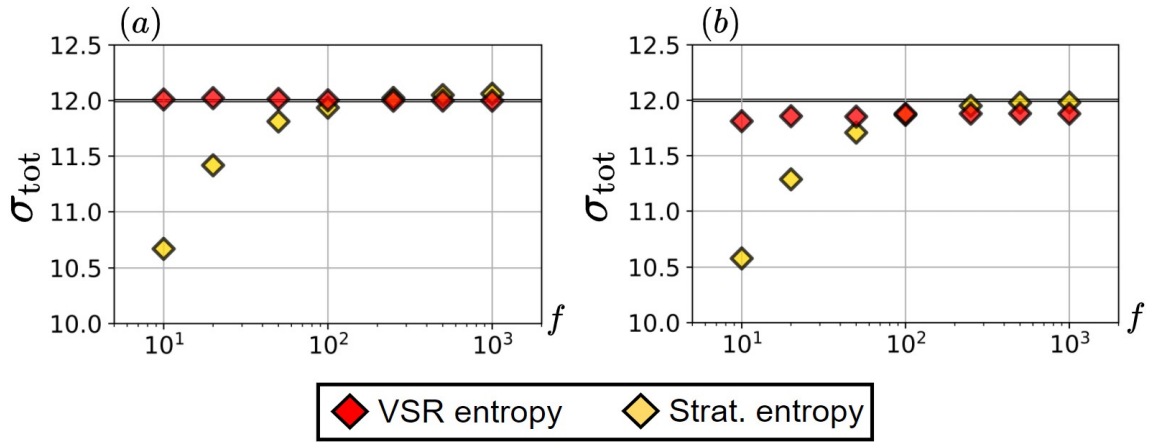

Figure 7.6: Estimate of the entropy production rate for the model described in 6.1 with two equations: the VSR method (7.51) and the estimation procedure based on the Stratonovich integral (7.53). Results are as a function of the sampling frequency. We generate 1000 trajectories and parameters are set to $\mu = \kappa = 1$ and $\alpha = \rho = 2$, implying an exact entropy production rate $\sigma_{tot} = 12$ (black lines). Panel (a) is for $k_B T = 1$ while panel (b) corresponds to $k_B T = 4$. One sees that, in both cases, our VSR method is more stable and estimates entropy production in a more precise way especially for low sampling frequencies.

the set of coupled Langevin equations

$$\begin{cases} \dot{x}(t) = -\alpha\mu\kappa x(t) - \mu\rho y(t) + \sqrt{2k_B T\mu}\,\xi^x(t) \\ \dot{y}(t) = -\mu\kappa y(t) + \alpha\mu\rho x(t) + \sqrt{2k_B T\mu}\,\xi^y(t) \end{cases} \tag{7.54}$$

with stationary entropy production rate equal to

$$\sigma_{\rm tot} = \frac{\mu\rho^2(1+\alpha)}{\kappa}\,. \tag{7.55}$$

We generate traces on a time interval $[0,4]$ with numerical integration time step $dt = 10^{-3}$. We then calculate the entropy production rate using our formula (7.51), and (7.53). To test the performances of these two methods as a function of the sampling frequency, we analyse results for subsets including a fraction $\varphi = 1/2$, $1/4, 1/10$, $1/20, 1/50$, $1/100$ of the available data by keeping one sample every $1/\varphi$ ones. The last step is equivalent to an empirical sampling frequency equal to $f = \varphi/dt$. From the results depicted in Figure 7.6 one sees that the new method (7.51) shows better performances when the sampling frequency is small and, furthermore, it is much more stable. Hence, the new way of estimating entropy production could work for a slow apparatus that would not sample fast enough for the standard computation of a Stratonovich integral. As the sampling frequency increases, the performances of the two methods become comparable. Further applications of this procedure will be presented in future papers.

7.4 Chapter conclusions

To sum up, in this chapter we presented a novel formula, which we term the variance sum rule (VSR), that can be useful for the characterisation of equilibrium and non-equilibrium Langevin systems. As opposite to the uncertainty relations discussed in Chapter 5, the VSR is an equality and hence it can be used for precise estimation of relevant model parameters. Indeed, for a bead in an harmonic potential at equilibrium and in a stochastically jumping trap, we tested our method by estimating some model parameters whose true value is known a priori and found a very good agreement between the estimated values an the real ones. This adds further evidence that the variance of stochastic motion can be exploited for measuring physical quantities. Furthermore, we also showed that the small time limit of the VSR leads to a novel formula for the entropy production rate (7.51) which is more stable and accurate (especially for low sampling frequency) with respect to the textbook estimation approach based on the definition of the entropy production in terms of a Stratonovich integral (see Figure 7.6). In the next chapter, we will show how a similar VSR holds for equilibrium non-Markovian systems , governed by an overdamped generalised Langevin equation (GLE), which again may be used for the estimation of relevant quantities, such as the parameters defining the memory kernel $\Gamma(t)$ appearing in the GLE.

CHAPTER 8

NON-MARKOVIAN VARIANCE SUM RULE

8.1 Introduction

In this chapter we introduce an equivalent of the variance sum rule (VSR) (7.2) for a system with memory. Specifically, we consider the non-Markovian equilibrium Langevin dynamics of N Brownian identical particles in one dimension, trapped by an external potential $U(x_t)$ and subject to a pairwise interaction force $f(x_t^n, x_t^m) = -f(x_t^m, x_t^n)$, that is

$$\int_{-\infty}^{t} \mathrm{d}t' \Gamma(t-t')\dot{x}_{t'}^n = -\partial_{x_t^n} U\left(x_t^n\right) + \sum_{m\neq n} f(x_t^n, x_t^m) + \eta^n(t). \tag{8.1}$$

with $n, m \in \{1, \ldots, N\}$. By defining the center of mass variable $x(t) = \sum_n x^n(t)/N$, we will show that the non-Markovian VSR reads

$$\begin{aligned} &\int_0^t \mathrm{d}t' \, \Gamma(t-t') \int_0^{t'} \mathrm{d}t'' \, \Gamma(t'-t'') \mathrm{Var}\left(x_{t''} - x_0\right) + \\ &\quad + \int_0^t \mathrm{d}t' \int_0^t \mathrm{d}t'' \, \mathrm{Cov}(F(\{x_{t'}^n\}), F(\{x_{t''}^n\})) = 2\, k_B T \int_0^t \mathrm{d}t' \int_0^{t'} \mathrm{d}t'' \, \Gamma(t'') \end{aligned} \tag{8.2}$$

where

$$F(\{x_t^n\}) = -\frac{1}{N} \sum_n \partial_{x_t^n} U\left(x_t^n\right) \tag{8.3}$$

can be regarded as the "average" external force exerted on each Brownian particle. We point out that, in equilibrium, the variances of the relative displacement and the covariance of the forces are experimentally accessible quantities making it possible, as we will show in Section 8.3, to extract the functional form of the memory kernel from experimental data. We also add that a very similar relation to (8.2) can be found for an external potential being dragged at a constant speed, i.e $U(x_t, t) = U(x_t - vt)$. Indeed, for the same reasons discussed in 3.7.2.1, this constant dragging leads to a non-equilibrium steady state that can be mapped to an equivalent equilibrium dynamics by means of a Galilean transformation, which in turn helps in obtaining the VSR in this stationary regime. In this context, by identifying the double integral of the covariance of the average forces with the variance of the thermodynamic work, it will be also straightforward to obtain the upper bound to the Fano factor of the thermodynamic work,

$$\frac{\langle \Delta W^2 \rangle_T^{\mathrm{st}}}{\langle W \rangle_t^{\mathrm{st}}} \leq 2\, k_B\, T\,. \tag{8.4}$$

Note that this inequality is opposite to the TUR which, instead, gives a lower bound to the Fano factor of the entropy production. Indeed, we will also show how the non-Markovian VSR naturally leads to a *reversed thermodynamic uncertainty relation* (RTUR) for the thermodynamic work. These inequalities will be presented in more detail in Section 8.3.1 while the derivation of the non-Markovian VSR can be found in Section 8.2. Its consequences and applications, instead, are depicted in Section 8.3.

8.2 Non-Markovian variance sum rule: derivation

We start from the set of overdamped Generalised Langevin equations

$$\int_{-\infty}^{t} \mathrm{d}t'\, \Gamma(t-t')\dot{x}^n_{t'} = -\partial_{x^n_t} U\left(x^n_t - vt\right) + \sum_{m\neq n} f(x^n_t, x^m_t) + \eta^n(t) \tag{8.5}$$

describing a system of N Brownian particles in one dimension, subject to a confining potential $U(x_t, t)$ and interacting through a pairwise force such that $f(x^n_t, x^m_t) = -f(x^n_t, x^m_t)$. The latter could be central forces arising from an interaction potential $U^{\mathrm{int}}(|x^n_t - x^m_t|)$, i.e such that

$$f(x^n_t, x^m_t) = -\partial_{x^n_t} U^{\mathrm{int}}(|x^n_t - x^m_t|) = \partial_{x^m_t} U^{\mathrm{int}}(|x^n_t - x^m_t|) = -f(x^m_t, x^n_t)\,. \tag{8.6}$$

Moreover, we have that $\langle \eta^n(t)\rangle = 0$ and $\langle \eta^n(t')\eta^m(t'')\rangle = \delta_{nm}\, k_B T\, \Gamma(|t'-t''|)$. Note that we already included the velocity term inside the potential. Indeed, once the non-Markovian VSR will be derived for the steady state determined by $v \neq 0$, the equilibrium relation will be readily obtained for $v = 0$.

In order to prove the VSR, we integrate and sum over n both sides of (8.1)

$$\begin{aligned}\sum_n \int_0^t \mathrm{d}t' \int_{-\infty}^{t'} \mathrm{d}t''\, \Gamma(t'-t'')\dot{x}^i(t'') = \\ = -\sum_n \int_0^t \mathrm{d}t'\, \partial_{x^n_t} U\left(x^n_{t'} - vt'\right) + \sum_{n,\, m\neq n} \int_0^t \mathrm{d}t' f(x^n_{t'}, x^m_{t''}) + \sum_n \int_0^t \mathrm{d}t'\, \eta^n(t')\end{aligned} \tag{8.7}$$

and, by further doing a change of variables on the left hand side of (8.7) and noting that $\sum_{n,\, m\neq n} f(x^n_{t'}, x^m_{t'}) = 0$, we get that

$$\int_0^t \mathrm{d}t' \int_0^\infty \mathrm{d}t''\, \Gamma(t'')\dot{x}(t'-t'') = -\frac{1}{N}\sum_n \int_0^t \mathrm{d}t'\, \partial_{x^n} U\left(x^n_{t'} - vt'\right) + \int_0^t \mathrm{d}t' \eta(t')\,. \tag{8.8}$$

where we defined $x(t) = \sum_n x^n(t)/N$ and $\eta(t) = \sum_n \eta^n(t)/N$. The latter is a sum of independent Gaussian noises whose mean and variance are equal to the sum of all mean and variances, respectively, characterising $\eta^n(t)$ for each index n. This fact, together with the $1/N$ normalisation factor, implies that with $\langle \eta(t)\rangle = 0$ and $\langle \eta(t')\eta(t'')\rangle = k_B T \Gamma(|t'-t''|)$. For a steady state, we have that a change of variable $y^n(t) = x^n(t) - vt$ in (8.1) maps the system into a reference frame where $y(t)$ is an

equilibrium variable, so that $\langle y \rangle_t = const$. With this change of reference frame, and by defining $y(t) = x(t) - vt$, equation (8.8) becomes

$$\begin{aligned}\int_0^t \mathrm{d}t' \, F(\{y^n_{t'}\}) &= \int_0^t \mathrm{d}t' \eta(t') - \int_0^t \mathrm{d}t' \int_0^\infty \mathrm{d}t'' \, \Gamma(t'') \dot{y}(t' - t'') - \widehat{\gamma} \, v \, t = \\ &= \int_0^t \mathrm{d}t' \eta(t') - \int_0^\infty \mathrm{d}t'' \, \Gamma(t'') \left(y(t - t'') - y(-t'') \right) - \widehat{\gamma} \, v \, t \, ,\end{aligned} \tag{8.9}$$

where $\widehat{\gamma} = \int_0^\infty \mathrm{d}t' \, \Gamma(t')$, defined in Chapter 3, and we further defined the "average" external force

$$F(\{y^n_t\}) = \frac{1}{N} \sum_i \int_0^t \mathrm{d}t' \, \partial_{y^n} U \left(y^n_{t'} \right) \, . \tag{8.10}$$

This change of reference allows us to consider equilibrium averages, which are of course easier to handle, and to use the equilibrium FDT, as it will be clear in few lines. We proceed by considering the variance of both sides of (8.9), hence obtaining

$$\begin{aligned}\int_0^t \mathrm{d}t' \int_0^t \mathrm{d}t'' \, \mathrm{Cov}(F(\{y^n_{t'}\}), F(\{y^n_{t''}\})) \; &= \int_0^t \mathrm{d}t' \int_0^t \mathrm{d}t'' \, \langle \eta_{t'} \, \eta_{t''} \rangle + \\ &+ \int_0^\infty \mathrm{d}t' \Gamma(t') \int_0^\infty \mathrm{d}t'' \Gamma(t'') \mathrm{Cov} \left(y_{t-t'} - y_{-t'}, y_{t-t''} - y_{-t''} \right) + \\ &- 2 \int_0^t \mathrm{d}t' \int_0^\infty \mathrm{d}t'' \, \Gamma(t'') \left(\langle y_{t-t''} \, \eta_{t'} \rangle \right) - \langle y_{-t''} \, \eta_{t'} \rangle) = \\ = 2 k_B T \int_0^t \mathrm{d}t' \int_0^{t'} \mathrm{d}t'' \, \Gamma(t'') &+ \\ &+ \int_0^\infty \mathrm{d}t' \Gamma(t') \int_0^\infty \mathrm{d}t'' \, \Gamma(t'') \langle (y_{t-t'} - y_{-t'})(y_{t-t''} - y_{-t''}) \rangle + \\ &- 2 \int_0^t \mathrm{d}t' \int_0^\infty \mathrm{d}t'' \, \Gamma(t'') \left(\langle y_{t-t''} \, \eta_{t'} \rangle \right) - \langle y_{-t''} \, \eta_{t'} \rangle) \, .\end{aligned} \tag{8.11}$$

where we used that $\langle \eta(t) \rangle = \langle y_t - y_{t'} \rangle = 0$. Furthermore, by exploiting that $y(t)$ is an equilibrium variable, which implies that the correlations involving $y(t)$ are homogeneous in time $\langle y_{t'} \, y_{t''} \rangle = \langle y_{t'-t''} \, y_0 \rangle = \langle y_{t''-t'} \, y_0 \rangle = \langle y_{t''} \, y_{t'} \rangle$, we can rewrite (8.11)

$$\int_0^t \mathrm{d}t' \int_0^t \mathrm{d}t'' \, \mathrm{Cov}(F(\{y^n_{t'}\}), F(\{y^n_{t''}\})) + \mathcal{R}(t) - \phi(t) = 2 k_B T \int_0^t \mathrm{d}t' \int_0^{t'} \mathrm{d}t'' \, \Gamma(t'') \tag{8.12}$$

where we defined

$$\phi(t) = 2 \int_0^\infty \mathrm{d}t' \, \Gamma(t') \int_0^\infty \mathrm{d}t'' \, \Gamma(t'') \big(C(t'' - t') - C(t + t'' - t') \big) \tag{8.13}$$

$$\mathcal{R}(t) = 2 \int_0^\infty \mathrm{d}t' \, \Gamma(t') \int_0^t \mathrm{d}s \, \left\langle \left(y_{t-t'} - y_{-t'} \right) \eta_s \right\rangle . \tag{8.14}$$

and $C(t' - t'') = \langle y_{t'} \, y_{t''} \rangle$. Let us focus on (8.14). Because $\eta(t)$ can be regarded as the noise generating the randomness of the equilibrium variable $y(t)$, we can consider the latter as a functional of the noise $\eta(t)$, i.e. $y(\eta_t)$. Again, the Furutsu-Novikov

formula [127, 128] gives us an expression for the correlation of a functional $O(\eta_t)$ of the noise and the noise itself, that is

$$\langle O(\eta_u)\eta_s\rangle = k_B T \int_{-\infty}^{\infty} \mathrm{d}t''\, \Gamma(|s-t''|)\left\langle \frac{\delta O(\eta_u)}{\delta \eta(t'')}\right\rangle . \tag{8.15}$$

From this we see that for $\Gamma(t) = 2\gamma_0\delta(t)$, i.e Markovian dynamics, one recovers (7.11) (except for a factor $2\,k_B T\,\gamma_0$ arising from a different definition of the noise) where the correlation function is equal to 0 for $s > u$. This is not true instead for coloured noise. For an equilibrium scenario [132], even for non Markovian dynamics it holds that

$$\chi_O(u,t'') = \left\langle \frac{\delta O_u(\eta)}{\delta \eta(t'')}\right\rangle = \langle O_u\, \dot{y}_{t''}\rangle\, \theta(u-t'')/k_B T\,, \tag{8.16}$$

where $\chi_O(t,s)$ is the response function associated to the observable O and the Heaviside step function $\theta(t-s)$ is needed to preserve causality. For $O = y$, (8.15) hence specialises to

$$\langle y(\eta_u)\eta_s\rangle = \int_{-\infty}^{\infty} \mathrm{d}t''\, \Gamma(|s-t''|)\langle y_u\, \dot{y}_{t''}\rangle\, \theta(u-t'')\,. \tag{8.17}$$

By dropping the explicit noise dependence for the variable y_t and by looking at (8.14), one sees that the terms to calculate have the form

$$\begin{aligned}\int_0^t \mathrm{d}s\, \langle y_u\, \eta_s\rangle &= \int_{-\infty}^{\infty} \mathrm{d}t'' \int_0^t \mathrm{d}s\, \Gamma(|s-t''|)\langle y_u\, \dot{y}_{t''}\rangle\theta(u-t'') = \\ &= \int_{-\infty}^{\infty} \mathrm{d}t'' \int_0^t \mathrm{d}s\, \Gamma(|t''|)\langle y_u\, \dot{y}_{t''+s}\rangle\theta(u-t''-s) = \\ &= \int_{-\infty}^{\infty} \mathrm{d}t''\, \Gamma(|t''|) \int_0^t \mathrm{d}s\, \partial_s C(u-t''-s)\theta(u-t''-s)\end{aligned} \tag{8.18}$$

where in the second line we performed a change of variables $\widetilde{t}'' = t'' - s$ renaming $\widetilde{t}'' = t''$ afterwards. Moreover, we again used that $C(u-s) = C(u,s) = \langle y_u y_s\rangle$. Moving forward, one sees that (8.18) can we rewritten as

$$\begin{aligned}\int_0^t \mathrm{d}s\, \langle y_u \eta_s\rangle &= \int_{-\infty}^{\infty} \mathrm{d}t''\, \Gamma(|t''|)\theta(u-t'')\theta(t-u+t'') \int_0^{u-t''} \mathrm{d}s\, \partial_s C(u-t''-s) + \\ &\quad + \int_{-\infty}^{\infty} \mathrm{d}t''\, \Gamma(|t''|)\theta(u-t-t'') \int_0^t \mathrm{d}s\, \partial_s C(u-t-t'') = \\ &= \int_{u-t}^{u} \mathrm{d}t''\, \Gamma(|t''|)\big(C(0) - C(u-t'')\big) + \\ &\quad + \int_{-\infty}^{u-t} \mathrm{d}t''\, \Gamma(|t''|)\big(C(u-t''-t) - C(u-t'')\big) = \\ &= \int_{u-t}^{u} \mathrm{d}t''\, \Gamma(|t''|)C(0) + \int_0^{\infty} \mathrm{d}t''\, \Gamma(|t''|)C(u+t''-t) + \\ &\quad - \int_0^{t-u} \mathrm{d}t''\, \Gamma(|t''|)C(u+t''-t) - \int_0^{\infty} \mathrm{d}t''\, \Gamma(|t''|)C(u+t'') + \\ &\quad + \int_0^{-u} \mathrm{d}t''\, \Gamma(|t''|)C(u+t'')\end{aligned} \tag{8.19}$$

Using this we see that equation (8.14) becomes

$$\begin{aligned}
\mathcal{R}(t) = 2\int_0^\infty \mathrm{d}t'\,\Gamma(t')\Bigg[&\int_0^\infty \mathrm{d}t''\,\Gamma(|t''|)C(t''-t) - \int_0^\infty \mathrm{d}t''\,\Gamma(|t''|)C(t+t''-t') \\
&- \int_0^{t'} \mathrm{d}t''\,\Gamma(|t''|)C(t''-t') + \int_0^{t'-t} \mathrm{d}t''\,\Gamma(|t''|)C(t+t''-t') + \\
&- \int_0^\infty \mathrm{d}t''\,\Gamma(|t''|)C(t''-t'-t) + \int_0^\infty \mathrm{d}t''\,\Gamma(|t''|)C(t''-t') + \\
&+ \int_0^{t+t'} \mathrm{d}t''\,\Gamma(|t''|)C(t''-t'-t) - \int_0^{t'} \mathrm{d}t''\,\Gamma(|t''|)C(t''-t') + \\
&+ \int_{-t'}^{t-t'} \mathrm{d}t''\,\Gamma(|t''|)C(0) - \int_{-t'-t}^{-t'} \mathrm{d}t''\,\Gamma(|t''|)C(0)\Bigg] = \\
= 2\int_0^\infty \mathrm{d}t'\,\Gamma(t')\Bigg[&\int_0^{t-t'} \mathrm{d}t''\,\Gamma(|t''|)\big(C(0) - C(t-t'-t'')\big) + \\
&- \int_{t+t'}^\infty \mathrm{d}t''\,\Gamma(|t''|)C(t''-t'-t) + \\
&+ \int_{t'}^\infty \mathrm{d}t''\,\Gamma(|t''|)C(t''-t') - \int_0^{t'} \mathrm{d}t''\,\Gamma(|t''|)C(t''-t') + \\
&- \int_0^{t+t'} \mathrm{d}t''\,\Gamma(|t''|)C(0) + 2\int_0^{t'} \mathrm{d}t''\,\Gamma(|t''|)C(0)\Bigg] + \phi(t)\,,
\end{aligned} \tag{8.20}$$

where $\phi(t)$ is defined in (8.13). By further noting that

$$\int_0^\infty \mathrm{d}t' \int_0^{t'} \mathrm{d}t'' = \int_0^\infty \mathrm{d}t'' \int_{t''}^\infty \mathrm{d}t' \tag{8.21}$$

i.e. these integrals define the same region of integration, one readily sees that the second to last line of (8.20) is equal to 0.

Consider now the variance of $y(t) - y(0)$,

$$\begin{aligned}
\mathrm{Var}(t) &= \mathrm{Var}\left[y_t - y_0\right] = \\
&= \langle y_t^2\rangle + \langle y_0^2\rangle - 2\langle y_t\, y_0\rangle = 2\left(\langle y_0^2\rangle - \langle y_t\, y_0\rangle\right) = 2\left(C(0) - C(t)\right)\,.
\end{aligned} \tag{8.22}$$

With this definition, $\mathcal{R}(t)$ becomes equal to

$$\begin{aligned}
\mathcal{R}(t) = \int_0^\infty \mathrm{d}t'\,\Gamma(t')\Bigg[\int_0^{t-t'} \mathrm{d}t''\,\Gamma(|t''|)\mathrm{Var}(t-t'-t'') + \\
- 2\int_{t+t'}^\infty \mathrm{d}t''\,\Gamma(|t''|)C(t+t'-t'') + \\
- 2\int_0^{t+t'} \mathrm{d}t''\,\Gamma(t'')C(0) + 4\int_0^{t'} \mathrm{d}t''\,\Gamma(t'')C(0)\Bigg] + \phi(t) = \\
= \int_0^\infty \mathrm{d}t'\,\Gamma(t')\Bigg[\int_0^{t-t'} \mathrm{d}t''\,\Gamma(|t-t'-t''|)\mathrm{Var}(t'') + \\
- 2\int_{-\infty}^0 \mathrm{d}t''\,\Gamma(|t+t'-t''|)C(t'') + \\
- 2\int_{t'}^{t+t'} \mathrm{d}t''\,\Gamma(t'')C(0) + 2\int_0^{t'} \mathrm{d}t''\,\Gamma(t'')C(0)\Bigg] + \phi(t) = \\
= \phi(t) + \int_{-\infty}^t \mathrm{d}t'\,\Gamma(t-t')\int_0^{t'} \mathrm{d}t''\,\Gamma(t'-t'')\mathrm{Var}(t'') + \\
+2\int_0^\infty \mathrm{d}t'\,\Gamma(t')\Bigg[\int_{t'+t}^\infty \mathrm{d}t''\,\Gamma(t'')C(0) - \int_0^\infty \mathrm{d}t''\,\Gamma(t+t'+t'')C(t'')\Bigg],
\end{aligned} \tag{8.23}$$

where again we used (8.21) to obtain the term proportional to $C(0)$ in the eighth line from the sixth.

Let us focus on the integral of the second last line, i.e.

$$r(t) = \int_{-\infty}^t \mathrm{d}t'\,\Gamma(t-t')\int_0^{t'} \mathrm{d}t''\,\Gamma(t'-t'')\mathrm{Var}(t'')\,. \tag{8.24}$$

We immediately see that

$$\begin{aligned}
r(t) = \int_0^t \mathrm{d}t'\,\Gamma(t-t')\int_0^{t'} \mathrm{d}t''\,\Gamma(t'-t'')\mathrm{Var}(t'') + \\
- \int_0^\infty \mathrm{d}t'\,\Gamma(t+t')\int_0^{t'} \mathrm{d}t''\,\Gamma(t'-t'')\mathrm{Var}(t'') = \\
= \int_0^t \mathrm{d}t'\,\Gamma(t-t')\int_0^{t'} \mathrm{d}t''\,\Gamma(t'-t'')\mathrm{Var}(t'') + \\
- 2\int_0^\infty \mathrm{d}t'\,\Gamma(t+t')\int_0^{t'} \mathrm{d}t''\,\Gamma(t'-t'')C(0) + \\
+ 2\int_0^\infty \mathrm{d}t''\int_{t''}^\infty \mathrm{d}t'\,\Gamma(t+t')\Gamma(t'-t'')C(t'')
\end{aligned} \tag{8.25}$$

where again equation (8.21) was used along with (8.22). Let us consider the last two

terms of (8.25) separately.

$$\begin{aligned}2\int_0^\infty \mathrm{d}t'\,\Gamma(t+t')\int_0^{t'}\mathrm{d}t''\,\Gamma(t'-t'')C(0) =& 2\int_0^\infty \mathrm{d}t'\,\Gamma(t+t')\int_0^{t'}\mathrm{d}t''\,\Gamma(t'')C(0) = \\ =& 2\int_0^\infty \mathrm{d}t''\int_{t''}^\infty \mathrm{d}t'\,\Gamma(t+t')\Gamma(t'')C(0) = \\ =& 2\int_0^\infty \mathrm{d}t''\int_{t+t''}^\infty \mathrm{d}t'\,\Gamma(t')\Gamma(t'')C(0) = \\ =& 2\int_0^\infty \mathrm{d}t'\,\Gamma(t')\int_{t+t'}^\infty \mathrm{d}t''\,\Gamma(t'')C(0)\end{aligned} \tag{8.26}$$

where in the last line we renamed the integration variables. As for the second term we get

$$\begin{aligned}2\int_0^\infty \mathrm{d}t''\int_{t''}^\infty \mathrm{d}t'\,\Gamma(t+t')\Gamma(t'-t'')C(t'') = & \\ =& 2\int_0^\infty \mathrm{d}t''\int_0^\infty \mathrm{d}t'\,\Gamma(t+t'+t'')\Gamma(t')C(t'') = \\ =& 2\int_0^\infty \mathrm{d}t'\,\Gamma(t')\int_0^\infty \mathrm{d}t''\,\Gamma(t+t'+t'')C(t'')\,.\end{aligned} \tag{8.27}$$

Putting (8.25), (8.26) and (8.27) all together we hence obtain

$$\begin{aligned}r(t) =& \int_0^t \mathrm{d}t'\,\Gamma(t-t')\int_0^{t'}\mathrm{d}t''\,\Gamma(t'-t'')\mathrm{Var}(t'')+ \\ &-2\int_0^\infty \mathrm{d}t'\,\Gamma(t')\left[\int_{t+t'}^\infty \mathrm{d}t''\,\Gamma(t'')C(0)-\int_0^\infty \mathrm{d}t''\,\Gamma(t+t'+t'')C(t'')\right].\end{aligned} \tag{8.28}$$

Moreover, from (8.23) and (8.28) one gets

$$\begin{aligned}\mathcal{R}(t) =& \phi(t)+r(t)+ \\ &+2\int_0^\infty \mathrm{d}t'\,\Gamma(t')\left[\int_{t+t'}^\infty \mathrm{d}t''\,\Gamma(t'')C(0)-\int_0^\infty \mathrm{d}t''\,\Gamma(t+t'+t'')C(t'')\right] = \\ =& \phi(t)+\int_0^t \mathrm{d}t'\,\Gamma(t-t')\int_0^{t'}\mathrm{d}t''\,\Gamma(t'-t'')\mathrm{Var}(t'')\,.\end{aligned} \tag{8.29}$$

Finally, by plugging (8.29) into (8.12) we get

$$\begin{aligned}&\int_0^t \mathrm{d}t'\,\Gamma(t-t')\int_0^{t'}\mathrm{d}t''\,\Gamma(t'-t'')\mathrm{Var}(t'')+ \\ &+\int_0^t \mathrm{d}t'\int_0^t \mathrm{d}t''\,\mathrm{Cov}(F(\{y^n_{t'}\}),F(\{y^n_{t''}\})) = 2\,k_BT\int_0^t \mathrm{d}t'\int_0^{t'}\mathrm{d}t''\,\Gamma(t'')\,.\end{aligned} \tag{8.30}$$

The last step of the derivation consists in rewriting the terms involving the covaraiances in terms of the original variable $x_t = y_t + vt$. Indeed, because vt is a deterministic variable, one trivially finds that

$$\mathrm{Var}(t) = \mathrm{Var}\left(y_t - y_0\right) = \mathrm{Var}\left(x_t - x_0\right) \tag{8.31}$$

As regards the covariance of the forces, because for a Galilean transformations it holds that $\widetilde{P}(y_t) = \widetilde{P}(x_t - vt) = P(x_t)$ [85], where $\widetilde{P}$ is the probability defined in the rest frame while P is the one defined in the laboratory frame, one can easily show that

$$\mathrm{Cov}(F(\{y^n_{t'}\}), F(\{y^n_{t''}\})) = \mathrm{Cov}(F(\{x^n_{t'}\}), F(\{x^n_{t''}\}))\,. \tag{8.32}$$

As a consequence, one immediately sees that (8.30) becomes

$$\begin{aligned} &\int_0^t \mathrm{d}t'\,\Gamma(t-t')\int_0^{t'} \mathrm{d}t''\,\Gamma(t'-t'')\mathrm{Var}\,(x_{t''}-x_0) + \\ &+\int_0^t \mathrm{d}t'\int_0^t \mathrm{d}t''\,\mathrm{Cov}(F(\{x^n_{t'}\}), F(\{x^n_{t''}\})) = 2\,k_BT\int_0^t \mathrm{d}t'\int_0^{t'} \mathrm{d}t''\,\Gamma(t'')\,, \end{aligned} \tag{8.33}$$

that is our final result. We further add that, by exploiting the symmetries of the correlation functions in a steady state, the latter can be rewritten in Laplace space as

$$\big(k\,\hat{\Gamma}(k)\big)^2\mathcal{L}_k[\mathrm{Var}\,(x_t - x_0)] + 2\,\mathcal{L}_k\big[\big\langle F(\{x^n_t\})\,F(\{x^n_0\})\big\rangle\big] = 2\,k_BT\,\hat{\Gamma}(k)\,. \tag{8.34}$$

8.3 Non-Markovian variance sum rule: discussion and applications

The non Markovian VSR

$$\begin{aligned} &\int_0^t \mathrm{d}t'\,\Gamma(t-t')\int_0^{t'} \mathrm{d}t''\,\Gamma(t'-t'')\mathrm{Var}\,(x_{t''}-x_0) + \\ &+\int_0^t \mathrm{d}t'\int_0^t \mathrm{d}t''\,\mathrm{Cov}(F(\{x^n_{t'}\}), F(\{x^n_{t''}\})) = 2\,k_BT\int_0^t \mathrm{d}t'\int_0^{t'} \mathrm{d}t''\,\Gamma(t'') \end{aligned} \tag{8.35}$$

is another novel result relating the variance of the relative displacement and the covariance of the averaged force acting on the beads. For a single colloidal particle, the latter becomes the external force acting on the bead through the confinement potential. For this case, analytical and numerical verification of the VSR have been performed for harmonic and non-harmonic potentials, respectively, as for the examples shown in figure 8.1. Furthermore, in comparison to the Markovian VSR (7.39), here there appears a double convolution between the memory kernel and the variance of the relative displacement while on the right hand side there appears the double integral of the memory kernel. Even though these additional features seem to complicate the functional form of the VSR, the latter can be recast in a more elegant and simple form in Laplace space (8.34) where it can be used to estimate the parameters characterising the memory kernel $\Gamma(t)$. Indeed, by rewriting (8.34) as

$$\big(k\,\hat{\Gamma}(k)\big)^2\mathcal{L}_k[\mathrm{Var}\,(x_t - x_0)] - 2\,k_BT\,\hat{\Gamma}(k) + 2\,\mathcal{L}_k[\mathrm{Cov}\,(F(\{x^n_t\})\,F(\{x^n_0\}))] = 0\,, \tag{8.36}$$

one immediately sees that it can be regarded as a second order algebraic equation for the unknown variable $\hat{\Gamma}(k)$, hence leading to

$$\hat{\Gamma}_\pm(k) = \frac{1 \pm \sqrt{\Delta(k)}}{\beta\,k^2\,\mathcal{L}_k[\mathrm{Var}\,(x_t - x_0)]}\,, \tag{8.37}$$

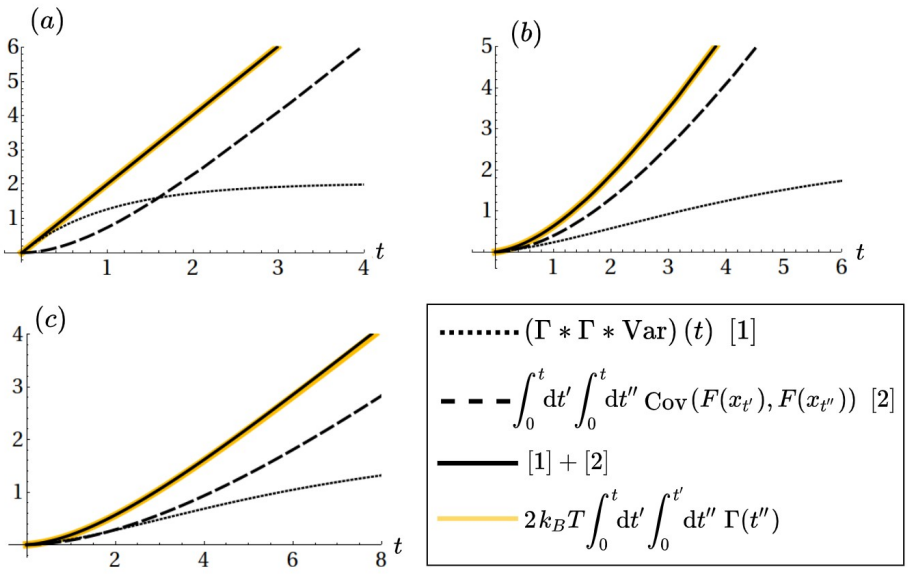

Figure 8.1: Behaviour or the non-Markovian VSR as a function of time ($k_BT = 1$) and where $(\Gamma * \Gamma * \mathrm{Var})(t) = \int_0^t \mathrm{d}t' \, \Gamma(t-t') \int_0^{t'} \mathrm{d}t'' \, \Gamma(t'-t'') \mathrm{Var}\,(x_{t''} - x_0)$. Panel (a) corresponds to a particle trapped in a harmonic potential $U(x_t) = \kappa \, x_t^2/2$ ($\kappa = 1$) in a Markovian medium with $\Gamma(t) = 2\,\gamma_0\,\delta(t)$ ($\gamma_0 = 1$). The case of a non-Markovian kernel $2\,\gamma_0\,\delta(t) + \gamma_1 \mathrm{e}^{-t/\tau}/\tau$ ($\gamma_0 = 0.1$, $\gamma_1 = 1$, $\tau_1 = 2$) in the same harmonic potential is depicted in panel (b). All these results have been analytically obtained with the formulas shown in Chapter 3. Panel (c) instead is obtained via simulated data in a double well potential $U(x_t) = \frac{a}{2}x_t^2 + \frac{b}{4}x_t^4$ ($a = -1$, $b = 1$) and kernel $\Gamma(t) = 2\,\gamma_0\,\delta(t) + \gamma_1 \mathrm{e}^{-t/\tau}/\tau$ ($\gamma_0 = 0.1$, $\gamma_1 = 1$, $\tau_1 = 2$).

$$\Delta(k) = 1 - 2\,\beta^2\,k^2\,\mathcal{L}_k[\mathrm{Var}\,(x_t - x_0)]\,\mathcal{L}_k[\mathrm{Cov}\,(F(\{x_t^n\})\,F(\{x_0^n\}))] \tag{8.38}$$

where $\beta = (k_BT)^{-1}$. Equation (8.37) shows that, similarly to the Markovian VSR, one is able to extract relevant model parameters, in this case those defining the memory kernel, by measuring variances and correlations of operationally accessible quantities. Indeed, by gathering a good statistics to estimate these quantities and by numerically calculating their Laplace transform (only for real k in this case), the two solutions $\hat{\Gamma}_\pm(k)$ of equation (8.37) can be readily evaluated. To understand which of these two solutions must be taken, we perform a consistency check by considering the solutions in the limits of small and large k. This can be done by first evaluating the small/large time limits of $\mathrm{Var}\,(x_t - x_0)$ and $\mathrm{Cov}\,(F(\{x_t^n\})\,F(\{x_0^n\}))$, which can be readily extrapolated from the VSR itself. Indeed, for small times, corresponding to large k, and similarly to what has been done in Appendix A.1, these quantities behave as follows

$$\begin{aligned} \lim_{t\to 0} \mathrm{Var}\,(x_t - x_0) \propto t \quad &\Longrightarrow \quad \lim_{k\to\infty} \mathcal{L}\,[\mathrm{Var}\,(x_t - x_0)] \propto k^{-2}\,, \\ \lim_{t\to 0} \big\langle F(\{x_t^n\})\,F(\{x_0^n\})\big\rangle \propto const \quad &\Longrightarrow \quad \lim_{k\to\infty} \mathcal{L}_k[\mathrm{Cov}\,(F(\{x_t^n\})\,F(\{x_0^n\}))]] \propto k^{-1}\,. \end{aligned} \tag{8.39}$$

As a consequence, the right hand side of (8.37) becomes

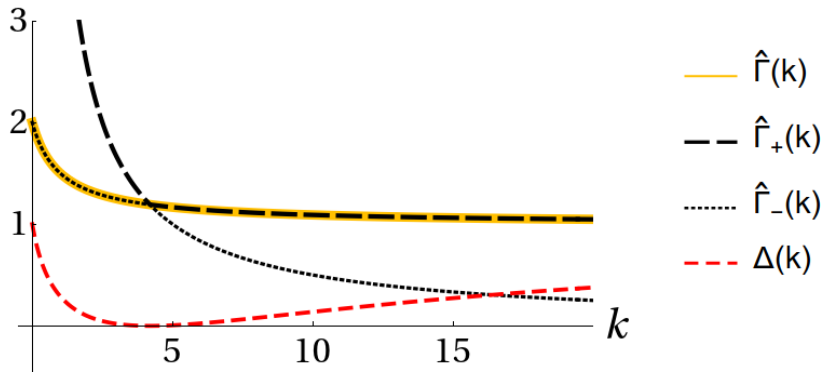

Figure 8.2: Plot of the solutions for Brownian particle in a parabolic potential, modelled by (3.4) with $m = 0$, $\lambda(t) = 0$, $\kappa = 5$ and memory kernel $\Gamma(t) = 2\gamma_0 + \gamma_1 e^{-t/\tau}/\tau$ with Laplace transform $\hat{\Gamma}(k) = \gamma_0 + \gamma_1/(1 + k\tau)$ ($\gamma_0 = \gamma_1 = \tau = 1$). The solutions $\hat{\Gamma}_\pm(k)$ and the discriminant $\Delta(k)$ have been analytically computed from (8.37) and (8.38) by using the formulas presented in Chapter 3. As it is clear from the figure, when the discriminant becomes equal to zero, the correct solution switches from $\hat{\Gamma}_-(k)$ to $\hat{\Gamma}_+(k)$ (as k grows).

$$\hat{\Gamma}_\pm(k) \overset{k\to\infty}{\approx} c_1 \left(1 \pm \sqrt{1 - c_2\, k^{-1}}\right), \tag{8.40}$$

for some constants c_1, c_2. As discussed in Chapter 3 and in the context of the unidimensonal overdamped GLE, the large k limit of $\hat{\Gamma}(k)$ must be finite, which in turn implies that in this regime the correct solution of (8.40) is $\hat{\Gamma}_+(k)$, while for the other solution one finds $\hat{\Gamma}_-(k) \propto k^{-1}$. In a similar way and finite effective friction coefficient $\widehat{\gamma}$, the large times (small k) limit leads to

$$\begin{aligned} \lim_{t\to\infty} \mathrm{Var}\,(x_t - x_0) \propto const \quad &\Longrightarrow \quad \lim_{k\to 0} \mathcal{L}\left[\mathrm{Var}\,(x_t - x_0)\right] \propto k^{-1}, \\ \lim_{t\to\infty} \left\langle F(\{x_t^n\})\, F(\{x_0^n\})\right\rangle \propto e^{-t/\tau} \quad &\Longrightarrow \quad \lim_{k\to 0} \mathcal{L}_k[\mathrm{Cov}\,(F(\{x_t^n\})\, F(\{x_0^n\}))]] \propto const, \end{aligned} \tag{8.41}$$

for some typical time τ characterising the long time behaviour of the correlation functions. Moreover, the constant variance of the relative displacement is constant because of the presence of the confining potential. Hence, in this limit, equation (8.37) becomes

$$\hat{\Gamma}_\pm(k) \overset{k\to 0}{\approx} \frac{c_1}{k}\left(1 \pm \sqrt{1 - c_2\, k}\right), \tag{8.42}$$

implying that, because $\hat{\Gamma}(0) = \widehat{\gamma}$ is finite, $\hat{\Gamma}_-(k)$ is the right solution. Indeed, for small k one finds that $\hat{\Gamma}_+(k) \propto k^{-1}$.

To summarise, we found that for large (small) k the right solution to consider is $\hat{\Gamma}_+(k)$ ($\hat{\Gamma}_-(k)$). Moreover, from equations (8.40) and (8.42) one sees that the discriminant $\Delta(k) \approx 1$ in these regimes. Indeed, because the memory kernels are continuous and real function, their Laplace transform must be continuous and real (for real k) as well. This implies that there must be at lest one k such that the solution can smoothly switch from $\hat{\Gamma}_-(k)$ to $\hat{\Gamma}_+(k)$ as k grows. For all the cases we analysed, there is always a single point where the discriminant $\Delta(k)$ becomes zero (which is a global minimum for $\Delta(k)$) and, from a practical point of view, by detecting this point one is able to discriminate which part of the solution must be used for

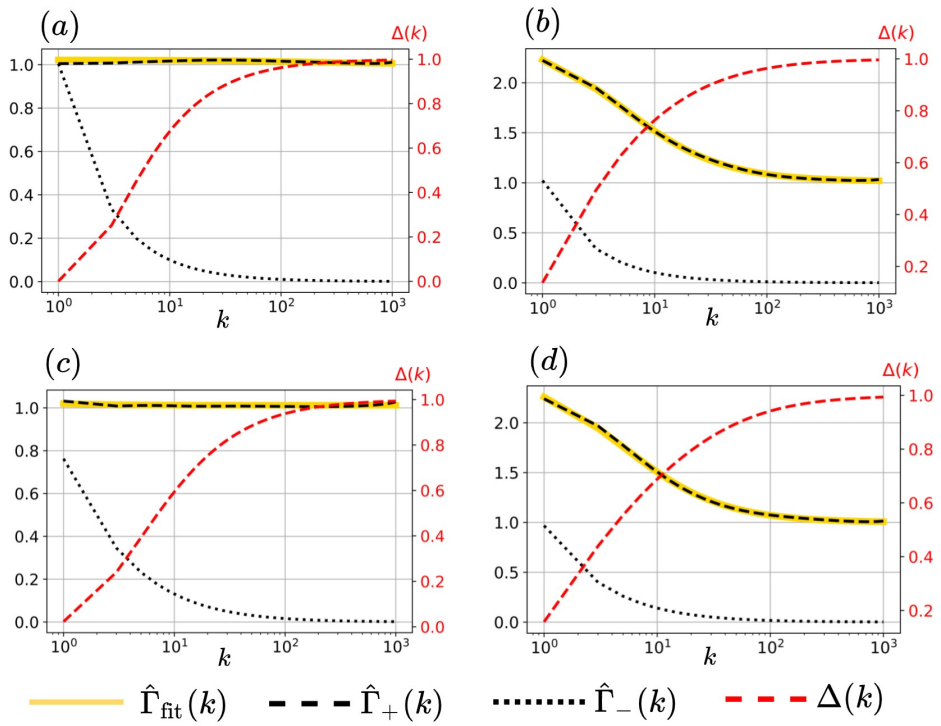

Figure 8.3: Estimation of the memory kernel from simulated data (10^4 trajectories) on a time window of 10s and $dt = 10^{-3}$. The upper row corresponds to a particle in a harmonic potential $U(x_t) = \kappa\, x_t^2/2$ ($\kappa = 1$) while the second row corresponds to $U(x_t) = \frac{a}{2}\, x_t^2 + \frac{b}{4}\, x_t^4$ ($a = -1$, $b = 1$). The column on the left is generated using a Markovian kernel $\Gamma(t) = 2\,\gamma_0\,\delta(t)$ ($\gamma_0 = 1$). Instead, the column on right corresponds to the non-Markovian kernel equal to $2\,\gamma_0\,\delta(t) + \gamma_1 e^{-t/\tau}/\tau$ ($\gamma_0 = 1$, $\gamma_1 = 1.5$, $\tau_1 = 0.2$). By numerically evaluating the Laplace transform for $k \in \{1, 2, \ldots, 10^3\}$ one is able to fit the solution ($\Gamma_+(k)$ in this case because $\Delta(k)$, whose scale is the red one on the right of each panel, has already become 0 for $k < 1$) with the analytical formula of the kernels above in Laplace space. In real world application, of course, one does not know the functional form of the kernel a priori and, as a consequence, the strategy would be to try different analytical forms and chose the one that fits the data better. For the cases above, we fit the solutions with $\hat{\Gamma}_{\rm fit}(k) = \widetilde{\gamma}_0 + \widetilde{\gamma}_1/(1 + k\widetilde{\tau})$ finding for:
(a) $\widetilde{\gamma}_0 = 1.003 \pm 0.001$, $\widetilde{\gamma}_1 = 0.01 \pm 0.001$ and $\widetilde{\tau} = 0.007 \pm 0.002$;
(b) $\widetilde{\gamma}_0 = 1.005 \pm 0.001$, $\widetilde{\gamma}_1 = 1.48 \pm 0.01$ and $\widetilde{\tau} = 0.191 \pm 0.005$;
(c) $\widetilde{\gamma}_0 = 1.005 \pm 0.001$, $\widetilde{\gamma}_1 = 0.02 \pm 0.02$ and $\widetilde{\tau} = 0.01 \pm 0.02$;
(d) $\widetilde{\gamma}_0 = 0.999 \pm 0.001$, $\widetilde{\gamma}_1 = 1.506 \pm 0.04$ and $\widetilde{\tau} = 0.197 \pm 0.002$.

the fitting procedure of the parameters of the memory kernel. An example of this behaviour is depicted in Figure 8.2.

Simulations In order to study the performances of our fitting method, we first simulate 10^4 stochastic trajectory for the equilibrium dynamics of a single Brownian particle in a harmonic potential $U(x_t) = \kappa\, x_t^2/2$ and a in double well potential $U(x_t) = a\, x_t^2/2 + b\, x_t^4/4$ (with $a < 0$), both in a Markovian $\Gamma(t) = 2\,\gamma_0\,\delta(t)$ and in a non-Markovian $\Gamma(t) = 2\,\gamma_0\,\delta(t) + \gamma_1\, e^{-t/\tau}/\tau$ bath. From these trajectories,

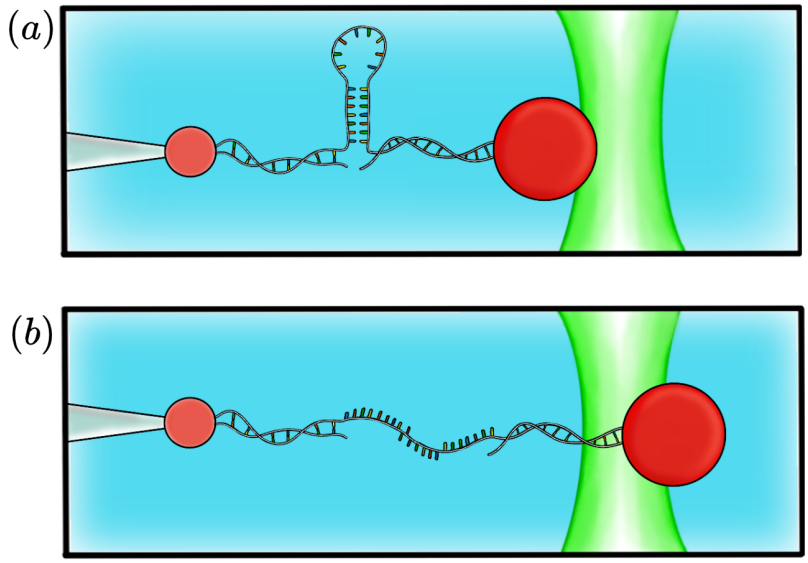

Figure 8.4: Schema of a DNA hairpin i a (a) folded and (b) unfolded state.

we compute the variance of the relative displacement and the double integral of the covariance of the forces and numerically evaluate their (real valued) Laplace transform. Because the traces are defined in a time interval $[0, 10]$ with sampling frequency of $dt = 10^{-3}$, we decide to evaluate the numerical Laplace transforms for the discrete set of values in Laplace space, $k \in \{1, 2, 3, \ldots, 1000\}$. As shown in Figure 8.3 and in its caption, the result of the parameter estimation is in very good agreement with the original values used for generating the traces. However, one can note that, in many cases, an underestimation of the errors occurs (see caption of Figure 8.3). This is probably due to the systematic error occurring during the numerical evaluation of the Laplace transforms, especially for small k (remember that the traces are up to $t = 10$). Nevertheless, this issue is of secondary importance and indeed, encouraged by these good results, we proceed by applying this same method to experimental data coming from traces of a Brownian particle attached to a DNA hairpin whose dynamics may be described by a GLE equation.

DNA hairpins are well known biological systems formed by a single stranded DNA molecule which can be studied by using optical tweezers [133, 134, 135, 136]. In this case, one end of the DNA is fixed by a pipette while the other end is chemically attached to a colloidal bead which in turn is trapped by the laser beams of the optical tweezers. What can be observed, in this setting, is that the hairpin undergoes a zipping/unzipping dynamics between a folded (Figure 8.4(a)) and an unfolded (Figure 8.4(b)) state. The GLE has already been used to model this kind of system in terms of a reaction coordinate dynamics [137] but has never been used, to our knowledge, to model the motion of a colloidal bead attached to a DNA hairpin. Indeed, we are going to suppose that the effects of the hairpin on the dynamics of the colloidal bead can be modelled by some effective potential $V_{\text{eff}}(x_t)$ where, because the system is complex and many degrees of freedom have been integrated out in this effective model, there are also memory effects. We thus assume that such equilibrium dynamics can be effectively described by a GLE where the position PDF equals $p(x_t) \propto \exp\left[-\beta V_{\text{eff}}(x_t)\right]$ and, as a consequence, the force acting

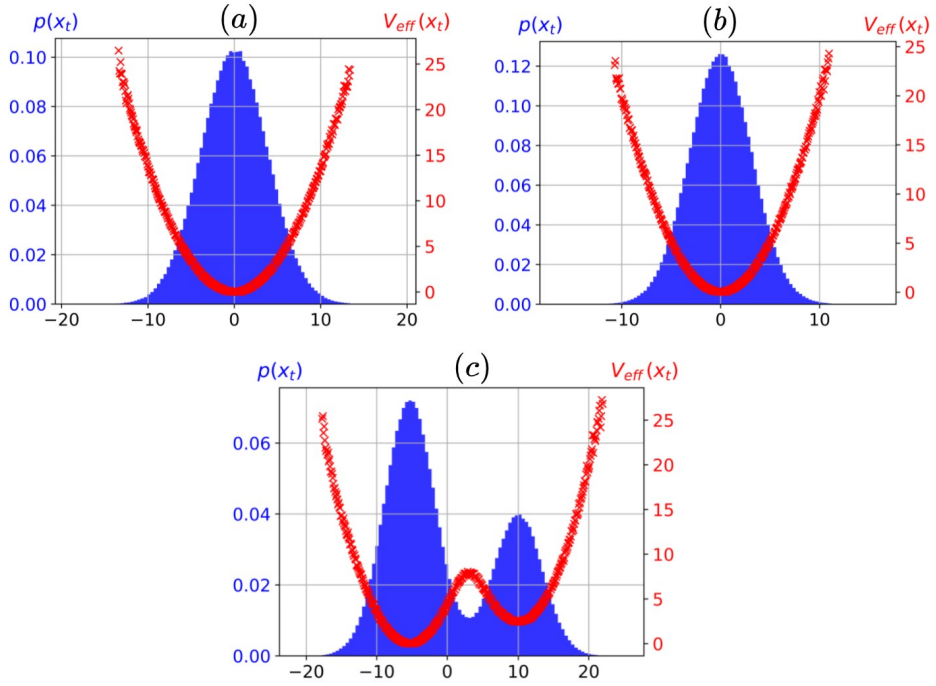

Figure 8.5: Reconstructed PDF from experimental measurements (blue scale on the left) and effective potential $V_{\text{eff}}(x_t) = -k_B T \ln p(x_t) + const$ (red scale on the right in [pN nm]). Figure (a) corresponds for the trace in a unfolded state, (b) to the folded state and (c) to the zipping/unzipping dynamics.

on the particle is $F(x_t) = -\partial_{x_t} V_{\text{eff}}(x_t)$. We are going to consider three traces for a hairpin always in an unfolded case, always in a folded state and while undergoing zipping/unzipping dynamics. For each of these traces, the effective potential can be readily obtained by empirically estimating the PDF $p(x_t)$ from experimental measurements and by considering $V_{\text{eff}}(x_t) = -k_B T \ln p(x_t)$, as shown in Figure 8.5. These potential data points can be be fitted with a polynomial $\mathcal{P}_n(x)$ of degree n, with $n = 2$ for the folded and unfolded state and $n = 12$ for the zipping/unzipping dynamics. The forces, and hence their variances, can be then readily evaluated by considering (minus) the derivative of the effective potential with known analytical form and fitted parameters.

By applying this procedure, we are now able to apply the VSR method as for the simulation case depicted in the previous paragraph and the results of the estimation procedure are shown in Figure 8.6. The first thing we observe is that, for all cases, the Markovian friction coefficient γ_0 is always higher then the nominal value $\approx 2.5 \cdot 10^{-5}$[pN s/nm], also observed in the section dedicated to the Markovian VSR. Such an effect is expected, of course, because of the presence of the hairpin. Moreover, the estimated γ_0 for the folded case is slightly higher then that in the unfolded case. We interpret this as hydrodynamic backflow effects due to the increased proximity of the bead to the pipette. In addition, for the folded and unfolded cases, we already obtain very good fits by only using one additional exponential to the memory kernel, i.e. $\Gamma(t) = 2\gamma_0 \delta(t) + \gamma_1 e^{-t/\tau_1}/\tau_1$. The non-Markovian friction coefficients γ_1 are one order of magnitude larger then γ_0 and for the folded state it is four times larger then that in the unfolded case. This could be due to the more rigid configuration of the hairpin in the folded state. The es-

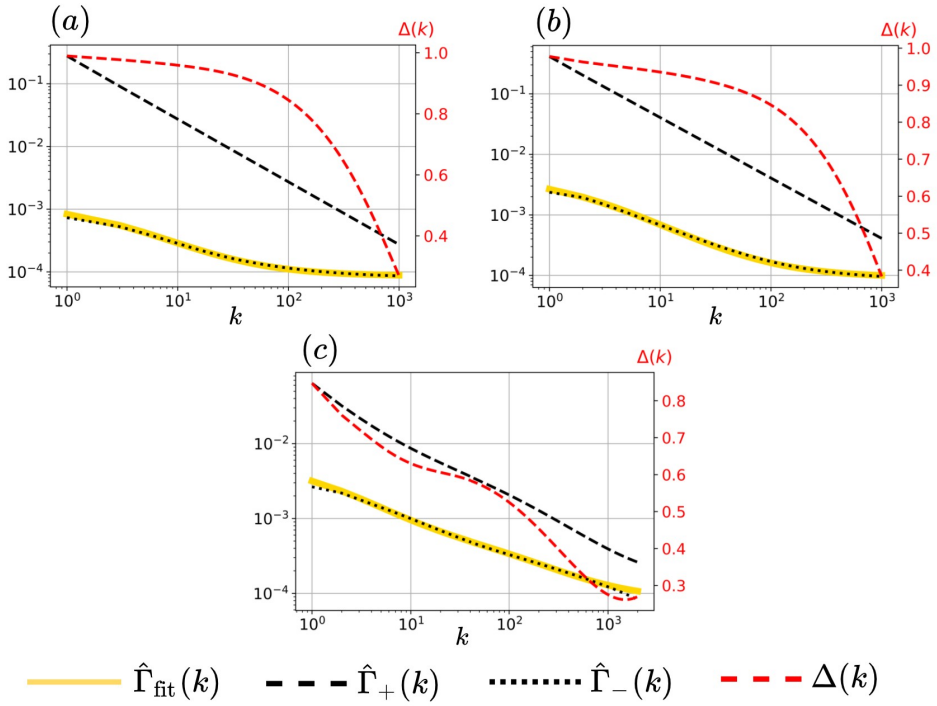

Figure 8.6: Experimental data derived from traces with (a) unfolded hairpin, (b) folded hairpin and (c) jumping hairpin. Again, we numerically evaluate $\hat{\Gamma}_{\pm}(k)$ but this time we fit $\hat{\Gamma}_{-}(k)$ because $\Delta(k)$ (red scale on the right) still has not reached 0 in the k interval we are considering. The fitting procedure has been performed by choosing different functional forms for the memory kernel (a Markovian component plus a number of exponentials with parameters $\{\widetilde{\gamma}_i, \widetilde{\tau}_i\}$) and we present the best results coming from these fits, which read:
(a) $\widetilde{\gamma}_0 = (8.6 \pm 1 \cdot 10^{-1}) \cdot 10^{-5}\,\mathrm{pN\,s/nm}$, $\widetilde{\gamma}_1 = (1.06 \pm 2 \cdot 10^{-2}) \cdot 10^{-3}\,\mathrm{pN\,s/nm}$ and $\widetilde{\tau}_1 = (0.43 \pm 0.01)\mathrm{s}$;
(b) $\widetilde{\gamma}_0 = (9.3 \pm 1 \cdot 10^{-1}) \cdot 10^{-5}\,\mathrm{pN\,s/nm}$, $\widetilde{\gamma}_1 = (4.06 \pm 2 \cdot 10^{-2}) \cdot 10^{-3}\,\mathrm{pN\,s/nm}$ and $\widetilde{\tau}_1 = (0.582 \pm 0.008)\mathrm{s}$;
(c) $\widetilde{\gamma}_0 = (1.5 \pm 1 \cdot 10^{-2}) \cdot 10^{-4}\,\mathrm{pN\,s/nm}$, $\widetilde{\gamma}_1 = (2.12 \pm 3 \cdot 10^{-2}) \cdot 10^{-3}\,\mathrm{pN\,s/nm}$, $\widetilde{\tau}_1 = (0.76 \pm 0.02)\mathrm{s}$, $\widetilde{\gamma}_2 = (1.08 \pm 8 \cdot 10^{-2}) \cdot 10^{-3}\,\mathrm{pN\,s/nm}$ and $\widetilde{\tau}_2 = (1.29 \cdot 10^{-2} \pm 1 \cdot 10^{-4})\mathrm{s}$

timated typical times τ_1 are of the same order of magnitude (≈ 0.5s) and slightly higher for the folded case. Such typical times are rather large for a DNA hairpin dynamics. We are currently evaluating how these parameters could be connected with the molecular construct of the hairpin and eventually to some pink noise from the apparatus. Moreover, because one needs long time traces for the small k estimation of the numerical Laplace transform, there is the possibility that some experimental drift effects could have altered the measured data. Indeed, such effects have been detected in data of free beads, even though this VSR analysis applied to the latter still gives compatible results to the nominal value of the friction coefficient (we do not present these data here for shortness).

However, it is worth noting that, for the trace undergoing zipping/unzipping dynamics, the best fit was given by a memory kernel with two exponentials, whose estimated parameters are again presented in the caption of Figure 8.6. Here, we

observe an increase of the Markovian friction coefficient (one order of magnitude) while γ_1 and γ_2 have the same order of magnitude as γ_1 for the folded unfolded case. Again we observe a large typical time $\tau_1 \approx 0.76$, for which the same considerations as above can be made, in addition to a smaller typical time $\tau_2 \approx 10^{-2}$ which is more compatible with molecular timescales.

To sum up, in this paragraph we showed how the VSR can be used to deduce the memory kernel characterising the effective dynamics of a bead attached to DNA hairpin. Due to the lack of a sufficiently large pool of analysed traces and to the possibility of systematic errors occurred during the measurements, we cannot yet assert precisely how the fitted parameters are related to molecular constructs of the hairpin. However, we are confident that this VSR based procedure could be useful for future applications and for similar estimation tasks as those shown in this section.

8.3.1 Reversed TUR and Fano factor

Another interesting consequence of the non-Markovian VSR can be derived by considering the total external work done on the particles for a constant dragging at velocity $v \neq 0$. This is given by the generalisation of (3.41) for N particles and for $\lambda(t) = vt$, i.e.

$$\begin{aligned} W_{\text{tot}}(x_t, t) =& v \sum_n \int_0^t \mathrm{d}t' \, \partial_{vt'} U\left(x_{t'}^n - vt'\right) = \\ =& - v \sum_n \int_0^t \mathrm{d}t' \, \partial_{x_{t'}^n} U\left(x_{t'}^n - vt'\right) = N\, v \int_0^t \mathrm{d}t' \, F(\{x_{t'}^n\}) \,. \end{aligned} \tag{8.43}$$

Its average can be readily evaluated by switching to the equilibrium reference frame, corresponding to a change of variables $y_t^n = x_t^n - vt$ and characterised by the equilibrium PDF

$$\widetilde{P}^{\text{eq}}(\{y_t^n\}) \propto \exp\left[-\beta\left(\sum_n V(y_t^n) + \sum_{n,\, m\neq n} U^{\text{int}}(|y_t^n - y_t^m|)\right]\right) , \tag{8.44}$$

where $U^{\text{int}}(|x_t^n - x_t^m|)$ is defined in (8.6), $V(y_t^n) = U(y_t^n) + \widehat{\gamma}\, v\, y_t^n$ is a tilted potential for the variables in the moving frame and $v\, y_t^n$ comes from the transformed GLE in terms of y_t, obtained from (8.5) by setting $x_t^n = y_t^n + vt$. From this one readily sees that the average of (8.43) becomes

$$\begin{aligned} \langle W_{\text{tot}} \rangle_t =& - v \sum_n \int_0^t \mathrm{d}t' \int \prod_{n'} \mathrm{d}y_{t'}^{n'} \; \widetilde{P}^{\text{eq}}(\{y_t^n\})\, \partial_{y_{t'}^n} U(y_{t'}^n) = \\ =& - v \sum_n \int_0^t \mathrm{d}t' \int \prod_{n'} \mathrm{d}y_{t'}^{n'} \; \widetilde{P}^{\text{eq}}(\{y_{t'}^n\}) \left(\partial_{y_{t'}^n} V(y_{t'}^n) - \sum_{m\neq n} f(y_{t'}^n, y_{t'}^m) - \widehat{\gamma}\, v\right) = \\ =& N\, \widehat{\gamma}\, v^2\, t + v\, k_B T \sum_n \int_0^t \mathrm{d}t' \int \prod_{n'\neq n} \mathrm{d}y_{t'}^{n'} \int \mathrm{d}y_{t'}^n \, \partial_{y_{t'}^n} \widetilde{P}^{\text{eq}}(\{y_{t'}^n\}) \; = \\ =& N\, \widehat{\gamma}\, v^2\, t \,. \end{aligned} \tag{8.45}$$

where in the second line we used that $\sum_{n,m\neq n} f(y^n_{t'}, y^m_{t'}) = 0$ while in the third line we noted that $\partial_{y^n_{t'}} \widetilde{P}^{\rm eq}(\{y^n_{t'}\}) = -\beta \left(\partial_{y^n_{t'}} V(y^n_{t'}) - \sum_{m\neq n} f(y^n_{t'}, y^m_{t'})\right) \widetilde{P}^{\rm eq}(\{y^n_{t'}\})$ and that $\int \mathrm{d}y^n_{t'}\, \partial_{y^n_{t'}} \widetilde{P}^{\rm eq}(\{y^n_{t'}\}) = 0$ because the PDF becomes zero at the boundaries. As regards its variance, one readily sees from (8.43) that

$$\langle \Delta W^2_{\rm tot}\rangle_t = N^2\, v^2 \int_0^t \mathrm{d}t' \int_0^t \mathrm{d}t''\, \mathrm{Cov}(F(\{y^n_{t'}\}), F(\{y^n_{t''}\}))\,. \tag{8.46}$$

This in turn implies that, the non-Markovian VSR (8.35) can be rewritten as

$$\begin{aligned}\int_0^t \mathrm{d}t'\, \Gamma(t-t') \int_0^{t'} \mathrm{d}t''\, \Gamma(t'-t'')\mathrm{Var}\,(x_{t''} - x_0) + \langle \Delta W^2_{\rm tot}(x_t, t)\rangle / N^2\, v^2 = \\ = 2\, k_B T \int_0^t \mathrm{d}t' \int_0^{t'} \mathrm{d}t''\, \Gamma(t'')\,.\end{aligned} \tag{8.47}$$

For the class of positive memory kernel, i.e. such that $\Gamma(t) \geq 0$ for every t and including a large number of relevant examples, one clearly sees that (8.47) leads to

$$\frac{\langle \Delta W^2_{\rm tot}\rangle_t}{N^2\, v^2} \leq 2\, k_B T \int_0^t \mathrm{d}t' \int_0^{t'} \mathrm{d}t''\, \Gamma(t'') \leq 2\, k_B T \int_0^t \mathrm{d}t' \int_0^{\infty} \mathrm{d}t''\, \Gamma(t'') = 2\, k_B T\, \widehat{\gamma}\, t\,, \tag{8.48}$$

i.e.

$$\frac{\langle \Delta W^2_{\rm tot}\rangle_t}{\langle W_{\rm tot}\rangle_t} \leq 2\, N\, k_B T \tag{8.49}$$

where we used (8.45) to get this last inequality. The ratio on the left hand side of (8.49) is also known as the Fano factor [138] of the total work. By the ratio of variance over average, it quantifies how an observable is relatively spread in a way opposite to a signal to noise ratio (SNR). By further exploiting that, in a steady state and in analogy with equation (3.40), it holds that

$$\langle \Sigma_{\rm tot}\rangle_t = \langle \Sigma_{\rm env}\rangle_t = \beta \langle \Delta Q\rangle = \beta\, (\langle W_{\rm tot}\rangle_t - \langle \Delta E\rangle_t) = \beta \langle W_{\rm tot}\rangle_t\,, \tag{8.50}$$

where we noted that $\langle \Delta E\rangle_t = \langle U\rangle_t - \langle U\rangle_0 = 0$, one also readily sees that (8.49)

$$\frac{\langle W_{\rm tot}\rangle^2_t}{\langle \Delta W^2_{\rm tot}\rangle_t} \geq \frac{\langle \Sigma_{\rm tot}\rangle_t}{2\, N}\,, \tag{8.51}$$

that is a form of *reversed thermodynamic uncertainty relation* (RTUR) for the observable work. The latter is not an integrated current and, moreover, even for Markovian dynamics, the drift vector of the LE associated to this model is time dependent, hence the TUR was not expected to hold. However, it is a curious fact that for a simple constant-velocity dragging, this TUR is reversed at all times. This violation of the TUR at all times was noted in [20] for Markovian systems: it is as a byproduct of their generalisation of the TUR for arbitrary time-dependent protocols and a wider class of observables (such as the work).

To conclude, we add that also the TUR (5.29) leads to a bound to the Fano factor, this time for the entropy production. Indeed, the latter can be taken as observable the $R(\omega_t)$ in (5.29), i.e.

$$\frac{\langle \Delta \Sigma^2_{\rm tot}\rangle_t}{\langle \Sigma_{\rm tot}\rangle_t} \geq 2\, k_B T\,. \tag{8.52}$$

This lower bound on a Fano factor contrasts with the upper bound of (8.49). These examples show that it is not trivial to predict which kind of inequalities may hold for non-autonomous, driven systems. Either upper and lower bounds can be found for Fano factors of thermodynamic observables not so different from each other.

8.4 Chapter conclusions

To conclude, in this chapter we presented a non-Markovian version of the VSR whose main use, at the moment, is the estimation of the parameters defining the non-Markovian memory kernel $\Gamma(t)$. We first tested the performances of our estimation method on simulated data obtaining a nearly perfect agreement between the estimated parameters and those used to simulate the data. Encouraged by this result, we apply the same method to experimental time traces of a bead attached to a DNA hairpin and trapped by optical tweezers. In this case, the estimated characteristic times seem to be too large if compared to the typical times associated to a molecular dynamics, such that of a jumping DNA hairpin. We believe that such overestimation is due to experimental noise (pink noise) and drift effects, which must be removed. As a consequence, a more complete and refined analysis of such traces is postponed to future work. Finally, we also show that the non-Markovian VSR leads to a lower bound to the Fano factor of the thermodynamic work (8.49) for a system dragged at constant velocity v, differently from the TUR which, instead, leads to an upper bound of the Fano factor for the total entropy production.

CHAPTER 9

CONCLUSIONS

In Brownian motion, from the variance of displacements it is possible to measure a physically relevant quantity as the diffusion constant or the friction coefficient of a particle. We have generalised this approach by providing variance sum rules for systems of confined particles, which can be used to infer other relevant parameters also for regimes far from equilibrium. Estimations of parameters and entropy production via a new formula are favoured by our approach. A specific sum rule is also used to estimate an effective memory kernel describing the dynamics of complex systems where many degrees of freedom are involved and where a detailed Markovian description of the system is hard to handle. All of this shows that the indetermination of stochastic motion is a resource that we should continue to understand and exploit for measuring physical quantities.

Of course, the very same variance is a negative factor for the precision of stochastic processes, as characterised by thermodynamic uncertainty relation. This says that dissipation is needed for having currents with low variance. Nevertheless, with the kinetic uncertainty relation we have shown that the degree of agitation, as quantified by the mean jumping rate in a discrete system, is a *kinetic* upper limit to precision as well. In fact, we have often found that it is the main limit to precision in systems far from equilibrium.

Let us conclude by listing again some original results we have discussed in this work

- A generalisation of the Laplace transform, which allows to study steady states of dragged particles (Chapter 3).
- The kinetic uncertainty relation (Section 5.3).
- Some uncertainty relations for systems with memory (Section 5.5).
- The exact solution of some linear models also in regimes not solved previously (Chapter 6).
- The variance sum rule for a multidimensional system, in which one observes a deviation from linearity of the sum of variances that quantifies non-equilibrium (Chapter 7).
- The variance sum rule for a non-Markovian system and its utility in estimating memory kernels (Chapter 8).
- A new formula for the entropy production rate, based on the variance sum rule at short times (Section 7.3.2.1).

APPENDIX A

APPENDICES

A.1 Appendix A: Limits of susceptibilities

In this section we discuss the limits of the position susceptibility defined in Laplace space as

$$\hat{\chi}_x(k) = [mk^2 + k\hat{\Gamma}(k) + \kappa]^{-1} \tag{A.1}$$

along with the limit of its integral and and of its derivative,

$$\chi(t) \equiv \int_0^t \mathrm{d}t' \chi_x(t')\,, \qquad\qquad \chi_v(t) \equiv \partial_t \chi_x(t)\,. \tag{A.2}$$

To this end we use that for a given function $g(t)$ it holds

$$\lim_{t\to 0} g(t) = \mathcal{L}_t^{-1}\left[\lim_{k\to\infty} \hat{g}(k)\right], \qquad \lim_{t\to\infty} g(t) = \mathcal{L}_t^{-1}\left[\lim_{k\to 0} \hat{g}(k)\right]. \tag{A.3}$$

We first consider the long time limit of the susceptibilities

$$\begin{aligned}
\lim_{t\to\infty} \chi_x(t) &= \mathcal{L}_t^{-1}\left[\lim_{k\to 0} \frac{1}{mk^2 + k\hat{\Gamma}(k) + \kappa}\right] \approx \mathcal{L}_t^{-1}\left[\frac{1}{\kappa}\right] = \frac{2\delta(t)}{\kappa} \overset{t\to\infty}{=} 0\,,\\
\lim_{t\to\infty} \chi(t) &= \mathcal{L}_t^{-1}\left[\lim_{k\to 0} \frac{1}{k(mk^2 + k\hat{\Gamma}(k) + \kappa)}\right] \approx \mathcal{L}_t^{-1}\left[\frac{1}{k\kappa}\right] = \frac{\theta(t)}{\kappa} \overset{t\to\infty}{=} 1/\kappa\,,\\
\lim_{t\to\infty} \chi_v(t) &= 0\,,
\end{aligned} \tag{A.4}$$

where the last line immediately follows from the first line. Note that all this limits do not depend on m and hence they hold for both underdamped and overdamped dynamics. Things become different in the limit of $t \to 0$, where the the mk^2 term becomes dominant. Indeed, for underdamped dynamics, i.e. for finite m, we get

$$\lim_{t\to 0} \chi_x^{\text{under}}(t) = \mathcal{L}_t^{-1}\left[\lim_{k\to\infty} [mk^2 + k\hat{\Gamma}(k) + \kappa]^{-1}\right] \approx \mathcal{L}_t^{-1}\left[\frac{1}{mk^2}\right] = \frac{t}{m} \overset{t\to 0}{=} 0\,, \tag{A.5}$$

where we used that $\lim_{k\to\infty} \dfrac{mk^2}{k\hat{\Gamma}(k)} \gg 1$. In fact $\hat{\Gamma}(k) \overset{k\to\infty}{\propto} k$ would correspond to ballistic motion which we do not consider, see [77] for more details. As for its integral and derivative of course we have that

$$\lim_{t\to 0} \chi^{\text{under}}(t) = \lim_{t\to 0} \int_0^t \mathrm{d}t' \chi_x^{\text{under}}(t') \approx \frac{t^2}{2m} \overset{t\to 0}{=} 0\,, \quad \lim_{t\to 0} \chi_v^{\text{under}}(t) = \lim_{t\to 0} \partial_t \chi_x^{\text{under}}(t) \approx \frac{1}{m}\,. \tag{A.6}$$

We see that this result does not depend on the kernel form, in fact inertial effects dominate the particle behaviour in the small time limit. Moreover, it is clear from the last formulae that one can not simply take the massless limit $m \to 0$ a posteriori to recover overdamped dynamics, because otherwise the limit of the susceptibilities would be ill defined. Instead, the correct procedure would correspond to calculate all the susceptibilities taking the mass m exactly equal to zero a priori, i.e. one should compute

$$\lim_{t\to 0} \chi_x^{\text{over}}(t) = \mathcal{L}_t^{-1}\left[\lim_{k\to\infty}[k\hat{\Gamma}(k)+\kappa]^{-1}\right] \tag{A.7}$$

that now depends on the details of the memory kernel. Consider for example a memory kernel consisting of a piece proportional to a Dirac delta, which alone would make the dynamics Markovian, plus a sum of exponentials.

$$\Gamma^{\text{exp}}(t) = 2\gamma_0\delta(t) + \sum_i \frac{\gamma_i}{\tau_i} e^{-t/\tau_i}\,, \tag{A.8}$$

Its Laplace transform is equal to

$$\hat{\Gamma}^{\text{exp}}(k) = \gamma_0 + \sum_i \frac{\gamma_i}{1+k\tau_i}\,. \tag{A.9}$$

This is an important example, as a finite sum of appropriately chosen exponentials can approximate, up to a certain time scale, every memory kernel even if $\widehat{\gamma}$ does not converge, see [77] for more details.

Going back to the overdamped susceptibility, we have that

$$\begin{aligned}\lim_{t\to 0}\chi_x^{\text{exp, over}}(t) &= \mathcal{L}_t^{-1}\left[\lim_{k\to\infty}[k\hat{\Gamma}^{\text{exp}}(k)+\kappa]^{-1}\right] \approx \mathcal{L}_t^{-1}\left[\frac{1}{k\gamma_0(1+\frac{1}{k\gamma_0}\sum_i\frac{\gamma_i}{\tau_i}+\frac{\kappa}{k\gamma_0})}\right] \approx \\ &\approx \mathcal{L}_t^{-1}\left[\frac{1}{k\gamma_0} - \frac{1}{(k\gamma_0)^2}\left(\sum_i\frac{\gamma_i}{\tau_i}+\kappa\right)\right] = \frac{1}{\gamma_0} - \frac{t}{\gamma_0^2}\left(\sum_i\frac{\gamma_i}{\tau_i}+\kappa\right)\,,\end{aligned} \tag{A.10}$$

$$\lim_{t\to 0}\chi^{\text{exp, over}}(t) = \lim_{t\to 0}\int_0^t dt'\chi_x^{\text{exp, over}}(t') \approx \frac{t}{\gamma_0} \overset{t\to 0}{=} 0\,, \tag{A.11}$$

$$\lim_{t\to 0}\chi_v^{\text{exp, over}}(t) = \lim_{t\to 0}\partial_t\chi_x^{\text{exp, over}}(t) \approx -\frac{1}{\gamma_0^2}\left(\sum_i\frac{\gamma_i}{\tau_i}+\kappa\right)\,. \tag{A.12}$$

We see that that, for this particular kernel, the overdamped limit requires the presence of the piece proportional to the Dirac delta. A more detailed discussion of this problem can be found in [87].

A.2 Appendix B: Calculation of $\mathcal{C}(t',t'')$

This appendix is dedicated to the calculation of the following quantity

$$\begin{aligned}\mathcal{C}(t',t'') = \langle\phi(t')\phi(t'')\rangle &= \int_{t_m}^{t'} ds' \int_{t_m}^{t''} ds''\chi_x(t'-s')\chi_x\left(t''-s''\right)\langle\eta(s')\eta\left(s''\right)\rangle = \\ &= k_BT\int_{t_m}^{t'} ds' \int_{t_m}^{t''} ds''\chi_x(t'-s')\chi_x\left(t''-s''\right)\Gamma\left(|s'-s''|\right)\,.\end{aligned} \tag{A.13}$$

In the last line we used the second fluctuation-dissipation theorem $\langle \eta(t')\eta(t'')\rangle = k_B T \Gamma(|t'-t''|)$ that relates the correlation of the noise to the memory kernel. Taking the double modified Laplace transform of both sides of equation (A.13) we get

$$\begin{aligned}
&\beta \mathcal{L}_{k'}^{t_m}\left[\mathcal{L}_{k''}^{t_m}\left[C(t',t'')\right]\right] = \\
&= \int_{t_m}^{\infty} \mathrm{d}t' \mathrm{e}^{-k't'} \int_{t_m}^{\infty} \mathrm{d}t'' \mathrm{e}^{-k''t''} \int_{t_m}^{t'} \mathrm{d}s' \int_{t_m}^{t''} \mathrm{d}s'' \chi_x(t'-s')\chi_x\left(t''-s''\right)\Gamma\left(|s'-s''|\right) = \\
&= \int_{t_m}^{\infty} \mathrm{d}s' \int_{t_m}^{\infty} \mathrm{d}s'' \int_{s'}^{\infty} \mathrm{d}t' \mathrm{e}^{-k't'} \int_{s''}^{\infty} \mathrm{d}t'' \mathrm{e}^{-k''t''} \chi_x(t'-s')\chi_x\left(t''-s''\right)\Gamma\left(|s'-s''|\right) = \\
&= \int_{t_m}^{\infty} \mathrm{d}s' \mathrm{e}^{-k's'} \int_{t_m}^{\infty} \mathrm{d}s'' \mathrm{e}^{-k''s''} \int_{0}^{\infty} \mathrm{d}u' \mathrm{e}^{-k'u'} \int_{0}^{\infty} \mathrm{d}u'' \mathrm{e}^{-k''u''} \chi_x(u')\chi_x\left(u''\right)\Gamma\left(|s'-s''|\right) = \\
&= \hat{\chi}_x(k')\hat{\chi}_x\left(k''\right) \int_{t_m}^{\infty} \mathrm{d}s' \mathrm{e}^{-k's'} \int_{t_m}^{\infty} \mathrm{d}s'' \mathrm{e}^{-k''s''} \Gamma\left(|s'-s''|\right) ,
\end{aligned} \tag{A.14}$$

where $\beta = 1/k_B T$ as usual. Moreover, we again used that $\int_{t_m}^{\infty} \mathrm{d}t \int_{t_m}^{t} \mathrm{d}t' = \int_{t_m}^{\infty} \mathrm{d}t' \int_{t'}^{\infty} \mathrm{d}t$ between the second and the third line and then we made the change of variable $u = t - s$. Focusing on the remaining integrals, we have that

$$\begin{aligned}
&\int_{t_m}^{\infty} \mathrm{d}s' \mathrm{e}^{-k's'} \int_{t_m}^{\infty} \mathrm{d}s'' \mathrm{e}^{-k''s''} \Gamma\left(|s'-s''|\right) = \\
&= \int_{t_m}^{\infty} \mathrm{d}s' \int_{t_m}^{\infty} \mathrm{d}s'' \mathrm{e}^{-k'(s'-s'')} \mathrm{e}^{-s''(k'+k'')} \Gamma\left(|s'-s''|\right) = \\
&\overset{\sigma = s'-s''}{=} \int_{t_m}^{\infty} \mathrm{d}s'' \mathrm{e}^{-s''(k'+k'')} \int_{t_m - s''}^{\infty} \mathrm{d}\sigma\, \mathrm{e}^{-k'\sigma} \Gamma\left(|\sigma|\right) = \\
&= \int_{t_m}^{\infty} \mathrm{d}s'' \mathrm{e}^{-s''(k'+k'')} \left(\int_{0}^{\infty} \mathrm{d}\sigma\, \mathrm{e}^{-k'\sigma} \Gamma\left(\sigma\right) + \int_{t_m - s''}^{0} \mathrm{d}\sigma\, \mathrm{e}^{-k'\sigma} \Gamma\left(-\sigma\right) \right) = \\
&= \frac{\mathrm{e}^{-t_m(k'+k'')}}{k'+k''} \hat{\Gamma}(k') + \int_{t_m}^{\infty} \mathrm{d}s'' \mathrm{e}^{-s''(k'+k'')} \int_{t_m - s''}^{0} \mathrm{d}\sigma\, \mathrm{e}^{-k'\sigma} \Gamma\left(-\sigma\right) ,
\end{aligned} \tag{A.15}$$

where in the last line we recognised the Laplace transform of $\Gamma(t)$ and used that

$$\int_{t_m}^{\infty} \mathrm{d}s'' \mathrm{e}^{-s''(k'+k'')} = \frac{\mathrm{e}^{-t_m(k'+k'')}}{k'+k''} . \tag{A.16}$$

As for the second term in the last line of equation (A.15), using integration by parts we get

$$\begin{aligned}
&\int_{t_m}^{\infty} \mathrm{d}s'' \mathrm{e}^{-s''(k'+k'')} \int_{t_m - s''}^{0} \mathrm{d}\sigma\, \mathrm{e}^{-k'\sigma} \Gamma\left(-\sigma\right) = \\
&= -\left(\frac{\mathrm{e}^{-s''(k'+k'')}}{k'+k''} \int_{t_m - s''}^{0} \mathrm{d}\sigma\, \mathrm{e}^{-k'\sigma} \Gamma\left(-\sigma\right) \right) \Big|_{t_m}^{\infty} + \int_{t_m}^{\infty} \mathrm{d}s'' \frac{\mathrm{e}^{-k''s''-k't_m}}{k'+k''} \Gamma\left(s''-t_m\right) = \\
&= \int_{t_m}^{\infty} \mathrm{d}s'' \frac{\mathrm{e}^{-k''s''-k't_m}}{k'+k''} \Gamma\left(s''-t_m\right) \overset{u = s''-t_m}{=} \frac{\mathrm{e}^{-t_m(k'+k'')}}{k'+k''} \hat{\Gamma}(k'') .
\end{aligned} \tag{A.17}$$

where we noted that the first term in the second line is equal to zero. Going back to equation (A.15) and remembering that we started from (A.14) we finally obtain

$$\beta\mathcal{L}^{t_m}_{k'}\left[\mathcal{L}^{t_m}_{k''}\left[\mathcal{C}(t',t'')\right]\right] = \hat{\chi}_x(k')\hat{\chi}_x\left(k''\right)\frac{\hat{\Gamma}(k')+\hat{\Gamma}(k'')}{k'+k''}\mathrm{e}^{-t_m(k'+k'')}\,. \tag{A.18}$$

Recalling the definition of the position susceptibility via its Laplace transform and its relation with the memory kernel $\hat{\chi}_x(k) = [mk^2 + k\hat{\Gamma}(k) + \kappa]^{-1}$ and doing some algebra it is possible to show that

$$\begin{aligned}\beta\mathcal{L}^{t_m}_{k'}\left[\mathcal{L}^{t_m}_{k''}\left[\mathcal{C}(t',t'')\right]\right] =& \left[\frac{\hat{\chi}_x(k')}{k''(k'+k'')} + \frac{\hat{\chi}_x(k'')}{k'(k'+k'')} + \right.\\ &\left. - \kappa\frac{\hat{\chi}_x(k')}{k'}\frac{\hat{\chi}_x(k'')}{k''} - m\hat{\chi}_x(k')\hat{\chi}_x(k'')\right]\mathrm{e}^{-t_m(k'+k'')}\,.\end{aligned} \tag{A.19}$$

The inverse transformation back to real time yields

$$\begin{aligned}\beta\mathcal{C}(t',t'') =& \mathcal{L}^{t_m,-1}_{t'}\left[\hat{\chi}_x(k')\mathrm{e}^{-t_mk'}\mathcal{L}^{t_m,-1}_{t''}\left[\frac{\mathrm{e}^{-t_mk''}}{k''(k'+k'')}\right]\right] + \\ &+ \mathcal{L}^{t_m,-1}_{t''}\left[\hat{\chi}_x(k'')\mathrm{e}^{-t_mk''}\mathcal{L}^{t_m,-1}_{t'}\left[\frac{\mathrm{e}^{-t_mk'}}{k'(k'+k'')}\right]\right] + \\ &- \kappa\mathcal{L}^{t_m,-1}_{t'}\left[\frac{\hat{\chi}_x(k')\mathrm{e}^{-t_mk'}}{k'}\right]\mathcal{L}^{t_m,-1}_{t''}\left[\frac{\hat{\chi}_x(k'')\mathrm{e}^{-t_mk''}}{k''}\right] + \\ &- m\mathcal{L}^{t_m,-1}_{t'}\left[\hat{\chi}_x(k')\mathrm{e}^{-t_mk'}\right]\mathcal{L}^{t_m,-1}_{t''}\left[\hat{\chi}_x(k'')\mathrm{e}^{-t_mk''}\right]\,.\end{aligned} \tag{A.20}$$

Using that

$$\mathcal{L}^{t_m,-1}_{t'}\left[\frac{1}{k'(k'+k'')}\right] = \frac{1}{k''} - \frac{\mathrm{e}^{-t'k''}}{k''}\,, \qquad \mathcal{L}^{t_m,-1}_{t'}\left[\mathrm{e}^{-t_mk'}\right] = 2\delta(t'-t_m)\,, \tag{A.21}$$

along with the generalised convolution theorem, we are able to show that (A.20) becomes

$$\begin{aligned}\mathcal{C}(t',t'') =& k_BT\Big[\chi(t'-t_m) + \chi(t''-t_m) - \theta(t'-t'')\chi(t'-t'') + \\ &- \theta(t''-t')\chi(t''-t') - \kappa\chi(t'-t_m)\chi(t''-t_m) - m\chi_x(t'-t_m)\chi_x(t''-t_m)\Big]\,.\end{aligned} \tag{A.22}$$

A.3 Multidimensional covariance matrix

We show how to calculate the components of the $2n \times 2n$ covariance matrix associated to the multidimensional GLE (5.109). In order to do so, we use the expressions for the position and velocity which read

$$x^i(t) = x^i_{t_m}\left(1 - \kappa^i\chi^i(t-t_m)\right) + mv^i_{t_m}\chi^i_x(t-t_m) + \int_{t_m}^{t}\mathrm{d}t'\chi^i_x(t-t')\left[F^i(t') + \eta^i(t')\right]\,, \tag{A.23}$$

$$v^i(t) = -\kappa^i x^i_{t_m}\chi^i_x(t-t_m) + m v^i_{t_m}\chi^i_v(t-t_m) + \int_{t_m}^{t} \mathrm{d}t' \chi^i_v(t-t')\left[F^i(t') + \eta^i(t')\right]. \tag{A.24}$$

The velocity, if not averaged, is not defined in the overdamped limit (there should be an additional term of the form $\chi^i_x(0)(F^t + \eta^i(t))$ which is singular for overdamped dynamics and equal to zero in the underdamped case). Nevertheless, for $m = 0$, the covariance matrix has only $n \times n$ components and the cross correlation between position and velocity are not needed to define such matrix. Hence the expression above perfectly works for our scopes. In a similar way as done in [80] we define

$$\phi^i(t) = \int_{t_m}^{t} \mathrm{d}t' \chi^i_x(t-t')\eta^i(t') \tag{A.25}$$

and, by doing so, one can show that

$$\begin{aligned}\mathcal{C}_{ij}(t',t'') =& \langle \phi^i(t')\phi^j(t'')\rangle = \int_{t_m}^{t'} \mathrm{d}s' \int_{t_m}^{t''} \mathrm{d}s'' \chi^i_x(t'-s')\chi^j_x\left(t''-s''\right)\langle \eta^i(s')\eta^j\left(s''\right)\rangle \\ =& k_B T_i \delta_{ij}\Big[\chi^i(t'-t_m) + \chi^i(t''-t_m) - \theta(t'-t'')\chi(t'-t'') - \theta(t''-t')\chi^i(t''-t') + \\ & - \kappa^i\chi^i(t'-t_m)\chi^i(t''-t_m) - m\chi^i_x(t'-t_m)\chi^i_x(t''-t_m)\Big].\end{aligned} \tag{A.26}$$

Using this result, one can finally calculate the four matrices composing the the multidimensional covariance matrix

$$\mathcal{S}_{t,t_m} = \begin{pmatrix} \mathrm{Cov}_{t_m}(x^i_t, x^j_t) & \mathrm{Cov}_{t_m}(x^i_t, v^j_t) \\ \mathrm{Cov}^T_{t_m}(x^i_t, v^j_t) & \mathrm{Cov}_{t_m}(v^i_t, v^j_t) \end{pmatrix} \tag{A.27}$$

that are respectively

$$\begin{aligned}\mathrm{Cov}_{t_m}(x^i_t, x^j_t) =& \langle x^i x^j\rangle_{t_m,t} - \langle x^i\rangle_{t_m,t}\langle x^j\rangle_{t_m,t} = \\ =& \mathrm{Cov}(x^i_{t_m}, x^j_{t_m})\left(1-\kappa^i\chi^i(t-t_m)\right)\left(1-\kappa^j\chi^j(t-t_m)\right) + \\ & + m\mathrm{Cov}_{t_m}(x^i_{t_m}, v^j_{t_m})\left(1-\kappa^i\chi^i(t-t_m)\right)\chi^j_x(t-t_m) + \\ & + m\mathrm{Cov}_{t_m}(x^j_{t_m}, v^i_{t_m})\left(1-\kappa^j\chi^j(t-t_m)\right)\chi^i_x(t-t_m) + \\ & + m^2\mathrm{Cov}_{t_m}(v^i_{t_m}, v^j_{t_m})\chi^i_x(t-t_m)\chi^j_x(t-t_m) + \\ & + k_B T^i \mathcal{C}_{ij}(t,t) = \\ =& \mathrm{Cov}(x^i_{t_m}, x^j_{t_m})\left(1-\kappa^i\chi^i(t-t_m)\right)\left(1-\kappa^j\chi^j(t-t_m)\right) + \\ & + m\mathrm{Cov}_{t_m}(x^i_{t_m}, v^j_{t_m})\left(1-\kappa^i\chi^i(t-t_m)\right)\chi^j_x(t-t_m) + \\ & + m\mathrm{Cov}_{t_m}(x^j_{t_m}, v^i_{t_m})\left(1-\kappa^j\chi^j(t-t_m)\right)\chi^i_x(t-t_m) + \\ & + m^2\mathrm{Cov}_{t_m}(v^i_{t_m}, v^j_{t_m})\chi^i_x(t-t_m)\chi^j_x(t-t_m) + \\ & + k_B T^i\delta_{ij}\left[2\chi^i(t-t_m) - \kappa^i\left(\chi^i(t-t_m)\right)^2 - m\left(\chi^i_x(t-t_m)\right)^2\right],\end{aligned} \tag{A.28}$$

$$
\begin{aligned}
\mathrm{Cov}_{t_m}(x^i_t, v^j_t) =& \langle x^i v^j \rangle_{t_m,t} - \langle x^i \rangle_{t_m,t} \langle v^j \rangle_{t_m,t} = \\
=& -\kappa^j \mathrm{Cov}(x^i_{t_m}, x^j_{t_m}) \left(1 - \kappa^i \chi^i(t-t_m)\right) \chi^j_x(t-t_m) + \\
&+ m \mathrm{Cov}_{t_m}(x^i_{t_m}, v^j_{t_m}) \left(1 - \kappa^i \chi^i(t-t_m)\right) \chi^j_v(t-t_m) + \\
&- m\kappa^j \mathrm{Cov}_{t_m}(x^j_{t_m}, v^i_{t_m}) \chi^j_x(t-t_m) \chi^i_x(t-t_m) + \\
&+ m^2 \mathrm{Cov}_{t_m}(v^i_t, v^j_t) \chi^i_x(t-t_m) \chi^j_v(t-t_m) + \\
&+ k_B T^i \left(\partial_{t'} \mathcal{C}_{ij}(t', t'') \Big|_{t'=t''=t} = \right. \\
=& -\kappa^j \mathrm{Cov}(x^i_{t_m}, x^j_{t_m}) \left(1 - \kappa^i \chi^i(t-t_m)\right) \chi^j_x(t-t_m) + \\
&+ m \mathrm{Cov}_{t_m}(x^i_{t_m}, v^j_{t_m}) \left(1 - \kappa^i \chi^i(t-t_m)\right) \chi^j_v(t-t_m) + \\
&- m\kappa^j \mathrm{Cov}_{t_m}(x^j_{t_m}, v^i_{t_m}) \chi^j_x(t-t_m) \chi^i_x(t-t_m) + \\
&+ m^2 \mathrm{Cov}_{t_m}(v^i_{t_m}, v^j_{t_m}) \chi^i_x(t-t_m) \chi^j_v(t-t_m) + \\
&+ k_B T^i \delta_{ij} \Big[\chi^i_x(t-t_m) - \kappa^i \chi^i_x(t-t_m) \chi^i(t-t_m) - \\
&- m \chi^i_v(t-t_m) \chi^i_x(t-t_m) \Big],
\end{aligned}
\tag{A.29}
$$

$$
\begin{aligned}
\mathrm{Cov}_{t_m}(v^i_{t_m}, v^j_{t_m}) =& \langle v^i v^j \rangle_{t_m,t} - \langle v^i \rangle_{t_m,t} \langle v^j \rangle_{t_m,t} = \\
=& \kappa^j \kappa^i \mathrm{Cov}(x^i_{t_m}, x^j_{t_m}) \chi^i(t-t_m) \chi^j_x(t-t_m) + \\
&- m\kappa^i \mathrm{Cov}_{t_m}(x^i_{t_m}, v^j_{t_m}) \chi^i_x(t-t_m) \chi^j_v(t-t_m) + \\
&- m\kappa^j \mathrm{Cov}_{t_m}(x^j_{t_m}, v^i_{t_m}) \chi^j_x(t-t_m) \chi^i_v(t-t_m) + \\
&+ m^2 \mathrm{Cov}_{t_m}(v^i_{t_m}, v^j_{t_m}) \chi^i_v(t-t_m) \chi^j_v(t-t_m) + \\
&+ k_B T^i \left(\partial_{t'} \partial_{t''} \mathcal{C}_{ij}(t', t'') \Big|_{t'=t''=t} = \right. \\
=& \kappa^j \kappa^i \mathrm{Cov}(x^i_{t_m}, x^j_{t_m}) \chi^i(t-t_m) \chi^j_x(t-t_m) + \\
&- m\kappa^i \mathrm{Cov}_{t_m}(x^i_{t_m}, v^j_{t_m}) \chi^i_x(t-t_m) \chi^j_v(t-t_m) + \\
&- m\kappa^j \mathrm{Cov}_{t_m}(x^j_{t_m}, v^i_{t_m}) \chi^j_x(t-t_m) \chi^i_v(t-t_m) + \\
&+ m^2 \mathrm{Cov}_{t_m}(v^i_{t_m}, v^j_{t_m}) \chi^i_v(t-t_m) \chi^j_v(t-t_m) + \\
&+ k_B T^i \delta_{ij} \Big[\frac{1}{m} - \kappa^i \left(\chi^i_x(t'-t_m) \right)^2 - m \left(\chi^i_v(t'-t_m) \right)^2 \Big].
\end{aligned}
\tag{A.30}
$$

BIBLIOGRAPHY

[1] A. Einstein. *Über die von der molekularkinetischen Theorie der Wärme geforderte Bewegung von in ruhenden Flüssigkeiten suspendierten Teilchen*. Annalen der Physik **4** (1905).

[2] I. Goychuk, V. O. Kharchenko, and R. Metzler. *How Molecular Motors Work in the Crowded Environment of Living Cells: Coexistence and Efficiency of Normal and Anomalous Transport*. PLoS One **9** e91700 (2014).

[3] M. Baiesi and C. Maes. *Life efficiency does not always increase with the dissipation rate*. J. Phys. Comm. **2** 045017 (2018).

[4] A. C. Barato and U. Seifert. *Thermodynamic Uncertainty Relation for Biomolecular Processes*. Phys. Rev. Lett. **114** 158101 (2015).

[5] P. Pietzonka, A. C. Barato, and U. Seifert. *Universal bound on the efficiency of molecular motors*. J. Stat. Mech. page 124004 (2016).

[6] M. Polettini, A. Lazarescu, and M. Esposito. *Tightening the uncertainty principle for stochastic currents*. Phys. Rev. E **94** 052104 (2016).

[7] T. R. Gingrich, J. M. Horowitz, N. Perunov, and J. L. England. *Dissipation Bounds All Steady-State Current Fluctuations*. Phys. Rev. Lett. **116** 120601 (2016).

[8] C. Nardini and H. Touchette. *Process interpretation of current entropic bounds*. Eur. Phys. J. B **91** 16 (2018).

[9] P. Pietzonka, F. Ritort, and U. Seifert. *Finite-time generalization of the thermodynamic uncertainty relation*. Phys. Rev. E **96** 012101 (2017).

[10] T. R. Gingrich, G. M. Rotskoff, and J. M. Horowitz. *Inferring dissipation from current fluctuations*. J. Phys. A: Math. Gen **50** 184004 (2017).

[11] J. M. Horowitz and T. R. Gingrich. *Proof of the finite-time thermodynamic uncertainty relation for steady-state currents*. Phys. Rev. E **96** 020103 (2017).

[12] K. Proesmans and C. Van den Broeck. *Discrete-time thermodynamic uncertainty relation*. EPL **119** 20001 (2017).

[13] K. Macieszczak, K. Brandner, and J. P. Garrahan. *Unified Thermodynamic Uncertainty Relations in Linear Response*. Phys. Rev. Lett. **121** 130601 (2018).

[14] A. Dechant and S.-i. Sasa. *Current fluctuations and transport efficiency for general Langevin systems*. J. Stat. Mech. page 063209 (2018).

[15] S. Ito and A. Dechant. *Stochastic Time Evolution, Information Geometry, and the Cramér-Rao Bound*. Physical Review X **10** 021056 (2020).

[16] A. M. Timpanaro, G. Guarnier, J. Goold, and G. T. Landi. *Thermodynamic Uncertainty Relations from Exchange Fluctuation Theorems*. Phys. Rev. Lett. **123** 090604 (2019).

[17] D. M. Busiello and S. Pigolotti. *Hyperaccurate currents in stochastic thermodynamics*. Phys. Rev. E **100** 060102 (2019).

[18] A. Dechant. *Multidimensional thermodynamic uncertainty relations*. J. Phys. A: Math. Theor. **52** 035001 (2019).

[19] A. Dechant and S.-i. Sasa. *Fluctuation–response inequality out of equilibrium*. Proc. Natl. Acad. Sci. **117** 6430 (2020).

[20] T. Koyuk and U. Seifert. *Thermodynamic uncertainty relation for time-dependent driving*. Physical Review Letters **125** 260604 (2020).

[21] P. Fischer, H.-M. Chun, and U. Seifert. *Free diffusion bounds the precision of currents in underdamped dynamics*. Phys. Rev. E **102** 012120 (2022).

[22] P. Pietzonka, A. C. Barato, and U. Seifert. *Universal bounds on current fluctuations*. Phys. Rev. E **93** 052145 (2016).

[23] J. P. Garrahan. *Simple bounds on fluctuations and uncertainty relations for first-passage times of counting observables*. Phys. Rev. E **95** 032134 (2017).

[24] D. Chiuchiu and S. Pigolotti. *Mapping of uncertainty relations between continuous and discrete time*. Phys. Rev. E **97** 032109 (2018).

[25] G. Gallavotti and E. G. D. Cohen. *Dynamical ensembles in nonequilibrium statistical mechanics*. Phys. Rev. Lett. **74** 2694 (1995).

[26] C. Maes, F. Redig, and A. Van Moffaert. *On the definition of entropy production, via examples*. J. Mat. Phys. **41** 1528 (2000).

[27] C. Maes and K. Netočný. *Time-reversal and Entropy*. J. Stat. Phys. **110** 269 (2003).

[28] C. Maes. *On the origin and the use of fluctuation relations for the entropy*. Séminaire Poincaré **2** 29 (2003).

[29] C. Maes and M. H. van Wieren. *Time-Symmetric Fluctuations in Nonequilibrium Systems*. Phys. Rev. Lett. **96** 240601 (2006).

[30] P. Baerts, U. Basu, C. Maes, and S. Safaverdi. *Frenetic origin of negative differential response*. Phys. Rev. E **88** 052109 (2013).

[31] C. J. Fullerton and R. L. Jack. *Dynamical phase transitions in supercooled liquids: Interpreting measurements of dynamical activity*. J. Chem. Phys. **138** 224506 (2013).

[32] C. Maes. *Frenetic Bounds on the Entropy Production*. Phys. Rev. Lett. **119** 160601 (2017).

[33] U. Basu and C. Maes. *Nonequilibrium Response and Frenesy*. J. of Phys.: Conf. Ser. **638** 012001 (2015).

[34] U. Basu, M. Krüger, A. Lazarescu, and C. Maes. *Frenetic aspects of second order response*. Phys. Chemistry Chem. Physics **17** 6653 (2015).

[35] M. Baiesi and G. Falasco. *Inflow rate, a time-symmetric observable obeying fluctuation relations*. Phys. Rev. E **92** 042162 (2015).

[36] U. Seifert and T. Speck. *Fluctuation-dissipation theorem in nonequilibrium steady states*. Europhys. Lett. **89** 10007 (2010).

[37] R. Kubo. *The fluctuation-dissipation theorem*. Rep. Prog. Phys. **29** 255 (1966).

[38] L. Boltzmann. *Weitere Studien über das Wärmegleichgewicht unter Gasmolekülen*. Sitzungberichte der Kaiserlichen Akademie der Wissenschaften **66** 275–370 (1877).

[39] L. Boltzmann. *On the Relationship between the Second Fundamental Theorem of the Mechanical Theory of Heat and Probability Calculations Regarding the Conditions for Thermal Equilibrium*. Sitzungberichte der Kaiserlichen Akademie der Wissenschaften **76** (1877).

[40] J. W. Gibbs. *Elementary principles in statistical mechanics developed with especial reference to the rational foundation of thermodynamics*. New York: C. Scribner 1902.

[41] P. Langevin. *Sur la théorie du mouvement Brownien*. Comptes Rendus Hebdomadaires des Seances de l'Academie des Sciences **46** 530–533 (1908).

[42] U. Seifert. *Stochastic thermodynamics, fluctuation theorems and molecular machines*. Reports on Progress in Physics **75** 126001 (2012).

[43] E. Lippiello, F. Corberi, and M. Zannetti. *Off-equilibrium generalization of the fluctuation dissipation theorem for Ising spins and measurement of the linear response function*. Phys. Rev. E **71** 036104 (2005).

[44] E. Lippiello, F. Corberi, and M. Zannetti. *Fluctuation dissipation relations far from equilibrium*. J. Stat. Mech. page 07002 (2007).

[45] E. Lippiello, F. Corberi, A. Sarracino, and M. Zannetti. *Nonlinear response and fluctuation dissipation relations*. Phys. Rev. E **78** 041120 (2008).

[46] M. Baiesi, C. Maes, and B. Wynants. *Fluctuations and response of nonequilibrium states*. Phys. Rev. Lett. **103** 010602 (2009).

[47] M. Baiesi, C. Maes, and B. Wynants. *Nonequilibrium Linear Response for Markov Dynamics, I: Jump Processes and Overdamped Diffusions*. J. Stat. Phys. **137** 1094 (2009).

[48] M. Baiesi, E. Boksenbojm, C. Maes, and B. Wynants. *Linear response of nonequilibrium states, II: inertial dynamics*. J. Stat. Phys. **139** 492 (2010).

[49] C. Maes and B. Wynants. *On a response function and its interpretation*. Markov Proc. Rel. Fields **16** 45 (2010).

[50] M. Baiesi, C. Maes, and B. Wynants. *The modified Sutherland-Einstein relation for diffusive non-equilibria*. Proc. Royal Soc. A **467** 2792 (2011).

[51] M. Baiesi and C. Maes. *An update on the nonequilibrium linear response*. New J. Phys. **15** 013004 (2013).

[52] C. Maes. *Frenesy: Time-symmetric dynamical activity in nonequilibria*. Physics Reports **850** 1 (2020).

[53] C. Maes. *Non-Dissipative Effects in Nonequilibrium Systems*. Springer Briefs in Complexity. Springer Cham, Switzerland 2018.

[54] G. E. Crooks. *Nonequilibrium measurements of free energy differences for microscopically reversible Markovian systems*. J. Stat. Phys. **90** 1481 (1998).

[55] G. Crooks. *Entropy production fluctuation theorem and the nonequilibrium work relation for free energy differences*. Phys. Rev. E **60** 27212726 (1999).

[56] P. G. Bergmann and J. L. Lebowitz. *New Approach to Nonequilibrium Processes*. Phys. Rev. **99** 578 (1955).

[57] S. Katz, J. Lebowitz, and H. Spohn. *Nonequilibrium steady states of stochastic lattice gas models of fast ionic conductors*. Journal of Statistical Physics **34** 497 (1984).

[58] S. Katz, J. L. Lebowitz, and H. Spohn. *Phase transitions in stationary nonequilibrium states of model lattice systems*. Phys. Rev. B **28** 1655 (1983).

[59] J. Schnakenberg. *Network theory of microscopic and macroscopic behavior of master equation systems*. Rev. Mod. Phys. **48** 571 (1976).

[60] H. Kramers. *Brownian motion in a field of force and the diffusion model of chemical reactions*. Physica **7** 284 (1940).

[61] J. E. Moyal. *Stochastic Processes and Statistical Physics*. Journal of the Royal Statistical Society. Series B (Methodological) **11** 150 (1949).

[62] H. Risken. *The Fokker-Planck Equation*. Springer-Verlag Berlin 2nd edition 1989.

[63] C. W. Gardiner. *Handbook of stochastic methods for physics, chemistry and the natural sciences* volume 13 of *Springer Series in Synergetics*. Springer-Verlag Berlin third edition 2004.

[64] R. E. Spinney and I. J. Ford. *Entropy production in full phase space for continuous stochastic dynamics*. Phys. Rev. E **85** 051113 (2012).

[65] K. Sekimoto. *Stochastic Energetics* volume 799 of *Lecture Notes in Physics*. Springer 2010.

[66] R. van Zon and E. G. D. Cohen. *Stationary and transient work-fluctuation theorems for a dragged Brownian particle*. Phys. Rev. E **67** 046102 (2003).

[67] M. Baiesi, T. Jacobs, C. Maes, and N. S. Skantzos. *Fluctuation symmetries for work and heat*. Phys. Rev. E **74** 021111 (2006).

[68] L. Rondoni and C. Mejia-Monasterio. *Fluctuations in nonequilibrium statistical mechanics: models, mathematical theory, physical mechanisms*. Nonlinearity **20** R1 (2007).

[69] S. Ciliberto. *From space-time chaos to stochastic thermodynamics*. Comptes Rendus Physique **20** 529 (2019).

[70] G. R. Kneller and K. Hinsen. *Fractional Brownian dynamics in proteins*. The Journal of Chemical Physics **121** 10278 (2004).

[71] W. Min, G. Luo, B. J. Cherayil, S. C. Kou, and X. S. Xie. *Observation of a Power-Law Memory Kernel for Fluctuations within a Single Protein Molecule*. Phys. Rev. Lett. **94** 198302 (2005).

[72] R. Zwanzig. *Nonequilibrium statistical mechanics*. Oxford University Press 2001.

[73] U. Weiss. *Quantum dissipative systems* volume 13. World scientific 2012.

[74] H. Mori. *Transport, Collective Motion, and Brownian Motion*)*. Progress of Theoretical Physics **33** 423 (1965).

[75] E. Fodor, D. Grebenkov, P. Visco, and F. Wijland. *Generalized Langevin Equation with Hydrodynamic Backflow: Equilibrium Properties*. Physica A: Statistical Mechanics and its Applications **422** 107112 (2014).

[76] V. Lisy and J. Tóthová. *Generalized Langevin equation and the fluctuation-dissipation theorem for particle-bath systems in a harmonic field*. Results in Physics **12** 12121213 (2019).

[77] I. Goychuk. *Viscoelastic subdiffusion: Generalized Langevin equation approach*. Advances in Chemical Physics **150** 187 (2013).

[78] D. Molina-Garcia, T. Sandev, H. Safdari, G. Pagnini, A. Chechkin, and R. Metzler. *Crossover from anomalous to normal diffusion: truncated power-law noise correlations and applications to dynamics in lipid bilayers*. New Journal of Physics **20** 103027 (2018).

[79] R. F. Fox. *The generalized Langevin equation with Gaussian fluctuations*. Journal of Mathematical Physics **18** (1977).

[80] I. Di Terlizzi, F. Ritort, and M. Baiesi. *Explicit solution of the generalised Langevin equation*. J. Stat. Phys. **181** 1609 (2020).

[81] T. Mai and A. Dhar. *Nonequilibrium work fluctuations for oscillators in non-Markovian baths*. Phys. Rev. E **75** 061101 (2007).

[82] J. Berner, B. Müller, J. R. Gomez-Solano, M. Krüger, and C. Bechinger. *Oscillating modes of driven colloids in overdamped systems*. Nature communications **9** 1 (2018).

[83] S. Loos and S. Klapp. *Heat flow due to time-delayed feedback*. Scientific Reports **9** 2491 (2018).

[84] T. Speck and U. Seifert. *The Jarzynski relation, fluctuation theorems, and stochastic thermodynamics for non-Markovian processes*. Journal of Statistical Mechanics: Theory and Experiment **2007** L09002 (2007).

[85] A. Cairoli, R. Klages, and A. Baule. *Weak Galilean invariance as a selection principle for coarse-grained diffusive models*. Proceedings of the National Academy of Sciences **115** 5714 (2018).

[86] M. Tassieri. *Microrheology with Optical Tweezers: Principles and Applications* chapter 6. Pan Stanford Publishing Singapore 2016.

[87] E. d. S. Nascimento and W. A. Morgado. *Non-Markovian effects on overdamped systems*. EPL (Europhysics Letters) **126** 10002 (2019).

[88] T. Van Vu and Y. Hasegawa. *Uncertainty relations for time-delayed Langevin systems*. Phys. Rev. E **100** 012134 (2019).

[89] T. Van Vu and Y. Hasegawa. *Uncertainty relation under information measurement and feedback control*. J. Phys. A: Math. Gen **53** 075001 (2020).

[90] S. ichi Amari. *Information Geometry and Its Applications*. Applied mathematical sciences 194. Springer 1st ed. edition 2016.

[91] S. M. Carroll. *Spacetime and geometry*. Cambridge University Press 2019.

[92] H. Poincaré. *Analysis Situs*. Journal de l'École Polytechniqu **2** 1–123 (1895).

[93] S. Ito. *Stochastic Thermodynamic Interpretation of Information Geometry*. Phys. Rev. Lett. **121** 030605 (2018).

[94] A. K. Bhattacharya. *On a measure of divergence between two statistical populations defined by their probability distributions*. Bulletin of the Calcutta Mathematical Society **35** 99–109 (1943).

[95] M. Okuyama and M. Ohzeki. *Quantum Speed Limit is Not Quantum*. Phys. Rev. Lett. **120** 070402 (2018).

[96] H. Cramér. *Mathematical methods of statistics*. Princeton University Press 1946.

[97] C. Rao. *Information and the accuracy attainable in the estimation of statistical parameters*. Bulletin of the Calcutta Mathematical Society **37** 81–91 (1945).

[98] T. Van Vu and Y. Hasegawa. *Uncertainty relations for underdamped Langevin dynamics*. Phys. Rev. E **100** 032130 (2019).

[99] Y. Hasegawa and T. Van Vu. *Uncertainty relations in stochastic processes: An information inequality approach*. Phys. Rev. E **99** 062126 (2019).

[100] Y. Hasegawa. *Thermodynamic Uncertainty Relation for General Open Quantum Systems*. Phys. Rev. Lett. **126** 010602 (2021).

[101] I. Di Terlizzi and M. Baiesi. *Kinetic uncertainty relation*. J. Phys. A: Math. Gen **52** 02LT03 (2019).

[102] S. Deffner and S. Campbell. *Quantum speed limits: from Heisenberg's uncertainty principle to optimal quantum control*. J. Phys. A: Math. Theor. **50** 453001 (2017).

[103] G. Falasco and M. Esposito. *The dissipation-time uncertainty relation*. Phys. Rev. Lett. **125** 120604 (2020).

[104] A. C. Barato, R. Chetrite, A. Faggionato, and D. Gabrielli. *A unifying picture of generalized thermodynamic uncertainty relations*. J. Stat. Mech. page 084017 (2019).

[105] U. Seifert. *From Stochastic Thermodynamics to Thermodynamic Inference*. Annual Review of Condensed Matter Physics **10** 171 (2019).

[106] J. Li, J. M. Horowitz, T. R. Gingrich, and N. Fakhri. *Quantifying dissipation using fluctuating currents*. Nature Comm. **10** 1666 (2019).

[107] S. K. Manikandan, D. Gupta, and S. Krishnamurthy. *Inferring Entropy Production from Short Experiments*. Phys. Rev. Lett. **124** 120603 (2020).

[108] S. Otsubo, S. Ito, A. Dechant, and T. Sagawa. *Estimating entropy production by machine learning of short-time fluctuating currents*. Phys. Rev. E **101** 062106 (2020).

[109] T. Van Vu, V. T. Vo, and Y. Hasegawa. *Entropy production estimation with optimal current*. Phys. Rev. E **101** 042138 (2020).

[110] G. Falasco, M. Esposito, and J.-C. Delvenne. *Unifying thermodynamic uncertainty relations*. New Journal of Physics **22** 053046 (2020).

[111] A. W. C. Lau, D. Lacoste, and K. Mallick. *Nonequilibrium fluctuations and mechanochemical couplings of a molecular motor*. Phys. Rev. Lett. **99** 158102 (2007).

[112] D. Lacoste, A. W. C. Lau, and K. Mallick. *Fluctuation theorem and large deviation function for a solvable model of a molecular motor*. Phys. Rev. E **78** 011915 (2008).

[113] J. P. Garrahan, R. L. Jack, V. Lecomte, E. Pitard, K. van Duijvendijk, and F. van Wijland. *First-order dynamical phase transition in models of glasses: an approach based on ensembles of histories*. J. Phys. A: Math. Gen **42** 075007 (2009).

[114] A. J. McKane and T. J. Newman. *Predator-prey cycles from resonant amplification of demographic stochasticity*. Phys. Rev. Lett. **94** 218102 (2005).

[115] D. T. Gillespie. *Exact Stochastic Simulation of Coupled Chemical Reactions*. J. Phys. Chem. **81** 2340 (1977).

[116] I. D. Terlizzi and M. Baiesi. *A thermodynamic uncertainty relation for a system with memory*. Journal of Physics A: Mathematical and Theoretical **53** 474002 (2020).

[117] J. R. Gomez-Solano, A. Petrosyan, and S. Ciliberto. *Heat Fluctuations in a Nonequilibrium Bath*. Phys. Rev. Lett. **106** 200602 (2011).

[118] S. Ito and A. Dechant. *Stochastic Time Evolution, Information Geometry, and the Cramér-Rao Bound*. Phys. Rev. X **10** 021056 (2020).

[119] R. Filliger and P. Reimann. *Brownian Gyrator: A Minimal Heat Engine on the Nanoscale*. Phys. Rev. Lett. **99** 230602 (2007).

[120] A. Crisanti, A. Puglisi, and D. Villamaina. *Nonequilibrium and information: The role of cross correlations*. Phys. Rev. E **85** 061127 (2012).

[121] V. Dotsenko, A. Maciołek, O. Vasilyev, and G. Oshanin. *Two-temperature Langevin dynamics in a parabolic potential*. Phys. Rev. E **87** 062130 (2013).

[122] V. Mancois, B. Marcos, P. Viot, and D. Wilkowski. *Two-temperature Brownian dynamics of a particle in a confining potential*. Phys. Rev. E **97** 052121 (2018).

[123] S. Cerasoli, V. Dotsenko, G. Oshanin, and L. Rondoni. *Asymmetry relations and effective temperatures for biased Brownian gyrators*. Phys. Rev. E **98** 042149 (2018).

[124] E. dos S Nascimento and W. A. M. Morgado. *Stationary properties of a non-Markovian Brownian gyrator*. Journal of Statistical Mechanics: Theory and Experiment **2021** 013301 (2021).

[125] J. Gieseler, J. R. Gomez-Solano, A. Magazzù, I. P. Castillo, L. P. García, M. Gironella-Torrent, X. Viader-Godoy, F. Ritort, G. Pesce, A. V. Arzola, K. Volke-Sepúlveda, and G. Volpe. *Optical tweezers — from calibration to applications: a tutorial*. Adv. Opt. Photon. **13** 74 (2021).

[126] I. Di Terlizzi, M. Gironella, M. Baiesi, and F. Ritort. *Variance sum rule for non-equilibrium systems*. In preparation.

[127] K. Furutsu. *On the statistical theory of electromagnetic waves in a fluctuating medium (I)*. Journal of Research of the National Bureau of Standards, Section D: Radio Propagation page 303 (1963).

[128] E. A. Novikov. *Functionals and the random-force method in turbulence theory*. Soviet Journal of Experimental and Theoretical Physics **20** 1290 (1965).

[129] K. Berg-Sørensen and H. Flyvbjerg. *Power spectrum analysis for optical tweezers*. Review of Scientific Instruments **75** 594 (2004).

[130] S. Otsubo, S. Ito, A. Dechant, and T. Sagawa. *Estimating entropy production by machine learning of short-time fluctuating currents*. Phys. Rev. E **101** 062106 (2020).

[131] S. K. Manikandan, D. Gupta, and S. Krishnamurthy. *Inferring Entropy Production from Short Experiments*. Phys. Rev. Lett. **124** 120603 (2020).

[132] C. Maes, S. Safaverdi, P. Visco, and F. van Wijland. *Fluctuation-response relations for nonequilibrium diffusions with memory*. Phys. Rev. E **87** 022125 (2013).

[133] A. Mossa, M. Manosas, N. Forns, J. M. Huguet, and F. Ritort. *Dynamic force spectroscopy of DNA hairpins: I. Force kinetics and free energy landscapes*. Journal of Statistical Mechanics: Theory and Experiment **2009** P02060 (2009).

[134] A. Alemany and F. Ritort. *Determination of the elastic properties of short ssDNA molecules by mechanically folding and unfolding DNA hairpins*. Biopolymers **101** 1193 (2014).

[135] J.-D. Wen, M. Manosas, P. T. Li, S. B. Smith, C. Bustamante, F. Ritort, and I. Tinoco Jr. *Force unfolding kinetics of RNA using optical tweezers. I. Effects of experimental variables on measured results*. Biophysical journal **92** 2996 (2007).

[136] M. Manosas, J.-D. Wen, P. T. Li, S. B. Smith, C. Bustamante, I. Tinoco Jr, and F. Ritort. *Force unfolding kinetics of RNA using optical tweezers. II. Modeling experiments*. Biophysical journal **92** 3010 (2007).

[137] H. Vandebroek and C. Vanderzande. *The effect of active fluctuations on the dynamics of particles, motors and DNA-hairpins*. Soft Matter **13** 2181 (2017).

[138] U. Fano. *Ionization Yield of Radiations. II. The Fluctuations of the Number of Ions*. Physical Review **72** 26 (1947).